Transactions of the ASME

TRANSACTIONS OF THE AMERICAN SOCIETY OF MECHANICAL ENGINEERS

VOLUME 76 JULY 1954 NUMBER 5

Transactions

of The American Society of Mechanical Engineers

Published on the tenth of every month, except March, June, September, and December

Published monthly by The American Society of Mechanical Engineers. Publication office at 20th and Northampton Streets, Easton, Pa. The editorial department is located at the headquarters of the Society, 29 West Thirty-Ninth Street, New York 18, N. Y. Cable address, "Dynamic," New York. Price $1.50 a copy, $12.00 a year for Transactions and the *Journal of Applied Mechanics*; to members and affiliates, $1.00 a copy, $6.00 a year. Changes of address must be received at Society headquarters seven weeks before they are to be effective on the mailing list. Please send old as well as new address.... By-Law: The Society shall not be responsible for statements or opinions advanced in papers or...printed in its publications (B13, Par. 4) ....Entered as second-class matter March 2, 1928, at the Post Office at Easton, Pa., under the Act of August 24, 1912....

Design and Operation of High-Recovery Regenerative-Type Air Preheaters

Part 1 Special Features of the Regenerative-Type Air Preheaters[1]

By GEORGE BRADDON,[2] WELLSVILLE, N. Y.

Air preheating has become the most widely accepted method of recovering heat from flue gases of high-efficiency steam-generating units. The drive to reduce stack losses further and improve over-all efficiencies continues. The regenerative air preheater possesses unique characteristics which contribute to its ability to achieve maximum reduction in stack losses while permitting continuous operation over long periods. This paper deals with those features of the regenerative air preheater which are inherent in the type and are created expressly for the purpose of realizing high efficiency coexistent with high availability.

Introduction

THE purpose of this paper is to broaden understanding of the regenerative-type air preheater which continues to be one of the most effective means at the disposal of the designer in his striving for higher efficiency of steam generation.

The High-Efficiency Boiler

In today's modern steam-electric station, optimum economy is realized principally by attaining high efficiency of the vapor cycle and high efficiency of steam generation. The boiler unit must be matched to the requirements of the vapor cycle. The resulting demands on the boiler unit place a limitation on the heat which may be transferred to water and steam so that the products of combustion leave the surfaces of the pressure components at an elevated temperature. But, to generate steam at high efficiency, the heat loss in the products of the combustion discharged to the stack must be kept as low as possible. To achieve low exit-gas temperature, the designer of the modern steam generator resorts to air preheating. There is no alternative. Fig. 1, from the work of Arthur R. Weismantle,[3] illustrates this point. These curves show the duty of an economizer, or an air preheater; also combinations of both, to effect a given desired exit-gas temperature as a function of the boiler pressure. A terminal difference of 150 F between the temperature of the flue gas and the temperature of the water is assumed to be the practical minimum. This difference applies to temperatures in the boiler as well as the economizer. If the desired exit-gas temperature be 350 F, the shaded area shows air preheating to be indicated at operating pressures above 250 psi. For a 1400-psi boiler, equipped with economizer and air preheater, the air preheater has to effect a drop in the temperature of the flue gas from 600 to 350 F.

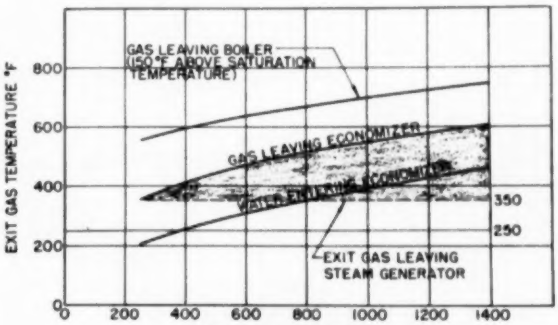

Fig. 1 Exit-Gas Temperature as a Function of Boiler Pressure

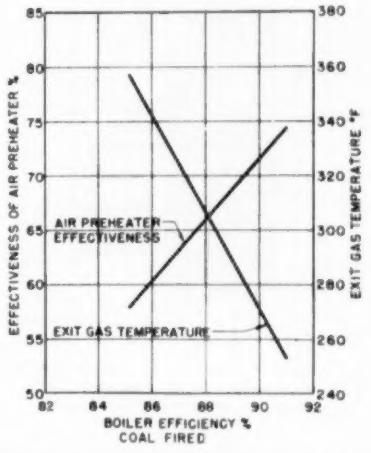

Fig. 2 Boiler Efficiency Versus Air-Preheater Effectiveness and Exit-Gas Temperature Corresponding to Coal Firing

Today, exit-gas temperatures in the proximity of 250 F are being specified for high-efficiency boilers when fuel characteristics permit. The air preheater, to serve a 1400-psi boiler with no economizer, would have to effect a drop in flue-gas temperature from about 740 to 250 F. The trend in the design of the modern boiler is to assign to the air preheater the task of recapturing the major share of the recoverable heat in the flue gases leaving the boiler proper. Heat-transfer surface added to an air preheater to increase its duty is accomplished at lower cost than that of equiva-

[1] Part 2 of this paper, by Joseph Waitkus, is on page 706.

[2] Assistant Chief Engineer, The Air Preheater Corporation. Mem. ASME.

[3] "Some Comments on Air Preheat" by A. R. Weismantle, Lecture to employees of Air Preheater Corporation, November, 1950.

Contributed by the Power Division and presented at the Fall Meeting, Rochester, N. Y., October 5-7, 1953, of The American Society of Mechanical Engineers.

 Manuscript, slightly condensed, received at ASME Headquarters, January 25, 1953. Paper No. 53—F-22.

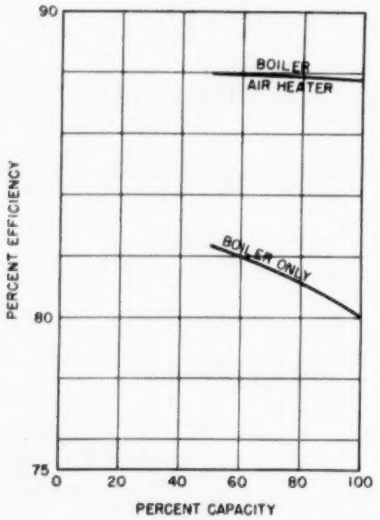

Fig. 3 Boiler Efficiency as a Function of Load

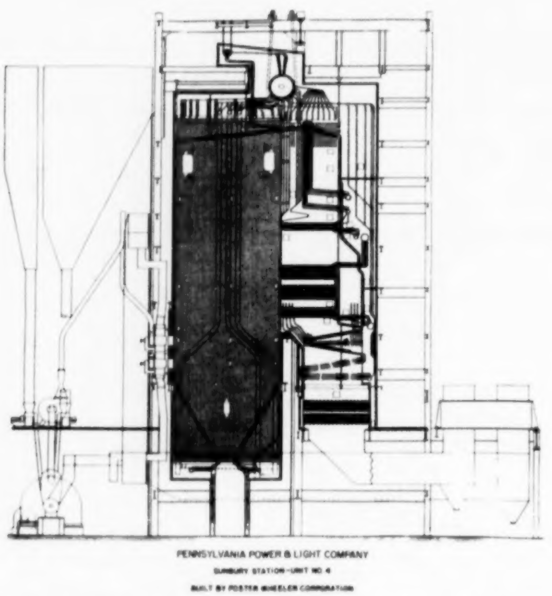

Fig. 4 Foster Wheeler Boiler Unit, No. 4 Sunbury Station, Pennsylvania Power & Light Company, With Vertical-Type Air Preheater

lent economizer surface. The modern high-pressure boiler then, demands an air preheater of high effectiveness, that is, one which recovers a high proportion of the heat available to it.

The curves in Fig. 2 are based upon specifications of about 20 high-efficiency boiler units equipped with air preheaters. They show the relation between boiler efficiency corresponding to coal-firing and gas-side effectiveness, also between boiler efficiency and exit-gas temperature. The high-recovery air preheater in such steam-generating units contributes approximately 10 points to the over-all boiler efficiency. More than that, the air preheater tends to offset the drooping efficiency characteristic at high

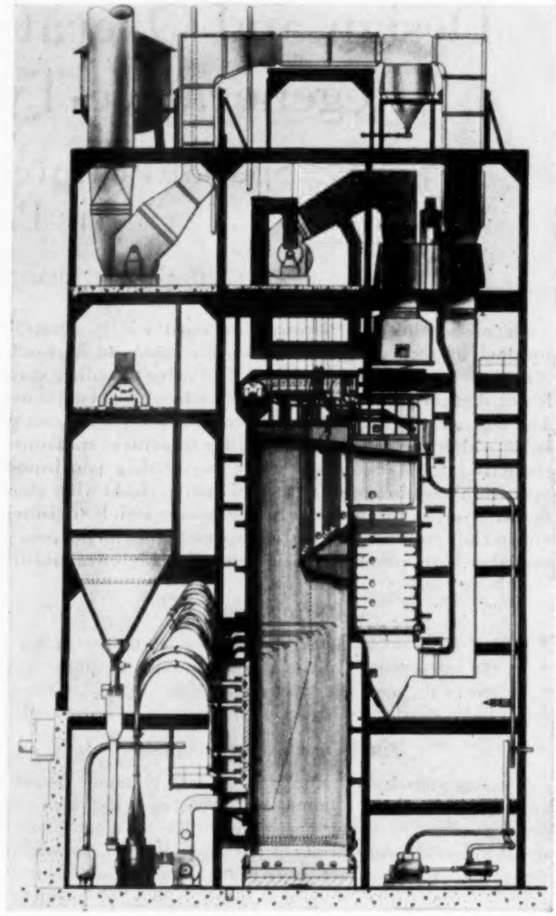

Fig. 5 Babcock & Wilcox Boiler Unit, Gorgas Station, Alabama Power Company With Vertical-Type Air Preheater

rating. Fig. 3, also from the work of Weismantle,[3] illustrates the influence of the air preheater upon boiler efficiency as load increases.

Combustion air at high temperature, such as is exemplified in the foregoing, brings about savings other than betterment of boiler efficiency. For a given duty, the furnace size of a boiler fired by pulverized coal, oil, or gas may be reduced appreciably by the use of preheated air. The higher the preheat, the greater the reduction obtainable. This saving in boiler cost results from acceleration of the combustion process, which diminishes the necessary resident time for the fuel particle in the furnace.

Description of the Regenerative-Type Air Preheater

The place occupied by the air preheater of the regenerative type in a modern high-efficiency boiler unit is illustrated in Figs. 4 to 8, inclusive. In all these illustrations, as in nearly all applications, the flue gas and the combustion air flow through the preheater in opposite directions. In Figs. 4 and 5 the gas flow is vertically upward. In Figs. 6 and 7 it is vertically downward and in Fig. 8 it is horizontal. The duct connections of this type air preheater can be fashioned to suit a wide variety of shapes and sizes of ducts.

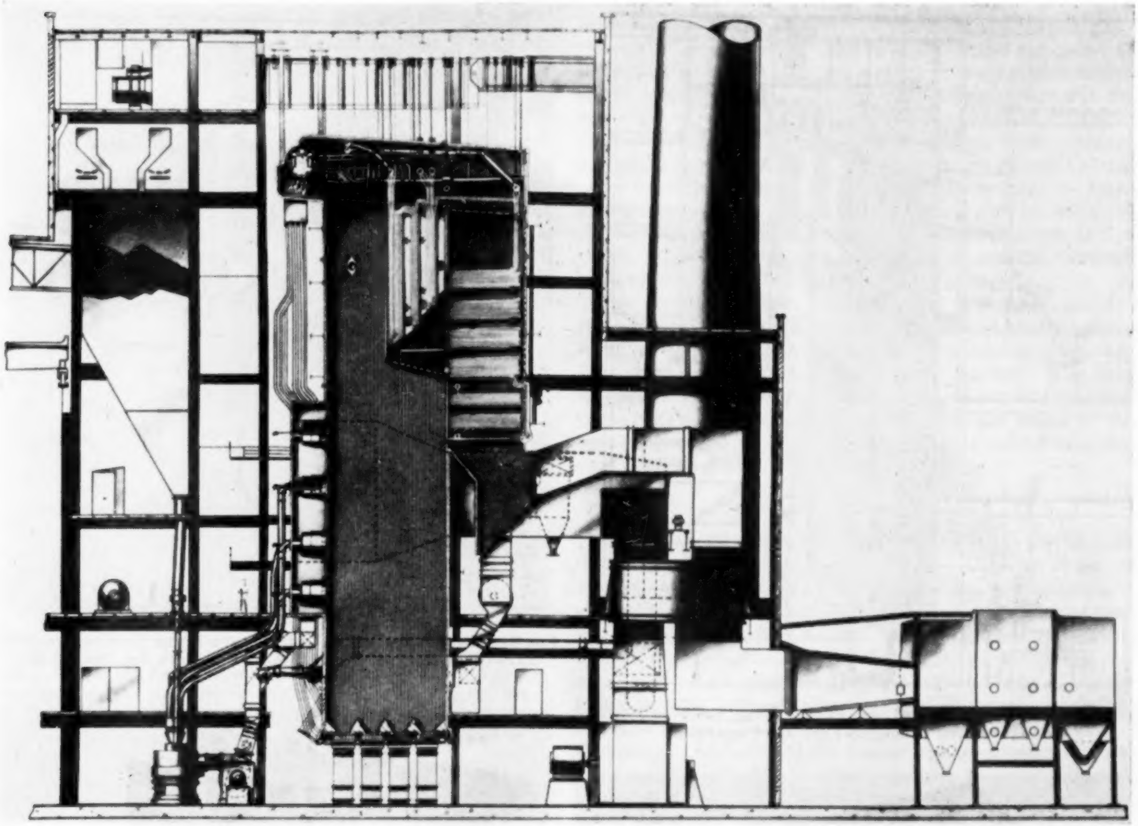

FIG. 6 BABCOCK & WILCOX BOILER UNIT, ASTORIA STATION, CONSOLIDATED EDISON COMPANY OF NEW YORK, WITH INVERTED-TYPE AIR PREHEATER

In all of the installations represented by these views, two regenerative air preheaters connected in parallel to the ductwork serve the boiler unit. Such is usually the case for boiler units having capacities in excess of approximately 300,000 lb per hr. Usually located side by side at the rear of the boiler, the pair of heaters occupies a space within the width of the boiler bay. For a boiler unit of 1,000,000-lb per hr capacity, each of the two structures of the regenerative air preheaters is about 22 ft diam, 15 ft high, and weighs approximately 250,000 lb. A few users of regenerative air preheaters recently have chosen to employ three heaters in parallel side by side across the rear of a 1,000,000-lb per hr reheat-boiler unit.

The essence of the regenerative-type heat exchanger is the heating element. In the regenerative-type air preheater the heating elements are contained in a slowly turning rotor of cellular construction. As the rotor turns, heat is absorbed continuously by the heating elements from the gas while a like amount of heat is released simultaneously to the combustion air as these fluids flow axially through the rotor. The rotor is enclosed in a gastight housing which is fitted at each end to make connection with air and flue-gas ducts. These components are evident in Fig. 9 which is a view of a typical regenerative air preheater of average size for gas and air flowing downward and upward, respectively. Also showing in this view is the rotor drive unit. Regenerative-type air preheaters having upward gas flow are termed "vertical" type and designated by the letter V. Those having downward gas flow are termed "vertical inverted" type and are designated by the letters VI.

Fig. 10 is a view of a large-sized regenerative air preheater for horizontal flow of gas and air. Its components are similar to the corresponding parts of the vertical types. The rotor is carried on two radial bearings, one of which shows in the view. The rotor-drive unit also appears. It is termed "horizontal" type and designated by the letter H.

In counterflow preheaters, the part where the gas enters and air leaves is termed "the hot end" and, similarly, the part where air enters and gas leaves is termed "the cold end." These terms apply to the structures as a whole as well as the rotor and heating elements. All of these views referred to in the foregoing are of shop assemblies just before shipping. Heating elements are not installed until final erection.

Fig. 11 is an artist's drawing showing a section in elevation through the center line of a large vertical inverted-type air preheater. Here the rotor is shown with heating elements in place. For large-size heaters, the weight of the rotor is transmitted to a specially designed beam out of the way of the flue gases. This view shows the rotor support bearing and the rotor guide, or steady, bearing. The rotor drive also is shown.

The components of the structure joined to each end of the rotor housing are termed "connecting plates." Aside from affording connections for attachment of gas and air ducts, the connecting plates also serve to keep separate the two streams and

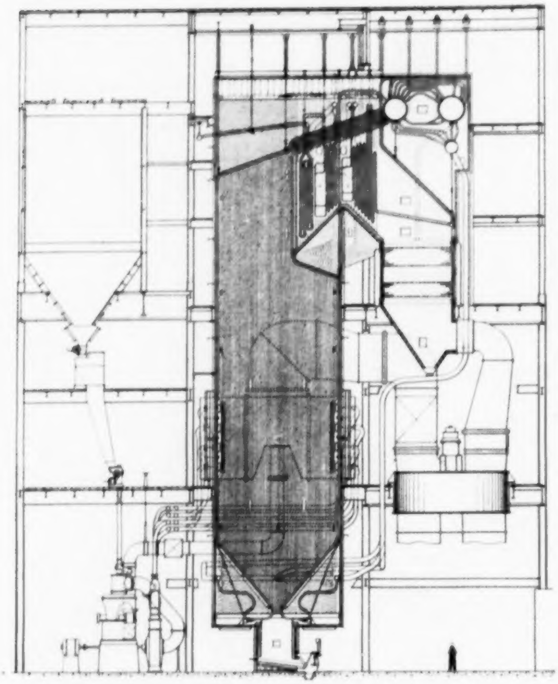

Fig. 7 Combustion Boiler Unit, Plant Yates, Georgia Power Company With Inverted-Type Air Preheater

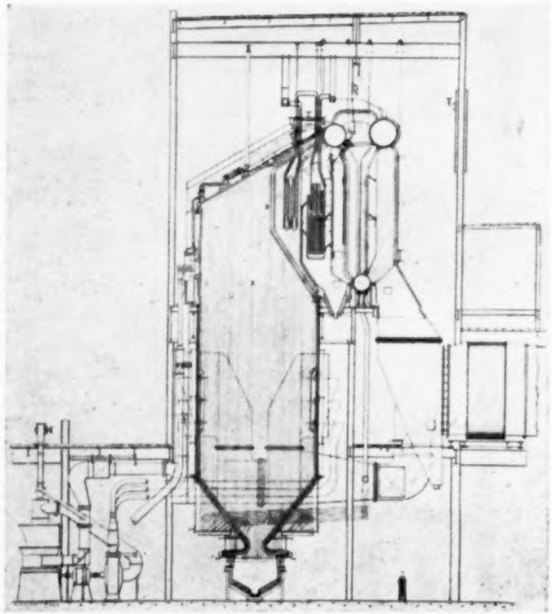

Fig. 8 Combustion Boiler Unit, Possum Point Station, Virginia Electric Company, With Horizontal-Type Air Preheater

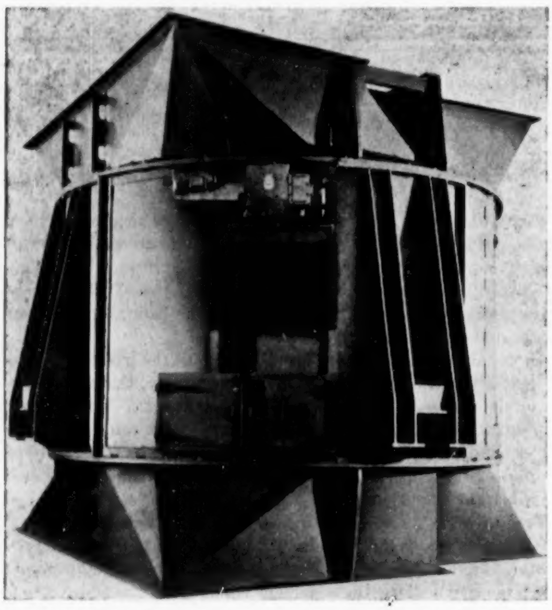

Fig. 9 Shop Assembly of Typical Inverted Heater of Medium Size—Side View

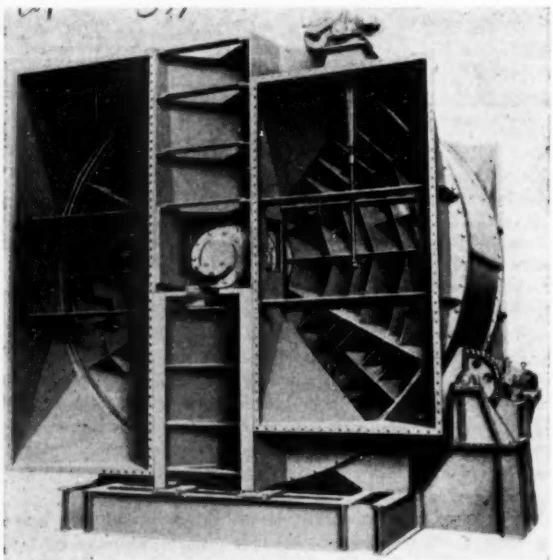

Fig. 10 Shop Assembly of Typical Horizontal Heater of Large Size

to guide them into and away from the rotor. Sealing strips fastened to the rotor are set to clear stationary machined surfaces of the connecting plates as closely as practicable. Leakage from the higher-pressure air to the lower-pressure gas in typical high-recovery regenerative air preheaters is of the order of 8 per cent when seals are set properly and in good condition.

The connecting plates are constructed so as to guide the separate air and gas streams into the rotor according to a predetermined division of the rotor area in order to realize the most advantageous proportionment of pressure losses for optimum economy in fan selection and in fan operation.

A balanced-draft application for which about 90 per cent of the

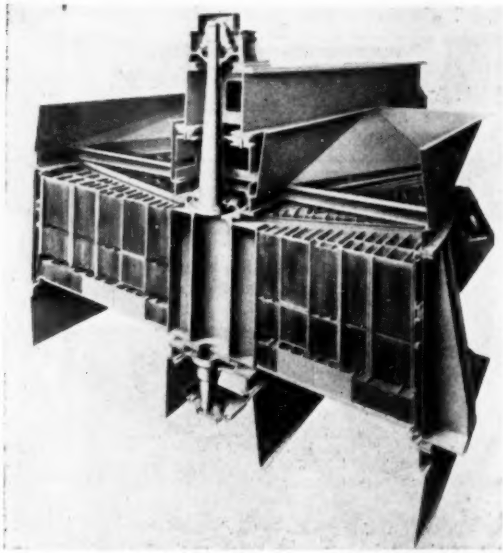

Fig. 11 Sectional View Through Large-Sized Inverted-Type Heater

combustion air passes through the air preheater would be designed to pass the gas through approximately 60 per cent of the rotor area and to pass the air through 40 per cent of the rotor area. For a pressure-fired boiler all of the combustion air (except tempering air) is taken through the air preheater. It would be designed to pass gas through approximately 55 per cent of the rotor area and air through the remaining 45 per cent.

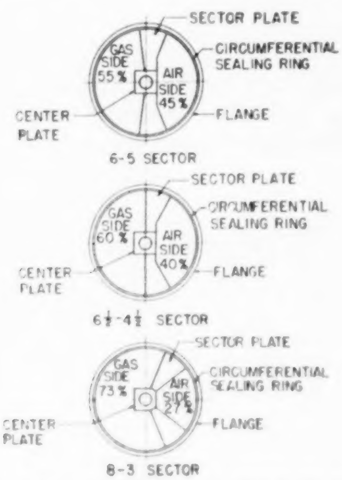

Fig. 12 Three Typical Arrangements of Sectors

Fig. 12 shows arrangement of partitions of the connecting plate for three typical divisions. By resort to special construction, any ratio of gas to air-side areas may be chosen to suit the relative pressure losses desired.

Problems in Design and Operation for High Recovery

Today the low limit in temperature of exit gas depends upon the dew point of the gas or, more exactly, upon the extent to which the constituents of the gas combine to form deposits on the heat-transfer surfaces, upon the character of the deposit and nature of the surface as well as upon the severity of the corrosion attack on the metal of the surface. While there is steady progress in the search for knowledge of the complex causes of these ill effects, there are as yet no known measures to prevent them. Certain techniques and operating devices to be dealt with in Part 2 of this paper have been developed. They contribute much to deter fouling and corrosion of the cold-end heating surfaces when the air preheater is operated under conditions inviting trouble of this nature. These problems and a discussion of remedial measures is the subject of a paper by Karlsson and Hammond.[4]

Aside from the resort to operational techniques, the regenerative-type air preheater possesses unique characteristics which, along with some special provisions, constitute salient advantages in coping with operation in the trouble zone. The combination of inherent characteristics, of special provisions, and of appropriate techniques, permits the selection and design of the regenerative-type air preheater for deliberate operation under conditions which otherwise would be untenable.

Inherent Characteristics

Relatively uniform distribution of the flow of gas and air past the heating surface is one of the best-known properties of the regenerative-type air preheater. It results in uniform heating and cooling of the heating elements by which the existence of cold spots toward the cold end of the heating elements is avoided. The mean metal temperature at the cold end of the heating elements of the regenerative air preheater is known to be as high or higher than the arithmetical average of temperatures of entering air and exit gas. The work of Karlsson and Hammond,[4] also of Karlsson and Holm,[5] treat this subject and give results of some experimental work whereby element-metal temperatures were measured. These findings are quite significant in the light of results of some field measurements of tube-metal temperature in a recuperative air heater. A difference of as high as 120 deg F between average of entering air and leaving temperature and the temperature of tube metal is reported by Rothemich and Parmakian.[6]

The added property, whereby all the edges of the heating elements near which deposits accumulate at the cold end can be conveniently reached by a single cleaning jet, makes for simplicity in the cleaning equipment needed to halt the growth of deposits.

Heating elements are stacked in the rotor in layers, usually two, and seldom more than three. This property permits the replacement of elements which are subject to deterioration without disturbing the main body of heat-transfer surface.

Special Provisions

The special features devised expressly to implement operation at low exit-gas temperature are as follows: Cleaning apparatus; cold-end heating elements arranged for rapid and convenient replacement.

Provision for cleaning the cold-layer elements where troublesome deposits form is standard equipment for the regenerative air preheater.

The apparatus for directing a jet of steam or compressed air on

[4] "Air-Preheater Design as Affected by Fuel Characteristics," by Hilmer Karlsson and W. E. Hammond, Trans. ASME, vol. 75, 1953, pp. 711–722.

[5] "Heat Transfer and Fluid Resistances in Ljungström Regenerative-Type Air Preheaters," by Hilmer Karlsson and Sven Holm, Trans. ASME, vol. 65, 1943, pp. 61–72.

[6] "Tubular-Air-Heater Problems," by E. F. Rothemich and G. Parmakian, Trans. ASME, vol. 75, 1953, pp. 723–728.

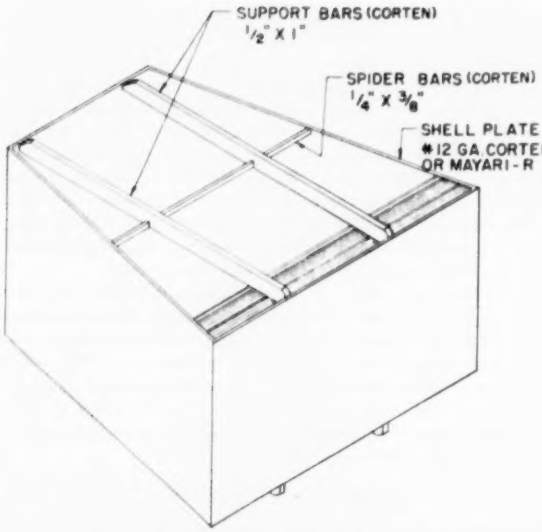

Fig. 13 Typical Basket for Cold-End Layer

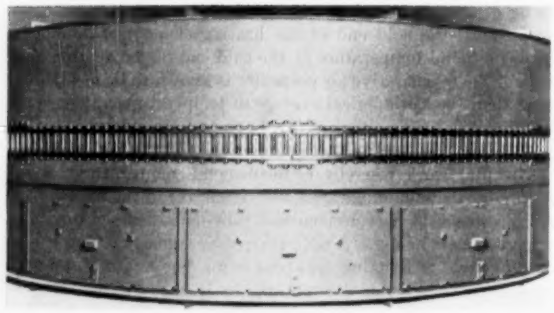

Fig. 14 Rotor With Panels in Place Closing Openings Through Which Cold-End Baskets Are Withdrawn

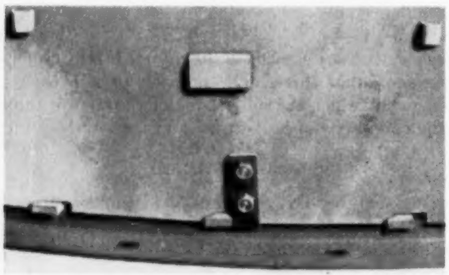

Fig. 15 Close-Up of Panel Fastener

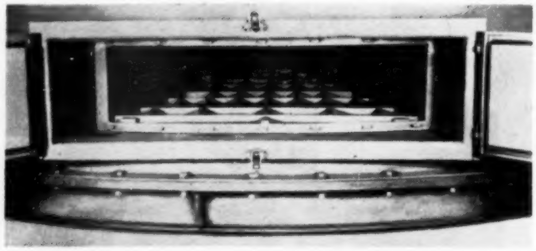

Fig. 16 View Through Open Basket-Removal Door Into Space for Cold-Layer Baskets

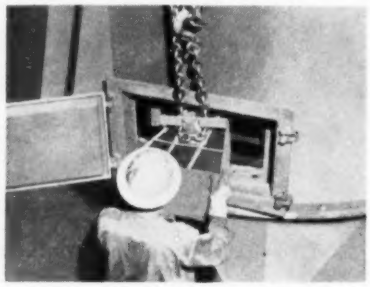

Fig. 17 Cold-Layer Basket Being Loaded Into Rotor

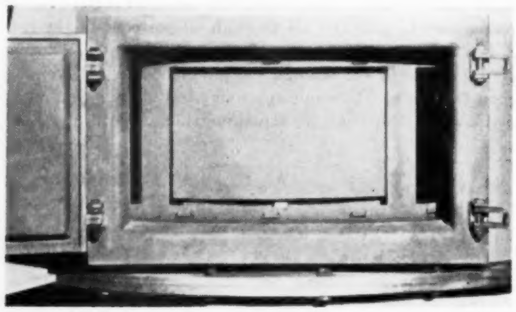

Fig. 18 Cold-Layer Basket in Place

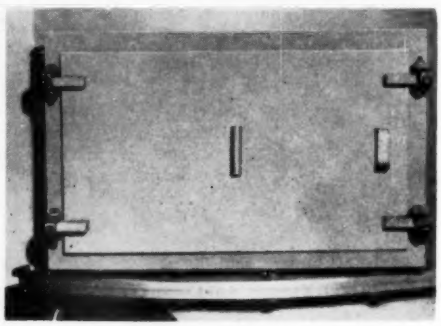

Fig. 19 View of Basket-Removal Door for Cold-End Element, Closed Position

the deposit where it forms and for the effective introduction of wash water is described in detail in an article by Waitkus.[7]

Replaceable Heating Elements for the Cold Layer

The cold-layer heating elements, 12-in. in depth, are packed in baskets convenient for handling, Fig. 13. Each basket is reversible so that the portion of elements thinned by corrosion can be turned away from the zone of corrosion and the unaffected portion exposed to it. This feature nearly doubles the useful element life.

An access door through the rotor housing, and removable panels

[7] "Cleaning Regenerative Air Preheaters," by Joseph Waitkus, *Combustion*, vol. 25, 1953, August, pp. 40–45; September, pp. 43–46; October, pp. 49–53.

in the rotor shell, allow for quick removal and replacement of basketed cold-layer elements without disturbing sealing members or any other components. Such replacement is effected without the need for maintenance crews to work inside the heater or ductwork. This feature allows removal and replacement while the interior is too hot to enter. Furthermore, the work can be done with the boiler unit under light load. The work can be accomplished conveniently during a week-end outage or while in operation at any convenient time that load reduction can be arranged.

Thus the cold layers of elements may be removed for washing external to the heater and subsequently returned to the rotor. This feature is attractive to those designers and operators who prefer to avoid the introduction of water to the interior of the air preheater and ductwork.

Figs. 14 to 19, inclusive, with their respective captions, are self-explanatory.

The heating elements of the cold layer are fabricated from 18-gage corrosion-resistant low-alloy steel. The plate and the bars of the baskets containing the elements, as well as the grating for

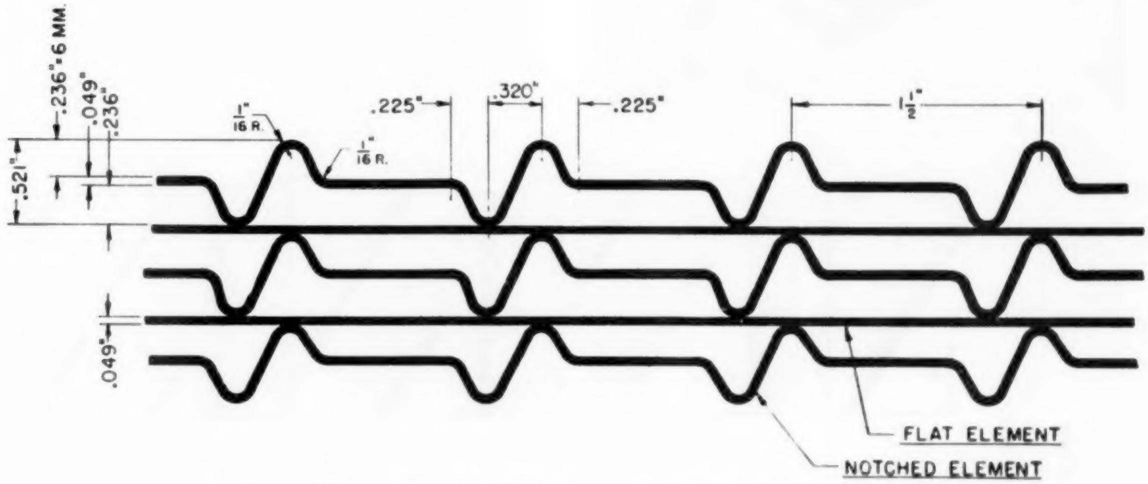

Fig. 20 Form of Heating Elements for Cold-End Layer

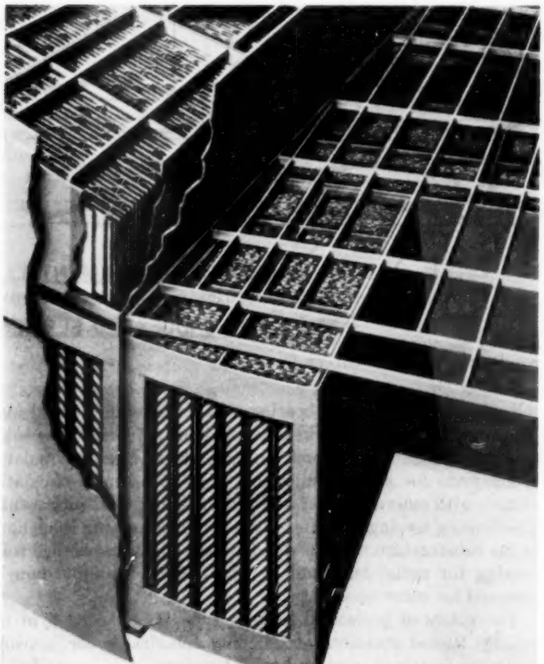

Fig. 21 Sectional View Through Portion of Rotor of Inverted Heater Showing Arrangement of Basketed Heating Elements

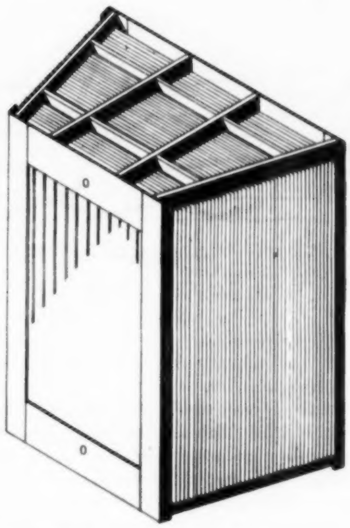

Fig. 22 Typical Basket for Hot and Intermediate Layers of Heating Elements

supporting the baskets (across which they are skidded) are all fabricated from the same or equivalent alloy.

The heating elements have the form illustrated in Fig. 20. This configuration provides straight-through passages, free of crevices or undulations, in which deposits might be sheltered from the action of the cleaning jet or wash water.

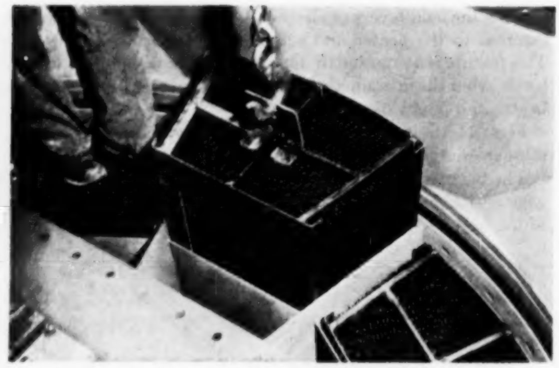

Fig. 23 Hot-Layer Basket Being Lowered Into Rotor

as cold layers. Shop-packaging also assures control over tightness of the pack. A typical arrangement of basketed heating elements and method of supporting them in the rotor is shown in Fig. 21 applying to the rotor of an inverted air preheater. Fig. 22 shows a typical basket for the hot and intermediate layers of heating element. In Fig. 23 a hot-layer basket is shown being lowered into the rotor.

The heating elements of the hot and intermediate layers have the form shown by Fig. 24. This configuration achieves a high coefficient of heat transfer with low pressure loss.

Other Features of the Regenerative Air Preheaters

The following is a brief description of improvements in design put into use in recent years:

Rotor Support. The rotor of V and VI-type air preheaters is suspended by a carrying shaft from the superstructure. The current design of rotor support employs a spherangular type of self-aligning roller thrust bearing capable of taking radial load. The bearing is contained in a simple housing, easily accessible. Cooling by a submerged coil, through which water is circulated, is adequate for most installations, Fig. 25. An oil-circulating system with external cooler and filter is being used successfully. The bearing serving to center the rotor in its housing is anchored in the substructure. It is a standard self-aligning spherical roller bearing for radial load and is contained in a simple housing jacketed for water cooling.

The rotors of horizontal heaters, type H, are carried in two equally loaded standard self-aligning spherical roller bearings. They are contained in water-cooled housings. Cooling and filtering by oil circulation also has been practiced successfully.

Rotor Drive. In the regenerative air preheater of modern design the driving force for turning the rotor is applied at its

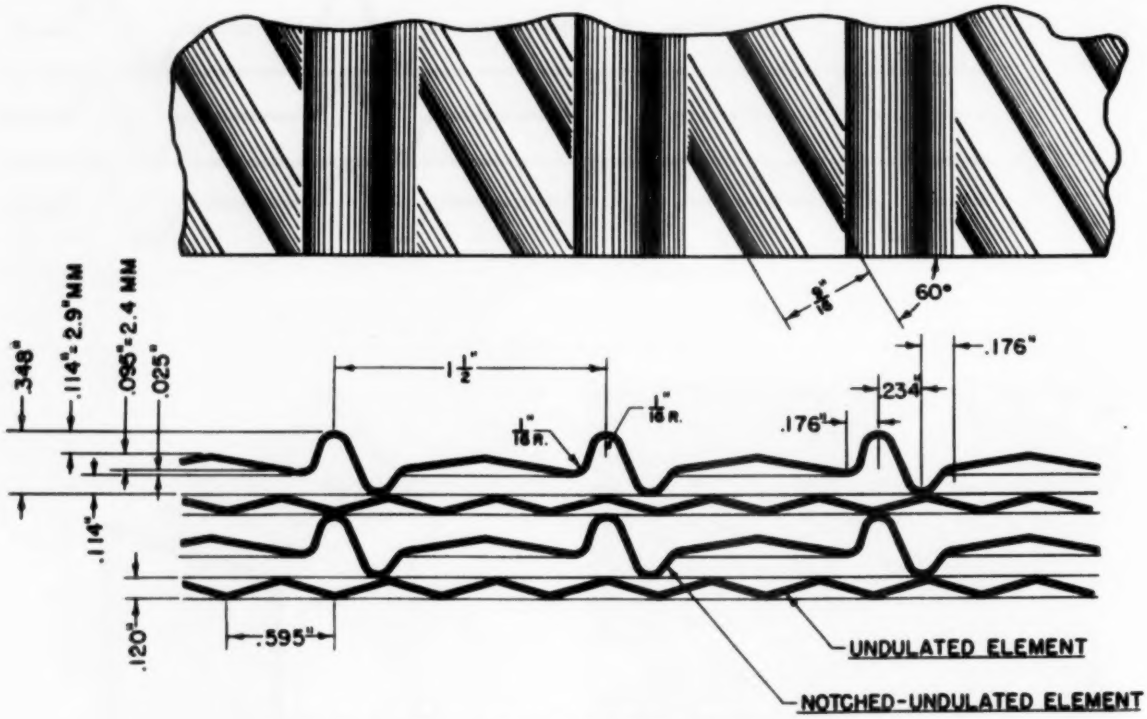

Fig. 24 Form of Heating Elements for Hot and Intermediate Layers

Under certain severe conditions, notably those attending operation while firing high-sulphur or high-vanadium-bearing fuel oil the trouble zone may extend beyond the cold layer. To cope with such conditions, an intermediate layer of heating elements, formed similarly to that of the cold layer and fabricated also from corrosion-resistant alloy, can be furnished basketed for convenient handling through the side of the structure in the manner described in the foregoing for the cold layer.

Replaceable Heating Elements for Hot and Intermediate Layers

With the growth in the use of large-sized regenerative-type air preheaters, the need to shorten field time for installation of heating elements assumed increased importance. The answer to this problem was to shop-package hot and intermediate layers as well

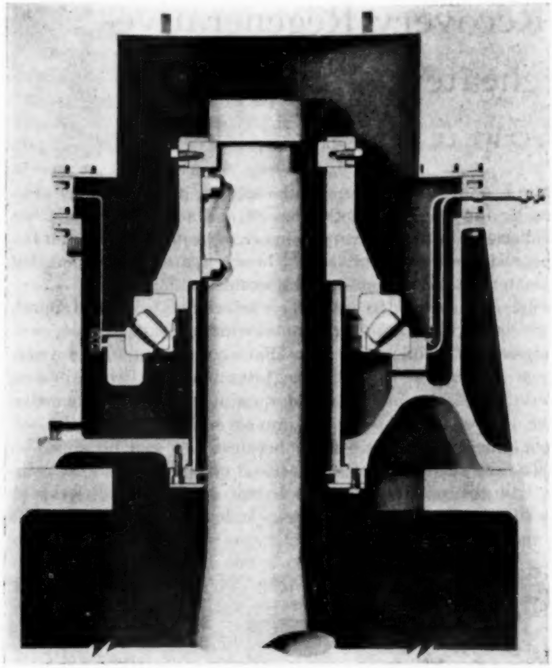

Fig. 25 Typical Rotor Support of Current Design Employing Spherangular Roller Thrust Bearing

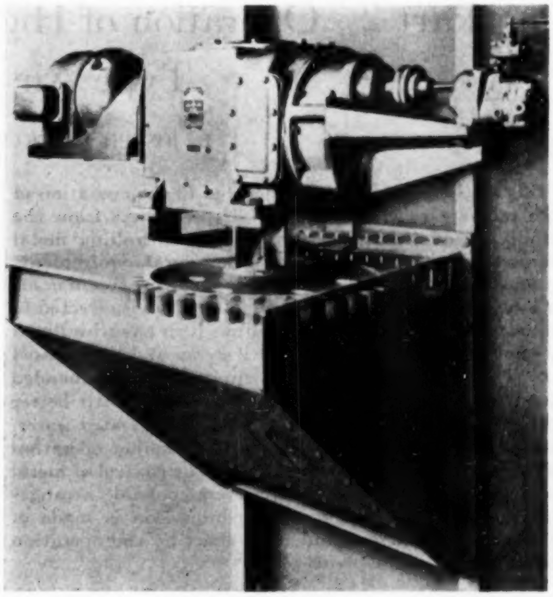

Fig. 26 Typical Drive Unit With Auxiliary Air Motor for Vertical or Inverted Heater

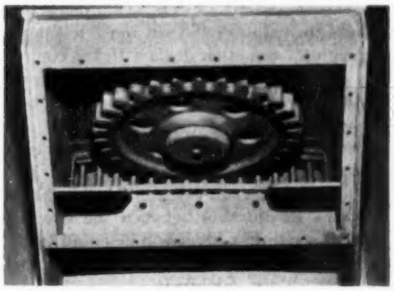

Fig. 27 View of Pinion-and-Pin Rack Engagement

periphery. A pin rack, or ring gear, is mounted on the rotor shell and is engaged by a pinion driven from the low-speed shaft of an electric-motor-driven speed reducer.

The principal advantage of this type of drive is accessibility for convenient attendance and maintenance. Flexibility in position permits the designer and user to choose the most desirable location.

Fig. 26 shows a typical rotor drive unit for a vertical or inverted-type air preheater. The unit shown here is provided with an auxiliary air motor, although this feature is the exception rather than the rule. Fig. 27 shows elements of the pin rack and the pinion and shows engagement between them.

The Future

As long as electric energy is generated by burning fuels under pressure vessels, the regenerative air preheater probably will continue to fill a place of prominence in the process.

It is not overoptimistic to expect that further progress in efficiency of fuels utilization will evolve from research which has been under way, and which continues unabated. One phase of this research is concerned with means to remove solid particles from the flue gases before they come in contact with the surfaces where troublesome deposits collect under conditions prevailing today. Another phase is concerned with the treatment of fuels to remove constituents which are responsible for the ill effects, or with treatment to render such constituents passive in so far as concerns their trouble-making properties.

The foreseeable possibilities of progress within the next five years is an approach to an exit-gas temperature of 200 F at full load with fuels that today cause distress under prevailing conditions, and an approach to even lower temperatures with fuels that can be coped with under those prevailing conditions which today can be considered practical though troublesome.

Part 2 Operation of High-Recovery Regenerative-Type Air Preheaters

By JOSEPH WAITKUS,[8] WELLSVILLE, N. Y.

This section of the paper is devoted to the operation of high-recovery regenerative-type air preheaters from the standpoint of removing deposits and controlling metal temperature. Emphasis is placed on several requirements for an effective removal of deposits by blowing steam or air and washing with treated water. Attention is directed to the need for a dry cleaning medium which has stimulated interest in the use of superheater steam and compressed air. The washing procedure currently recommended assures a higher degree of deposit removal with better protection from acid action. Alkalized or treated water, instead of raw water, accelerates the washing operation and produces a more thorough job. The control of metal temperature is discussed from several possible arrangements and combinations. The comparison is made of corresponding features and their effect on the operation and efficiency of the plant.

Introduction

In discussing the operation of the regenerative-type air preheater to obtain and sustain high recovery, consideration might be directed to two important aspects: One deals with the removal of deposits to maintain the air and flue-gas passages in condition for free flow; the other deals with the control of metal temperature to avoid dew-point conditions and subsequent corrosion and thinning of the heating surface. Since both aspects dominate the operation of high-recovery equipment, it should be of immediate interest to review a few of the latest developments and practices as applied to the regenerative-type air preheater.

As an introduction to the subject, it might be wise to emphasize and clarify the relationship between the two aspects just mentioned. Referring to Fig. 28, it will be noted that, basically, flue gases resulting from combustion contain solid particles and vapors. The particles are sulphur-bearing and accumulate to form deposits; the vapors of SO_2, SO_3, and H_2O condense to form moisture or sweating. The combination of deposits and moisture, under certain conditions of operation, develops an acid or corrosive state. In other words, deposits, moisture, and corrosion are interconnected very much the same as elements in a chemical formula. Each element contributes to, or stimulates, the influence of the other two elements separately or in combination. The control of corrosion, therefore, logically requires control of the accumulation of deposits and the formation of moisture. For deposits, the solution is found in an effective soot blower or cleaning device; in the case of moisture, the solution is found in some means of elevating the temperature of the metal at the point where condensation takes place.

Character of the Deposit

The technique for removing deposits has advanced, in recent years, to a high degree of effectiveness. It is the result of new equipment, new cleaning mediums, and new procedures. Since Part 1 of this paper covers the design of new equipment, Part 2 will emphasize some of the important factors related to cleaning mediums and procedures.

[8] Assistant to Technical Manager, The Air Preheater Corporation. Mem. ASME.

For a proper development of the subject, it might be logical to consider the character of the deposit and recognize some of its peculiarities. Deposits vary in many respects depending on the type, analysis, and quantity of fuel burned, and on the operating characteristics of the fuel-burning equipment.

Fuels are identified as one of three principal types—solid, liquid, or gaseous. Each type varies to take into account differences in analysis, heat value, and so on. For example, solid fuels generally are referred to as anthracite, bituminous, or lignite, in consideration of the presence and quantity of definite elements. Each of these in turn is divided into several subclasses or grades. Liquid fuels vary considerably because they can be mixed so easily from several sources. Residual or process gases are coming into greater prominence and their use is likely to grow as developments are made in various industries—particularly the oil and chemical industry.

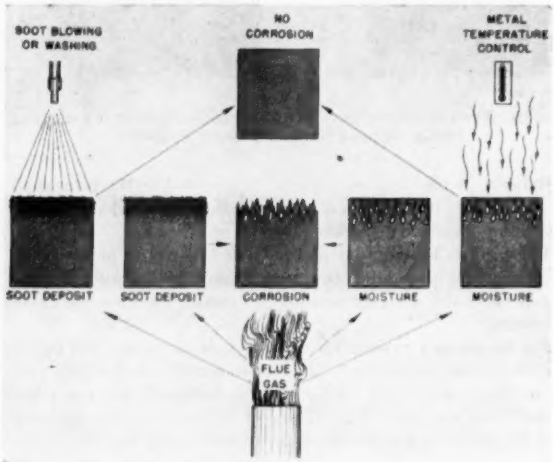

Fig. 28 Origin and Relationship Between Deposits, Moisture, and Corrosion

The significance of fuel analysis cannot be emphasized too strongly in the light of the current introduction and use of low-grade fuels of various types and combinations. Mixed fuels are particularly uncertain in their analysis, and from the combination of certain elements arises an acute problem in deposit formations. Constituents such as sulphur, vanadium, ash, moisture, and the like, are recognized today as basically responsible for difficulties with deposits. There is no prospect of returning to operation with high-grade fuels since the supply is diminishing rapidly. With gradual and continual deterioration of the quality of the fuel supply, fuel analysis takes on increased significance and importance.

The quantity of fuel burned is of interest because many steam-generating units today consume at least two types of fuels and, very often, in several grades. Economic considerations create this situation, demanding combustion equipment of flexible design and suited to multifuel-burning in a wide range of types and grades. It is important to recognize how much of each type of

fuel is consumed, how often the change is made from one to the other, and the conditions when the change is conducted.

Under operating characteristics of the steam-generating unit, consideration should be extended to the type and efficiency of the combustion equipment. Pulverized coal varies in fineness, depending on the action of the mills, and produces an ash of varying size and character. The ash may vary from comparatively large abrasive particles to a soft, fine, or dusty texture. In liquid fuels, the importance of atomization cannot be overlooked. Mechanical, steam, and air-atomization systems vary in their influence on combustion, depending on the characteristics of the fuel. There is no doubt that the degree of atomization plays an important part in the formation of deposits in so far as liquid fuels are concerned. Generally, if combustion is complete in the furnace, some of the detrimental constituents are oxidized to a less active state and entrained as an ash in the flue gases. If combustion is poor or incomplete, then the various constituents, separately or in combination, extend their influence to the formation of deposits.

The texture of the deposit—whether it is a dry dust, a soft mass, a gummy or sticky residue, or a hard, cementlike mass—depends on the fuel, type of combustion, and metal temperature. It determines to a large measure the cleaning medium and procedure required. Some deposits can be removed by just an occasional blowing of the cleaning device; others require regular and strong blowing action, with an occasional washing operation. Still other deposits cannot be removed by blowing, and require the extreme action of a washing operation at regular and frequent intervals.

The uncertainties and intangibles involved in deposit formation make it one of the most elusive problems to predict and analyze in the steam-generating field. There are as many types and combinations of deposits as there are installations. No two deposits are alike or show the same results. Too often, what might be considered as the solution for difficulties with deposits at one installation may be found completely inadequate for another.

The removal of deposits can be divided into two separate functions. The most common one is performed with steam or air as a cleaning medium. Another is performed with water as a washing medium. The effectiveness of the first function determines the necessity for resorting to the second function.

Cleaning the regenerative-type air preheater was recently the subject of a series of three articles by Joseph Waitkus[7] to which the reader is referred for complete details on equipment, cleaning mediums, and procedures.

Temperature Control

Elevating the metal temperatures to avoid condensation of acid vapors in the flue gases has long been recognized as important to sustaining satisfactory operation at high recovery in the regenerative-type air preheater. Since several types of controls are available, a problem arises as to which type or combination of types to apply. An introduction to the several types should be helpful to an understanding of the problem as it exists today.

Cold-Air By-Passing. The most widely used type of temperature control is the cold-air by-pass system in Fig. 29. It is arranged to remove cold air ahead of the air preheater and discharge it into the duct after the preheater. By so doing, metal temperature is controlled by reducing air-preheater recovery. The reduction in recovery is indicated by a rise in exit-gas temperature.

This control is simple and popular, and, if provided with the dampers indicated, gives excellent metal-temperature control. With constant inlet-air temperature, the cold-end metal temperature is elevated approximately one half the rise in exit-gas

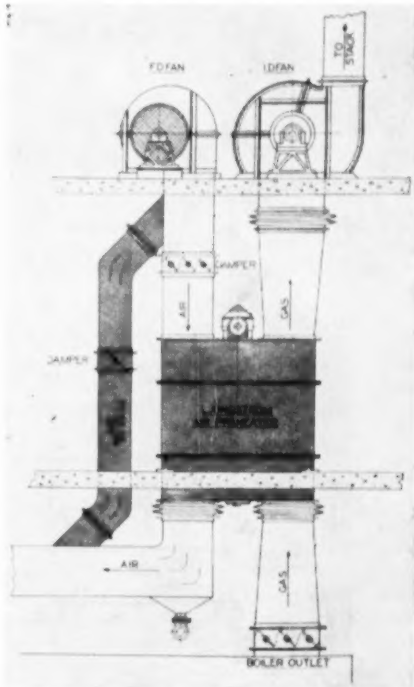

Fig. 29 Cold-Air By-Passing System

temperature. This is based on the principle that the metal temperature is very close to the arithmetic mean of the inlet-air and exit-gas temperature.

Increased exit-gas temperature affects over-all efficiency of the steam-generating unit and is the main reason for some lack of interest for this type of temperature control. The fact that it is inexpensive and effective does not always offset the loss in boiler efficiency.

One other objection to this control is the great reduction in air temperature resulting from mixing cold air with hot air. This is serious for certain types of fuels—particularly those with high moisture content. To help correct this situation for primary-air purposes, a slight modification can be made as shown in Fig. 30. A crossover duct, with suitable dampers, provides control of primary-air temperature for pulverizer mills to the limit of the temperature of the hot air leaving the air preheater.

Hot-Air Recirculating. This type of temperature control provides means for mixing cold air from the forced-draft fan with hot air from the outlet of the air preheater to elevate the air-preheater inlet-air temperature. The cold-end metal temperature in turn is elevated approximately one half the rise in inlet-air temperature, based on the arithmetic mean of air and gas temperatures.

Two arrangements are available—one admits hot air directly into the forced-draft fan inlet under natural flow as in Fig. 30, and the other with a recirculating fan to control the hot-air flow as in Fig. 31. Note in the latter arrangement the unique means for distributing hot air in the cold-air stream to obtain thorough mixing and uniform air temperature.

The first arrangement is the simplest and most widely used. However, it has one disadvantage—hot air from the regenerative-type air preheater is usually contaminated and, when discharged into the forced-draft fan to mix with incoming cold air, may cause an accumulation of deposit on the fan blading. This can

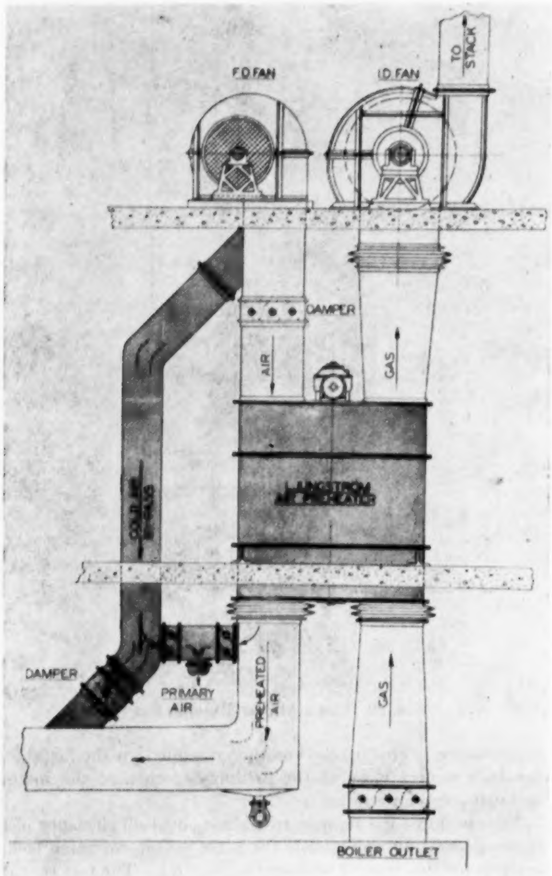

FIG. 30 COLD-AIR BY-PASSING SYSTEM WITH CONTROLLED PRIMARY AIR-TEMPERATURE DUCT

throw the fan out of balance and force the equipment out of service to clean or wash the fan.

The second arrangement overcomes the disadvantages mentioned by keeping the contaminated hot air out of the forced-draft fan. But, in doing so, it adds to the cost of the control. Obviously, the recirculating fan must be selected correctly to handle high air temperatures, and additional expense, therefore, will be involved. However, it insures wider control over the extraction and movement of the hot air. The design and construction of the recirculating fan in some measure can anticipate the condition or contamination of the hot air. Furthermore, with the recirculating fan at practically the same temperature as the hot recirculated air, there is less tendency for deposits to accumulate within the fan.

With hot-air recirculation, there is apparently less sacrifice in recovery than experienced with the cold-air by-passing. In other words, the exit-gas temperature is nearly the same as obtained without temperature control.

The explanation is in the fact that the increased quantity of air—consisting of air for combustion plus recirculated hot air—offsets the effect of a lower-temperature head, and results in practically the same heat transfer. With no change in inlet-gas quantity and temperature, the outlet-gas temperature, with or without hot-air recirculation, is nearly the same. The result is that the temperature control is obtained with practically no loss

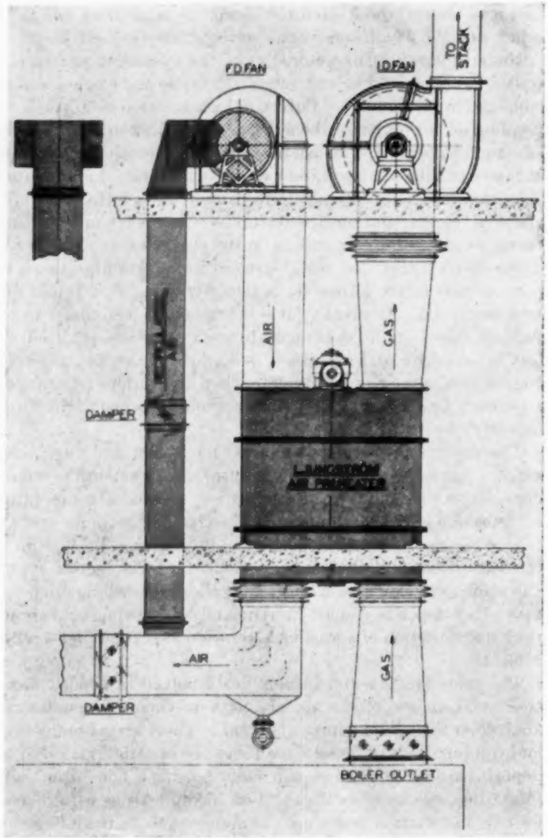

FIG. 31 HOT-AIR RECIRCULATING SYSTEM WITH AIR ADMITTED INTO FORCED-DRAFT-FAN INLET

in over-all efficiency and, for this reason, the hot-air recirculating type of temperature control is attractive.

However, the hot-air recirculating system does affect the steam-generating-plant economy. In the case of Fig. 31, increased fan power is required to handle air at elevated temperatures. Instead of handling air at room temperature, the forced-draft fan is moving air at temperatures up to 200 F. In addition, stratification resulting from nonuniform temperature distribution can upset the fan performance and increase the power input. The arrangement in Fig. 32 also increases the power demand but it is appreciably less than for the arrangement in Fig. 31. The separate recirculating fan, selected to balance the pressure loss through the air preheater, requires less power than the extra power required by the forced-draft fan when hot air is admitted into it directly.

In addition to the foregoing there is a substantial drop in outlet-air temperature. However, it is not as great as in the case of the cold-air by-pass system.

Hot-Gas By-Passing. Another type of temperature control, and one which has had little recognition, is the gas by-pass around the heating surface of the boiler, superheater, or economizer. None of these is viewed with much favor in current power-plant design practice, so there are few such installations. Fig. 33 is a typical arrangement of a gas by-pass around an economizer.

Lack of interest in this type of control is due to the loss in over-all efficiency since exit-gas temperatures will be higher than normal operation. There is also the additional expense for large

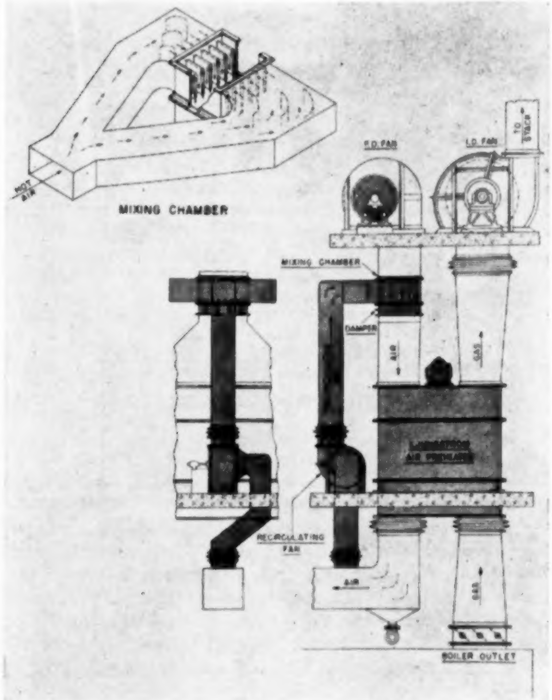

Fig. 32 Hot-Air Recirculating System With Air-Mixing Chamber After Forced-Draft Fan Outlet

ducts, dampers, and the like, to be considered. However, with gas temperatures entering the preheater at a higher level, recovery on the air side increases accordingly. The additional air temperature resulting may be advantageous for fuels with high moisture content and improve the combustion of some low-grade fuels.

Steam Air Heater

Last, but not least in importance as a means of cold-end temperature control, is the steam air heater. Installing heating coils, either at the inlet or outlet of the forced-draft fan, elevates the inlet-air temperature to the air preheater with the same effect on metal temperature as obtained with the hot-air recirculating systems. Fig. 34 is a typical arrangement with a heating coil at the forced-draft-fan inlet. Fig. 35 is an arrangement at the outlet of the fan, and is particularly interesting for the by-pass feature and control of air distribution over the heating coils.

The choice of a source of steam depends largely on the design and arrangement features of the plant. Bled steam, low-pressure service system, and low-pressure boilers, to mention a few, have been used with satisfactory results. The economics, favorable in most cases, considers the amount and cost of steam required to elevate the air temperature to the desired level, the size and cost of the heating coils, and arrangement with respect to other components of the plant.

One of the most significant advantages of this type of temperature control is that the air temperature is higher than obtained with any of the other types. However, there is some loss in over-all efficiency because the exit-gas temperature is usually higher than obtained with hot-air recirculation.

This temperature control is simple and compact. It usually fits into the duct arrangement without extensive modifications or need for special ducts and dampers.

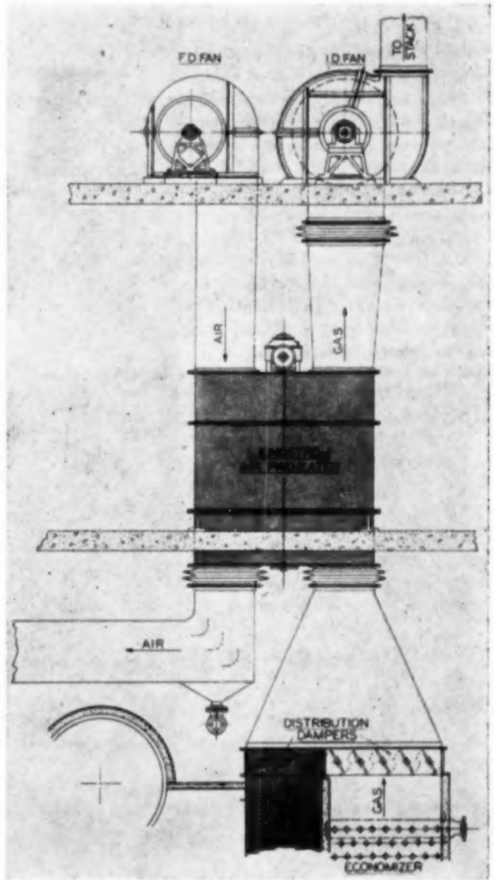

Fig. 33 Hot-Gas By-Passing System Arranged Around Economizer

General Observations

In the application of some type of temperature control, it is as much a problem to decide which one to use as to decide whether or not one is necessary to the satisfactory and continuous operation of the steam-generating unit. For a long time, cold-air by-passing and hot-air recirculation were considered basic to the control of metal temperatures in high-recovery regenerative-type air preheaters. Evidence now indicates that steam air heating is rapidly growing in prominence, and a number of such installations have been made. Since each of the systems described has its particular merits, and since all are equally effective in producing the desired metal temperature, the selection of a system must be decided in favor of the one having the best possibilities of performing under pre-established conditions significant to the design and operation of the steam-generating unit. The significant conditions might be pre-established from a consideration of the following factors:

Load and Efficiency:

1 Will the load be at a continuous high level from day to day over an extended period?

2 Will the load vary frequently and widely?

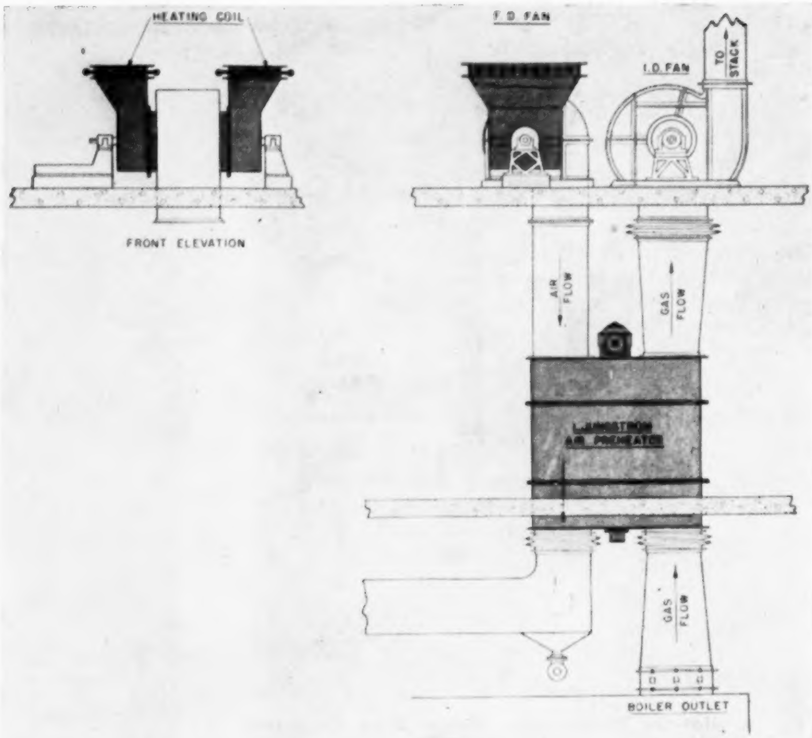

FIG. 34 (*right*) STEAM AIR HEATER AT FORCED-DRAFT-FAN INLET

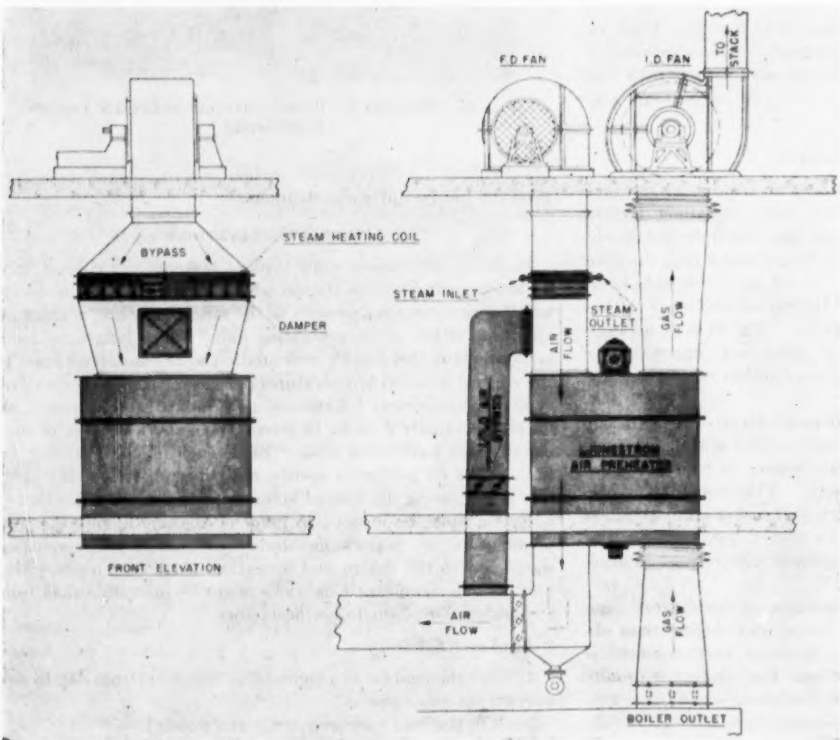

FIG. 35 (*left*) STEAM AIR HEATER AT FORCED-DRAFT-FAN OUTLET, WITH DAMPER CONTROL FOR AIR DISTRIBUTION AND INCLUDING COLD-AIR BY-PASSING SYSTEM

3 Will the unit be on bank at regular periods?
4 Will the unit be out of service frequently?
5 Can over-all efficiency be sacrificed?

Fuels:

1 What are the types of fuels to be consumed?
2 What quantity of each fuel will be consumed?
3 What is the analysis of the fuel?
4 How consistent is the fuel analysis?
5 Will the supply of fuel be adequate to assure uniform operation?
6 What will be the nature of the deposit it forms?

Ambient Air:

1 What will be the ambient-air temperature?
2 Will indoor air be used exclusively?
3 Will there be a mixture of indoor and outdoor air?
4 Will the air be heavy with entrained moisture?

If the steam-generating unit operates at maximum load continuously and there is sufficient forced-draft fan capacity and power available, then hot-air recirculation is preferred to the cold-air by-pass because the former will have little if any influence on the over-all efficiency whereas the latter will show an unfavorable high exit-gas temperature and corresponding loss in efficiency. On the other hand, if some efficiency can be sacrificed and the emphasis is placed on the need for a simple and easy to operate control, then the cold-air by-pass or the steam air heater might be worth considering.

Furthermore, if the steam-generating unit operates for appreciable periods at loads below half capacity and over-all efficiency is not important, the cold air by-pass or the steam air heater might be considered to some advantage. However, if efficiency is important, even at low loads, then hot-air recirculation might be the control to consider.

The foregoing views the selection of a temperature control from the standpoint of load and over-all efficiency only. A consideration of fuel characteristics influences mainly the decision on whether or not a temperature control is required and the range of the control. As the grade and quality of the fuel deteriorate, or as the quantity of poor fuels consumed increases, the sensitivity to dew point becomes more critical. To counteract this situation requires a temperature-control system carefully selected for size or capacity.

Fuel might influence the selection of the hot-air recirculating system in Fig. 31 if the fuel develops heavy deposits and ash in the flue gases. The hot air is then likely to be heavily contaminated and, as pointed out earlier, can unbalance the forced-draft fan.

From the standpoint of the condition of the ambient air, the influence will be in the matter of selection of the type of system and its range. If air is drawn exclusively from the boiler room, then a cold-air by-pass may be adequate. On the other hand, if outdoor air is mixed with boiler-room air, and if, in addition, the outdoor air is extremely low in temperature, or is high in entrained moisture due to weather conditions, steam air heating or hot-air recirculation may be desirable to condition the ambient air before it reaches the air-preheater heating surface.

The suggested list of conditions and typical design considerations are by no means complete. Others will come to mind as each project is studied in its design and development stages. The conclusion at this point can be that the decision for a temperature control, with respect to necessity and selection of a system, is a complex one and not easily resolved with any degree of assurance that the final decision is the correct one for this or that installation.

Combination Temperature-Control System

In view of the numerous facets of the problem of temperature control, many large installations consider a combination of cold-air by-pass with steam air heater or hot-air recirculation. Obviously, there is additional expense, but the flexibility is appreciably increased. It provides the widest range of temperature control for practically all conditions. Most important of all, it permits the use of the desirable features of each system at the most advantageous period in the operation of the steam-generating unit. Typical arrangements of combination systems are illustrated in Fig. 36 and Fig. 37.

The arrangement of a combined temperature-control system can vary in many respects to conform with the arrangement of the air preheater, forced-draft fan, ducts, and building features.

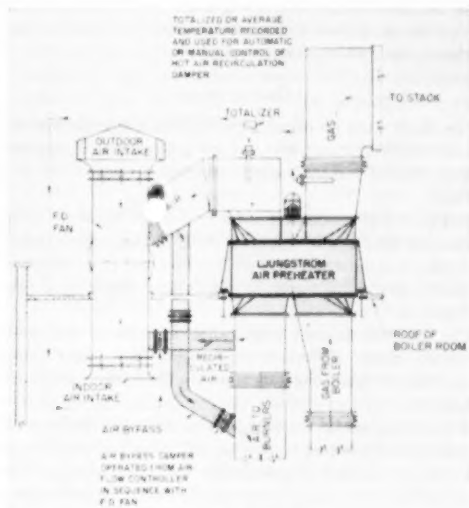

Fig. 36 Combination Cold-Air By-Passing and Hot-Air Recirculating System With Forced-Draft Fan Outdoors, and Arranged to Draw Either Indoor or Outdoor Air and Mix Both to Suit

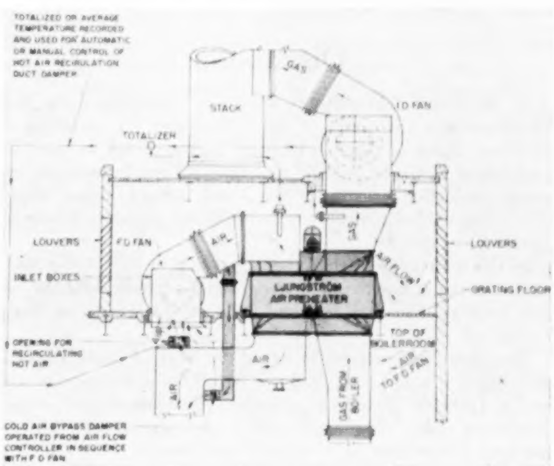

Fig. 37 Combination Cold-Air By-Passing and Hot-Air Recirculating System With Forced-Draft Fan Indoors and Drawing Warm Air From Above Boiler

Basically, however, the individual systems are the same as described earlier.

Attention is directed to one important feature, the mixing of outdoor air with boiler-room or indoor air. This feature is becoming increasingly necessary as steam-generating units become larger in size and number in a plant. To depend on indoor air entirely is often impossible and, in many cases, impractical because of the discomfort created by drafts and low temperatures on the operating level—particularly if the weather is cold and damp.

With seasonal changes in temperature and entrained moisture varying over a wide range, depending on the geographical location of the plant, the use of outdoor air creates a need for some type of temperature control or combination thereof, and the precise operation of the control with due recognition to the several factors mentioned in the foregoing. Protecting the forced-draft-fan inlets against inclement weather is a detail of no small importance and is too often overlooked.

Conclusions

While there may be other aspects influencing the operation of high-recovery regenerative-type air preheaters, it appears certain that deposit removal and temperature control are the most important.

Based on conclusions expressed in Joseph Waitkus' articles,[7] a dry cleaning medium is essential, and, in this connection, superheated steam and compressed air have proved most effective from the results of a wide range of conditions and a long period of investigation.

Under difficult deposit conditions, the use of water-washing may be required. Effective equipment and sound procedures are essential to meet the extreme conditions and should not be too objectionable nor difficult to provide.

The control of metal temperature to avoid dew-point conditions has been well developed to provide effective and reliable systems to suit the economics of practically any plant design. Most of the control systems have been applied over a sufficient length of time to prove to a reasonable degree their effectiveness.

Developments in cleaning and temperature control are by no means completed. The ever-changing picture in the steam-generating field as a result of design, fuel, materials, and so on, makes it necessary to review, amend, and revise equipment and procedures continually.

Discussion

A. Matiuk.[9] The authors are to be commended for their comprehensive treatment of the subject and for compiling an excellent digest of possible physical arrangements to meet the problem of corrosion. There is a serious need for suitable corrosion protection because of the trend toward higher steam-generating-unit efficiencies coupled with the generally downward trend of fuel quality.

In this connection, it may be interesting to outline the study made on one of our recent new installations, indicating the factors considered in that case and the economical solution finally employed.

The plant, being erected in one of the North Atlantic states, is comprised of a 132 mw, 1250 psi, 950 F turbine-generator unit and a 1,300,000 lb-per-hr pulverized bituminous-fired steam-generating unit. At times the plant may operate at extremely low-load factor because of special conditions of system loading and fuel costs. Under these conditions the plant will be subject to part-load operation and frequent shutdowns, resulting in an unusually severe air heater-corrosion problem.

The unit is designed for about 88 per cent efficiency at 1,300,000 lb-per-hr output, air heater-outlet flue-gas temperature at this load 291 F after allowing for air leakage. At 500,000-lb-per-hr output diluted outlet temperature would be 213 F.

The unit was proposed originally with combination steam-coil and hot-air-recirculation system for corrosion protection of the regenerative preheater. Subsequently, however, studies of annual operating costs and investment costs were prepared based on use of (*a*) cold-air by-pass, (*b*) hot-air recirculation, or (*c*) steam coils at the air-heater air inlet. These studies took into account all variable operating or investment-cost items, including, of course, influence of the various systems on boiler efficiency and on auxiliary power usage. Operating economics were predicated on average seasonal temperature variations coupled to the plant-loading regimen.

In the case of the steam-coil arrangement, coils were designed for a minimum ambient-air temperature of 10 F. Source of steam at higher loads would be one of the turbine-bleed points; at lower loads steam source would be a higher bleed point in order to assure adequate temperature head in the coils; and at extremely low loads reduced drum pressure would be used.

The economics of this particular situation pointed to the use of the steam-coil arrangement.

In another instance, involving a boiler of 1,150,000-lb per hr capacity, 1450 psi, 1000 F with reheat to 1000 F, gas-fired, stand-by fuel-oil-fired, located in the Southwest, studies indicated the economy of the hot-air-recirculation system. In contrast to the first case mentioned, the Southwest situation involved much higher load factor; continuous operation rather than on-off regimen; lower fuel costs; higher ambient temperatures; but generally comparable outlet-gas temperatures.

These two instances demonstrate briefly the care that must be exercised in considering the basic design and operating factors before a proper evaluation can be made. Generalization on a problem of this kind is, of course, not possible.

G. U. Parks.[10] The use of basketed-type cold-end elements has not proved entirely satisfactory. Although the basket plates are of the same corrosion-resistant alloy as the elements, they disintegrate at a more rapid rate due, probably, to the inability to have wash water penetrate the interstices between them. It has been necessary on several occasions to install new wrappers on the baskets although the elements were in good condition.

It has been our experience that it is necessary to wash the baskets before they are removed if Venezuelan oil is burned. Deposits wedge the baskets in place so that they cannot be removed without damage if dirty. Unless clean elements are removed, corrosive deposits are scattered on the premises. The handling of the dirty elements is also a hazard to the person and clothing of workers.

The authors' statement that use of soot blowers be kept at a minimum is proved by our experience. We find that washing can be reduced to a frequency of once in 10 to 12 weeks, using Venezuelan oil, if blowers are not used until differential pressure across the heater indicates it is necessary. Usually they are not used at all the first two weeks after washing, and then are used once a week, increasing to once every watch during the last week before washing.

Hot-air recirculation has not been entirely satisfactory. It has transferred substantial amounts of maintenance from the air heaters to forced-draft fans and ducts.

Even though corrosion is controlled at the cold end of the air heater by keeping exit gas at temperatures above 300 F, the prob-

[9] Mechanical Project Engineer, Ebasco Services, Inc., New York, N. Y. Assoc. Mem. ASME.

[10] Boston Edison Company, Boston, Mass.

lem persists in ductwork. The authors might initiate the desirability of coating the inside of ducts with corrosion-proof paint.

H. J. Petersen.[11] The subject of this paper is one which is of vital interest to every design engineer and operator of steam power plants. The gains in efficiency to be obtained by air preheaters are well known to all power-plant engineers. Any advance in the art which will permit lower exit-gas temperatures without excessive fouling of the elements (which is the goal of all air-preheater design), will be welcomed with open arms by all concerned.

Another feature which should be developed more fully is the design of larger air preheaters for horizontal flow. With the increasing unit capacities now taking place it would be desirable and economical to have preheaters of such design.

A typical case is the John Sevier plant of the Authority. This plant has three units each with a steam generator having a maximum rating of 1,410,000 lb of steam per hr. Each furnace is now designed with two No. $25^1/_2$-VI-48-in. air preheaters, each of which is capable of raising 759,000 lb of 80 F entering air to 532 F. At the present time there is no design for a regenerative-type air preheater for horizontal flow for that capacity. On our first two plants, which were of smaller capacity and hence used smaller air heaters, we used updraft boilers with upward gas flow through the heaters, which were installed on the fan floor above the boilers.

On our last five larger-capacity plants we used downdraft boilers with the gas flow vertically downward through the heaters. This design eliminated the fan floor above the boilers and permitted us to install the induced-draft fan outdoors. If we had been able to turn the downdraft duct of the furnace at right angles and direct the gas through horizontal preheaters we should have been able to put the air preheaters, the forced-draft fans, and the mechanical precipitators outdoors in addition to the induced-draft fans. That type of design would have saved us approximately 200,000 cu ft of building volume per unit or approximately $180,000. This saving in a multiunit plant would be very considerable.

E. B. Ripley.[12] The authors are to be congratulated on the very excellent presentation of a paper which cannot fail to be of extreme interest to any engineer concerned with the design and operation of large power plants. The paper gives definite evidence of the vast amount of development work which has been carried to a successful conclusion by the authors' company in its efforts to meet the growing problems arising from the use of fuels of poor quality, and with large amounts of moisture in the flue gases.

From the design point of view, we have been particularly interested in Part 2 of the paper, and more particularly in the discussion of the various devices which have been used to control the cold-end metal temperature. We believe that the summary of the advantages of the various methods is excellent. We feel, however, that additional emphasis should be placed on certain items, all of which are mentioned in the paper.

We have been totally unable to obtain satisfactory metal temperatures at the cold end of air heaters equipped only with a by-pass and dampers, when operating at low loads over cold week ends. This has resulted in several instances in plugging of the air heaters when the load was picked up on Monday mornings. For this reason we do not believe that a simple by-pass, even with dampers as indicated, is adequate in the neighborhood of New York City.

In any case, if by-passing alone is to be relied upon, careful provision should be made to obtain the greatest possible recirculation of air from within the plant, and a careful study of week-end operating conditions in zero weather should be made.

In connection with the use of hot-air recirculation, we believe that too-little emphasis is placed on the matter of the dust content in the recirculated hot air. There is not only the danger, which is pointed out in the paper, from unbalance in the forced-draft fans, but the very considerable nuisance value of the dust which comes with small leaks in the recirculating system. In our opinion, it is absolutely necessary to provide inlet boxes on the forced-draft fans if this system is to be used. The resulting increase in the cost of the fans is quite considerable.

For the reasons outlined, we have been strongly impelled to the use of steam air preheating. We have found it extremely difficult to make a satisfactory economic analysis of this method. Our particular difficulty has been in the inability to determine the actual performance of the air heater under varying loads and at less than maximum gas and air flows.

It appears that little if any data have been published with regard to the influence of changes in entering-air temperatures and flows upon the exit temperature of the flue gases. It would be helpful to engineers concerned with the design of these systems, if data were made available by the authors' company along these lines.

The foregoing remarks and, in fact, a great deal of the subject matter of the paper, might be understood by some to indicate that there had been an overwhelming amount of trouble in connection with the use of this type of heater when applied to obtain maximum boiler efficiency. It is a tribute to the authors' company and to the Society as a whole that such difficulties as have occurred are here brought out in the open for full and frank discussion. It is evident that, as a result of the effort and development which have been put into the study of these troubles, high efficiency can be obtained by the use of the regenerative heater without undue maintenance, and without sacrifice of availability.

E. F. Rothemich[13] and G. Parmakian.[14] This paper discusses very completely the inherent features of the regenerative air preheater in regard to efficiency and availability. The detailed discussion of current practices in operation and maintenance is of timely value to the power industry.

The paper refers to the desirability of removing solid particles before they collect on the regenerative-type heating surfaces to prevent troublesome deposits. The need for such separation, however, is also required by pulverized-coal-fired units burning high-ash coals because ash deposits dropped in air ducts and burner boxes and air-borne ash cause dust leakage and impaired burner operation. However, owing to general design considerations it is not always feasible to place dust-collecting equipment ahead of air preheaters. In many cases the size and cost of collecting equipment to handle higher-temperature gases ahead of the air preheater would be prohibitive.

Experience with tubular air heaters has indicated that the removal of coarse particles by a dust collector ahead of the air heater is not desirable from a point of view of reducing the extent of deposits. The coarse particles normally act as a scouring agent and result in a certain amount of self-cleaning. When this action is removed, the lighter particles of ash accumulate at an accelerated rate.

The recirculating arrangement, using an auxiliary fan and the

[11] Head Mechanical Engineer, Tennessee Valley Authority, Knoxville, Tenn. Mem. ASME.

[12] Mechanical Engineer, The Connecticut Light & Power Company, Berlin, Conn. Mem. ASME.

[13] Field Service Engineer, Riley Stoker Corporation, Worcester, Mass. Assoc. Mem. ASME.

[14] Mechanical Engineer, Riley Stoker Corporation. Mem. ASME.

mixing chamber, is of considerable interest. In a recuperative air-heater arrangement the absence of solid particles in the recirculated air eliminates deposits on the forced-draft-fan blading, and the simple arrangement without the added recirculation fan has proved completely satisfactory. Is the use of the auxiliary recirculation fan recommended for regenerative air preheaters when handling high-ash-content coals?

Authors' Closure

We are very appreciative of the interest indicated in our paper by those who have come forward with their comments.

We appreciate Mr. A. Matiuk's confirmation of the care to be exercised in the selection of a temperature-control system or combination. As pointed out in the paper by the author, each installation requires special consideration. A well-defined and specific procedure is practically out of the realm of possibility according to current observations and experiences. Too many factors influence the results, each of which can vary widely and uncertainly.

The statement by Mr. Parks is very interesting. The increased rate of corrosion of basket material compared to heating-surface material cannot be explained except for the possibility that the materials may not be the same. The baskets are usually fabricated of No. 10 USG material, and the cold-end heating surface from No. 18 USG material. If mild steel or OH material had been inadvertently used for the baskets instead of corrosion-resisting materials, it is very likely that the baskets would disintegrate more rapidly than the heating surface. Analysis of samples of the material in both components would be helpful in an explanation of this situation. It is quite possible, furthermore, that the corrosion-resisting materials may not have a uniform composition. The absence of certain constituents, important to the corrosion-resisting properties of the material, might explain the results reported by Mr. Parks. This situation bears further investigation.

Confirmation by Mr. Parks of the experience with reduced soot-blowing frequency and difficulties in the forced-draft fan with unbalance and dust accumulations are noted. It has been observed, in a few cases, that attention is being directed to coating the ductwork beyond the air preheater with some material or substance as protection against deterioration from corrosive conditions created by the flue gases. In most of these it seems the use of cement or ceramic materials has been considered. Painted coatings are no doubt being developed for this type of application, but they are of the character which require repeated application in order to continue the protection desired.

Mr. Petersen cites cases where the use of regenerative-type air preheaters designed for horizontal flow of gas and air would have permitted substantial savings in building costs.

The authors' company has recognized the benefits which horizontal-type air preheaters offer. Consequently, an announcement has been made to the effect that regenerative-type air preheaters for horizontal flow having equivalent features and, in the same size as those for vertical flow, are now available.

The thoughts expressed by Mr. Ripley are most appropriate to the subject of the paper. The experience cited with cold-air bypassing is typical of that encountered in a number of installations. It appears something more is necessary to meet the problem with plugging and corrosion, and that might well be a combination of hot-air recirculation or steam-air heating with cold-air by-passing. In other words, cold-air by-passing alone is not the full answer for the particular installations in mind.

The need for performance at varying loads, and at less than maximum air and gas flow, can be developed theoretically from basic calculations for the regenerative-type air preheater. A guide to selection of cold-end temperatures for various fuels has been published in a paper[15] by Hilmer Karlsson and W. E. Hammond.

In the second and third paragraphs of their discussion, Messrs. Rothemich and Parmakian question the desirability of removing solid particles from the gas stream ahead of the air preheater. They refer to their experience with tubular air heaters which indicates that the coarser particles act as scouring agents, helping to prevent in some measure the accumulation of fine particles on the cold-end surfaces.

The experience of the authors and their associates with the operation of regenerative-type air preheaters does not indicate that the presence of coarser particles in the gas stream of the average installation helps appreciably to prevent the accumulation of cold-end deposits. On the other hand, the removal of all particles ahead of the air preheater would amount to a direct approach to the elimination of the troublesome deposit.

As a response to the valued discussion by Messrs. Rothemich and Parmakian, it might be stated that a separate fan arrangement, such as illustrated in Fig. 32, is the best answer for a temperature-control system when the fuel is of high-ash content. What little ash does get into the air stream, and eventually into the separate recirculating fan, should not create any problem.

The authors express their appreciation to those who submitted discussion for their interest and for the valuable information offered; also, to those who gave us permission to make reference to their work. The help and encouragement given by our associates is gratefully acknowledged.

[15] "Air-Preheater Design as Affected by Fuel Characteristics," by Hilmer Karlsson and W. E. Hammond, Trans. ASME, vol. 75, 1953, pp. 711–722.

The Controlled-Circulation Boiler

By W. H. Armacost,[1] New York, N. Y.

From the standpoint of circulation there are two general types of boilers in operation in this country. These are natural circulation based on the conventional "thermal circulation head," and controlled circulation based on the use of a pump to distribute and circulate the water through the heat-absorption areas. The author's company supplies both types, having pioneered in the design and development of natural-circulation as well as controlled-circulation boilers. With the trend toward larger high-pressure units, industry is directing more and more attention to the controlled-circulation type. Therefore it appears desirable to summarize the information regarding these boilers. This paper deals largely with (*a*) the development of these boilers, (*b*) presently preferred designs, (*c*) operating features, results, and characteristics, and (*d*) brief reference to installations in this country.

Controlled Circulation

In the early days boiler designers had ample tolerance "to play with" in setting up circulation rates. This resulted from the large difference between the density of water and steam at relatively low pressures. In fact, in many cases it was necessary to retard the circulation rate to reduce turbulence in the drums. As pressures and heat inputs increased, more and more design attention was required and it was necessary to elevate the furnace-boiler system to obtain the necessary circulating head. One approach to this problem has been the development of controlled-circulation boilers.

Actually, there are only a few fundamental differences between controlled and natural-circulation boilers. A typical design of controlled-circulation boiler, as shown in Fig. 1, will make this clear. It will be noted that a steam-water drum is employed and a mixture of steam and water from the steam-generating tubes and feedwater from the economizer enters the drum. Small downtake tubes or large pipes carry the excess boiler water, after it has mixed with the feedwater, back to the entrance of the steam-generating circuits, and outlet tubes from the boiler drum deliver the separated steam to the superheater. All of these operations are quite similar to the conventional natural-circulation boiler, the chief differences being that pumps are used to "force" the circulation of water through the evaporative section of the boiler and orifices are used to "control" its distribution. More specifically, by controlled circulation is meant those features which permit the designer to proportion the water supply to a furnace wall, or boiler section, or to individual tubes in accordance with predetermined requirements, or to change the total flow or the distribution within limits at any subsequent time. This is accomplished by orifices in the inlet parts of the steam-generating circuits.

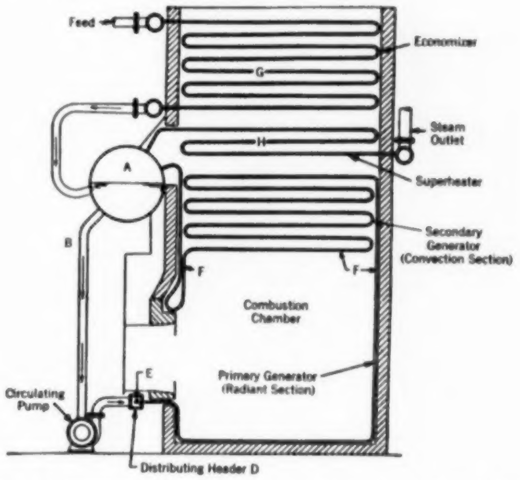

Fig. 1 Schematic Arrangement of Controlled-Circulation Boiler

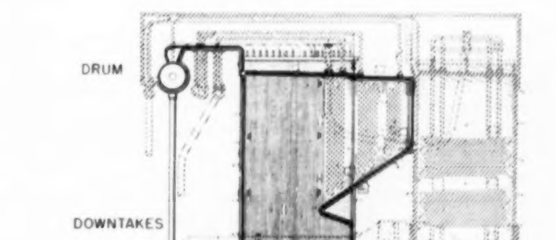

Fig. 2 Arrangement of Controlled Circulation at Chesterfield Station, Virginia Electric and Power Company

The controlled-circulation units employed in this country have been of two types. The first, Fig. 2, used in the early boilers, consists of one drum, waterwalls, superheater, reheater, and economizer as in any conventional boiler, but the water is distributed from the downtakes to a suction manifold through the pumps to a ring header, which supplies the entire waterwall through individual waterwall headers. In the ring header are

[1] Vice-President, Charge of Engineering, Combustion Engineering Inc. Fellow ASME.

Contributed by the Power Division and presented at a joint session with the Metals Engineering and Fuels Division, Research Committee on Furnace Performace Factors, High Temperature Steam Generation, and Joint ASTM-ASME Research Committee on Effect of Temperature on the Properties of Metals at the Annual Meeting, New York, N. Y., November 29–December 4, 1953, of The American Society of Mechanical Engineers.

 Manuscript received at ASME Headquarters, August 5, 1953. Paper No. 53—A-91.

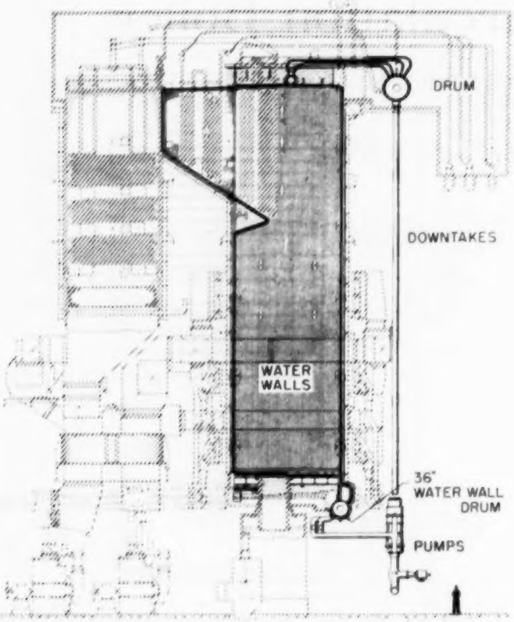

Fig. 3 Arrangement of Controlled Circulation at Kearny Station, Public Service Electric and Gas Company

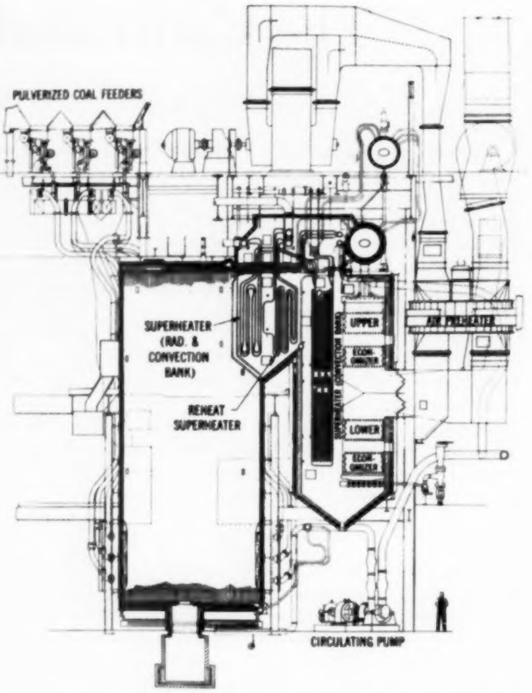

Fig. 4 General Arrangement of First High-Pressure Controlled-Circulation Boiler in the United States—Somerset Station, Montaup Electric Company

four master strainers. Distribution of the "strained water" to the waterwalls is controlled by orifice plates inside of the headers, each two orifice plates being protected by a strainer. In addition to the regular waterwall circuit, there is a second circuit, referred to as a panel wall, which cools the area in the vicinity of the reheater. The panel wall is supplied with water directly from the discharge header and has separate strainers. The steam-and-water mixture flows into the single drum where the steam is separated by means of turboseparators and from thence to the first or low-temperature section of the superheater.

The second type of controlled-circulation unit and that used in later installations, Fig. 3, is somewhat simpler than the first in that no headers or master strainers are employed. Instead, one or two distribution drums are used at the bottom of the unit. These are fed from the pump-discharge manifold and supply the waterwalls through orifice plates inside the drums. This makes for easier maintenance and general over-all simplicity.

One of the features of controlled circulation is that small tubes are used. These range from 1 in. to $1\frac{5}{8}$ in. OD. However, the controlled-circulation principle could be applied to a boiler with large tubes, but a great amount of water would have to be circulated to obtain satisfactory water velocities. To cut down on the amount of water circulated and for reasons pointed out later, the small tubes referred to are used.

For a more detailed consideration of controlled-circulation features, the reader is referred to the tabulation in the Appendix.

Early Installations

The first high-pressure boiler in the United States utilizing controlled circulation was installed at the generating plant of Montaup Electric Company at Somerset, Mass., Fig. 4. Several papers have discussed this installation, its early operation, and other characteristics (1, 2, 3, 4, 5, 6, 7).[2]

The Montaup boiler was completed in 1942. It was designed for 2000 psi drum pressure and a steam temperature of 960 F at the superheater outlet. It supplied 650,000 lb of steam per hr to a 25,000-kw topping turbine, the exhaust being reheated to 750 F. This was the first large boiler in which the furnace comprised all of the evaporative surface. The reasons for adopting controlled circulation at Montaup also have been discussed in detail and may be summarized by stating that the objective was to obtain the greatest possible amount of topping power from a given space in an existing building and within a definite appropriation.

During the early operation of the Montaup boiler unforeseen difficulties developed in boiler-water conditions. Similar difficulties arose with a "natural" or thermal circulation boiler, installed about the same time. In both cases, precipitation of salts occurred owing to the fact that the solubility of phosphate and sulphate decreases as the temperature rises. In the case of Montaup the difficulty was aggravated by condenser leakage which built up a considerable concentration of "soluble salts" in the boiler water. Marked improvement resulted from substitution of potassium water-treating chemicals for the sodium ones previously used. In addition to this, the ultimate solution of the problem involved close control of the addition of treating chemicals, lower excess of treating chemicals, and maintenance of condenser leakage at a minimum.

Another difficulty at Montaup was with the sealing of the circulating pumps. At no time was there failure of circulation or boiler outage due to pumps, but the glands had to be redesigned and rebuilt to hold down leakage.

A feature in the construction of the Montaup boiler was the use of welded connections for joining tubes to strength-welded nozzles on the headers and drums. A typical arrangement of the reinforced nozzles is shown in Fig. 5. This arrangement

[2] Numbers in parentheses refer to Bibliography at end of paper.

Fig. 5 Kearny Drum Showing Welded Reinforced Nozzles

eliminates rolled or mechanical joints and therefore danger of leaks. This is of extreme importance in the case of high-pressure boilers and the practice is being followed in present-day controlled-circulation units—also where it is applicable in natural-circulation units.

During the intervening years the early difficulties have been overcome; for the past several years the availability of this unit has equaled or exceeded the average reported for boilers of comparable size and operating conditions. Needless to say, the experiences gained have been invaluable in the design and development of present-day controlled-circulation boilers.

Later Installations

The first postwar controlled-circulation reheat unit to go into operation was at the Chesterfield Station of the Virginia Electric and Power Company, Fig. 6. Its capacity is 750,000 lb per hr at 1500 psi with 1000 F primary steam temperature and 1000 F reheat temperature. Note that waterwalls comprise the entire evaporation surface. Water from the drum passes through downcomers to the circulating pumps and thence to headers where it is distributed to the tubes. This boiler employs the lower distribution-header arrangement, as in Montaup, but an improved orifice arrangement was installed. Orifice plugs were not used for each tube; rather an orifice holder and screen were installed for each two or three tubes through a seal-welded handhole. This development greatly simplified the installation and maintenance of the units.

Another development in the case of the Chesterfield boiler concerned the circulating pumps. Based on experience at Montaup, pumps of the injection type were developed so that mechanical seals could be installed at a later date. At the present time satisfactory seals are in use to prevent sealing water entering the boiler. Seals are being developed to prevent leakage to atmosphere. For additional discussion of this subject see the section entitled Circulating Pumps.

Still another development involved the drum internals. Based on the experience at Montaup, a "centrifugal-type" separator was devised. The details of this equipment are given in the section entitled Turbo-Steam Separator Development. The equipment was previously found to be so efficient that no dry drum was included in the Chesterfield boiler. Operating experiences at Chesterfield have indicated satisfactory steam purity (see "Controlled Circulation at Chesterfield," by Crossan and Ryan, reference 8).

The unit recently put into operation at the Kearny Station of the Public Service Electric and Gas Company is typical of current installations of controlled-circulation boilers. This unit has a continuous capacity of 955,000 lb of steam per hr at 2650 psi. Primary steam temperature is 1100 F and reheat temperature, 1050 F. Fig. 7 gives further information regarding this boiler.

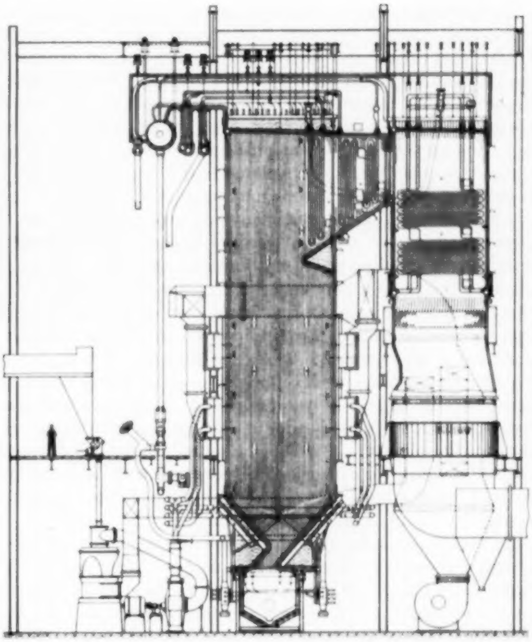

Fig. 6 Sectional Side Arrangement Controlled-Circulation Boiler—Chesterfield Station, Virginia Electric and Power Co.

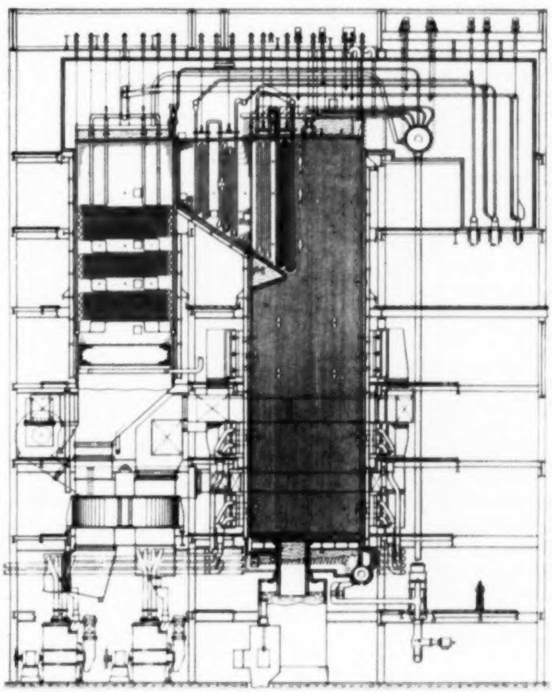

Fig. 7 Sectional Side Arrangement Controlled-Circulation Boiler—Kearny Station, Public Service Electric and Gas Company

In addition to further developments on steam purification and circulating pumps, this unit has several novel advancements. In the first place, the boiler-water circulating or distribution system was improved and simplified greatly. Instead of using headers and strainers, distribution drums are installed at the bottom of the unit, as shown in Figs. 3 and 19. These are fed from the pump-discharge manifold and supply the waterwalls through screens and orifice plates inside the drums. Such a system is much simpler from a maintenance standpoint.

Also, considerable improvement has been made in downtake piping and valves. In the case of Montaup the circulating pumps were installed on the floor below the unit. The supply pipes to the pumps were connected to a common header which received its water supply through two pipes connected to the bottom of the boiler drum. Provision for expansion was obtained by a system of pipe bends at the rear of the units. Discharge lines from all three pumps were connected to a common header. Expansion in the latter case was absorbed in the loops of tubing used to connect the discharge header to the main distributing header at the bottom of the unit. An objection to this scheme is the necessity of providing for expansion in large-diameter heavy-wall pipes without causing high stresses in the pipe connection to the pump casing.

An improved arrangement of pump supporting, downtake piping, pumps and valves, and that used in current installations, is shown in Fig. 8. Water is supplied to the common downtake header through four pipes connected to the bottom of the drum. The three pumps are mounted on the downtake header through the pump intake located at the bottom. Discharge lines from all three pumps connect to a common discharge header which, in turn, connects with the main distributing headers of the waterwalls. In this manner, piping and expansion loops are avoided since the pumps are not attached to the building structure.

Each pump is equipped with a motor-operated inlet valve with screwed down-stop check on the outlet. Normally, two pumps are in operation and a third is for stand-by. Provisions are made for maintaining all piping and the idle pump "hot" by 1-in. recirculating lines, through which hot water is recirculated continuously by utilizing the differential head across the pumps. This eliminates stresses caused by expansion.

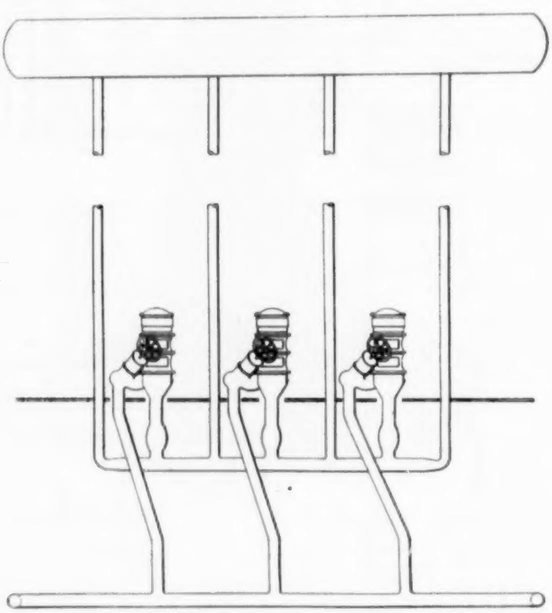

Fig. 8 Arrangement of Circulating Pumps and Piping of Controlled-Circulation Boilers

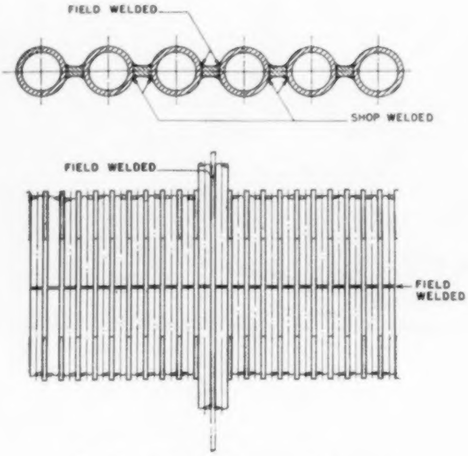

Fig. 9 Welded Waterwall Panels

Another feature of this boiler is the panel-wall construction. Panels are possible, due to uniform metal temperatures obtained with controlled circulation. Such a typical arrangement is shown in Fig. 9. Use of small tubes, $1^1/_4$ in. to $1^1/_2$ in. OD made possible by controlled circulation, greatly facilitate the wall construction; that is, these tubes readily may be made into panels and are easy to form into definite shapes, for example, around doors, inspection holes, and so on (see section entitled Welded Walls for more information on this subject).

Turbo-Steam Separator Development

In the case of the Montaup boiler, it was desired to have steam of maximum purity. Consequently, the design called for a dry drum. The drum internals for both the steam and the dry drum were described in a previous paper. When it was found that the steam purity was dependent on water level, replacement internals were installed. These gave a purity well within the guarantee. However, it was realized that still greater steam purity could be obtained by taking advantage of the relatively great pressure drop available on controlled-circulation boilers. After considerable development work, a greatly improved system resulted.

The steam-drum internals finally adopted and used on current controlled-circulation boilers consists of a steam-water mixture collecting compartment formed by internal baffles, with turbo-steam separators uniformly spaced and mounted on the collecting box or compartment. A symmetrical arrangement can be employed so that there are two rows of the turbo separators with a common internal baffle and a collecting box on either side of the drum. A typical arrangement is shown in Fig. 10. The operation of the steam-purifying equipment is as follows:

Steam-water mixture enters the top of the drum through nozzles discharging into an annular space formed by internal baffles. Flow of the mixture is directed downward behind symmetrical baffles around the entire drum surface, maintaining a uniform drum-wall temperature, and then into the turbo separators. The latter contain a center core and vanes which give the mixture a spinning or centrifugal motion, thereby throwing the water to the outer edge of the inner tube. Directly above the directional vanes and cores there is a skim-off lip which directs the water over the top of the inner tube and thence

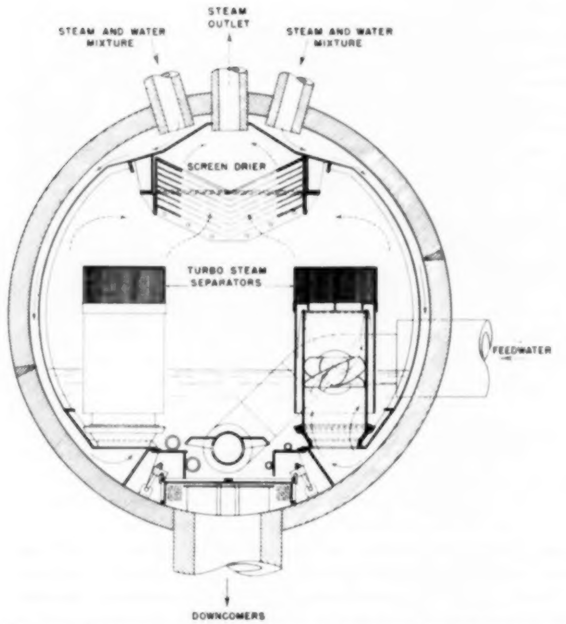

FIG. 10 SECTION OF DRUM SHOWING CYCLONE SEPARATOR AND DRUM INTERNALS

through the annular space to the drum. This is the primary separation stage. The relatively dry steam then passes through two opposed banks of closely spaced corrugated plates, which changes the direction of the steam many times and throws out much of the remaining water. This is the secondary separation stage. The third and final stage of purification is accomplished in the screen drier.

Steam-drum internals of this type were used first in controlled-circulation boilers built for the U. S. Navy Bureau of Ships. The units were checked thoroughly at the Naval Boiler and Turbine Laboratory at the Philadelphia Naval Shipyard. Excellent results were obtained.

In 1950, in order to test internals of this design in a large high-pressure boiler, a similar set of internals was installed in the controlled-circulation boiler at Montaup. Test results showed less than 0.5 ppm of solids in the steam when 960 ppm solids were present in the boiler water. Also, it was found that variation of water level had little if any effect on the steam purity. Furthermore, it was found that the dry drum was not required; therefore this is eliminated in current designs. Test results on recently installed controlled-circulation boilers show a solids content in the steam of less than 0.25 ppm. These data are backed by the fact that there has been no loss of capacity of turbines supplied with steam from these units.

A secondary advantage of the turbo-steam separator unit is that no "washing operation" is involved. Consequently, less steam condenses in the drum with the result that less water has to be circulated. Therefore a smaller drum can be used and the piping and pump for circulating the water may be smaller. This results in considerable saving in weight, especially since no dry drum is required.

CIRCULATING PUMPS

One of the major developments, in fact the one that made controlled circulation possible, concerned the circulating pumps. Generally three pumps are used, two for service and the third for stand-by. For general arrangement of pumps see Fig. 11.

The pumps raise the pressure of the water from the drum about 40 psi. This is sufficient to overcome the resistance of the orifice and the circuit proper. Distribution of the water is controlled by selection of the orifice size in accordance with calculated or desired requirements.

Several general types of pumps have been used. In no case has there been any real problem in preventing injection water from entering the boiler. This has been accomplished by using a low differential-pressure mechanical seal. As mentioned, some trouble has been experienced in developing a satisfactory mechanical seal between boiler pressure and atmospheric pressure.

In one type of pump a packing gland is supplemented by a water labyrinth which reduces the pressure stepwise until an ordinary packing gland can be used. Another type uses two impellers, one to circulate the boiler water and the other to circulate cooling water in a closed circuit so as to maintain a uniform temperature for the mechanical seal. It is possible to switch to injection sealing in case of mechanical seal failure.

As mentioned, at present pumps are available having satisfactory seals to prevent injection water entering the boiler through the pump. A development program is under way to obtain a seal of the mechanical type that will satisfactorily seal against the drop from boiler pressure to atmospheric. The current pumps, which are of the injection type, are designed so that mechanical seals can be installed.

The pertinent features of using circulating pumps in connection with controlled circulation are given in the Appendix. That involving starting up and shutting down a boiler warrants additional emphasis. If two pumps are required to handle the full capacity of the unit, they both may be started prior to firing or the second may be placed in operation when more circulation is required.

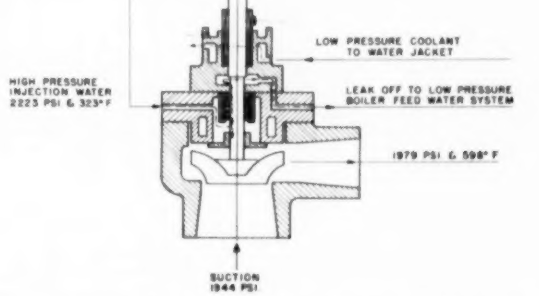

FIG. 11 SCHEMATIC ARRANGEMENT OF CIRCULATING-PUMP SEAL

Except for starting the circulating pumps, the procedure for putting a boiler in operation is the same as for a natural-circulation boiler. The advantages of having the water circulating during the starting-up period are obvious; that is, temperatures are maintained even throughout the unit which permits rapid starting. The same applies to shutting down the unit, at which time the pumps continue to operate and thus maintain even temperatures. Steaming of the economizer may be prevented by providing a connection between the circulating pump and the economizer-inlet header.

Owing to the importance of water circulation at all times, definite steps have been taken to "protect the system" in case of failure of a pump. An interlock-manometer arrangement is connected across the suction and discharge headers of the pumps

The manometer has a magnetic float which rises and falls with the differential pressure across the headers. Attached to the manometer are permanent-magnet-activated mercury switches, which are drawn in as the float rises. There are three of these switches, which are set at low, medium, and high differential; for example, 8 psi, 20 psi, and 40 psi. These switches activate lights on the control board. When all three are "lit" there is over 40 psi differential between the headers. This indicates that there are three pumps in service. When two lights are lit there is about 20 psi differential which is that developed by two pumps. When only one light is lit there is about 8 psi differential, meaning that only one pump is running; and an alarm is sounded so that load will be reduced manually to approximately 60 per cent. Actually, the one pump will circulate sufficient water at normal loads to prevent damage to the boiler for a short period of time. When no lights are lit, no pumps are running and all fuel is cut off to the unit by automatic firing relay.

Owing to the reliability of the current pumps and the use of the warning-alarm system, there is no longer any apprehension about the circulating features.

Use of Small-Diameter Tubes

Owing to the positive and controlled circulation of water in controlled-circulation boilers, and the fact that relatively low circulation ratios of the order of 4 or 5 to 1 are used for high pressures, it is possible to use small tubes, that is, of the order of $1^1/_4$ in. to $1^1/_2$ in. OD. Many advantages arise from the smaller tubes, the most important being listed in the Appendix. It will be noted that the weight and thickness of the tube are reduced greatly. As would be expected, the velocity is much greater through the tube. Since a thin tube is used, the temperature of the tube wall is low and as a result thermal and, therefore, total stress in the tubes is less. This results in a greater over-all "real" safety factor. This is illustrated in Table 1 which compares $1^1/_2$-in. and 3-in. tubes for 2650 psi.

TABLE 1 COMPARISON DATA FOR $1^1/_2$-IN. AND 3-IN. BOILER TUBES AT 2650 PSI

Tube diameter, in	3	$1^1/_2$
Wall thickness, in	0.34	0.165
Velocity ratio	1	1.96
Tube-weight ratio	1	0.49
Water weight ratio	1	0.51
Wall thickness, min and max., in.	0.34 and 0.435	0.165 and 0.219
Heat absorption, Btu/sq ft/hr	100000	100000
Temperature gradient wall, deg F	126	63
Temperature gradient film, deg F	10	10
Saturation temperature, deg F	679	679
Hot-face tube temperature, deg F	815	752

Referring more specifically to high-pressure conditions, as pressures are increased tube-wall thickness increases and, as a result of the thicker tube metal, there is a greater temperature difference or drop through the metal. This, together with the fact that saturation temperature increases with pressure, means that the tube skin temperature may become excessive and lead to danger of failure. The advantage of a small tube in these respects is obvious from the data in Table 1 and Fig. 12.

The temperature drop through the wall for a given tube thickness, of course, will depend on the heat-absorption rate. Temperature drops of more than 100 deg F may well exist. The higher metal temperature reduces the strength of the metal and requires an increase in thickness of the tube. This increases the temperature drop and a "vicious cycle" results.

The thermal stresses so developed may become appreciable as compared to the stress resulting from pressure inside the tube. Therefore, if a design is based on the ASME Boiler Code, which is based on pressure stress only, the desired factor of safety may not result; that is, the combined pressure and temperature stress

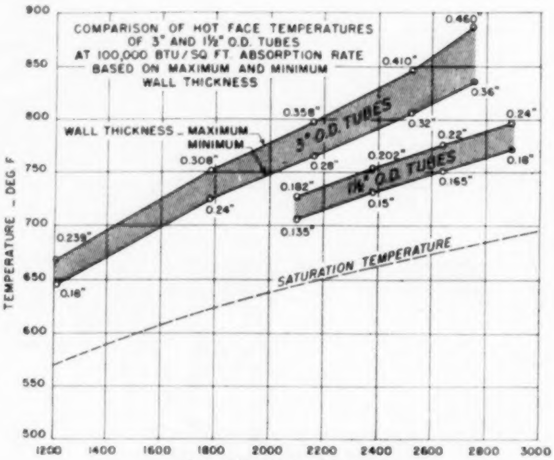

Fig. 12 Comparison of Tube Hot-Face Temperatures

may greatly exceed that for pressure alone. Table 1 illustrates this fact and again the advantage of a smaller tube is obvious. Also, it should be borne in mind that Code tube-metal thickness is the minimum requirement. Manufacturing tolerances on hot-finished tubes may be as much as 33 per cent over this minimum Thus, in the thicker sections of the tube, the temperature drop is greater and consequently the tube skin temperatures are higher, with the probability of higher thermal stresses being developed.

Some idea of the importance of this fact is shown in Fig. 12 where the upper curve shows tube skin temperatures for maximum wall thickness and the lower curve those for minimum wall thickness. Note that for an operating pressure of 2650 psi, using the minimum-thickness curve, the tube skin temperature for a 3-in. tube is 820 F, whereas that for a $1^1/_2$-in. tube it is only 752 F. Using the maximum-thickness curve the value for a 3-in. tube is 868 F whereas for a $1^1/_2$-in. tube it is only 777 F. Again the advantage of a smaller tube is evident.

Referring once more to tube diameters, the data in Table 1 on tube and water weight emphasize the advantages of small tubes. Note that in the case of a wall composed of $1^1/_2$-in. tubes, the tube weight is only 49 per cent as much as in the case of 3-in. tubes. The weight of water in the $1^1/_2$-in. tubes is only 51 per cent as much as that in the 3-in. tubes. The weight saved means less load on the foundations and reduced size and weight of structural supports. Owing to the smaller tubes, much less weld metal need be deposited in erection. A further advantage of the lower weight of the tube metal and water is that in starting up considerably less fuel is used and the boiler can be put on the line more quickly. For the same reason it can be shut down more quickly.

Still other advantages of small tubes are that they can be bent more easily to fit around burners, doors, soot blowers, and so on. They also are more readily butt-welded in the field because, even though there are more tubes to weld, the amount of weld metal required is much less.

Finally, a furnace wall made of small-diameter tubes presents a more nearly plane surface than one with larger tubes. This is advantageous from the standpoint of slag removal, as well as for the arrangement of wall backing and insulation.

A possible disadvantage of the small tubes is lack of structural strength in the wall. This, however, is readily offset by the use of girth members at closer intervals.

Welded Walls

A feature of the Kearny and some of the later boilers is the welded panel-wall construction. The Kearny boiler is designed for pressurized operation although induced-draft fans are provided in case suction operation is required. Owing to the even temperature in the walls resulting from controlled circulation, this welded design was made possible; it was facilitated somewhat by the small tubes used. These tubes were shop-welded into panels. Fig. 9 shows the general tube-bar construction, and Fig. 13 shows the sections by the different markings of the installed walls at Kearny. Employment of the panel construction eliminates the use of a steel casing for pressurized furnaces or making a gastight setting on suction firing. These advantages are obvious.

Considerable development and research work were carried out in connection with the panel-wall construction. The work especially was planned to determine the stability of the panel under severe thermal stress and to devise a satisfactory welding technique for those tubes which are aluminized.

The design of the test equipment was such as to simulate the condition that would result from uneven or increased heat absorption. Such a condition might result from slag falling off a tube surface and thus lead to increased heat absorption. Would this cause a considerable temperature gradient across the wall and result in high stresses and strains? If so, it would be desirable to determine the effect of these on a panel-type wall.

The waterwall panel-heater arrangement used in the test is shown in Fig. 14. It consisted of twenty-four $1^5/_8$-in-OD 0.165 MWT carbon-steel tubes on 2-in. centers with $^3/_8$-in. square bars welded between the tubes. The tube ends were rolled into an inlet and outlet header. A distribution orifice in each tube equalized the flow through the tubes.

The panel assembly, consisting of the tube bank, headers, and upper discharge pipe, was supported by the inlet and discharge in such a manner that it was not restrained from growth resulting from thermal expansion.

In order to heat the waterwall panel a combination of gas and oil-firing was employed. The gas burner, 44 in. × 84 in., was used to heat all of the panel except the 1-ft × 2-ft section near the center of the panel. This section, to which the heat was varied, was heated by an oil burner and at high heat-absorption rates the combustion air was supplemented by oxygen.

The waterwall-panel tube and bar temperatures were measured by means of thermocouples. Two methods were used to determine the heat absorbed. During runs when no steam was generated, the temperature rise of the water and the amount of water flow were used to calculate the heat flux. When steam was generated, the flux was calculated from data taken from calorimeters connected to the discharge pipes.

Panel deflections during operation were made by means of gages attached to the rear face.

Runs were made with various combinations of heating and at various heat rates. Most of the tests were conducted with local heating at the 1-ft × 2-ft rectangle at the center of the panel. Heat-absorption rates up to 244,000 Btu per sq ft per hr were obtained. During some of the runs, cycling was followed to introduce thermal shock. In these cases a temperature gradient was set up across the panel far in excess of that which would be anticipated in actual installations. The maximum distortion of the panel was 0.10 in. After the tests metallurgical and visual examinations of the panel showed no harmful effects. From these severe tests it may be concluded that the over-all design of the panel wall was satisfactory from the standpoints referred to.

In addition to the panel-wall features, there are others which warrant mention. These are easier handling during shipping and easier storage as the sections may be piled. In the actual construction operation there are many advantages, such as rapid closing of the wall using 4-ft × 40-ft panels, less time for welding as the panels are welded as a unit, and so on.

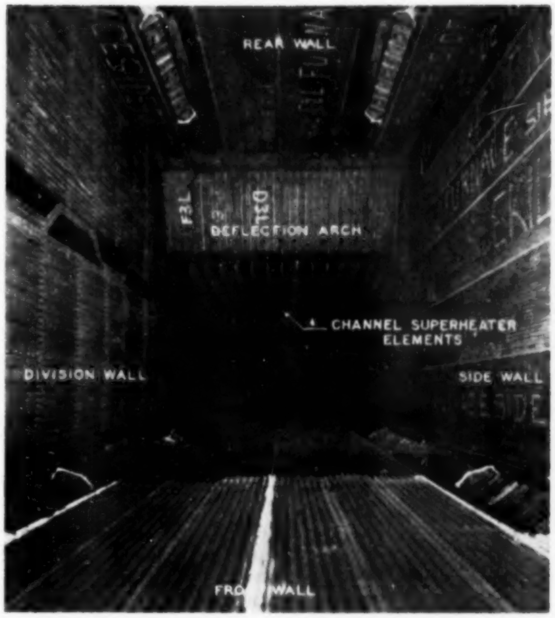

Fig. 13 Interior View of Kearny Boiler Showing Arrangement Panel, Waterwall Tubes, and Channel Superheater

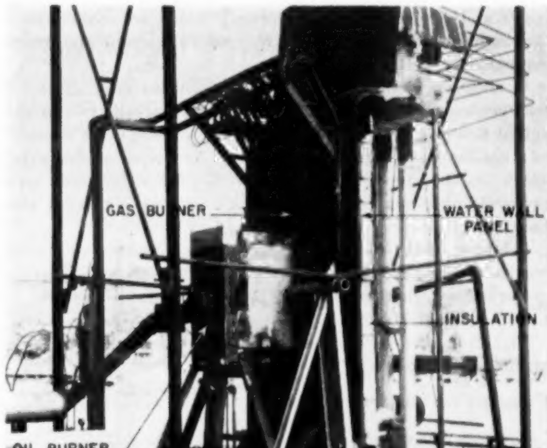

Fig. 14 Test Assembly Used in Development of Panel Walls

Operating Data and Performance

Fig. 15 shows the profile of the furnace walls on the Chesterfield boiler and just below this profile is shown the maximum tube temperatures recorded in reference to saturated temperatures in the tubes.

Fig. 16 shows the profile of the furnace walls on the Kearny

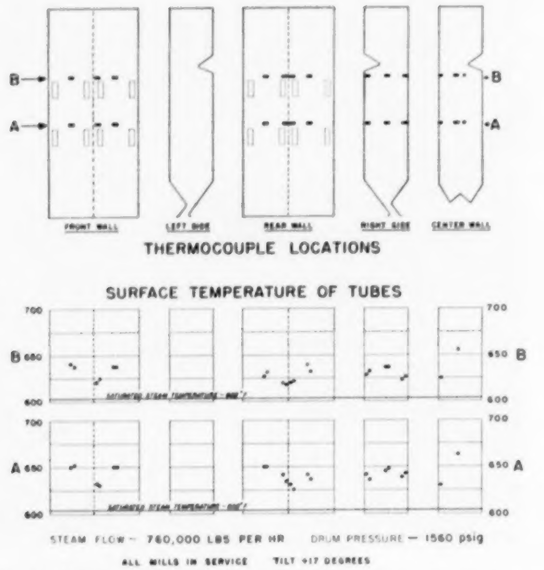

Fig. 15 Virginia Electric and Power Company—Chesterfield Station Unit No. 3

boiler and the resulting temperatures which are higher due to the higher saturated temperature resulting from the greater pressure within the tubes.

In addition to the thermocouples, calibrated pitot tubes with manometers were installed in representative circuits to check the actual flows against those expected. The flows were measured in a similar manner in the four downcomer pipes as this gave a check on the circulating performance. All performance measurements obtained came within the prescribed limits for these boilers.

It is interesting to compare expected performance with actual results. Therefore, in Fig. 17 the solid lines show the expected performance, whereas the dots show the actual results obtained at Chesterfield.

Fig. 18 shows the expected in relation to actual results obtained on the Kearny boiler.

Summary of Utility Installations of Controlled-Circulation Boilers

The following units either are in operation or will be in operation by the time this paper is presented or soon thereafter. For completeness the units previously discussed in this paper are listed again. It will be noted that the design pressures range from 1760 psi to 2650 psi.

Somerset Station, Montaup Electric Company—650,000 lb of steam per hr at 2000 psi, 960 F to a topping turbine. Reheat of the exhaust (400 psi) to 760 F. This installation was discussed in previous publications (1, 2).

Chesterfield Station, Virginia Electric and Power Company—750,000 lb of steam at 1670 psi, 1000 F primary steam temperature and 1000 F reheat. This is the lowest pressure controlled-circulation utility boiler to date, Fig. 6. Note that the furnace is arranged with center wall and tangential firing with steam and reheat temperatures controlled by tilting burners; this installation is discussed in the paper by Crossan and Ryan (8).

Portsmouth Station, Virginia Electric and Power Company—same as Chesterfield Station.

Kearny Station, Public Service Electric and Gas Company—two 1,055,000 lb steam per hr at 2650 psi, 1100 F primary steam

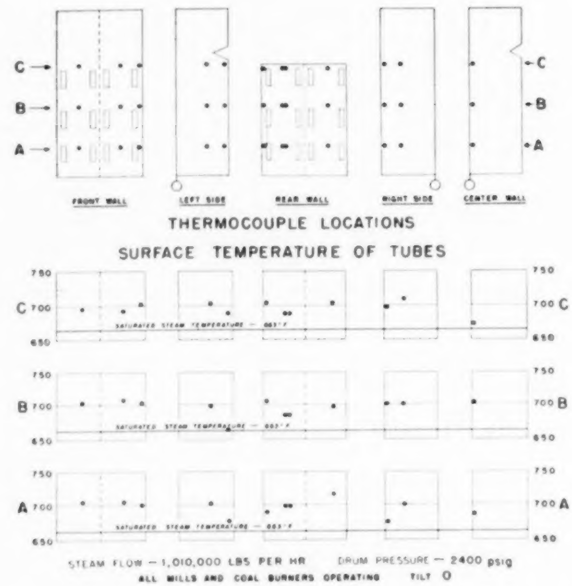

Fig. 16 Public Service Electric and Gas Company of New Jersey—Kearny Steam Generating Station Unit No. 7

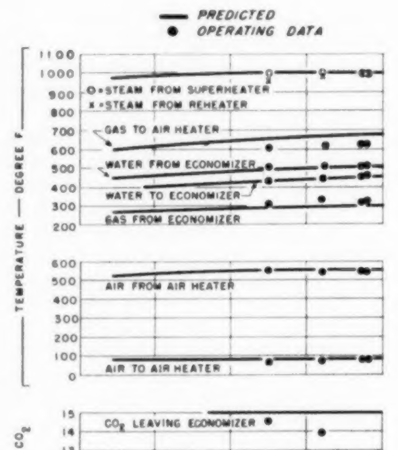

Fig. 17 Virginia Electric and Power Company—Chesterfield Station Unit No. 3

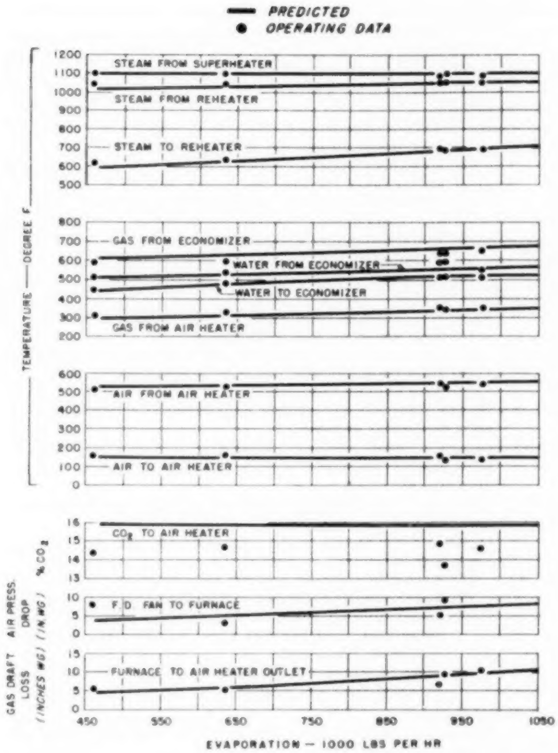

Fig. 18 Public Service Electric and Gas Company of New Jearsey—Kearny Steam Generating Station Unit No. 7

temperature and 1050 F reheat. This is the highest pressure controlled-circulation boiler to date, Fig. 7. Note that the furnace is of panel-wall construction. Another feature of this installation is the use of gas recirculation for control of steam and reheat temperature. Fig. 7 shows the gas-recirculating fan, duct, nozzles, and so on. This installation is described in the paper by Fairchild (9).

Etiwanda Station, Southern California Edison Company—two 920,000 lb of steam per hr at 2100 psi, 1000 F primary steam temperature and 1000 F reheat. This unit is of the low-head type (precaution against earthquakes). Its design was facilitated by the positive circulation resulting from controlled circulation.

Oak Creek Station, Wisconsin Electric Power Company—two 795,000 lb of steam per hr at 1775 psi (No. 1) and 2025 psi (No. 2), 1004 F primary steam temperature and 1000 F reheat. This unit differs from the previous ones in that radiant reheaters and combination radiant-and-convection superheaters are incorporated; burners are of the vertical type. A system of water-cooled header supports is used in the convection steam-generating sections and in the economizer. Water under controlled circulation passes serially through the several support headers.

Buck Steam Station, Duke Power Company—two 900,000 lb per hr at 2030 psi, 1000 F primary steam temperature and 1000 F reheat. Similar to Chesterfield, except for higher pressure and single furnace.

Eastlake Power Plant, Cleveland Electric Illuminating Company—three 875,000 lb of steam per hr at 2030 psi, 1050 F primary and 1000 F reheat steam temperatures; also one 1,500,000-lb steam/hour at 2750 psi, 1050 F primary and 1050 F reheat steam

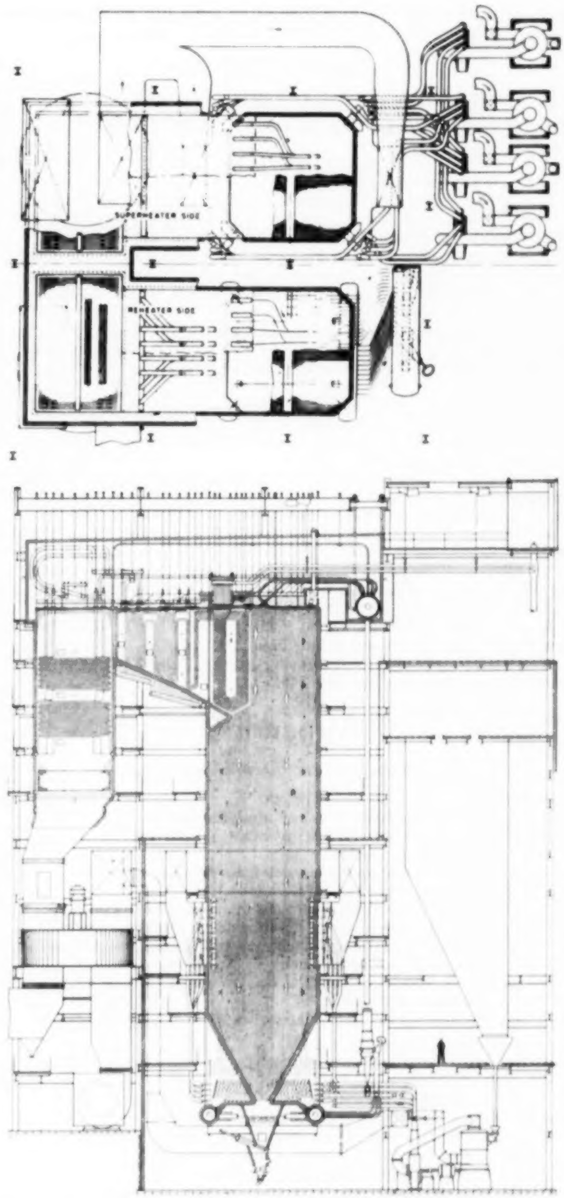

Fig. 19 General Arrangement—Controlled-Circulation Boiler, Cromby Station, Philadelphia Electric Company

temperature. Similar to Chesterfield except for higher pressure.

Cromby Station, Philadelphia Electric Company—one 1,450,000 lb of steam per hr at 2075 psi, 1000 F primary and 1000 F reheat steam temperatures. The chief development in this unit is the use of two separate furnaces, one arranged for control of primary steam temperature and the other for reheat. Both primary and reheat furnaces have independent tilting-burner controls thus insuring proper control of each, Fig. 19.

In addition to the foregoing controlled-circulation units, numerous others are in the installation or drawing-board stage. As is customary, once these boilers are in operation future papers

will summarize the improved developments and operating features and results.

ACKNOWLEDGMENT

The author gratefully acknowledges the assistance and suggestions of all associates in making this paper possible.

BIBLIOGRAPHY

1 "1825-Lb-Pressure Topping Unit With Special Reference to Forced-Circulation Boilers," by F. S. Clark, F. H. Rosencrants, and W. H. Armacost, Trans. ASME, vol. 65, 1943, pp. 461–477.

2 "Operating History and Performance of 2000-Psi Forced-Circulation Boiler at Somerset Station of Montaup Electric Company," by G. U. Parks, W. S. Patterson, and W. F. Ryan, Trans. ASME, vol. 68, 1946, pp. 411–427.

3 "Experience With Instruments and Control Equipment for 2000-Psi Boiler at Somerset Station of Montaup Electric Company," by W. D. Bissell and E. B. Powell, Trans. ASME, vol. 68, 1946, pp. 453–466.

4 "Special Studies of the Feedwater-Steam System of the 2000-Psi Boiler at Somerset Station at Montaup Electric Company," by W. D. Bissell, B. J. Cross, and H. E. White, Trans. ASME, vol. 68, 1946, pp. 429–442.

5 "Water Conditioning for the 2000-Psi Boiler at the Somerset Station of the Montaup Electric Company," by W. W. Cerna and R. K. Scott, Trans. ASME, vol. 68, 1946, pp. 443–451.

6 "Forced Circulation Boilers," by W. S. Patterson, *Paper Trade Journal*, September 5, 1946.

7 "Forced Circulation Boilers Tool for More Kwhrs Per Dollar," by W. F. Ryan, *Electrical World*, vol. 136, October 22, 1951, pp. 114–116.

8 "Controlled Circulation at Chesterfield," by T. E. Crossan and W. F. Ryan, published in this issue, pp. 727–734.

9 "The New Kearny Generating Station," by F. P. Fairchild, published in this issue, pp. 735–748.

Appendix

CONTROLLED-CIRCULATION FEATURES

1 General
- (a) Positive circulation before applying heat.
- (b) Controlled circulation in exact proportion to calculated heat distribution.
- (c) Steady water level on quick load swings.
- (d) Quick response to load demands.
- (e) Greater time available to act in event of tube failure due to small tubes and low discharge rate from rupture.
- (f) No loss of turbine capacity on tube rupture until load reduction can be planned.
- (g) Quick access to furnace due to rapid cooling and short outages for repairs.
- (h) No hideout of solids in boiler water.

2 Furnace-wall surface
- (a) Use of small-diameter tubes:
  - (1) Low weight of tubes.
  - (2) High velocity in tubes.
  - (3) Results in thin-wall tubes.
  - (4) Low hot-face temperature of tubes.
  - (6) Lower total stress in tubes.
  - (7) High factor of safety in tubes.
- (b) Circuits may be arranged either vertically or horizontally.
- (c) Tube circuits may be of unequal length or unequal heat absorption.
- (d) High permissible heat-absorption rate.
- (e) Minimum of time and expense for wall-tube repairs when necessary.
- (f) All-welded construction.
  - (1) Elimination of rolled joints.
  - (2) Elimination of handholes and gaskets.

3 Boiler-heating surface
- (a) Greater design flexibility:
  - (1) Horizontal multipass extended surface may be used.
  - (2) Cooling panels in superheater zone of multipass arrangement may be conveniently used.
  - (3) Water-cooled spacers and supports may be used for superheater, boiler, and economizer.

4 External circulating system
- (a) Low circulation rate is used in boiler surface and high velocities used thus:
  - (1) Small number and size of downtakes.
  - (2) Small number and size of risers.
  - (3) Improving steam quality.

5 Boiler drum
- (a) Low total circulation results in:
  - (1) Few drum nozzles for downtakes.
  - (2) Few drum nozzles for risers.
  - (3) Small space required for baffles and other internals.
  - (4) Small amount water to separate from steam.
  - (5) Low number of steam-separator units.
  - (6) Small-diameter drum.
  - (7) Thin drum wall.
  - (8) Large access space for given diameter.

6 Structural
- (a) Furnace-wall tubes small in diameter and thin, resulting in:
  - (1) Low water weight in operation.
  - (2) Low weight of structural supports.
  - (3) Small amount weld metal to be deposited in erection.
  - (4) Low load on foundations.
- (b) Use of water-cooled spacers and supports reduces special alloy structural members.

7 Maintenance
- (a) Low cost in replacing portions of tubing due to small-diameter thin-wall tubes.
- (b) Time saver because of quicker start-up, shutdown, and cool-off periods.
- (c) Quick and low amount of acid required for cleaning if found necessary.
  - (1) Less acid required and less time to drain.
  - (2) Less treatment time when circulating pumps are used.
  - (3) Quick flushing and neutralizing operations due to use of pumps, and because small amount of water required to fill boiler.
  - (4) Ease of inspecting tubes by cutting out samples before and after cleaning.

8 Operating economy
- (a) Large part of circulating-pump power goes into boiler as heat.
- (b) Low weight of pressure parts and water results in less fuel required to place unit in operation.
- (c) Time saved in heating up and cooling off, and short outages, means long operating time.

9 Flexibility of operation

Operating experience has indicated that flexibility and ease of control of controlled-circulation boilers is of great value in time of emergency. For example, owing to the small tubes used, a tube failure does not cause a violent disturbance and does not result in damage to adjacent parts and equipment. Also, owing to the positive controlled circulation, the circulation is not disrupted in other parts of the boiler. Therefore it is not necessary to drop load immediately; rather, operation may be continued for several hours.

Discussion

L. BAKER.[3] A review of the controlled-circulation boiler is long overdue. In Great Britain, too many people still shut their eyes to the many successful applications of the controlled-circulation boiler and continue to reiterate the fears about pump glands, and so on.

None of the bogeys has been significant in the three designs with which the writer has had personal experience, although the first one in the Royal Navy Destroyer met some gland difficulties in its initial operation.

The trends of development in the United States appear to be different from those in Great Britain. Duplication of pumps for service is not favored and in very few instances is a stand-by pump actually installed ready for operation. Experience justifies this view and there is no doubt that psychologically it is sound, as operating personnel soon became accustomed to the idea.

[3] Chief Superintending Engineer, Alfred Holt & Co., India Bldg., Liverpool 2, England.

The merits of the controlled-circulation boiler are twofold in the writer's opinion: (1) The easy steam/water separation and high purity steam resulting, and (2) the relatively low proportion of steam in the circulating mixture of steam and water that is exposed to the maximum rates of heat transfer, which results in a greater margin of safety from steam-blanketing.

The author is incorrect in his statement, "Steaming of the economizer may be prevented......" His intention surely is to show that the deleterious effects of adventitious steaming in an economizer can be overcome by converting it into generator surface by the direct circulation of boiler water into the economizer-inlet header. This fitting usually is controlled by the pressure drop across the economizer so that, below a safe flow, the economizer virtually is cut out or replaced by generating surface. In this way it is possible to design for a larger proportion of the heat extraction to be achieved in the economizer; i.e., the customary margin between economizer-outlet temperature and the saturation temperature can be reduced with advantage to the boiler design, and a lower pressure drop through the economizer can be adopted with advantages to the cycle efficiency.

Author's Closure

The author is gratified at the interest evidenced in controlled-circulation boilers. The discussion of Mr. Baker is appreciated in pointing out the differences in developments in Great Britain and the United States. His comment regarding steaming of the economizer apparently assumes that water is circulated through the economizer at all times. The author's discussion of this item applies only to starting up. During this period while pressure is raised without the generation of steam, no water flow to the economizer occurs. Steam is generated when gas temperatures exceed saturated temperatures of the trapped water in the economizer tubes. Steaming is avoided during the starting period by circulating water from the pump to the economizer inlet header.

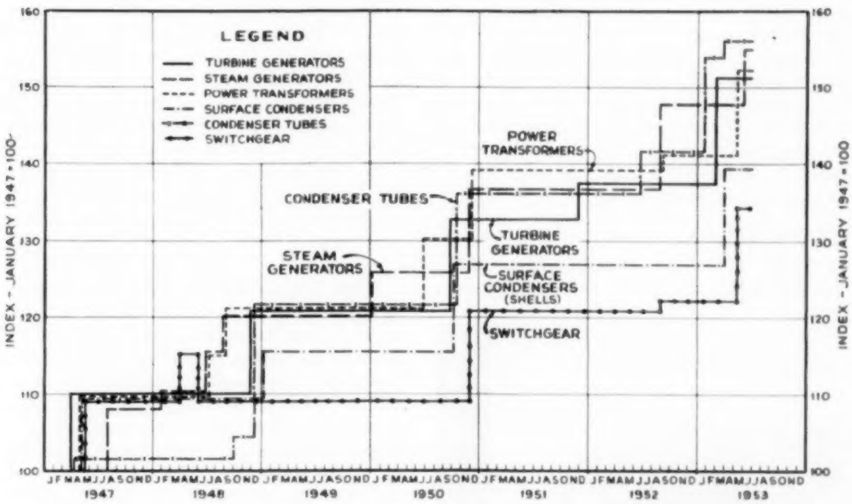

Fig. 1 Percentage Price Changes of Power-Station Equipment—January, 1947 = 100

Controlled Circulation at Chesterfield

By T. E. CROSSAN[1] and W. F. RYAN[2]

This paper deals with the reasons why controlled-circulation boilers were adopted for the Chesterfield Station and the economics of the installation. Early operating experience is described and more detailed descriptions of elements of the system are discussed.

Introduction

There were many reasons for using a controlled-circulation boiler in the latest extension of Virginia Electric and Power Company's Chesterfield Station. Many operating advantages have been outlined in another paper,[3] but the consideration we wish to emphasize in this presentation is that this type of design was selected in order to save some money.

The first large high-pressure controlled-circulation boiler installed by an American public utility was placed in operation in 1942 at the Somerset Station of the Montaup Electric Company.[4] There were two reasons for adopting this design at Montaup; a definitely limited amount of space was available in the existing power station, and a definitely limited amount of money in the company's treasury. The controlled-circulation design of boiler provided the greatest amount of capacity that could be obtained within these two limitations; in other words, it made possible more kilowatts per cubic foot and more kilowatts and kilowatt-hours per dollar than a natural-circulation boiler.

Early Problems

Serious difficulties were encountered in the early operation of that boiler. These were due in large measure to the unprecedented operating pressure; a natural-circulation boiler, designed for comparable conditions and installed at about the same time by another utility, experienced a great many of the same troubles. It was a long time before the owner, the engineers, and the boiler manufacturer were convinced that all of the problems had been solved. Nevertheless, the engineers never forgot the savings in space and money which the Montaup boiler provided, and this memory was kept keenly alive by the continuously rising costs of steam-electric generating plants during the years that followed.

For nearly 70 years our American public utilities maintained an enviable history of continuously lower selling prices for electric energy. This progressive reduction of rates was maintained through periods of war, depression, and inflation, almost until now, but recently a number of utilities have been compelled, regretfully and regrettably, to increase their charges to the consumer.

In combating inflation, higher thermal efficiencies have helped to offset rising fuel costs, and larger units have reduced the significance of higher wages for operating labor. The factor which engineers have been able to overcome only partially is the rising cost of plant, and this element of cost, which determines the demand charges in our rate schedules, will become even more embarrassing when a business recession occurs.

[1] Superintendent of Production, Virginia Electric and Power Company, Richmond, Va. Mem. ASME.

[2] Vice-President and Engineering Manager, Stone and Webster Engineering Corporation, Boston, Mass. Hon. Mem. ASME.

[3] "The Controlled-Circulation Boiler," by W. H. Armacost, published in this issue, pp. 715–726.

[4] See Trans. ASME, vol. 68, 1946, pp. 411–442.

Contributed by the Power Division and presented at a joint session of the Power, Metals Engineering, and Fuels Divisions, and Research Committees on Furnace Performance Factors, and High Temperature Steam Generation, and Joint ASTM-ASME Research Committee on Effect of Temperature on Properties of Metals at the Annual Meeting, New York, N. Y., November 29–December 4, 1953, of The American Society of Mechanical Engineers.

Note: Statements and opinions advanced in papers are to be understood as individual expressions of their authors and not those of the Society. Manuscript received at ASME Headquarters, October 14, 1953. Paper No. 53—A-96.

Fig. 1 shows the trend of major power-generating-equipment prices during the last few years and shows what the designing engineer has to contend with in his efforts to produce reliable and efficient capacity at reasonable cost. This chart is not an "index" but merely the experience of one engineering office in obtaining quotations on such items. The controlled-circulation-boiler design for the latest extension at Chesterfield was one of several measures adopted by the owner and the engineers in an effort to meet the challenge of rising plant cost.

The Chesterfield Plant

The Chesterfield Station is a strictly utilitarian design. It was started during World War II and, in the first section, every effort was made to economize on materials, particularly steel. Fig. 2 is an unretouched close-up showing an exterior view of the plant. The walls are of uninsulated corrugated asbestos; for unit No. 1, built during the war, this material was mounted on wood girts. This picture shows that the building, in spite of its economical design, is not unpleasing architecturally. Note the wood sash in the first section boiler and turbine rooms. The office building in the left foreground, built after the war, has steel sash. The first section was designed so that the walls could be rebuilt, using brick, at a later date, but the results have been so satisfactory with the original construction that no recent thought has been given to its replacement.

Fig. 2 Exterior of Chesterfield Power Station

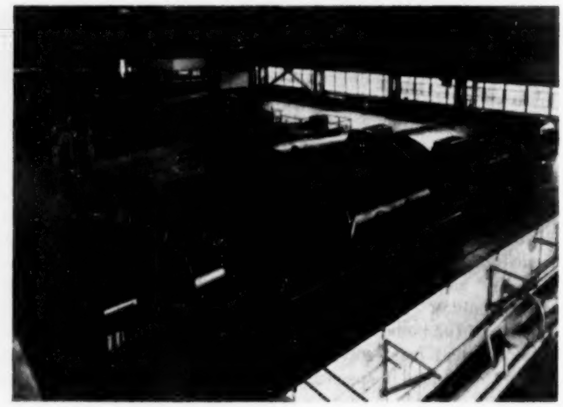

Fig. 3 Turbine-Room Interior of Chesterfield Power Station

Inside, the economy of construction shows up rather sharply, and the interior of the turbine room is not remarkable for architectural beauty, as shown in Fig. 3. Nothing was spent for aesthetic effect. Note the wood handrails and concrete girders in the first section built during wartime restrictions on use of steel. There are no tiled walls or even tiled floors, but complete protection is provided from the weather encountered in Tidewater, Va., at minimum cost. The savings which can be effected by out-of-door construction dwindle rapidly in the face of a building cost as low as this, and the added expense of out-of-door operation and maintenance would be difficult to justify.

No Funds for Glamor

While Virginia Electric and Power Company spends no money for glamor in its generating stations, it has never hesitated to pioneer when convinced it was getting more kilowatt capacity, more kilowatthours, greater safety, or a substantial saving in investment and operating costs. It was among the first of the utilities to accept the straight unit principle of design with a single boiler per turbine and no cross connections. Since the adoption of the preferred standards, it has never purchased any other kind of turbine generator. It was among the first purchasers of the 66,000-kw preferred standards, and unit No. 3 was the very first 100,000-kw preferred-standard turbine. The order was placed only three days after the revised standard including a unit of that size was adopted by the joint committee and three more have been purchased since—two for Portsmouth and one for Possum Point. These units also will be supplied with steam by controlled-circulation boilers.

It is the company's experience that standard machines provide more for the money than other types and the same philosophy of seeking the maximum return on investment led to the selection of controlled circulation to provide steam for unit No. 3, although it is the first post-Montaup design of this type.

The general simplicity of the station design is emphasized in the heat balance shown in Fig. 4. There are only five stages of extraction; make-up is provided by demineralizers rather than evaporators; and the final feedwater temperature is moderate (458 F). So also are the throttle pressure (1450 psig) and the throttle and reheat temperature (1000 F), factors which were fixed by the selection of a preferred standard unit.

Control is not overcentralized. Separate control boards are provided for high-tension switching, the boiler, the boiler-feed system and the turbine generator. The boiler control station is shown in Fig. 5 and the turbine-generator control station in Fig. 6. These boards are moderate in size and are not overburdened with dispensable instruments or controls.

Chesterfield Ranks Well

It will be deduced readily from these facts regarding design that Chesterfield has broken no world's records for thermal efficiency, but the station is by no means inefficient. Its heat rate is among the lowest 15 per cent reported in the Federal Power Commission's most recent report, although only units 1 and 2 were then running and their throttle pressure is only 850 psig (temperature 900 F). The sister station at Possum Point, also operating at these moderate steam conditions, is among the lowest 10 per cent. All of the Chesterfield units have ground out many millions of kilowatthours at gratifying production cost, and with an availability factor which would be difficult to excel.

The reduction of cost effected by using controlled circulation is now a matter of experience, not of estimate or conjecture. The engineers installed several natural-circulation boilers of substantially the same capacity and characteristics at about the same time. The delivered price of equipment was less for the controlled-circulation design, and the man-hour requirement for erection was less. The erection labor has further improved on

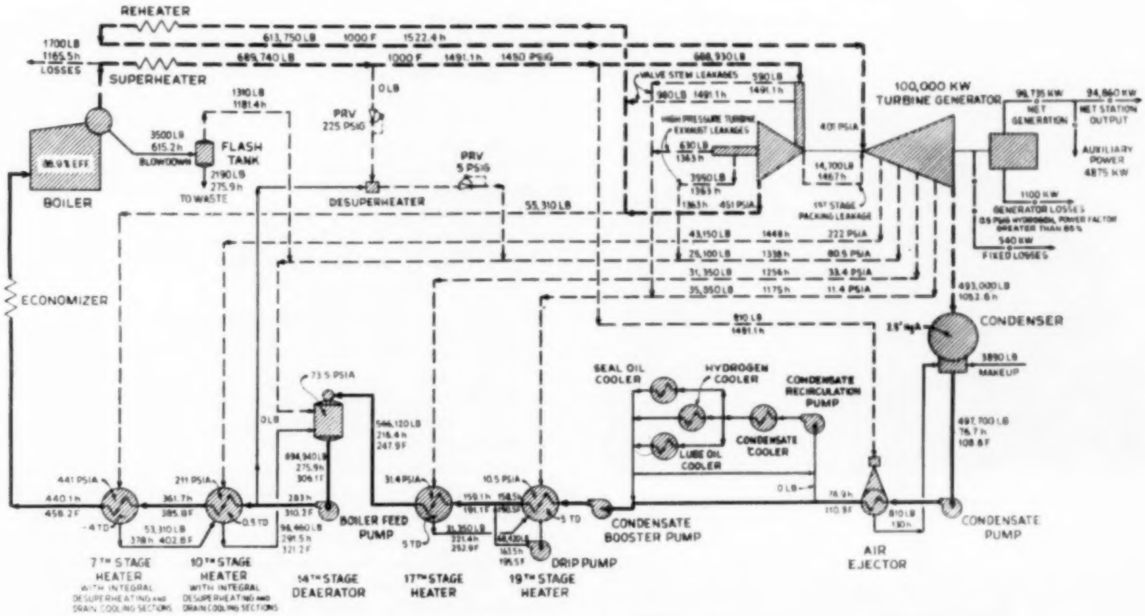

Fig. 4 Heat Balance of Chesterfield Unit No. 3

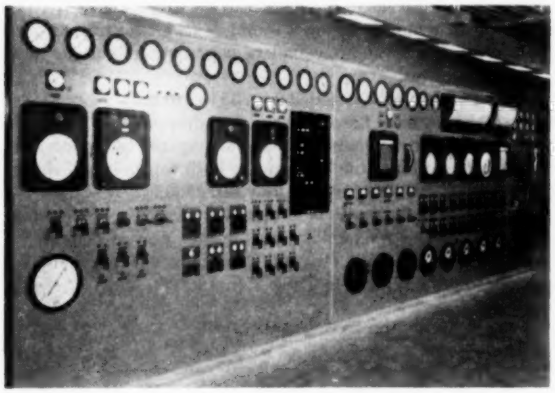

Fig. 5 Boiler-Gage Board

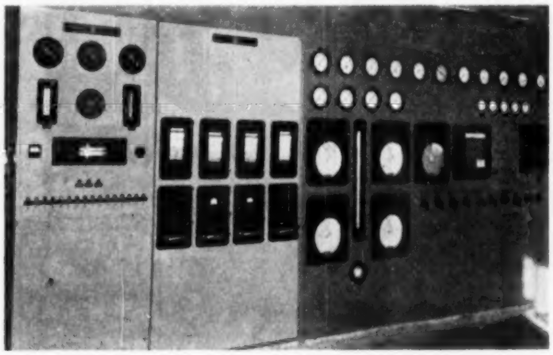

Fig. 6 Turbine-Gage Board

later installations as the manufacturer gained field experience with this new design. Substantial savings also were made in the cost of building.

Fig. 7 shows the over-all dimensions of steam-generating equipment for Chesterfield No. 3, and the corresponding dimensions of a natural-circulation boiler offered for the same capacity and operating characteristics. The controlled-circulation design shows a reduction of more than 30 per cent in required floor area and a reduction of more than 40 per cent in volume. This would be of less importance in an outdoor plant but, even in that case, it results in smaller floor area and reduction of weight on the foundations and structural steel. The weight of the Chesterfield No. 3 boiler is 1,000,000 lb less than the weight of an alternative natural-circulation design. The saving in supporting steel and foundations can be visualized readily.

How Savings Were Made

Fig. 8 shows the rear elevation of the boiler-plant building, indicating rather dramatically the saving in building effected by the boiler design. To the left is the section devoted to the first

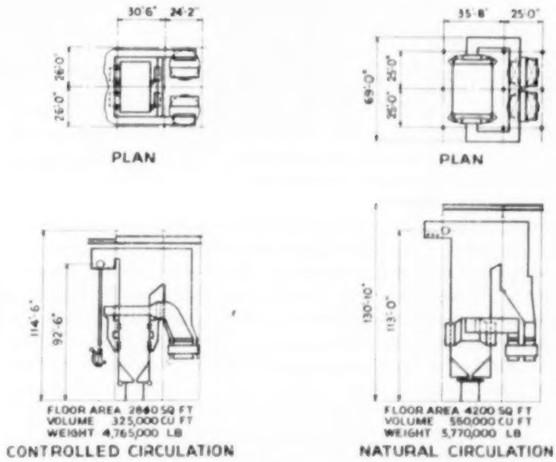

Fig. 7 Reheat Boiler
(Over-all dimensions—750,000 lb/hr 1000 F/1000 F)

Fig. 8 Chesterfield Boiler-Room Extensions

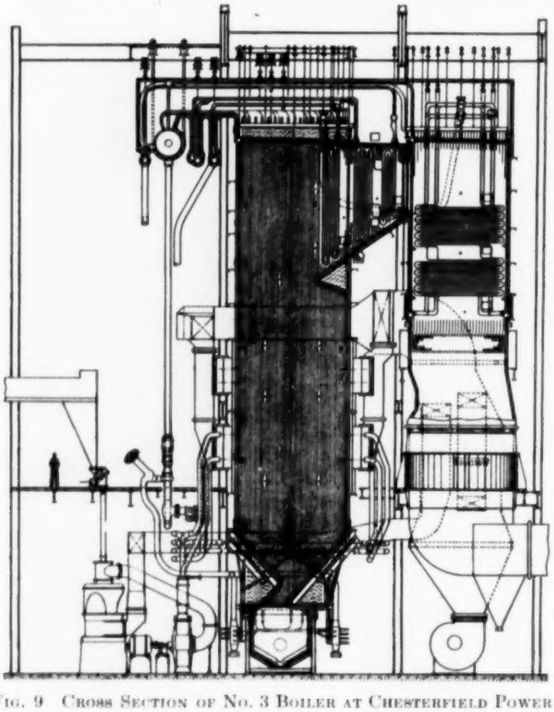

Fig. 9 Cross Section of No. 3 Boiler at Chesterfield Power Station

unit, a 50,000-kw handbook machine without reheat, the guaranteed capability of which is 62,500 kw. In the middle is the section devoted to unit No. 2, a 66,000-kw preferred standard, also nonreheat. The width is less, but it was necessary to raise the roof line a little and to add a larger protuberance at the rear for auxiliary equipment. At the right is the building for unit No. 3, a 100,000-kw preferred-standard reheat installation. Note that the width is substantially reduced, the roof level returns to the same elevation as for unit No. 1, and the proturberances required for units nos. 1 and 2 have been eliminated. The building for controlled-circulation unit No. 3 has 15 per cent less volume than for natural-circulation unit No. 1, in spite of its 50 per cent greater effective capacity expressed in terms of kilowatts.

That the savings in plant cost were obtained at no sacrifice of capacity or reliability, and that the operating advantages described by W. H. Armacost[3] have been realized, is clearly demonstrated by operating results.

The controlled-circulation boiler installed at the Chesterfield Station is rated at 750,000 lb of steam per hr at 1500 psi gage, 1000 F initial steam temperature, and 1000 F reheat. Mr. Armacost's paper[3] covers the boiler design and no description will be given except where some feature is of particular interest. A cross section of the unit is shown in Fig. 9.

Operating Experience

The boiler and 100-mw turbine generator first supplied energy to the Virginia Electric and Power Company system on November 9, 1952, and were in commercial operation as of December 1. Since the latter date, two outages have occurred, one forced and one scheduled.

The forced outage occurred when a normally latched-in relay, which trips the fires in case of low boiler circulating-pump differential, was accidentally de-energized by an electrician attempting to locate a direct-current ground. The load on the unit was reduced to station auxiliary power and, as soon as the cause of the trouble became known, the fires were relit and load restored. Approximately 30 min elasped between the start of load reduction and return to full load. Needless to say, the offending relay has been rewired to be de-energized normally.

The scheduled outage, from January 29 to February 4, 1953, was made to remove fine-mesh strainers from the turbine stop and intercept valves and to complete construction items and miscellaneous changes.

Loading of the unit has varied from 35 to 110 mw. Normal load is 105 to 110 mw from 12 to 18 hr per day, dropping to a minimum of 35 mw in the early morning hours, as required by system conditions. Operation of the boiler under both constant and changing load conditions has been entirely satisfactory.

The unit was in continuous operation from February 4 to August 21, 1953. Availability for the first year of commercial operation was 96.4 per cent. The various scheduled outages which occurred are given in Table 1.

TABLE 1 SCHEDULED OUTAGES

Date, 1953	Reason for outage	Hours out
1-29 to 2-4	Scheduled. Remove fine strainers from stop and intercept valves. Miscellaneous work.	124
8-21 to 8-24	Scheduled. Remove deposits from turbine-control valves.	51
10-28 to 11-2	Scheduled. Remove boiler-tube sections for inspection. Remove deposits from stems of stop and intercept valves.	96
11-25 to 11-29	Scheduled. Acid-clean boiler.	96
Total outage time		367

A hydrostatic test, after replacing the boiler-tube sections removed, showed two leaks. The first was a crack in a superheater tube and was repaired by replacing a short section of tubing. The second was a pinhole in a boiler tube, apparently caused by a stinger during erection. It was repaired by welding.

The tube sections removed contained a moderate amount of deposit, largely iron oxide. As the Thanksgiving Day week-end provided the only convenient opportunity for removing the unit from service for several months, it was decided to proceed with acid-cleaning at that time.

Fig. 10 shows the daily gross output in kilowatthours from November 10, 1952, to December 20, 1953.

Maintenance of design initial steam and reheat temperature of 1000 F is achieved readily by means of the combination of automatic burner tilt control and spray attemperation, with variations normally of about 5 deg F and not exceeding 10 deg F at outputs above about 550,000 lb of steam per hr.

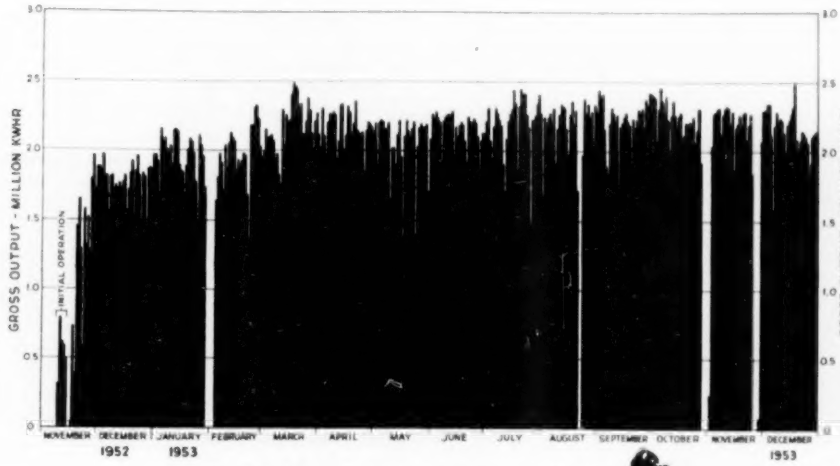

Fig. 10 Daily Output—Chesterfield Unit No.

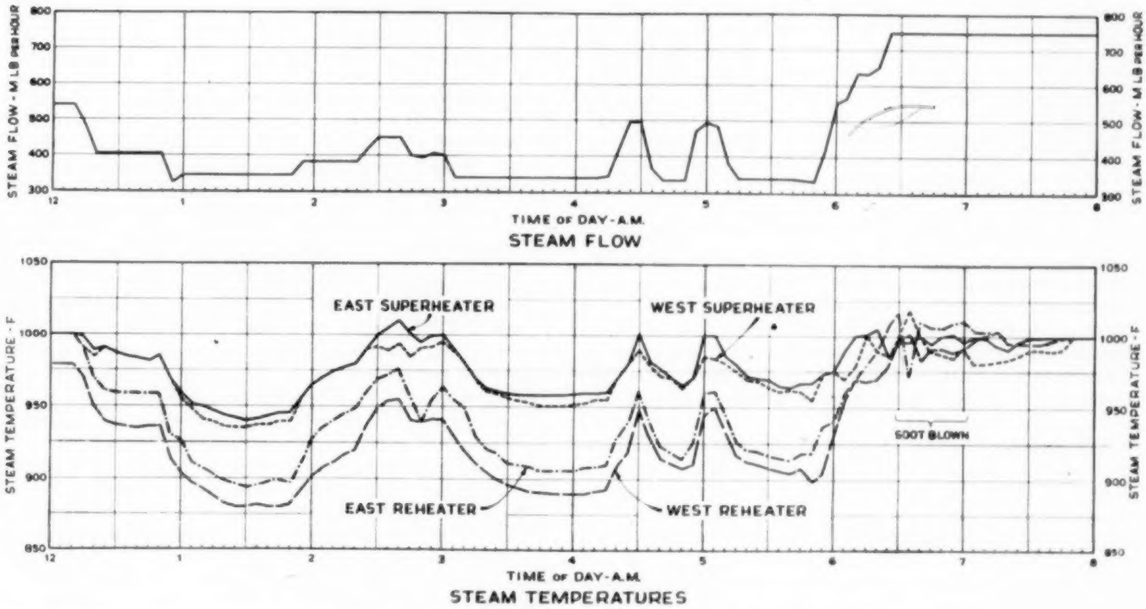

Fig. 11 Performance—Chesterfield No. 3 Boiler

Steam Conditions

Fig. 11 shows the steam flow and the initial and reheat steam-temperature records for a portion of August 7, 1953. The excellence of the control, especially of steam temperature over sudden and wide variations of steam output, is indicated clearly. The practically negligible difference in initial steam temperature from the two sides of the main superheater and the average difference of about 15 deg F from the two sides of the reheater during the large variations in load between 2.00 and 6.00 a.m. are especially satisfactory in view of the fact that combustion is being controlled in two separate furnaces.

Fig. 12 is a reproduction of the actual chart for the same day during a period of steady load. There is a maximum difference of less than 30 deg F for all four temperatures during this period, although all of the IR blowers were operated.

It is now believed that the difference in temperature in the two sides of the boiler is due to the unequal slagging of the two furnaces.

In a tangentially fired furnace, gas velocity is considerably higher in the left-hand side. Since the left wall of the right-hand furnace is a more or less flexible wall, it tends to shake loose slag deposits, whereas the left-hand wall of the left-hand furnace is not flexible and slag will accumulate. Work is presently in progress to change the blowing arc of the soot blowers in the boiler with the expectation of removing more slag in the rear corners of the furnaces.

A feature of interest is the vibration of the center wall tubes at the top. The maximum movement is approximately $^3/_8$ in., and this action appears to be very effective in keeping the upper part of the center screen wall free from slag.

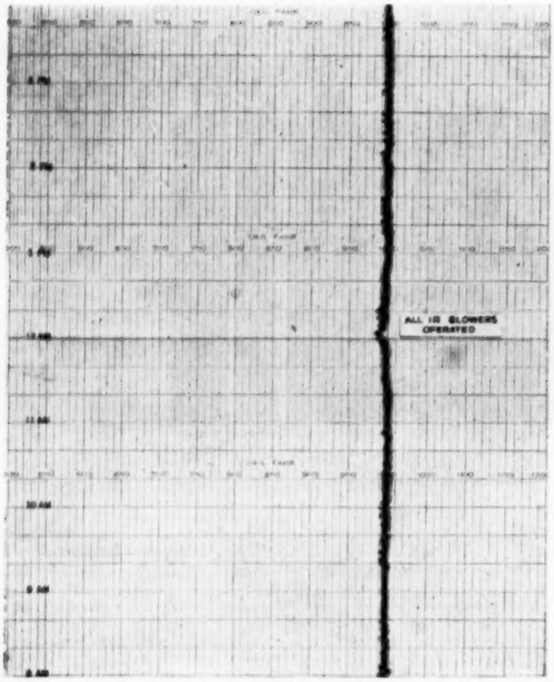

Fig. 12 Steam Temperature—Chesterfield No. 3 Boiler

Precautions Taken to Assure Clean Boilers

During the period of preliminary operation prior to putting the unit on the line, all possible precautions were taken to provide a commercially clean boiler. While this is a normal procedure with any boiler, experience with earlier controlled-circulation boilers indicated that special attention should be given to cleaning of the Chesterfield unit. Before boiling out, all tubes were pressure-flushed with a specially designed nozzle to insure that each tube was free from obstructions.

Boiling-out and acid-cleaning were accomplished with the secondary strainers and orifices removed but with the master strainers in place. During the draining of acid and water used for subsequent rinses, nitrogen was introduced to exclude air from the boiler. Acid was circulated periodically by a special pump installed for the purpose. When the boiler-circulating pumps were not in use during the acid wash-and-rinse period, they were pressurized with condensate containing caustic soda, sodium sulphite, and cobalt chloride to reduce the possibility of corrosion of the lower pump bearing.

Subsequent to the acid-wash and raw-water rinses of the boiler, a considerable amount of condensate was used for rinsing in an attempt to reduce the turbidity of the rinse water drained from the boiler, but this operation was not successful until the boiler was fired and the water temperature raised to 180 F. The heating of the unit, with the boiler circulating pumps in operation, apparently dislodged deposits of iron oxide and, after two subsequent rinses, the turbidity of the rinse water was acceptable.

After inspection of the drum and headers, all tubes were again pressure-flushed and the secondary strainers and orifices installed. The master strainers were removed and a considerable amount of welding beads and trash was found.

Subsequent to closing up the boiler, it was given a hydrostatic test, drained to firing level with nitrogen atmosphere above the water, and lit off to raise pressure for blowing out steam leads, setting safety valves, and preliminary operation of the turbine. After all the necessary tests had been made, the machine was phased out and synchronized with the system.

Operation for the first 2 weeks included the usual number of starts and stops for balancing the turbine, repairing leaks, and other details.

Heavy oil was fired during this preliminary period, and the change-over to coal was made during the latter part of November.

Feedwater Treatment

Feedwater treatment has been given careful attention. Total solids in the boiler water seldom exceed 100 ppm. Caustic soda and sodium hexametaphosphate are added to the boiler drum, cyclohexamine at the feed-pump suction, and sodium sulphite at the condenser hot well. The pH of the feedwater originally was controlled at 8.5, but tests have indicated that 8.8 to 9.0 is more effective in reducing iron and copper pickup in the system. A small amount of boiler water is recirculated through the economizer, from the boiler-circulating-pump discharge, to maintain the pH of the water in the economizer at 9.0 to 9.5. Limits set for the boiler water are as follows:

Alkalinity as NaOH, ppm	15 to 40
Phosphate as PO_4, ppm	1 to 3
Sulphite as Na_2SO_3, ppm	1 to 3
Silica as SiO_2, ppm	1

Initial checks of boiler performance by means of the regular station instruments indicate acceptably close agreement with the expected over-all boiler efficiency of 88.7 per cent at design capacity. Studies of various features of boiler operation are under way to furnish information on which to base adjustments of controls to assure optimum results throughout the usual capacity range.

Boiler Circulating Pumps

Since the date of commercial operation, neither capacity nor reliability of the steam-generating unit has ever been affected by the boiler circulating pumps. A cross section of one of the boiler circulating pumps is shown in Fig. 13 and a detail of the mechanical seal and injection sealing system in Fig. 14.

During most of the hours of pump operation, the mechanical seals have not been effective as such, but the sealing of the pumps has been accomplished by injecting water at a pressure slightly above the circulating-pump suction pressure. Recent tests have indicated that approximately 20 gpm per pump is required. This water is supplied by the main boiler feed pumps. Some injection water enters the boiler circuit, but most of it is returned to the main condensate stream at a back pressure of about 200 psi. The maximum time for which any mechanical seals have been fully effective has been approximately 2000 hr. A seal failure is not sudden, and the imminence of failure is indicated by a temperature rise in the sealing-water cooling circuit. A mechanical seal failure does not limit boiler operation, as sealing water is supplied and the pump continues in service.

During the outage of January 29 to February 4, 1953, all three pumps were overhauled completely and put in first-class condition. Since that time, two of the pumps have been dismantled for inspection. The first pump, inspected in June, 1953, was found to be in good condition; the second, overhauled early in August, 1953, required the replacement of several parts. On this latter pump there has been some indication that boiler water leaks through the seal and the resultant flashing contributes to the wear of various parts, particularly the breakdown bushing. Steps are being taken to remedy this condition.

More than normal wear of some pump parts was experienced during the period of preliminary operation. If it were feasible to

Fig. 14 Mechanical Seal and Injection Sealing System of Boiler Circulating Pump

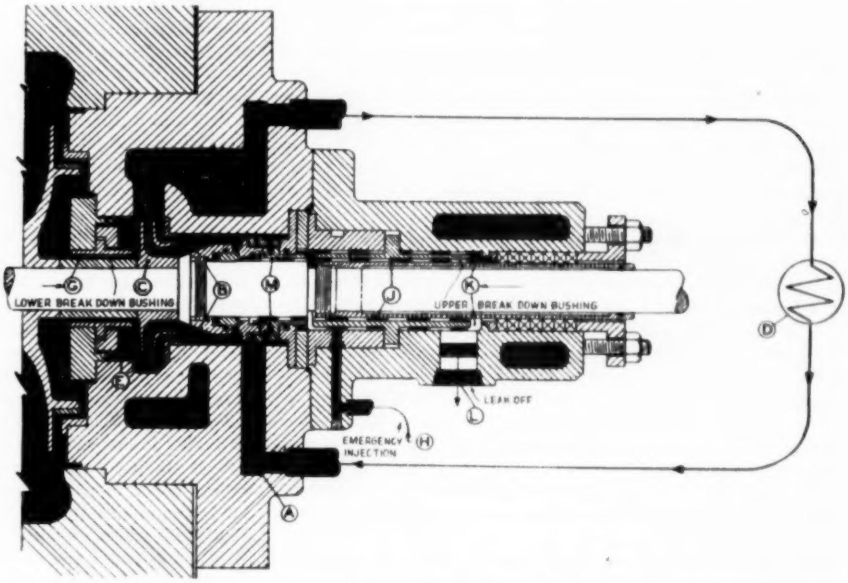

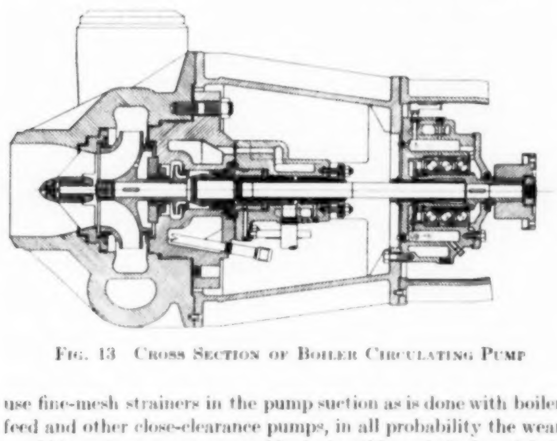

Fig. 13 Cross Section of Boiler Circulating Pump

use fine-mesh strainers in the pump suction as is done with boiler feed and other close-clearance pumps, in all probability the wear would have been more reasonable during this period when debris was being cleaned out of the system.

The power required by two boiler circulating-water pumps, 260 kw, amounts to approximately 5 per cent of the normal station auxiliary power.

Conclusion

In conclusion, all concerned are thoroughly satisfied with the choice of controlled circulation for Chesterfield—management, because of the low initial cost and dependable capacity, and plant personnel because of the freedom from operating difficulties. Confidence in the selection of controlled-circulation boilers is reflected further in the decision to install three more units of this design to meet future system demands of the Virginia Electric and Power Company.

Discussion

B. F. Hampshire.[5] The controlled-circulation boiler at the Somerset Station of the Montaup Electric Company has shown greatly improved reliability over the past four years. Tube failures resulting from internal deposits have been eliminated completely due primarily to the lowering of excess treatment chemicals, and also to the correction of condenser leakage. For instance, phosphate excess was originally carried at 25 to 30 ppm as is quite common in low-pressure boiler operation. Today, phosphate excess is carried at about $^1/_{10}$ of this amount.

Over this period, the boiler has been operated at full capacity during most of its operating hours—attaining an average of 94.5 per cent of rating for the calendar year 1950, and somewhat less since 1950, because of load sharing with new equipment.

The turbo steam purifiers and related equipment installed during July, 1950, have resulted in very satisfactory steam purity. Circulating-pump gland seals also have given trouble-free performance.

The authors point out the necessity for public utilities to hold down investment costs per kilowatt where possible. The controlled-circulation boiler undoubtedly will become an increasingly important factor in attaining this objective because of the space-saving and weight-saving possibilities with this type of boiler.

G. A. Plummer.[6] Having been associated throughout the development of the La Mont controlled forced-circulation boilers in Great Britain since 1936, and having been privileged to see the Chesterfield Plant in May, 1952, during the early stages of erection of the controlled-circulation boiler there, the writer has studied with great interest the valuable paper presented by the authors and should like to take this opportunity of congratulating them on their extremely interesting presentation.

The writer is particularly interested in the details given of the boiler circulating pumps employed. The related performance of these pumps indicates that the mechanical seals have not been fully effective nor entirely satisfactory. It would appear that the breakdown bushings have had to be relied upon, necessitating the injection of high-pressure sealing water.

From the writer's experience, extending over some 17 years, this system tends to become a "rake's progress."

Leakage commences from the mechanical seal. The increasing

[5] Vice-President and General Manager, Montaup Electric Company, Fall River, Mass.

[6] Director and Chief Engineer, John Thompson Water Tube Boilers, Limited, Wolverhampton, England.

amount of hot boiler water passing through the mechanical seal overloads the external cooler, thus raising the temperature under which the mechanical seal is called upon to operate, making its duty more arduous and throwing the work of sealing of the pump onto the breakdown bushings. The quantity of hot boiler water now leaking through the parts entirely overloads the external cooler and the resulting flashing of the boiler water in passing through the mechanical seal increases the wear of the various parts, and the injection of high-pressure sealing water must be resorted to.

It is indicated in the paper that the amount of sealing water used is approximately 12,000 lb per hr per pump. This quantity is limited only by the clearance between the breakdown bushings and the pump shaft. Again from the writer's experience, the suction eye bearing is not likely to contribute materially to the stability of the pump shaft for any length of time and, with such a long "overhang" of shaft it would appear that the radial clearances between the shaft and the breakdown bushings must increase rapidly, thus further increasing the quantity of injection sealing water employed, which eventually will become an embarrassment in the feed system.

In Great Britain we already have gone through a number of these experiences. They have been overcome largely by attention to details. For example, in the case of three La Mont boilers installed at the Taylors Lane Power Station which have now been in operation for 10 years employing packed stuffing boxes, a life of 2200 to 2700 hr is being obtained on the packing, while the shaft sleeves are giving over two years of service, which is considered a satisfactory maintenance position.

Recently, at another plant are installed a number of glandless boiler circulating pumps. These are of the submersible motor type. Some nine months entirely satisfactory service has now been obtained on these pumps. After the first six months of operation, two of these pumps were completely dismantled for examination; no measurable wear could be seen on any journal, thrust pad or other wearing face, and the insulation of the motor windings was perfectly satisfactory. The pumps were cleaned, reassembled, and it is now proposed to run these pumps for two years without opening up for any further mechanical examination. Periodic insulation tests of course will be taken.

The performance of these pumps is extremely promising and present indications are that boiler circulating pumps are no longer to be a maintenance problem.

Engineers in Great Britain are naturally watching with great interest the development of the controlled-circulation boiler in America and are considerably impressed by the technical achievements incorporated in the controlled-circulation boiler referred to by the authors. Nevertheless, there exists a solid and extensive background of experience with controlled circulation in Great Britain which if not ignored could no doubt contribute in some small measure to the success of the very much larger installations now being adopted in the United States of America.

Authors' Closure

The authors are indebted to Mr. Hampshire for additional data in regard to the performance of the first large American controlled-circulation boiler for high pressures, and to Mr. Plummer for his particularly helpful comments based on wide experience with circulating pumps for this service. On the latest installation for Virginia Electric and Power Company, at least one of the circulating pumps will be of the submerged type, that Mr. Plummer describes. This is the so-called "canned" pump developed by Westinghouse Electric Corporation for highly specialized work in connection with a nuclear reactor.

Since the paper was presented in December, 1953, the Chesterfield boiler has continued in regular station service without interruption until the present writing, May 1, 1954. The similar unit which was installed at Virginia Electric's Portsmouth Station and two somewhat larger steam generators installed in the Etiwanda Plant of Southern California Edison Company have equally good records for performance to date. The circulating pumps continue to be a source of maintenance expense, but the cost is not significant in terms of pounds of steam or kilowatt-hours produced. The intent of the manufacturer, the owner, and the engineer is, of course, to secure a pump substantially free from maintenance, or at least one which requires no more maintenance than is ordinarily experienced with high-pressure boiler feed pumps. Other designs of circulating pump have been installed on later projects, but have not been in operation long enough to indicate how much improvement has been effected.

The conclusion of the original paper was that all expectations with respect to low cost and dependable service had been realized. This conclusion is still valid after six additional months of high-capacity operation. Like all advances in the art of steam generation, the controlled-circulation boiler has had to pass through experimental and development stages. The results at Chesterfield demonstrate that this design has now achieved full commercial status.

The New Kearny Generating Station

Public Service Electric and Gas Company

By F. P. FAIRCHILD,[1] NEWARK, N. J.

The author describes the more important features of the design of the new Kearny Generating Station and points out the significant differences between Kearny and Sewaren. Outstanding features are the steam conditions, 2350 psig, 1100 F-1050 F; pressurized firing of boilers; controlled circulation in boilers; gas recirculation; side-exhaust turbines with twin condensers and no expansion joint between turbine and condenser; an experimental high-speed boiler feed pump; and a completely austenitic main steam system.

Introduction

This paper is intended to describe the salient design features of the recent installation of electric generating capacity at Kearny, N. J. While this project is the first capacity addition at the Kearny site in more than twenty years, it is actually another step in the technical progress which, after World War II, appears successively in the new capacity additions to the electric system of Public Service Electric and Gas Company as shown in Table 1. The new Kearny Generating Station is then the next step after Sewaren. The plant heat-rate curves for these installations, as shown in Fig. 1, show that substantial technical progress has occurred in this period. The Kearny units have a calculated net heat rate, based on equipment guarantees, of 8920 Btu per kwhr, as compared to 10,400 Btu per kwhr for No. 1 Unit at Essex. This is an improvement of more than 15 per cent in a little more than five years.

There is a striking contrast between the original Kearny, which commenced operation in 1925, and the new installation. Early in the design work it was realized that the compromises necessary to integrate the new structure with the old could not be justified, and it was then decided to design the new plant, as far as practicable, as a new generating station, disregarding the somewhat natural tendency to harmonize the two. This is manifest in the semioutdoor construction, the lower elevation of the operating floor, and many other features.

This paper will dwell principally upon the significant differences between the new Kearny Generating Station and the recently completed Sewaren Generating Station. The latter was described in a paper[2] presented by the author at the ASME Semi-Annual Meeting in 1949.

General Arrangement

This new station has, for its principal equipment, two turbine generators and two boilers arranged in the unit system. The entire plant is operated from a control room located at operating floor level in the center of the square formed by the four major items of equipment. The general arrangement is shown in Figs. 2 and 3, cross section and operating floor plan. At Kearny, the boilers are relatively closer to the turbines on account of the fact that the coal pulverizers are placed alongside and between boilers, rather than in front, between boiler and turbine, as they were at Sewaren. This arrangement makes it feasible to enclose the coal-preparation equipment in a separate room ventilated to draw the heat of motors and pulverizer radiation away from the remainder of the plant. It shortens the steam leads between boiler and turbine. It makes the feeders of all pulverizers accessible from one platform, as shown in Fig. 4.

As at Sewaren, the new Kearny Generating Station is designed for two-level operation. At Kearny, however, the two levels are 15 ft apart, against 26 ft at Sewaren. This arrangement makes travel between floors quicker and easier. It reduces building volume significantly. Saving in first cost is estimated at $300,000 for two units. The total and unit volumes enclosed by the building at Kearny and Sewaren are as follows:

		Kearny	Sewaren
Number of units		2	4
Guaranteed capability, mw		290	455
Enclosed building volume including basement:			
Total	1000 cu ft	3515	6600
Unit volume	cu ft per kw	12.1	14.5

These comparisons are for the enclosures of the principal operating equipment, excluding the coal-handling system, coal bunkers,

TABLE 1 CAPACITY ADDITIONS PUBLIC SERVICE ELECTRIC AND GAS COMPANY

Station	Unit no.	Guaranteed capability (mw)	Throttle Pres (psig)	Throttle Temp (F)	Reheat temp (F)	Starting date
Essex	1	110	1250	1000	...	Dec. 1947
Sewaren	1	110	1500	1050	...	Dec. 1948
	2	110	1500	1050	...	Nov. 1948
	3	110	1500	1050	...	Oct. 1949
	4	125	1500	1050	1000	July 1951
Kearny	7	145	2350	1100	1050	Mar. 1953
	8	145	2350	1100	1050	

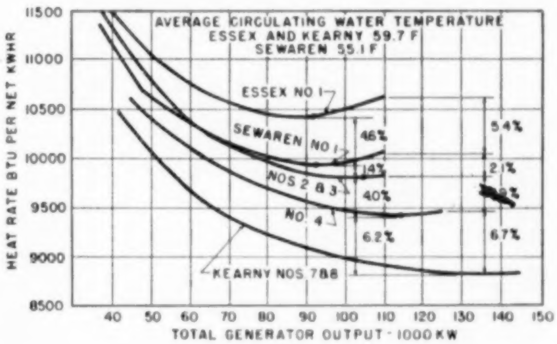

Fig. 1 Calculated Plant Heat Rates

[1] Chief Engineer, Electric Engineering Department, Public Service Electric and Gas Company. Fellow ASME.

[2] "The Design of Sewaren Generating Station and No. 1 Unit at Essex Station, Public Service Electric and Gas Company," by F. P. Fairchild, Trans. ASME, vol. 72, 1950, pp. 247-266.

Contributed by the Power Division and presented at the Annual Meeting, New York, N. Y., November 29-December 4, 1953, of The American Society of Mechanical Engineers.

Note: Statements and opinions advanced in papers are to be understood as individual expressions of their authors and not those of the Society. Manuscript received at ASME Headquarters, July 22, 1953. Paper No. 53—A-71.

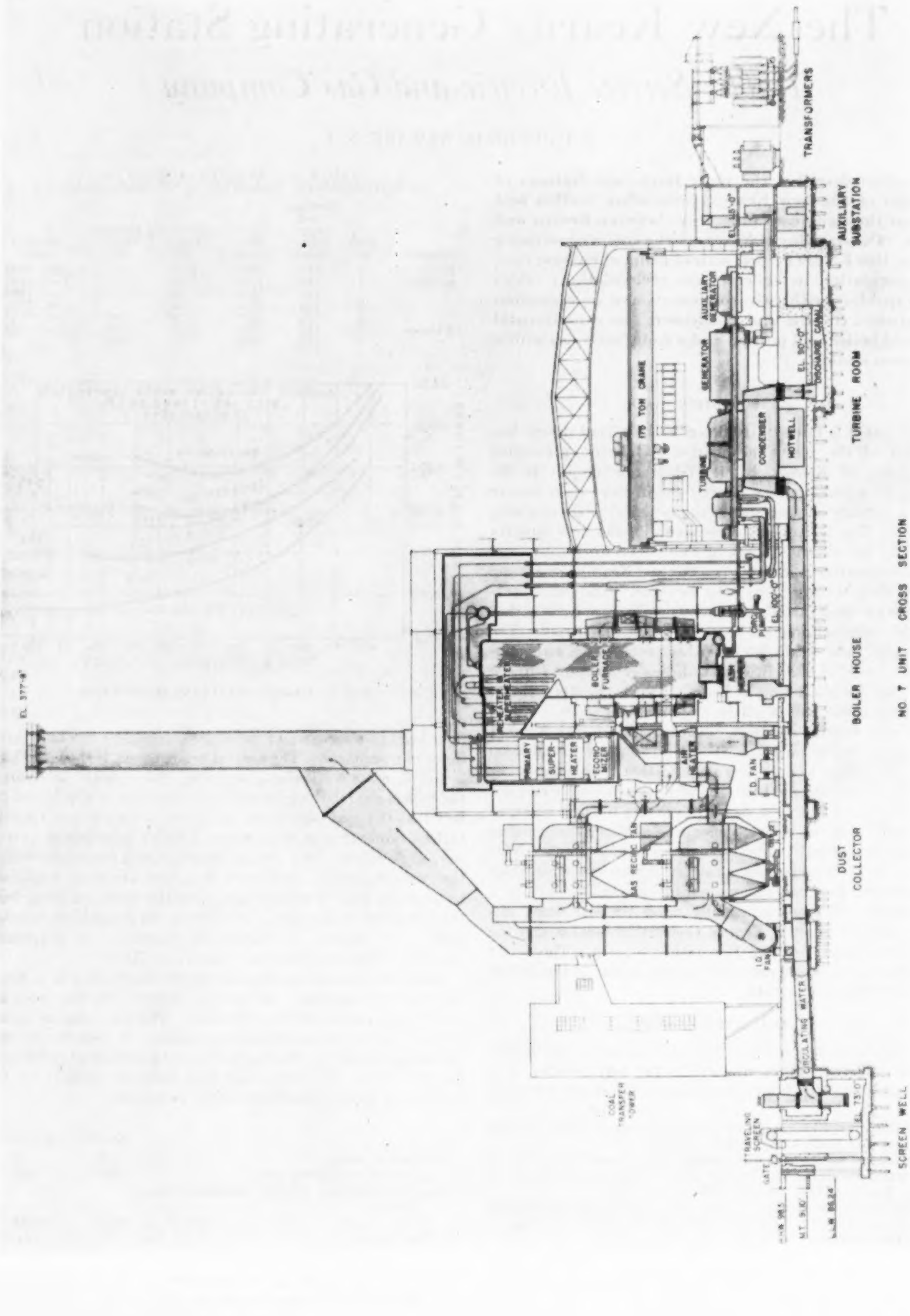
TRANSFORMERS
AUXILIARY SUBSTATION
TURBINE ROOM
BOILER HOUSE
DUST COLLECTOR
SCREEN WELL
NO 7 UNIT CROSS SECTION
175 TON CRANE
TURBINE
GENERATOR
AUXILIARY GENERATOR
CONDENSER
HOTWELL
DISCHARGE CANAL
EL 90'-0"
EL 100'-0"
EL 377'-8"
BOILER FURNACE
PRIMARY SUPER-HEATER
ECONO-MIZER
AIR HEATER
F.D. FAN
GAS RECIRC FAN
I.D. FAN
CIRCULATING WATER
COAL TRANSFER TOWER
TRAVELING SCREEN
GATE
EL 73'-0"

Fig. 2

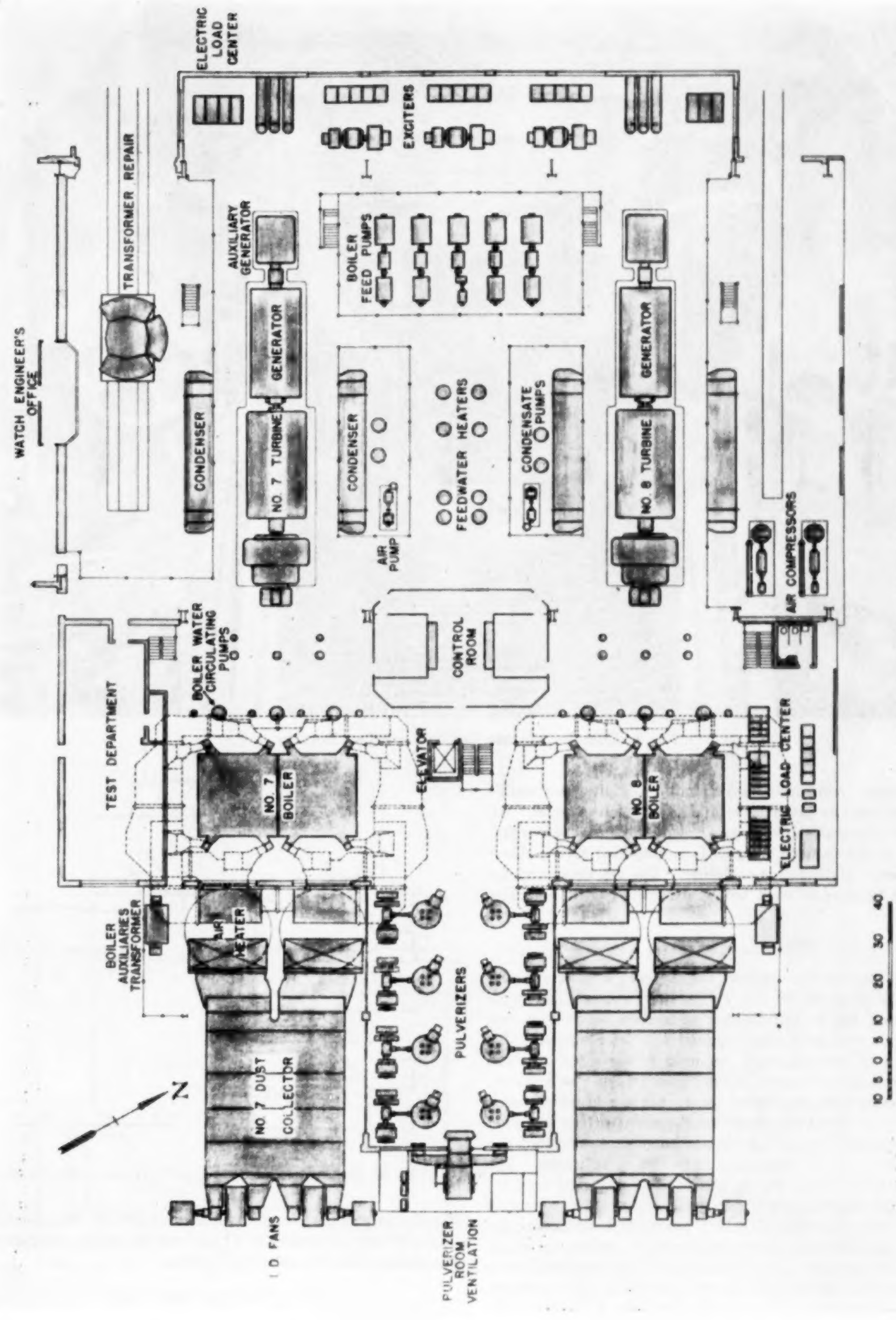

OPERATING FLOOR PLAN
NO. 7 & 8 UNITS

FIG. 3

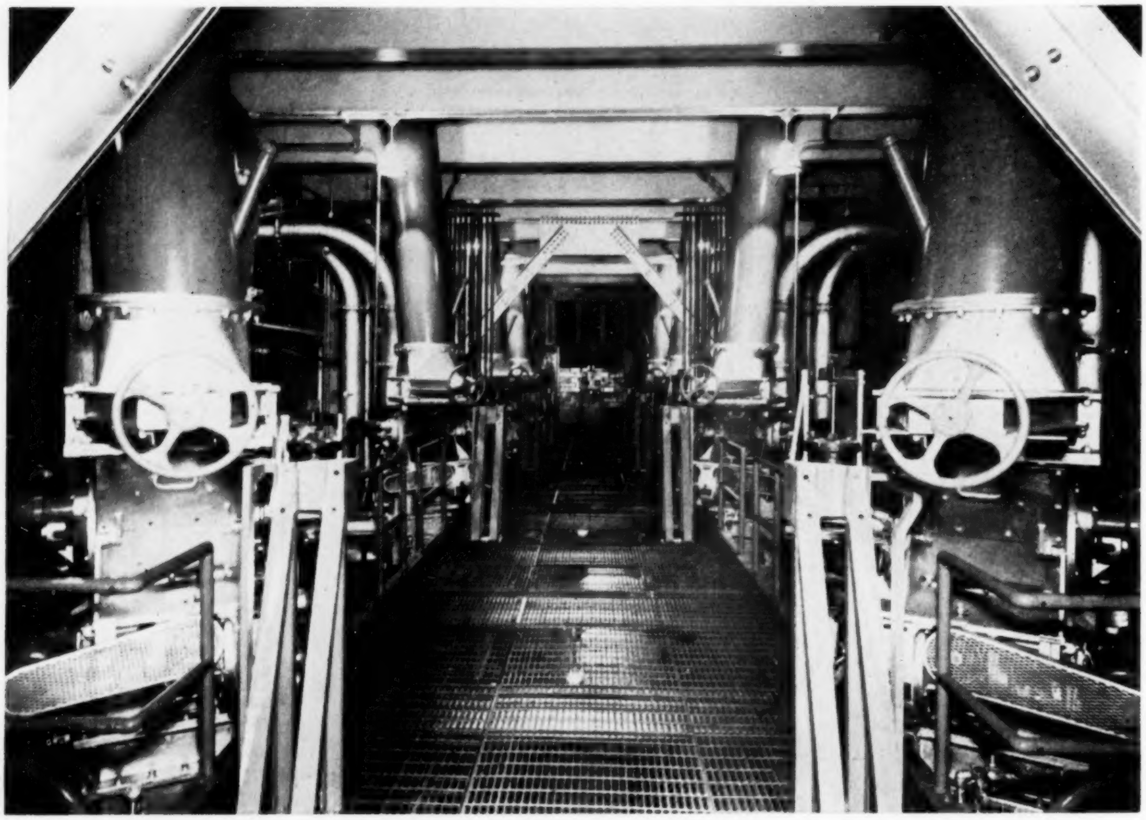

Fig. 4 Coal-Pulverizer Feeders for Two Boilers

service buildings, condenser cooling-water conduits, and auxiliary buildings such as gatehouses, and intake screen wells. All parts of the boilers are out-of-doors except the burner areas and the bottom of the furnace. Fig. 5 is a simplified sketch showing the extent of the building enclosure. The top drum and the three steam headers of each boiler are enclosed in the boiler casing.

Feedwater System

The feedwater-system diagram for Kearny, Fig. 6, is quite similar to the diagram for No. 4 Unit at Sewaren. The principal difference lies in the number of heaters before the feed pump, six per unit at Kearny against four at Sewaren. The total number of heaters, eight per unit, is the same. At full load, the pumping temperature is 395 F, against 265 F at Sewaren. Several schemes were considered to provide a cold-water emergency supply for the feed pumps in the event of the loss of a condensate-booster pump. A simple head tank required too much height; a pressurized tank was too complicated. The solution of the problem was to provide one electrical feed for each set of pumps, with the result that a failure of either pump stops both the condensate-booster pump and its associated boiler feed pump, leaving the remaining set of pumps operating. The condensate section of the condensate-booster pump takes its suction from the 10,000-gal storage hot well of the condenser. The spare feed pump can be paired with any of the four condensate-booster pumps of the two units. There is a cold-water connection from the head tank to feed-pump suction which is

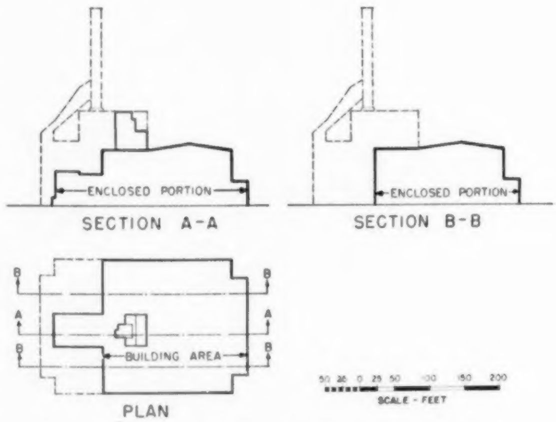

Fig. 5 Enclosed and Outdoor Portions of the Plant

effective at pumping temperatures below 275 F. A considerable saving in cost of heaters and high-pressure piping resulted from this change from the Sewaren diagram.

Steam-Generating Units

As compared to Sewaren the novel features of the Kearny boilers include controlled circulation, pressurized firing, twin

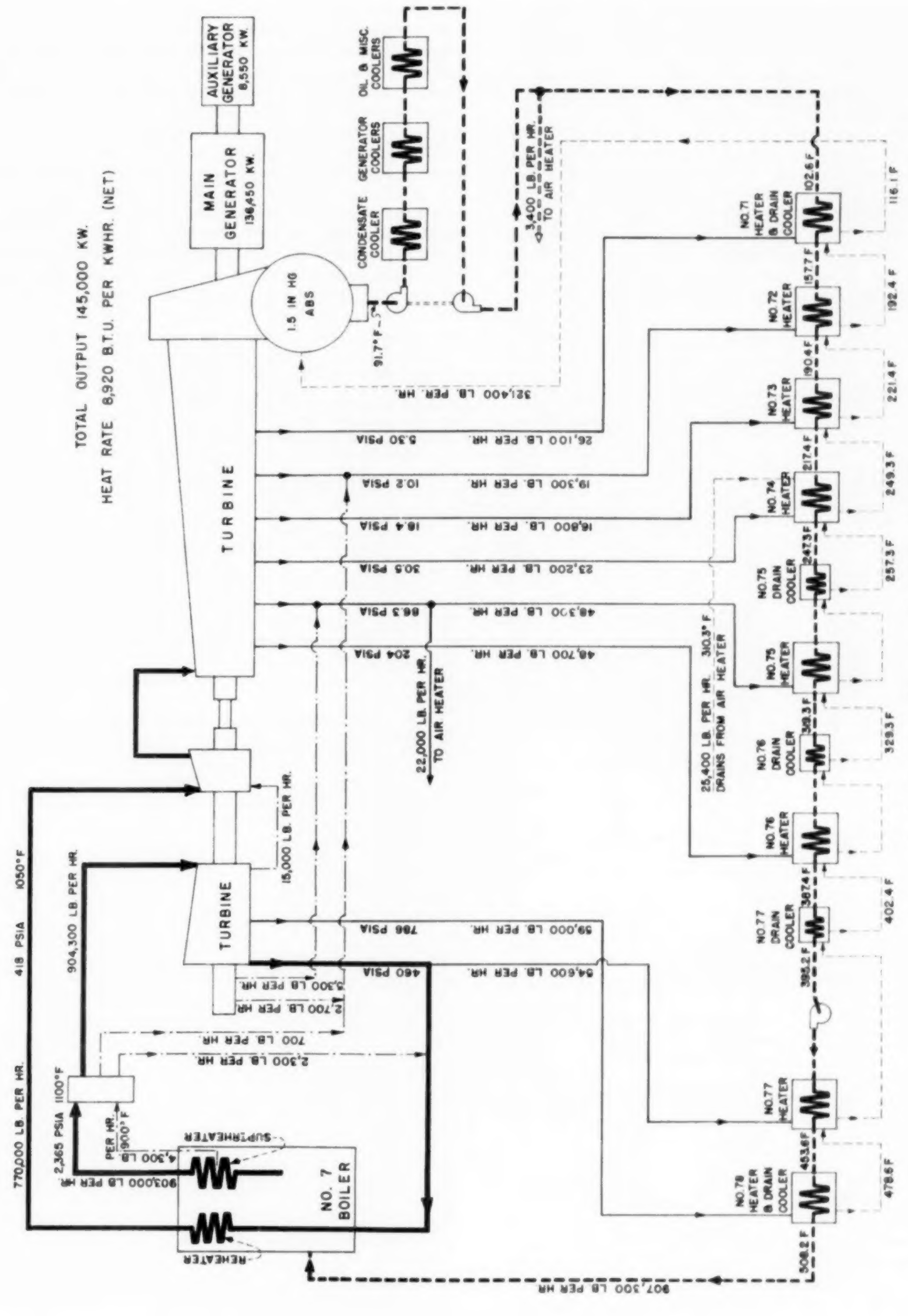

FIG. 6 DIAGRAM OF STEAM AND FEEDWATER SYSTEMS

furnaces, flue-gas recirculation, and higher steam temperatures and pressures. They have water-walled, divided furnaces of continuous-discharge, wet-bottom type. Each of the twin furnaces is about 20 ft square. The dividing waterwall has large openings to equalize furnace pressure. Fig. 7 is a cross-section elevation of the boilers.

The high-temperature stage of the superheater, which is located at the exit of the furnace, has its pendant tubes arranged in platens widely spaced to take advantage of radiant heat and to reduce fouling. These are shown in Fig. 8 which is a photograph made after preliminary oil firing but before coal had been burned. The reheater, which also has pendant tubes but not in platens, follows the high-temperature superheater in the gas path. In the downward pass, the gases flow over the three sections of horizontal tubes of the primary superheater, then the economizer, and finally the Ljungstrom air heaters. At this point the flow splits as it enters the two decks of flue dust collectors which are of the combined mechanical-electrostatic type. The width of single-deck collectors of equal efficiency was prohibitive. While the boilers normally operate as pressurized units, using only the forced-draft fans, they are provided with induced-draft fans to permit suction firing.

The gas-recirculation fans take part of the relatively cool flue gases leaving the economizer and deliver it to furnace ports located between the middle and lower levels of burners. By thus providing a means of increasing the mass flow through the heat-exchange surfaces, the control afforded by gas recirculation makes it possible to maintain design steam temperature with a lower furnace temperature when burning coal, thus minimizing slagging. These fans also perform the important function of

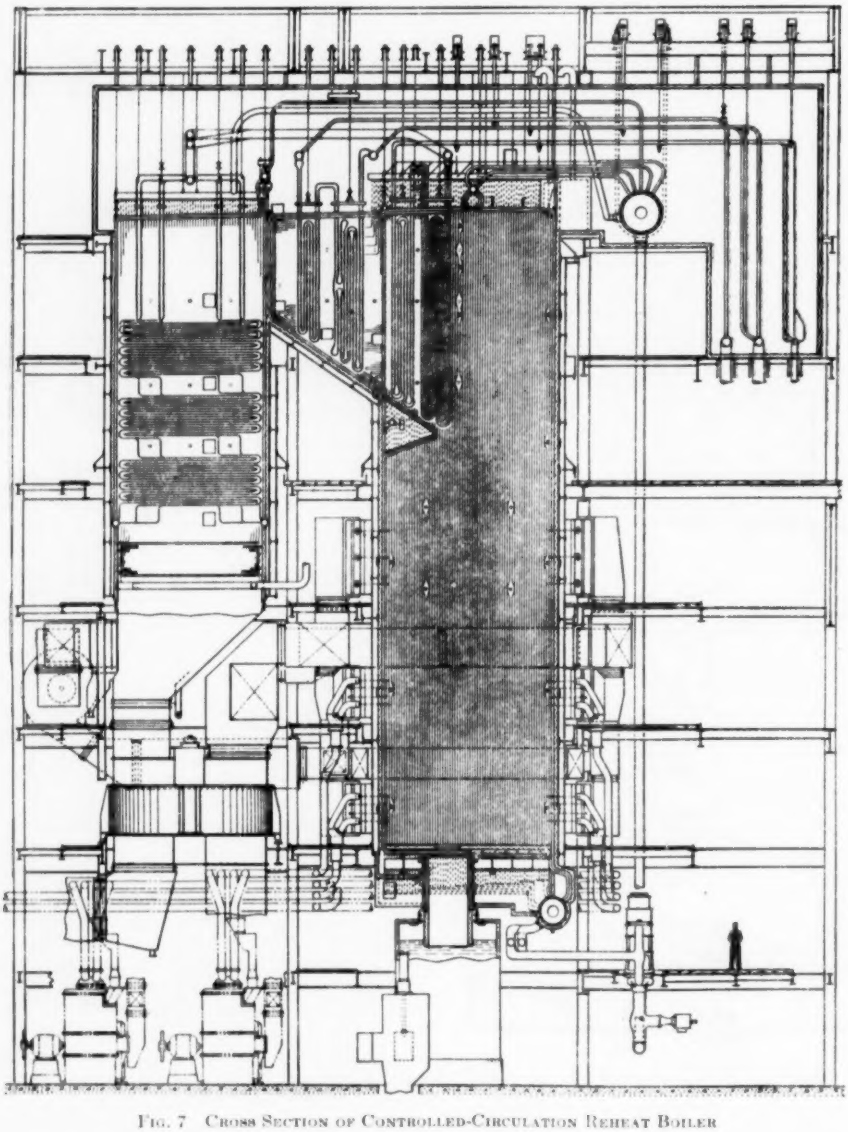

Fig. 7 Cross Section of Controlled-Circulation Reheat Boiler

making it possible to attain design steam temperature when burning oil. There are two gas-recirculating fans per boiler. Spray desuperheating is provided in both the superheater and reheater for steam-temperature control.

Because the boilers are designed for controlled circulation, considerably smaller furnace-wall tubes are used; $1^1/_2$ in. and $1^5/_8$ in. OD at Kearny against 3 in. and $3^1/_4$ in. OD at Sewaren. Each tube is provided with an orifice which is designed to control the flow so that it does its proper share of work. Design heat-transfer rates can be higher for controlled circulation because of known water velocity and relatively thinner tube walls.

Gas-leak tightness of the pressurized furnace is attained by making the pressure barrier at the waterwall tubes, each of which is welded to a bar spacer placed between adjacent tubes. Most of the joining for this construction was done in the shop, and the waterwalls were shipped to the site in panels ranging in width from 15 to 24 tubes, and in length from 24 ft to 49 ft. Fig. 9 shows the joints between four panels with the tube butt welds completed. This design feature avoids the necessity of constructing the furnace casing to be leaktight. It also effected a saving in the erection cost of the waterwalls.

For controlled circulation, each boiler has three vertical, single-stage circulating pumps, each rated for 40-psi differential head at a flow of 7300 gpm. Two pumps operate at full load. The boiler has been operated up to 145,000 kw with one circulating pump.

Turbine Generators

The turbine generators are unique in respect to their elevated steam conditions, 2350 psig, 1100 F at throttle and 1050 F reheat temperature. They are tandem-compound, 3600-rpm machines consisting of a high-pressure section, a single-flow reheat section, and a triple-flow low-pressure section, as shown in Fig. 10. Before entering the reheat section, the reheated

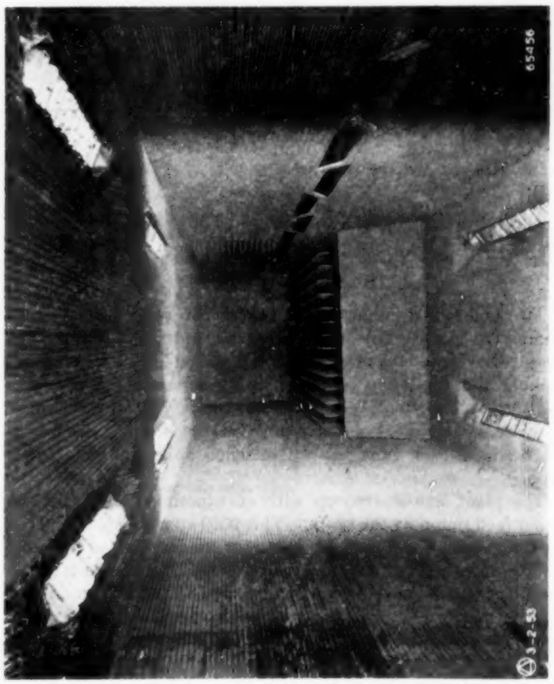

Fig. 8 Boiler Furnace After Initial Firing With Oil

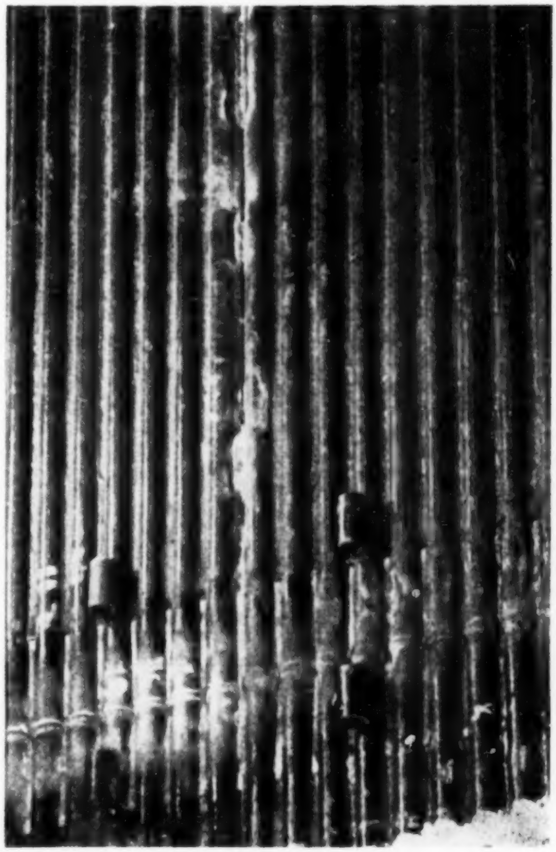

Fig. 9 Close-Up Showing Field-Welded Joints of Four Furnace-Wall Panels
(Welding not completed.)

steam returns to the inner portion of the high-pressure element and does work in three stages before crossing over to the intercept valves at the inlet of the reheat section. This arrangement saves the intercept valves from exposure to 1050 F steam. It also groups the high-temperature parts compactly to improve thermal-stress conditions in shaft and casing.

The side exhausts in the lower half of the low-pressure element make it possible to place the operating floor only 15 ft above the ground floor. A comparison of the Kearny and Sewaren turbine-exhaust arrangements is shown in Fig. 11.

Each turbine drives two generators in tandem. The main generator makes the outgoing product while the auxiliary generator supplies power to run the vital auxiliaries. The practice of installing shaft-end auxiliary generators started in the Public Service system in 1946, with No. 1 Unit at Essex Generating Station. When No. 8 is running at Kearny, there will be seven machines of this type in the system, as listed in Table 1. In 1946 there were two principal reasons for installing an auxiliary shaft-end generator. First, since all station auxiliaries were electric-motor driven, it seemed desirable to keep them running independently of electrical system disturbances in order to keep the boiler and turbine on the line ready to pick up load at the end of the disturbance. Second, as the size of the main generator limited the capability of the unit at that time, the auxiliary shaft-end generator made possible a gain in capacity

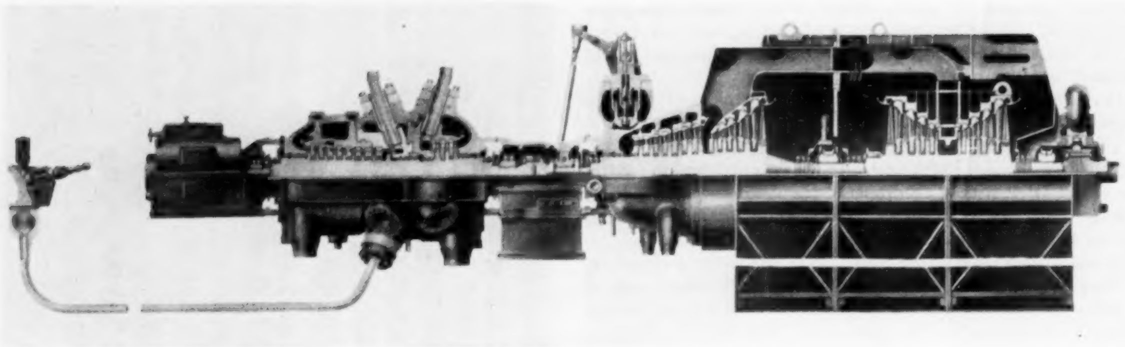

FIG. 10 TURBINE CROSS SECTION

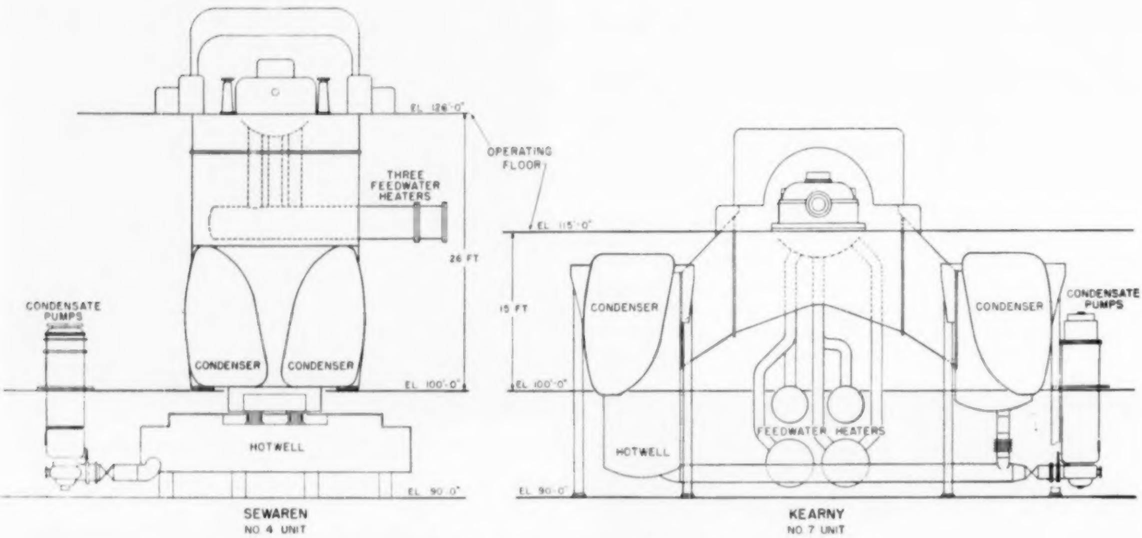

FIG. 11 TURBINE-EXHAUST ARRANGEMENT, KEARNY VERSUS SEWAREN

at a small incremental cost. Building volume was not increased because the auxiliary generator is placed in the space required to withdraw the rotor of the main generator. With the addition of reheat, the auxiliary generator has the added advantage of providing a fairly substantial residual turbine load in the event of the loss of the main generator. This keeps the turbine on the line, under control, and avoids closing of intercept valves and operation of safety valves.

Condensers

The Kearny condensers are arranged as twins to accommodate the side-exhaust turbine. In reference to the Sewaren condensers, see Fig. 11, the tube banks are inverted so that the turbine exhaust enters horizontally and flows up to the air cooler at the top, while the condensate falls down to the hot well. Deaeration of make-up and drains takes place in the steam space ahead of the tube banks. Each twin condenser is supported at about the same elevation as the turbine supports by four vertical columns connecting to support brackets at the top of the shell. This arrangement affords restraint vertically and freedom to expand horizontally by flexure of the vertical columns. This is similar to the arrangement used for two smaller outdoor installations in the southwest. Fig. 12 shows the No. 7 condenser during erection at Kearny.

Boiler Feed Pumps

Two boiler feed pumps in series with two condensate-booster pumps (re-entry type) are required to feed one boiler at full load. One spare boiler feed pump is installed for the two boilers, making the total five pumps. The spare pump is arranged to serve either unit. It does not start up automatically. A spare condensate-booster pump is kept in the storeroom. At Sewaren each unit has an installed spare pump of each type.

The plant was started up with an experimental, high-speed boiler feed pump as the spare. This 9000-rpm pump, compared to the conventional pumps, had four stages instead of nine, weighed (with gear) about 20 per cent less, and fitted into the same space. It was specified to operate with the same driver and the same pumping conditions. In preliminary operation certain modifications were indicated and the pump is being rebuilt and will be placed in trial operation at a later date. In the meantime, a conventional pump intended for Burlington Generating Station was installed in its place.

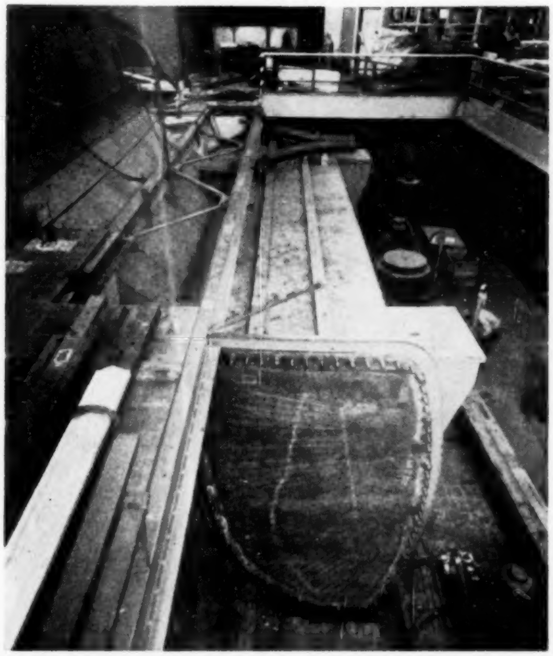

Fig. 12 Turbine-Exhaust Connection—During Construction

Central Control

One room, soundproofed and air conditioned, is provided for all the controls of the two units. Compared to Sewaren, the panel components are smaller and more compactly arranged. From his regular station the operator sees only the instruments that are necessary to operate the plant. Instruments for record purposes only are located in the wings of the control room. Telemetering is used more extensively at Kearny. Television apparatus is provided for viewing combustion conditions in one boiler. Space is provided for similar apparatus for the second boiler after a trial period on the first. Control-panel area for one unit at Kearny is about 350 sq ft, compared to 520 sq ft for one unit at Sewaren.

High-Temperature Parts

The entire main steam system, from the superheater-outlet header to the first-stage nozzle of the turbine, is made of austenitic stainless steel, chromium-nickel-columbium stabilized. This includes the main steam piping, turbine stop valves, control valve chest, and a section of the inner high-pressure turbine shell. The materials of the superheater tubes, starting from the primary end, are carbon steel, carbon-molybdenum steel, chromium-silicon-molybdenum steel, chromium-nickel-titanium stabilized steel. The main steam piping was made by forging and boring.

The hot reheat piping is made of $2^1/_4$ per cent chromium–1 per cent molybdenum steel, rolled from plate and welded. The materials of the reheater tubes of the steam generator, starting from the low-temperature end, are carbon-molybdenum steel, chromium-silicon-molybdenum steel, chromium-nickel-titanium

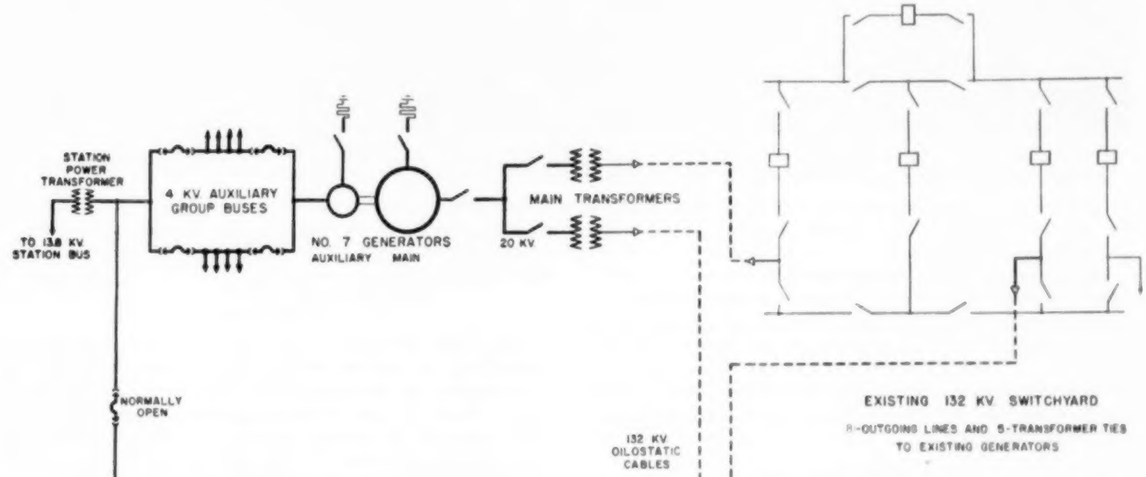

Fig. 13 One-Line Electrical Diagram

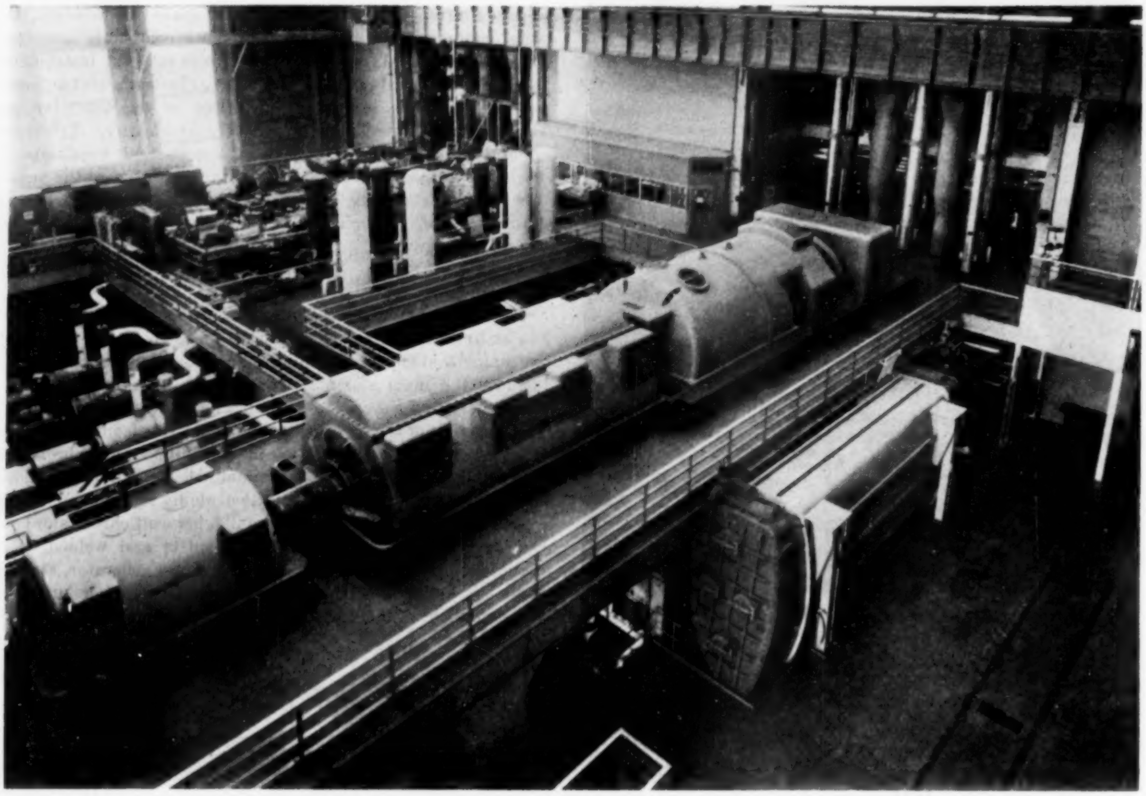

Fig. 14 Turbine Room—No. 7 in Foreground

stabilized steel. The tubes carrying the reheated steam outside the furnace to the principal header are made of chromium-molybdenum steel.

The welded joints in the main steam piping and the turbine high-temperature steam piping were made without backing rings, by the Heliarc inert-gas shielded tungsten-arc process for the first pass, and the shielded metal-arc process for the completion of the weld. A slight pressure of argon gas was applied to the inside of the joint during the first and second passes. Radiographic inspection was made on all joints over 3-in. pipe size or over $^{1}/_{2}$-in. wall thickness.

Coal-Handling System

Since the five units of boilers of the original station have been converted to oil-firing, the existing station facilities are adequate to supply unloading and storage of coal for the new station. Coal is conveyed from the existing station bunker to eight silos, one for each pulverizer. Each silo holds a 4-hr supply at full-load operation. Conveyer belts deliver the coal from the bunkers to small hoppers serving Redler conveyers, which are arranged to keep the silos full automatically. The coal for each boiler is weighed on the conveyer belts feeding the hoppers of the Redler conveyers.

Ash and Dust-Handling Systems

The ash and dust systems are separate at Kearny. The dust system is arranged so that it can be refired in the furnaces or sluiced by jetting to the disposal area. The ash system includes facilities for jetting the slag to the disposal area or to a dewatering bin for sale.

Electrical

Each main generator is connected by 20-kv stove-pipe bus construction to two 100,000-kva main transformers. The 132-kv leads from the transformers are oilostatic cable to the switchyard. There are two 9000-kva auxiliary power transformers with automatic throw-over switching to pick up the auxiliary power load in the event of failure of the auxiliary generators. The main electrical one-line diagram is shown in Fig. 13.

Summary

The objectives in the Kearny design were to achieve a plant design which, like Sewaren, would be a straightforward, simple arrangement that, with central control, would simplify operation and require minimum operating effort; a steam cycle that takes advantage of elevated steam conditions; and a simple, relatively small building for low maintenance and first cost.

Acknowledgment

The author gratefully acknowledges the assistance of Mr. P. A. Salmon and others of the Public Service Electric and Gas Company.

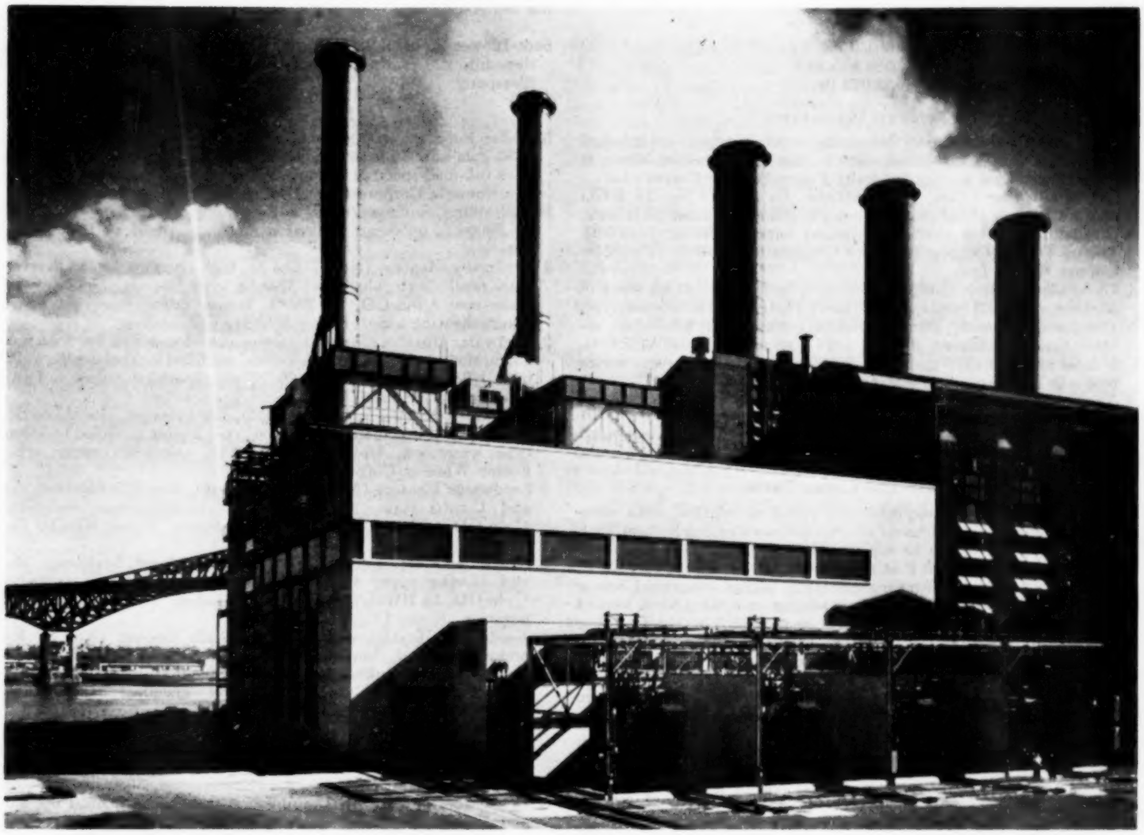

Fig. 15 Exterior View

MECHANICAL EQUIPMENT NO. 7 AND 8 UNITS
KEARNY GENERATING STATION

Turbine generators	General Electric Company
	Turbines
Number	2
Rated capacity	145,000 kw
Steam pressure	2350 psig
Steam temperature	1100 F
Reheat steam temperature	1050 F
Exhaust steam pressure	1.5 in. Hg abs
Speed	3600 rpm
Type	Tandem-compound, triple-flow, reheat, side exhaust
Number of stages:	
High-pressure section	9
Reheat section	10
Low-pressure section (triple flow)	5
Total	24
Extraction points	8
	Generators
Main generators	2—a-c, 3-phase, 60-cycle, 20,000 volts, 3600 rpm, 0.85 pf, 2-pole, wye-connected, hydrogen-cooled, single winding
Generator ratings	137,500 kw at 30 psig hydrogen pressure 129,082 kw at 15 psig hydrogen pressure 112,245 kw at 0.5 psig hydrogen pressure
Main generator exciters	3—400 kw, 375 volts, 900 rpm, self-excited, shunt-wound, including one spare
Auxiliary generators	2—a-c, 3-phase, 60-cycle, 4160 volts, 3600 rpm, 10,000 kw, 0.8 pf, 2-pole, wye-connected, air-cooled, single winding
Auxiliary generator exciters	3—45 kw, 250 volts, 900 rpm, self-excited, shunt-wound, including one spare
Generator ventilation	Self-ventilated with shaft-mounted fans
Hydrogen coolers (main generator)	8 fin-tube, two-pass, vertically mounted in generator housing, 1400 gpm cooling water at 95 F and 100 psig
Air coolers (auxiliary generator)	4 fin-tube, two-pass, vertically mounted in auxiliary generator housing, 270 gpm cooling water at 95 F and 100 psig
Lubrication system	2 oil coolers using 880 gpm cooling water at 104 F and 100 psig, 4 oil pumps: 1 main (shaft-driven), 2 a-c motor-driven auxiliary and 1 d-c motor-driven emergency for shutting down
Dimensions and weights of unit:	
Length, over-all	103 ft 5 1/8 in.
Width	19 ft
Height	11 ft 2 in.
Net turbine weight	735,000 lb
Net weight of main generator	603,307 lb
Net weight of auxiliary generator	131,200 lb
Total	1,469,507 lb

Dimensions of 3-piece exciter set:

Length	17 ft 2 in.
Width	6 ft 0 in.
Height	5 ft $8^3/_4$ in.
Net weight of set	32,075 lb

Turbine Auxiliaries

2 Condensers, single-pass, deaerating, surface-type, welded-steel shells, cast-iron water-boxes, each consisting of two 35,000-sq ft units; 10,000-gal storage hot well; Foster Wheeler Corporation

10,300 Condenser Tubes, per condenser, $^7/_8$ in. OD No. 18 BWG seamless drawn aluminum brass and aluminum bronze, 30 ft long, parallel to turbine shaft, ends rolled without flaring. (10,000) Phelps Dodge Copper Products Corporation; (300) Yorkshire Copper Works, Ltd.

4 Circulating Water Pumps, vertical, mixed-flow, bottom suction, 50,000 gpm at 19 ft total head, 390 rpm; Foster Wheeler Corporation.

5 Condensate-Booster Pumps, vertical, centrifugal five-stage, re-entry type, condensate element 1325 gpm at total head of 226 ft, booster element 1295 gpm at 945 ft total head, 1150 rpm. Spare pump in storeroom. Worthington Corporation

4 Vacuum Pumps, single-stage, rotating-plunger type, 550 cfm at 1.0 in. Hg, 400 rpm; Kinney Manufacturing Company

2 Turbine Oil Conditioners, dry type with 629-gal storage compartment, filtering capacity 1080 gph; Bowser, Incorporated

Steam-Generating Units

2 Boilers, two-drum, watertube, controlled circulation, with completely water-walled furnaces and continuous slagging bottom, each rated at 955,000 lb per hr continuous, and 1,055,000 lb per hr for 4 hr, at 2350 psig, 1100 F at superheater outlet, reheat to 1050 F, pressurized or suction furnace operation, tilting, tangential corner firing, coal burners at two levels, oil-firing on a third level, welded steel casing. Upper drum 54 in. ID × 48 ft × 5 in. thick; lower drum 36 in. ID × 43 ft × $3^{11}/_{16}$ in. thick; furnace tubes $1^1/_2$ in. and $1^5/_8$ in. OD; Combustion Engineering, Inc.

2 Reheaters, convection type, 232 four and a half loop elements presenting a heating surface of 14,344 sq ft, 1050 F outlet temperature at 800,000 lb per hr; temperature control by spray desuperheaters; Combustion Engineering, Inc.

2 Superheaters, two-stage, convection-type, high-temperature stage in two sections having 12,900 sq ft total heating surface, $2^1/_8$-in-OD tubes, low-temperature stage having 81,000 sq ft heating surface, 2-in-OD tubes, superheat control by desuperheaters; Combustion Engineering, Inc.

2 Economizers of the continuous-tube counterflow type, 2-in-OD tubes staggered in horizontal rows presenting 28,300 sq ft of heating surface, inlet water at 515 F and outlet water at 552 F with steam flow of 955,000 lb per hr; Combustion Engineering, Inc.

4 Air Heaters, each unit having two Ljungstrom regenerative-type heaters, vertical shaft, each having 67,500 sq ft heating surface; Air Preheater Corporation

8 Desuperheaters, four for each unit, two for the superheater of the steam-assisted spray type and two for the reheater of the pressure-spray type; Combustion Engineering, Inc.

6 Boiler Water Circulation Pumps, vertical, centrifugal, single-stage, 7300 gpm at 154 ft total head, 1165 rpm, including one spare for each boiler; Pacific Pumps, Inc.

4 Forced-Draft Fans, variable speed, 152,800 cfm at 80 F and 40.37 in. water, 1130 rpm maximum, driven through hydraulic couplings; American Blower Corporation

4 Hydraulic Couplings for Forced-Draft Fans, driven by constant-speed, 1500-hp motors, each having an air-cooled hydraulic fluid cooler unit with nine 1-hp motor-driven air-circulating fans; American Blower Corporation

4 Induced-Draft Fans, 255,700 cfm at 327 F and 23.7 in. water, 860 rpm, output controlled by inlet louver dampers; American Blower Corporation

4 Gas Recirculation Fans, 53,500 cfm at 683 F to a total head of 14.25 in. water, 880 rpm, radial paddle type; Sturtevant Division, Westinghouse Electric Corporation

Soot Blowers, automatic, sequential, pneumatically operated, air blowing, retractable units operate on 250 psi, air-puff units on 350 psi

Location	No. per boiler and type
Furnace	26, retracting
Superheater and reheater	14, retracting; 2, telescopic
Economizer and low-temperature superheater	6, rotating air puff
Induced-draft duct	2, stationary air puff
Air heaters	2, single nozzle

Diamond Power Specialty Corporation (soot blowers, furnace through induced-draft duct); Air Preheater Corporation (air heaters)

Soot-Blower Control and Power Air Dryer, dual tower, silica-gel desicant, 220 cfm maximum; The C. M. Kemp Manufacturing Company

Feedwater System

5 Boiler Feed Pumps, horizontal, barrel-type, 9-stage, centrifugal, 1380 gpm at 6650 ft total head, driven through hydraulic couplings with full-load speed of 3465 rpm, one installed spare for two units; Worthington Corporation

5 Hydraulic Couplings, for boiler feed pumps, variable speed, driven by 3000-hp, 3600-rpm induction motors; American Blower Corporation

4 Feedwater Heaters (Nos. 7 and 8), high-pressure, closed, vertical with head down, shell and U-tube type, 2-pass, lockhead-type water-box, $^5/_8$-in-OD, 17 BWG, monel tubes, constructed with desuperheating zone; Foster Wheeler Corporation

2 Feedwater Heaters (No. 6), low-pressure, closed, vertical with head down, shell and U-tube type, 2-pass, modified lockhead-type water-box, $^5/_8$-in-OD, 18 BWG, 80/20 copper-nickel tubes; Foster Wheeler Corporation

4 Feedwater Heaters (Nos. 4 and 5), low-pressure, closed, vertical with head down, shell and U-tube type, 2-pass, modified lockhead-type water-box, $^5/_8$-in-OD, 18 BWG, arsenical copper tubes; Foster Wheeler Corporation

2 Feedwater Heaters (No. 3), low-pressure, closed, horizontal, shell and U-tube type, 2-pass, modified lockhead-type water-box, $^3/_4$-in-OD, 18 BWG, arsenical copper tubes; Foster Wheeler Corporation

2 Feedwater Heaters (No. 2), low-pressure, closed, horizontal, shell and U-tube type, 4-pass, modified lockhead-type water-box, $^3/_4$-in-OD, 18 BWG, arsenical copper tubes; Foster Wheeler Corporation

2 Feedwater Heaters with Integral Drain Coolers (No. 1), low-pressure, closed, horizontal, shell-and-tube type with floating head, 4-pass (including one for drain cooling), modified lockhead-type water-box, $^5/_8$-in-OD, 18 BWG, arsenical copper tubes; Foster Wheeler Corporation

4 Drain Coolers (Nos. 6 and 7), low-pressure, vertical with head up, shell and U-tube type, single-pass, modified lockhead-type water-box, $^7/_8$-in-OD, 18 BWG, 80/20 copper-nickel tubes; Foster Wheeler Corporation

2 Drain Coolers (No. 5), low-pressure, vertical with head up, shell and U-tube type, single-pass, modified lockhead-type water-box, $^5/_8$-in-OD, 18 BWG, arsenical copper tubes; Foster Wheeler Corporation

2 Condensate Coolers, horizontal, shell-and-tube, single-pass, salt-water counterflow in tubes, capable of cooling 900,000 lb per hr of condensate from 115 F to 95 F with salt water at 85 F maximum, 5200 sq ft cooling surface, 110 psig maximum pressure; Condenser Service and Engineering Company

Demineralizing Equipment, two 50-gpm demineralizing tanks to treat condensate make-up; Illinois Water Treatment Company

1 Condensate Cooler, horizontal shell-and-tube to cool 100 gpm of condensate to 100 F ahead of demineralizers; Condenser Service and Engineering Company

Pulverizing Equipment

8 Pulverizers, Raymond bowl type, pressurized, integral exhauster, nominal capacity 18 tons per hr each, based on coal with grindability of 60 Hardgrove scale, 8 per cent moisture, and pulverizing 75 per cent through a 200-mesh screen; Combustion Engineering, Inc.

8 Pyrites Conveying Systems, one per pulverizer, capacity 15 tons per hr, 450 gpm salt water at 100 psig; United Conveyor Corporation

Coal Handling

4 Redler Conveyers, 19-in., horizontal, "over and under" arrangement, 150 tons per hr capacity, operating as feeders from bunkers to belt conveyers

2 Redler Conveyers, 19-in., horizontal, "over and under" arrangement, 165 tons per hr capacity, each serving four silos of one boiler

1 Redler Conveyer, 19 in., horizontal, closed-circuit arrangement, 165 tons per hr capacity, serving eight silos of two boilers; Stephens-Adamson Manufacturing Company

4 Belt Conveyers, two 30-in-wide, 270-ft-long conveyers with 155 tons per hr capacity; two 30 in. wide, 103 ft long with capacity of 160 tons per hr.; Robins Engineers Division, Hewitt-Robins Inc.

2 Weightometers; Merrick Scale Manufacturing Company

2 Magnetic Separators; Dings Magnetic Separator Company
32 Coal Valves; Stock Equipment Company

ASH HANDLING

Ash System, each boiler having two ash-storage hoppers, 60,000-lb slag capacity, sump tank, clinker grinder, and jet pump; The Allen-Sherman-Hoff Company

DUST HANDLING

4 Dust Collectors on Two Levels, integral Multiclone-Cottrell; each Multiclone unit has 396 cast-iron tubes and each Cottrell electric precipitator has 20 electrode curtains on 10-in. centers forming 19 gas ducts; each boiler has 24 dust hoppers, draft loss through precipitators 3.0 in. water at 460,000 cfm gas flow, 97 per cent efficient; Western Precipitation Corporation
2 Screw Conveyers, 14 in. diam, horizontal, motor-driven, dust-tight, capacity of 6 tons per hr fly ash for refiring system; Link Belt Company
4 Flight Conveyers, two 11-in. side-pull 90-deg Redlers handling 25 tons per hr, two 5-in. horizontal Redlers handling 3 tons per hr; Stephens-Adamson Manufacturing Company
2 Dry-Dust Pumping Systems, Fuller-Kinyon, each to pump dust to storage bin, each capable of 25 to 28 tons per hr fly ash; Fuller Company
48 Dust Feeder Valves, rotary vane feeders on precipitator hoppers, 10,000 lb per hr fly ash each; 12 on gas recirculating dust-collector hoppers 16,000 lb per hr for a group of six; United Conveyor Corporation
Wet-Dust-Handling System, 4 × 6 in. hydrovactor requiring 710 gpm water, two type C windswept valves; The Allen-Sherman-Hoff Company
4 Gas Recirculation System Fly Ash Collectors, multitube mechanical type with 147 tubes; draft loss at 60,000 cfm is 0.6 in. water; American Blower Corporation

FUEL-OIL HEATERS

3 Fuel-Oil Heaters, straight-tube, fixed-bundle, oil inside tubes, heat 180 gpm from 100 F to 225 F with steam at 350 psig, 500 F; The Griscom-Russell Company

AIR COMPRESSORS

3 Air Compressors, two for soot blowers, one for station service, horizontal, rotary, two-stage, low-pressure, 1592 cfm at 125 psig, 575 rpm; Fuller Company
2 Booster Air Compressors for soot blowers, horizontal, duplex single-stage, reciprocating, high-pressure (120 to 500 psi); 1500 cfm at 500 psi, 300 rpm; Ingersoll-Rand Company
3 Control Air Compressors, horizontal, carbon-ring, single-stage, 300 cfm, at 80 to 100 psi, 300 rpm; Ingersoll-Rand Company
1 Dust System Air Compressor, horizontal, rotary, single-stage, 603 cfm at 27 psi; Fuller Company
3 Control Air Dryers, dual tower, silica-gel desiccant, 300 cfm air; C. M. Kemp Manufacturing Company

PUMPS

4 Heater Drain Pumps, vertical, centrifugal, two-stage, 800 gpm at 36 ft total head, 1170 rpm; Worthington Corporation
3 Fuel-Oil Pumps, vertical, screw-type, 180 gpm, 1865 ft total head, 1150 rpm; Quimby Pump Division, Warren Steam Pump Company, Inc.

MECHANICAL CONTROL SYSTEMS

Combustion Control; Hagan Corporation
Fuel-Oil Pressure Control; Hagan Corporation
Temperature Controls; The Swartwout Company
Water-Level Controls; The Swartwout Company
Three-Element-Type Feedwater Control; Bailey Meter Company
Superheat and Reheat Temperature Control; Bailey Meter Company

INSTRUMENTS AND METERS

Boiler Meters; Bailey Meter Company
Miniature Indicators and Draft Gages; Bailey Meter Company
Multipoint Recorders for superheater and reheater-tube temperatures, bearing temperatures, and miscellaneous temperatures; Leeds and Northrup Company
Conductivity Recorders; Leeds and Northrup Company
Boiler Gage Glasses for boiler-drum water level; Diamond Power Specialty Corporation
Television Equipment for viewing furnace; Diamond Power Specialty Corporation
Ashcroft Duragages; Manning, Maxwell & Moore, Inc.
Sight-Flow Indicators, Water Level Gages; Ernst Water Column and Gage Company; Yarnall-Waring Company
Indicating Thermometers; Taylor Instrument Company
Liquid-Level Controllers; Moore Products Company; The Swartwout Company; Fisher Governor Company
Oxygen Recorders for combustion guide; Hays Corporation
Boiler Performance Indicators; Panalarm Products, Inc.

MAJOR ELECTRICAL EQUIPMENT

4 Main Transformers—100,000 kva, 20/138 kv; Westinghouse Electric Corporation
2 Station Power Transformers—9000 kva, 13.2/4.16 kv; Allis-Chalmers Manufacturing Company
Lightning Arresters on generator leads; General Electric Company
Oil Circuit Breakers—auxiliary power
1—Westinghouse Electric Corporation 2000 amp, 14.4 kv
1—Existing
Main Generator Leads—isolated phase, 5000-amp, 23-kv; Westinghouse Electric Corporation
Auxiliary Generator Leads—segregated phase, 2000-amp, 7500-volts; Westinghouse Electric Corporation
Auxiliary Power Switchgear—all metal-clad, 5 kv, Westinghouse Electric Corporation; 220 volts and 440 volts, I-T-E Circuit Breaker Company; Westinghouse Electric Corporation
High-Voltage Transformer Leads—4 lines of oilostatic pipe-type cable, 450 amp, 138 kv; Okonite Company
Motors; Allis-Chalmers Manufacturing Company; Westinghouse Electric Corporation; General Electric Company

DESIGNERS: Electric Engineering Department, Public Service Electric and Gas Company
BUILDERS: United Engineers and Constructors Inc.
ARCHITECTURAL CONSULTANT: Alfred Easton Poor

Discussion

W. H. ROWAND.[3] The Society and the authors are to be commended for the excellent papers[4] describing the early stages of a most interesting development in the design of steam generators.

This development is a striking example of some of the factors which have promoted the tremendous progress of the utility industry. Such factors—wholesome technological competition and courage to experiment on a sufficiently large scale—permit the acid test of commercial operation over a period of years to write the answer on the best ways to accomplish the desired results in the pressure range from 1700 to 2700 psi.

Our company has more than 30 natural-circulation boiler units operating in this pressure range and many have been operating for several years. We are now building 70 more units of similar designs for these pressures and, therefore, later judgment certainly can be made on a very broad base.

The comparison made by Messrs. Ryan and Crossan of the difference in weight and building volume between forced and natural-circulation boilers is not too good for generalization because the two units cited are not comparable. If the natural-circulation unit had a furnace division wall, and the same furnace design factors as the forced-circulation unit, the required building volumes would have been almost identical—and the saving in the weight of the tubing in the forced-circulation unit would have been less than 100 tons to balance against the additional buckstay steel weight, and the weight of the recirculating pumps. Incidentally, we have built scores of high-pressure natural-circulation boilers with furnace division walls; these have been operating successfully for years, and many more are now under construction.

[3] Vice-President, The Babcock & Wilcox Company, New York, N. Y. Mem. ASME.

[4] In addition to the present paper, this discussion has reference to "The Controlled-Circulation Boiler," by W. H. Armacost, and "Controlled Circulation at Chesterfield," by T. E. Crossan and W. F. Ryan. Published in this issue, pp. 715–748.

We do not believe that any academic factors, such as a difference of 30 to 50 deg in the average wall temperatures of the furnace tubes, will play a role in the long-term evaluation of forced and natural-circulation boilers, since boiler tubes fail because of internal and external corrosion, or because of several hundred degrees of overheating resulting from internal deposits or steam blanketing. Instead, we feel sure that the broad evaluation will be based on long-term analyses of first cost, operating reliability, operating flexibility, and operating cost.

Looking to the future, neither natural-circulation boilers nor the Lamont type of forced-circulation boiler described by the authors—nor, for that matter, other types of forced-circulation boilers such as the Steamotive or the Sulzer operating with spill-over—are suitable for operation at, and above, the critical pressure. It will be necessary for such operation, to use the once-through type of boiler such as the Universal Pressure steam generator we are now building for the Philo Station of the American Gas & Electric System. This type of unit does not require recirculating pumps, but instead, uses extra pressure developed by the feed pumps.

Author's Closure

The first unit initially carried full load on March 31, 1953. There is nothing to date to indicate any difficulty in the new Kearny operation so far as steam temperature or pressure is concerned.

In designing the boilers for this station, much consideration was given to the problem of slagging or deposits in the gas passages of the 1100 F and 1050 F superheaters. Experience with the units to date in this respect is quite satisfactory.

An unusual number of service interruptions has taken place, due principally to auxiliary difficulties—pumps for various services, heaters, gas recirculation fans, et cetera. The unit was shut down for several weeks in midsummer, due to the material of a defective seal weld in the turbine control valve having broken loose causing certain damage to the high-pressure turbine buckets and diaphragms. During this shutdown, some surface was removed from the reheater in order to reduce attemperator water to a minimum.

The second unit went into commercial operation November 10, 1953. There has been no further difficulty with either of the turbines.

The high-speed spare boiler feed pump mentioned in the paper developed casing leakage difficulties, to the extent that the manufacturer decided to redesign it. At present, the spare pump is of the same design as the other boiler feeders at Kearny.

Pressurized operation in the new Kearny Station has averaged so far only about 20 per cent. The furnace itself has been in general satisfactorily tight, the panel construction proving quite ideal in this respect. However leaks in the dust-removal system from the precipitators, difficulties with expansion joints, and sealing system in connection with ash removal from the furnace bottoms, and other such items have prevented continuous pressurization. Changes in these items being presently made should allow satisfactory operation.

As to controlled circulation, the only difficulties so far have been those resulting from boiler circulating pump design. Some of these difficulties have been alleviated, others will undoubtedly be in time.

The boilers perform very well, are fast-steaming, and reach a steady state, after load or other operating changes, very quickly. As to physical characteristics, it is interesting to note that each of these reheat boilers produces 20 per cent more kilowatts than the fourth unit at Sewaren, with a total weight of 15 per cent less.

An Experimental and Theoretical Investigation of Two-Dimensional Centrifugal-Pump Impellers

By A. J. ACOSTA,[1] PASADENA, CALIF.

An experimental and theoretical investigation on a series of two-dimensional centrifugal-pump impellers has been made in an effort to determine the usefulness of potential theory for the description of the flow. Computed values of the developed head and pressure distribution on the vane surfaces are compared with measurements on two, four, and six-vaned logarithmic spiral impellers. The agreement between the observed and predicted quantities is reasonably good for operating points where the influence of the inlet turn on the internal flow is least. The discrepancies which occur at other flow rates are attributed to real fluid effects which are observed in the impeller passages.

Nomenclature

The following nomenclature is used in the paper:

$z = x + iy$ = complex variable of the physical plane
w = complex variable of the mapped plane
$w_0 = ae^{i\delta}$ = complex constant in the w plane
V = absolute velocity
U = peripheral velocity ($r\omega$)
W = relative velocity
ω = angular speed
N = number of vanes
β = vane angle
γ = complement of the vane angle
Γ = circulation strength
r = radius
q = complex constant
C_v = constant for the through flow
ψ = head coefficient = head rise$/U_2^2/g$
ψ_d = measured head coefficient
ψ' = work coefficient (input head)
φ = flow-rate coefficient = discharge/exit area $\times U_2$
p = pressure
P_T = inlet total pressure
C_p = pressure coefficient = $p - P_T/{}^1/_2 U_2^2$
ζ_r = relative loss coefficient

Subscripts:

a = displacement flows in the w (circle plane)
b = the through flow in the w-plane, and as noted
e = shockless entry
m = meridional (radial) component
n = normal component
r = relative or radial component
t = tangential component
u = component in direction of rotation
w = quantities in w-plane
z = quantities in z-plane
2 = vane-exit tips
1 = vane-entrance tips

Superscript:

$\bar{A}$ = complex conjugate of A

Introduction

In the past most of the experimental work in the field of hydraulic machinery has been conducted on complete machines. Because of the mechanical difficulties involved, relatively little work has been done to determine the performance and behavior of the individual components. Roughly, a hydraulic machine may be considered to be composed of three parts; a stationary inlet or guide device, a rotating component or impeller, and volute or stationary diffusing and collecting device.

With a view to obtaining component performance, much experimental work has been done in testing combinations of impellers in various volutes. Individual performance is then inferred from changes in over-all behavior. A separate study of the components permits a more ready understanding of the processes occurring and through simplification allows analysis to be undertaken. If the complete characteristics of the individual elements of the machine were then either known or predictable, design would become more straightforward.

Since the impeller is responsible for energy input to the flow, it seems clear that it should be the item of first interest. It would be highly desirable to be able to predict the head developed and the distributions of pressure which occur by other than empirical methods. However, a satisfactory theory embracing all of the effects of real fluids and the complex geometries found in practice is not yet available. For that reason the problem must be simplified as far as possible, retaining only the essentials. Profile sections of pump impellers range from those in which the cross sections are purely axial throughout to those wherein the flow approaches axially and leaves radially. For the intermediate or "mixed-flow" types the profile sections appear conical. In this work attention is directed at the radial flow or "centrifugal" type of impeller in which the characteristic feature is the rather great change of radius from impeller inlet to exit. In the interest of simplification the effect of the turn from the axial to radial direction is neglected and the impeller is assumed to be two-dimensional; that is, the flow is restricted to depend only on radial and angular co-ordinates. For analysis, the flow is further assumed to be inviscid, incompressible, and irrotational so that the methods of potential theory may be employed.

This approach is a familiar one in fluid mechanics and much success has been obtained with it. However, it should be noted at the outset that the limitations of potential theory for flows of the sort just described are as yet unknown.

---

[1] Research Engineer, Hydrodynamics Laboratory, California Institute of Technology, Pasadena, Calif. Assoc. Mem. ASME.

Contributed by the Hydraulic Division and presented at the Semi-Annual Meeting, Los Angeles, Calif., June 28–July 2, 1953, of The American Society of Mechanical Engineers.

Note: Statements and opinions advanced in papers are to be understood as individual expressions of their authors and not those of the Society. Manuscript received by ASME Headquarters on February 8, 1954. This paper was not preprinted.

The line of thought followed in this work is not novel. It is to be found in references (1 to 3),[2] to mention a few of the current efforts. However, in most of these works, the configurations studied are such that analysis or comparison with a theory in any systematic way is difficult. The blade shape chosen herein for analysis is a logarithmic spiral, that is, a vane of constant angle. This shape is the only one that is mathematically convenient but, since most blade designs used in practice are represented closely by such spirals, this restriction is not a major defect.

Theoretical Treatment

In this section the solution for the potential flow resulting from a rotating array of logarithmic spiral blades is outlined. The flow is assumed to be two-dimensional, thus permitting the application of complex variable theory. This problem has been treated previously by a number of authors, notably Busemann (4) and Sorensen (5), who were interested in the over-all behavior or performance. Consequently, in these works only the head versus flow-rate relation and the operating point for "shockless" entry, i.e., that flow rate for which the entering flow streams smoothly onto the blade leading edge, were determined. Blade-pressure distributions have been calculated for straight radial blades for one and two blades (6) and for a few cases by an approximate procedure (7, 8). In the following paragraphs the development outlined follows that of reference (4).

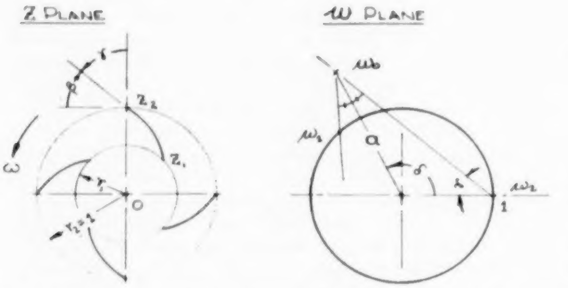

Fig. 1 Representation of Blade System in z and w-Planes
(Positive directions as shown.)

The velocity field due to a rotating impeller, Fig. 1, may be resolved into two components, namely, (a) that resulting from rotation of the vanes in still fluid designated as the "displacement" flow, and (b) the component due to a line source placed at the origin of a stationary vane system. This latter solution corresponds to pure "through flow" with no rotation and accounts for the net discharge of the impeller. Various operating conditions may then be obtained by a linear combination of solutions (a) and (b). This procedure is validated by the linearity of Laplace's equation and the fact that each solution separately satisfied its own boundary condition. In order to effect a solution of these boundary-value problems, a conformal mapping is employed which transforms the physical given plane into one in which the circular system of blades is mapped onto a circle.

The Mapping Function. The conformal mapping employed is credited originally to König (9) although it is presented here in slightly different form. The function is (Fig. 1)

$$z = \left[\frac{w_0 - w}{w_0 - 1}\right]^{1/N} \left[\frac{\bar{w}_0 - 1/w}{\bar{w}_0 - 1}\right]^{e^{2i\gamma}/N} \quad [1]$$

[2] Numbers in parentheses refer to the Bibliography at the end of the paper.

and

$$\frac{dz}{z} = \frac{e^{i\gamma}}{N}\frac{dw}{w}\left[\frac{e^{i\gamma}/w}{\bar{w}_0 - 1/w} - \frac{e^{-i\gamma}w}{w_0 - 1}\right] \quad [2]$$

where z and w are the physical and circle planes, respectively; N is the number of blades and $\pi/2 - \gamma$ is customarily called the vane angle. This function maps the system of N-vanes onto the unit circle in the w-plane in such a way that the region exterior to the unit circle is mapped onto the z-plane. The complex constant w_0 corresponds to the origin in the z-plane and its value depends on the various geometrical parameters of the impeller.

The singular points of the mapping are given by the roots of $dz/dw = 0$, and they determine the end points of the logarithmic spirals. The two solutions of this equation are denoted by w_1 and w_2. If the point representing the blade-exit tip is chosen as $w_2 = 1$, then the value of w_1 representing the blade-inlet tip is

$$w_1 = e^{i(2\gamma + 2\delta + \pi)} \quad [3]$$

in which $w_0 = ae^{i\delta}$. From the foregoing relations

$$a = \frac{\sin\gamma}{\sin(\gamma + \delta)} \quad [4]$$

The tip radius corresponds to $r_2 = |z_2| = 1$, so that the ratio of inlet to outlet radius is given by z_1, i.e.

$$r_1/r_2 = |z_1| = \left|\left[\frac{w_0 - w_1}{w_0 - 1}\right]^{1/N}\left[\frac{\bar{w}_0 - 1/w_1}{\bar{w}_0 - 1}\right]^{e^{i\gamma/N}}\right|$$

which becomes after suitable reduction

$$r_1/r_2 = \left[-\frac{\sin(2\gamma + \delta)}{\sin\delta}\right]^{\frac{1+\cos 2\gamma}{N}} e^{-\frac{2(\pi - \delta - \gamma)}{N}\sin 2\gamma} \quad [5]$$

It should be noted from Fig. 1 that $2\gamma + \delta \geqslant \pi$. If r_1/r_2, N, and γ are given, a and δ may be found from Equations [4] and [5].

(a) *The Displacement Flow.* The boundary condition at a solid surface is that there is no flow through the surface. Upon reference to Fig. 2(a) it is readily seen that this condition is fulfilled for a rotating blade if

$$V_{nz} = \omega\cos\gamma z_b e^{i(\pi/2 + \gamma)}$$

where V_{nz} is the vector velocity and z_b is the complex co-ordinate of the blade. Let F be the complex potential for the flow, then

$$\frac{dF}{dw} = \frac{dF}{dz}\frac{dz}{dw}$$

or

$$\frac{dF}{dw} = \bar{V}_{nz}\frac{dz}{dw}$$

Since polar co-ordinates are employed in the w-plane, the boundary condition there is expressed as

$$V_{rw}e^{-i\theta} = \omega\cos\gamma\bar{z}_b\frac{dz_b}{dw}e^{-i(\pi/2 + \gamma)} \quad [6]$$

By the use of Equations [1] and [2] and the substitution $w = e^{i\theta}$ the boundary condition in the w-plane becomes

$$V_{rw} = -i\frac{\omega\cos\gamma}{N}\left[\frac{w_0 - e^{i\theta}}{w_0 - 1}\right]^q\left[\frac{\bar{w}_0 - e^{i\theta}}{\bar{w}_0 - 1}\right]^q \times$$

$$\left[\frac{e^{i(\gamma - \theta)}}{\bar{w}_0 - e^{-i\theta}} - \frac{e^{-i(\gamma - \theta)}}{w_0 - e^{i\theta}}\right] \quad [7]$$

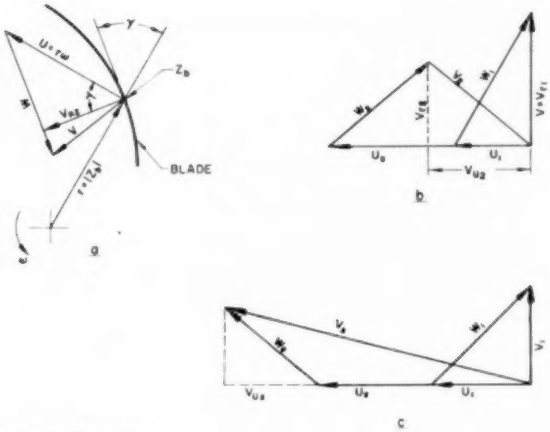

(*a*) Definition sketch
(*b*) Inlet and outlet velocity triangles—backward-curved vanes
(*c*) Same for forward-curved vanes

FIG. 2 DEMONSTRATING DISPLACEMENT FLOW

where
$$q = \frac{1}{N}\,[1 + e^{2i\gamma}]$$

In addition to the boundary condition on the blade, there is the further requirement that the velocity vanish at infinity in both planes since it is assumed that there will be no disturbance there. With this stipulation the tangential velocity on the unit circle in the w-plane may be found by using a form of Poisson's integral (10), i.e.

$$V_t(\theta) = -\frac{1}{2\pi}\int_0^{2\pi} V_r(\varphi)\cot\frac{\varphi-\theta}{2}\,d\varphi \quad\ldots\ldots [8]$$

and the principal value of this integral must be taken.[3]

Substitution of Equation [7] into Equation [8] then gives for the tangential displacement velocity the integral

$$V_{tw}(\theta) = i\,\frac{\omega\cos\gamma}{2\pi N}\int_0^{2\pi}\left[\frac{w_0 - e^{i\varphi}}{w_0 - 1}\right]^q\left[\frac{\bar w_0 - e^{-i\varphi}}{\bar w_0 - 1}\right]^q \times$$
$$\left[\frac{e^{i(\gamma-\varphi)}}{\bar w_0 - e^{-i\varphi}} - \frac{e^{-i(\gamma-\varphi)}}{w_0 - e^{i\varphi}}\right]\cot\frac{\varphi-\theta}{2}\,d\varphi \quad .. [9]$$

From Fig 1 it is evident that the point $w = 1$ maps into the blade trailing edge. The requirement of finite velocity there means that

$$V_{twa}(\theta = 0) = 0$$

This condition may be satisfied without disturbing the boundary condition of Equation [7] by introducing a vortex at the origin in the w-plane of such strength that

$$V_{tw}(\theta = 0) + \frac{\Gamma_a}{2\pi} = 0$$

The value of $V_t(\theta = 0)$ is given the special notation V_{a2}. The total tangential displacement velocity on the unit circle which satisfies Kutta's condition at the exit tip is thus

$$V_{twa} = V_{tw} - V_{a2} \quad\ldots\ldots\ldots\ldots [10]$$

where subscript a denotes the displacement flow.

[3] An explicit formula for V_t has been obtained by another procedure; however, it is quite difficult to evaluate in the general case, consequently recourse was made to numerical methods.

(*b*) *The Through Flow.* To obtain the effect of net discharge from the impeller, the vane system is regarded as being stationary and the flow resulting from a line source at the origin in the z-plane is determined.

The point w_0 is mapped by Equation [1] into the origin in the physical plane. Thus, in order to determine the complete through-flow potential, the flow about the unit circle due to a source at w_0 must be obtained. The required potential is readily found by the method of images to be

$$G(w) = \frac{Q}{2\pi}\log(w - w_0) + \frac{Q}{2\pi}\log(1/w - \bar w_0) \quad\ldots [11]$$

where Q may be complex and is the source strength in the w-plane. As yet no requirement has been put on Q. If it is complex, then the flow in the z-plane issues from the origin on logarithmic spirals with an angle (arg$Q$) between the spiral and any radius. Thus the effect of inlet guide vanes may be approximated by a suitable complex value of Q. Such "prerotation" has been observed on complete pumping installations in the inlet pipe (10) although observations on free impellers (11) indicate little or no prerotation. For free two-dimensional impellers there is no reason for prerotation to occur, and since these calculations are to be compared to experiments conducted on such impellers, Q is assumed to be real throughout the rest of this work. The velocity components are found by differentiation of Equation [11] and on the unit circle they are

$$V_r = 0$$
$$V_t = \frac{Qa\sin(\theta - \delta)}{\pi[1 + a^2 - 2a\cos(\theta - \delta)]} \quad\ldots\ldots [12]$$

The through flow also must satisfy Kutta's condition at the exit tip. As in (*a*), the addition of a simple vortex at the origin satisfies this condition if its strength is adjusted to give zero velocity at $w = 1$. Hence

$$\frac{\Gamma_b}{2\pi} = -V_{b2} = \frac{Qa}{\pi}\,\frac{\sin\delta}{1 + a^2 - 2a\cos\delta} \quad\ldots\ldots [13]$$

The total tangential through-flow velocity is thus

$$V_{twb} = a\,\frac{Q}{\pi}\left[\frac{\sin(\theta - \delta)}{1 + a^2 - 2a\cos(\theta - \delta)} + \frac{\sin\delta}{1 - a^2 - 2a\cos\delta}\right] \quad ..[14]$$

Equations [1], [9], [10], [14] constitute the required solution of the potential flow for a two-dimensional rotating-pump impeller with equally spaced logarithmic spiral blades. The velocity distribution for any operating condition may be obtained by a linear combination of V_{twa} and V_{twb}.

The Developed Head. The head developed by the impeller is

$$H = \frac{1}{g}\,[U_2 V_{u2} - U_1 V_{u1}]$$

where U_1, U_2 are the inner and outer tip speeds, respectively, and V_{u1}, V_{u2} are the average values of the tangential component of the absolute velocity in the direction of rotation. As in (*b*), prerotation is presumed to be zero, hence $V_{u1} = 0$. If Γ_z designates the value of the circulation in the z-plane measured positive counterclockwise, then

$$\psi = H/U_2^2/g = -\frac{\Gamma_2}{2\pi V_2 U_2} \quad\ldots\ldots\ldots [15]$$

where ψ is a dimensionless head coefficient. A circuit once in the positive (counterclockwise) direction about the unit circle in the

w-plane corresponds to a circuit in the positive direction around one impeller vane. The total circulation in the z-plane is thus equal to N times the circulation about one blade. Thus, if $\Gamma_a + \Gamma_b$ is the circulation in the w-plane, then

$$\Gamma_z = N[\Gamma_a + \Gamma_b] \qquad [16]$$

The dimensionless head coefficient ψ is then

$$\psi = \frac{NV_{a2}}{r_2U_2} + \frac{NV_{b2}}{r_2U_2}$$

The first term is dependent only on the rotation of the blades and the second is a function only of the flow rate. The dimensionless quantity NV_{a2}/r_2U_2 is incorporated into the single constant ψ_0 which is otherwise known as the shutoff head. According to Equation [13], one has

$$\frac{NV_{b2}}{r_2U_2} = \frac{NQ}{\pi r_2U_2}\, a \left[\frac{\sin\delta}{1 + a^2 - 2a\cos\delta}\right]$$

where Q is the flow rate in the w-plane and consequently represents the flow rate per passage per unit width in the physical plane. A flow-rate coefficient may be defined as

$$\varphi = \frac{V_{m2}}{U_2} = \frac{NQ}{A_2U_2} \qquad [17]$$

Thus the head versus flow-rate equation now takes the usual form

$$\psi = \psi_0 + \varphi C_v \tan\gamma \qquad [18]$$

in which

$$C_v = \frac{2a\sin\delta}{1 + a^2 - 2a\cos\delta}\,\frac{1}{\tan\gamma} \qquad [19]$$

Equation [18] is the required relation between the head developed and the flow rate. If the number of blades $N = \infty$, then ψ_0, $C_v = 1$, so that

$$\psi = 1 + \varphi\tan\gamma$$

This expression is the so-called Euler head, since it was first determined by him by assuming that the vanes perfectly guided the fluid.

Condition of Shockless Entry. Impellers with blades which are backward curved[4] have a particular flow-rate coefficient for which the velocity at the inlet edge is finite. For an infinite number of vanes this point (denoted by "shockless" entry) is equal to the flow rate at which the entering relative velocity is parallel to the inlet-vane section. However, for a finite number of vanes this flow rate must be determined from the condition that the tangential velocity is zero at the point in the circle plane corresponding to the vane-inlet tip. This condition is expressed by the equation

$$V_{twa}(\theta = \theta_1) + V_{twb}(\theta = \theta_1) = 0 \qquad [20]$$

The flow rate and head developed at shockless entry are designated as φ_e and ψ_e, respectively.

Pressure and Velocity Distribution. The velocities in the w-plane may be transformed to corresponding velocities in the z-plane by the relation

$$\frac{dF}{dZ} = \frac{dF}{dw}\frac{dw}{dz}$$

where F is the complex potential for the flow. Let V_{tz} be the tangential vector velocity on the blade surface in the z-plane. Equation [6] then gives

$$V_{tz} = iV_{tw}\frac{V_{nz}}{V_{rw}} \qquad [21]$$

on the blade.

From Fig. 2 it is evident that the relative velocity is

$$W = -r\omega\sin\gamma - V_{tz} \qquad [22]$$

along the blade for forward curved blades. Since the relative flow is steady and the absolute flow irrotational, blade pressures may be computed from Equation [22] by using the Bernoulli equation for rotating co-ordinates

$$p + \frac{1}{2}\rho\,[W^2 - r^2\omega^2] = \text{const} \qquad [23]$$

In this work the constant is chosen to be the inlet total pressure P_T. A pressure coefficient may then be defined as

$$C_p = p - P_T\Big/\frac{1}{2}\rho U_2^2 = [r/r_2]^2 - [W/U_2]^2 \qquad [24]$$

and by means of Equations [22], [21], [14], [10] values of C_p along the blade may be computed.

Numerical Evaluation and Results. The potential problem outlined was evaluated for three cases in which $r_1/r_2 = 0.54$, $\beta = \pi/2 - \gamma = -30$ deg were constants, and N was 2, 4, and 6. Numerical integration of Equation [9] offered no difficulty for $N = 2$ and 4; however, the integrand for $N = 6$ was quite sharp and peaked. For that reason a function whose conjugate was known was subtracted from the integrand and the resulting difference integrated. The numerical procedure of Peebles was used (13).[5] Values of the function were computed at 80 equally spaced points around the unit circle and in the case of $N = 6$ the value of a was very nearly equal to unity. As a consequence, the integrand of Equation [9] changed rapidly in the vicinity of $\theta = \delta$ which made it difficult to secure an exact value of φ_e. From the computations, it is believed that φ_e is good to two figures at least, whereas the values of ψ_0, C_p should be good to three figures.

Pressure distributions for shockless entrance and various other flow rates were computed for the cases noted in the foregoing and are plotted, together with the experimental values, in Figs. 8, 9, and 10. The computed head versus flow-rate relations are shown in Fig. 11.

The values of ψ_0 and φ_e are tabulated in Table 1 together with comparative values from reference (4) and with the results of infinite vane theory.

TABLE 1 VALUES OF ψ_0, φ_e, ψ_e

		ψ_0	φ_e	ψ_e
$N = 2$	This work	0.38	0.31	0.11
	Busemann (4)	0.38	0.31	0.11
$N = 4$	This work	0.63	0.27	0.24
	Ref. (4)	0.66	0.29	0.23
$N = 6$	This work	0.76	0.24	0.36
	Ref. (4)	0.76	0.26	0.35
$N = \infty$	....	1.00	0.168	0.66

The comparison is excellent for $N = 2$, while for $N = 4$ and 6 the results differ by a few per cent. The reasons for the discrepancy are unknown, for the computation procedure was such as to give at least three-figure accuracy.

Experimental Apparatus and Equipment

Three experimental impellers were constructed and tested in

[4] With reference to Fig. 1, backward-curved blades are obtained by letting γ be positive in the direction shown and the rotative speed be $(-\omega)$, or vice versa.

[5] This method is an 80-point numerical integration of Equation [8]. Second, third, and higher differences are used to provide corrections for excess curvature in the function $f(\phi)$.

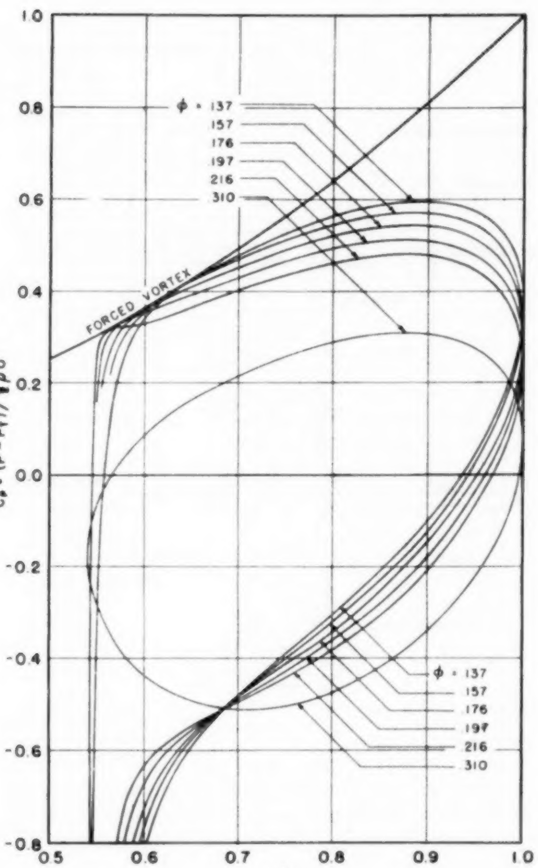

Fig. 3 Theoretical Pressure Coefficient Versus Dimensionless Radius at Various Flow-Rate Coefficients for Impeller With Two Log-Spiral, 30-Deg Vanes, and Radius Ratio of 0.54
(The forced vortex line represents a limit the theory cannot exceed.)

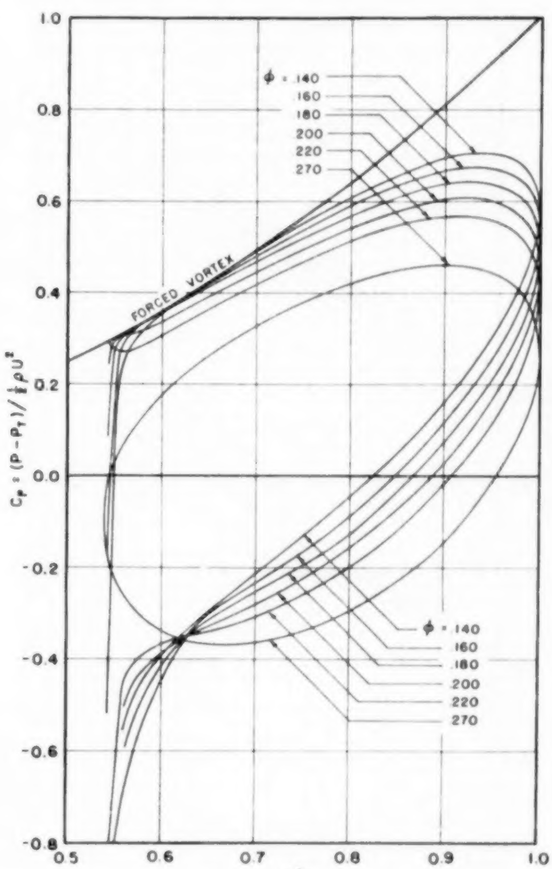

Fig. 4 Theoretical Pressure Coefficient Versus Dimensionless Radius at Various Flow-Rate Coefficients
($N = 4$, $r_1/r_2 = 0.54$, $\beta = 30$ deg.)

the Rotating Channels test stand of the Hydrodynamics Laboratory. Although this apparatus has been described elsewhere (1) it is appropriate to mention its salient features here.

Essentially, the equipment consists of a reservoir, a pump, and a system of piping to provide a flow of water in a closed circuit. Venturi meters are provided to measure flow of water. The flow may be distributed to any one of three test basins in either one of two directions. The test basin used for the present work was provided with a $^1/_2$-hp V-belt impeller drive. Water was delivered to the impeller via an approach section in which a honeycomb flow straightener five diameters upstream had been installed. The impeller discharged into an open tank and the flow was led back to the reservoir. A speed-control device attached to the drive mechanism maintained the impeller at a constant rotative speed which was measured by a "Strobotac."

The assembled impeller and drive mechanism are shown in Fig. 6 in cross section. A pair of stationary circular plates forms an annulus which serves to keep the flow parallel a short distance outside the impeller and provides a convenient support for flow-survey probes.

Test Impellers. Three test impellers, Fig. 7, were constructed with the same parameters as those cases theoretically treated, e.g., $r_1/r_2 = 0.54$, $\beta = 30$ deg; $N = 2$, 4, and 6. A relatively abrupt simple turn deflects the flow from the axial to radial direction, Fig. 7. It was impossible to use a vaned turn which would have given more uniform inlet velocities at the impeller entrance, as the setup limitations would have prevented the measurement of the head. Impeller vanes were made of $^1/_8$-in. brass sheet bent to the proper logarithmic spiral contour. Corresponding curved slots machined in the lucite shrouds positioned the blades. The resulting assembly was held together by screws tapped into the top and bottom sides of the vanes. The impellers were then turned to 12 in. in a lathe leaving the vane tips $^1/_4$ in. wide. The bottom shroud was jig-drilled to center and to run true on the driving assembly.

The breadth of the impellers is a nominal 1 in. This dimension is about the allowable maximum which does not impose a severe retardation of the average flow around the inlet turn with the approach nozzle used. The resulting low-aspect ratio of the passage is typical of impellers with design flow-rate coefficients of about 0.10 to 0.15.

Instrumentation. The determination of blade-pressure distributions requires the measurement of pressure signals on a rotating device. Customarily, such signals are measured with a stationary manometer in conjunction with a complicated system of rotating seals. The complexity of such a device was circum-

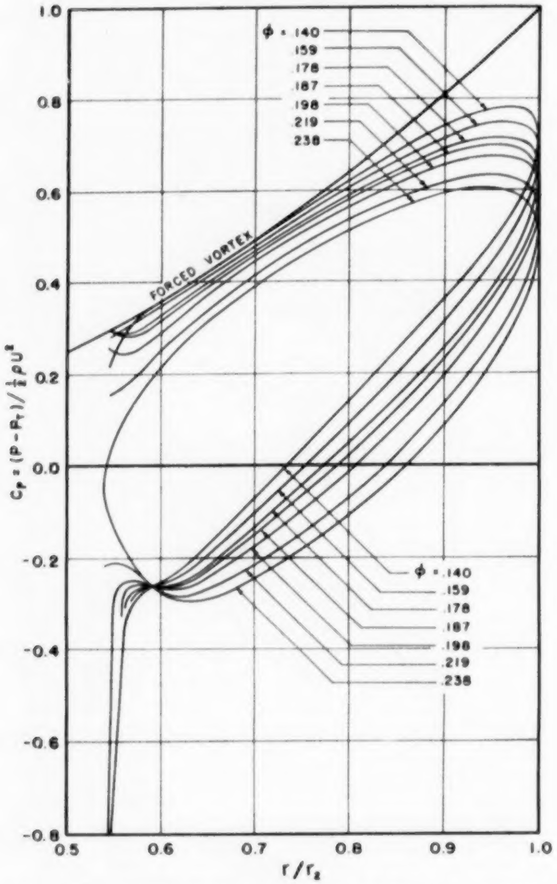

Fig. 5 Theoretical Pressure Coefficient Versus Dimensionless Radius at Various Flow-Rate Coefficients
(N = 6, r_1/r_2 = 0.54, β = 30 deg.)

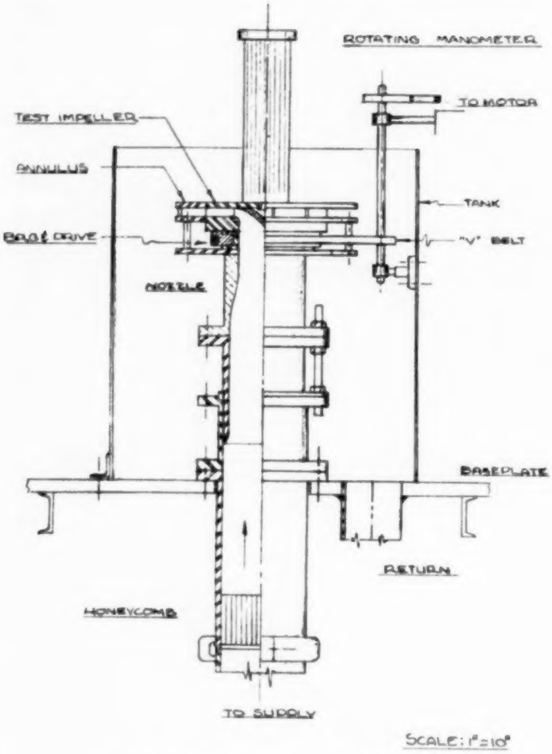

Fig. 6 Impeller Test-Basin Assembly

vented by constructing a multitube manometer which was attached rigidly to the impeller. The manometer was circular and mounted concentrically with the impeller center line and was equipped with twenty-seven 5-mm glass tubes 18 in. long. The manometer readings were converted into actual pressures by accounting for the relative centrifugal-force effects. In this way a complete determination of blade static pressures could be obtained in one setup by observing the tubes with the aid of a synchronized strobolight.

Thirteen piezometer taps 0.030 in. diam were installed on opposite sides of two diametrically opposite vanes at the mid-elevation of the passage. The taps communicated with $^1/_{16}$-in. holes drilled down the height of the vane. Transparent plastic tubing then led off the pressure signal to the rotating manometer.

The reference pressure was chosen to be the inlet total pressure. It was measured by a $^3/_{16}$-in. simple impact tube located on the impeller center line.

The head developed by the impeller was measured by two stationary total head probes aligned with the flow. A $^1/_4$-in. simple impact probe mounted on the impeller center line in the throat of the approach section measured the inlet total head and a venturi-type total head probe (kiel No. SKD 700) mounted $^1/_8$ in. from the impeller OD was used to survey the average discharge total head. The head was measured with a simple water manometer.

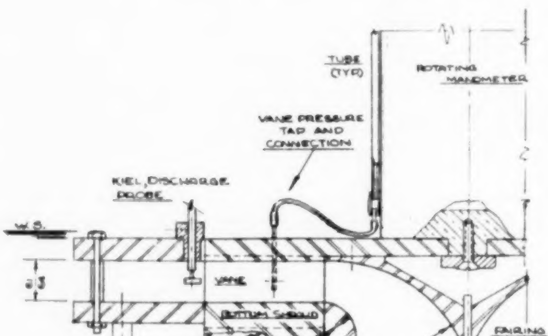

Fig. 7 Impeller Assembly Showing Instrumentation

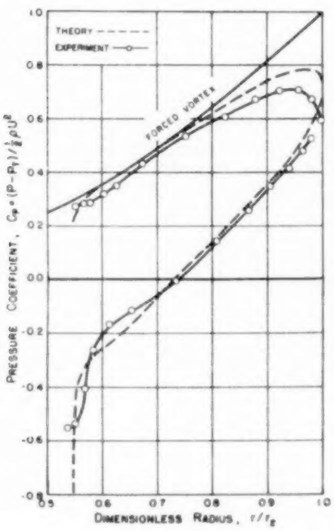

Fig. 8a. φ = 0.140

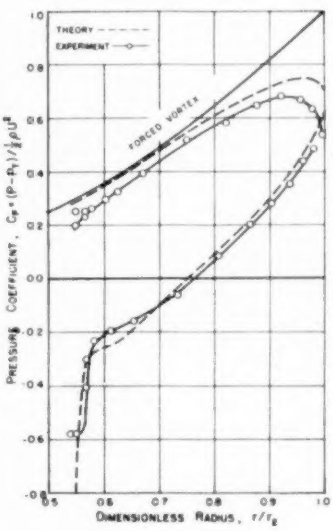

Fig. 8b. φ = 0.159

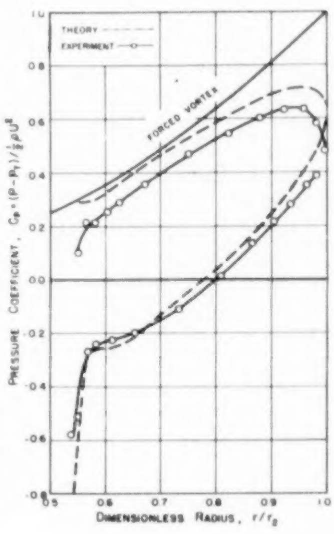

Fig. 8c. φ = 0.178

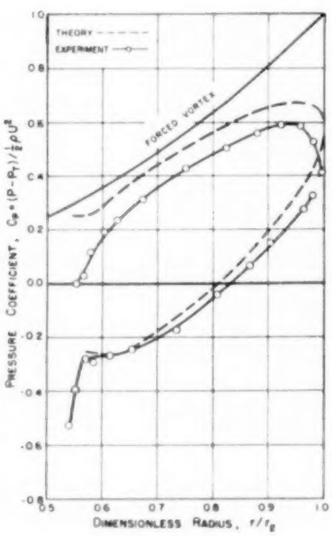

Fig. 8d. φ = 0.198

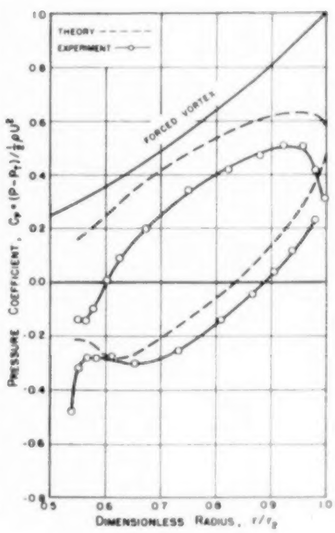

Fig. 8e. φ = 0.219

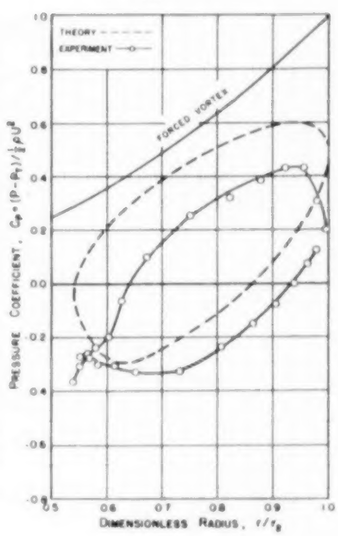

Fig. 8f. φ = 0.238

FIG. 8 EXPERIMENTAL AND THEORETICAL PRESSURE DISTRIBUTIONS AT SEVERAL VALUES OF FLOW-RATE COEFFICIENT FOR AN IMPELLER WITH SIX LOG-SPIRAL, 30-DEG VANES AND A RADIUS RATIO OF 0.54

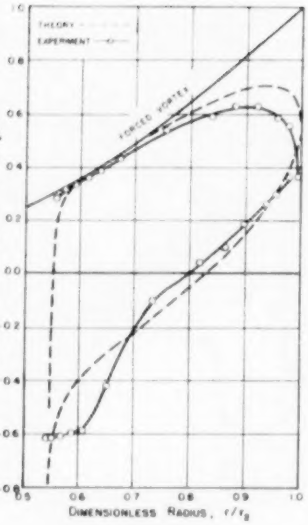

Fig. 9a. φ = 0.140

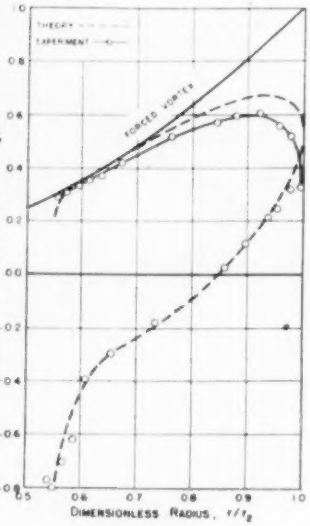

Fig. 9b. φ = 0.160

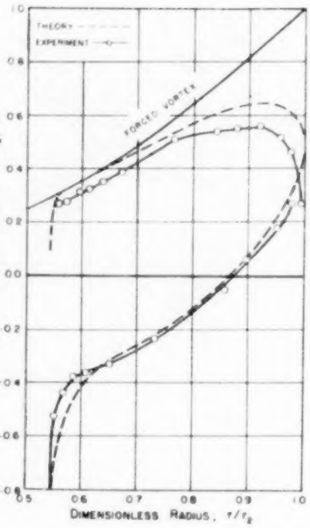

Fig. 9c. φ = 0.180

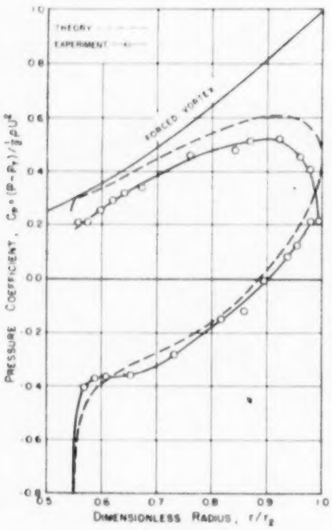

Fig. 9d. φ = 0.200

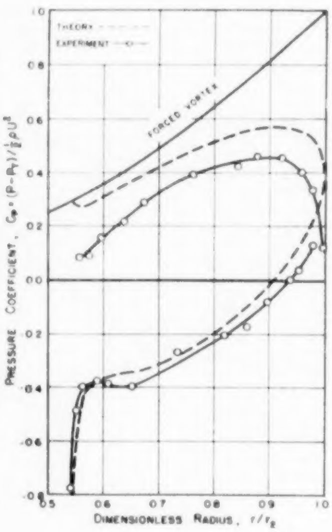

Fig. 9e. φ = 0.220

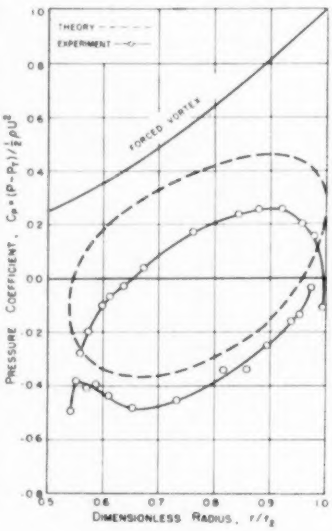

Fig. 9f. φ = 0.270

Fig. 9 Experimental and Theoretical Pressure Distributions at Several Flow Rates for $N = 4$

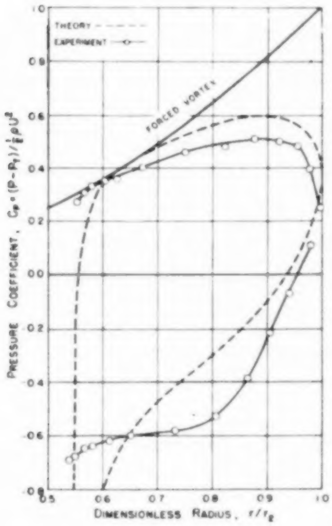

Fig. 10a. φ = 0.137

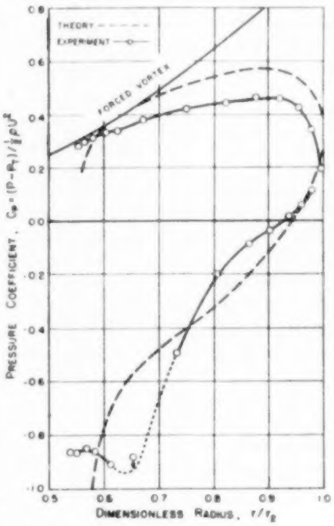

Fig. 10b. φ = 0.157

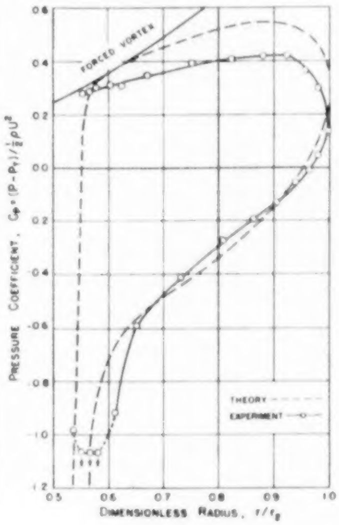

Fig. 10c. φ = 0.176

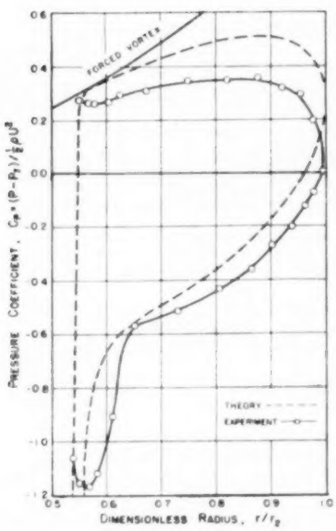

Fig. 10d. φ = 0.197

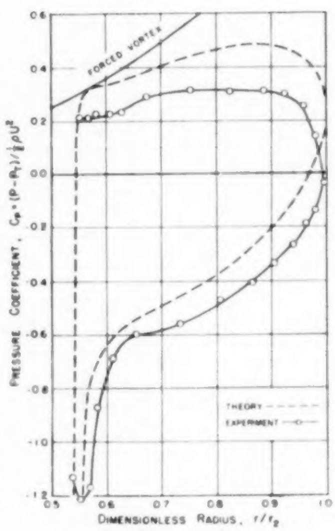

Fig. 10e. φ = 0.216

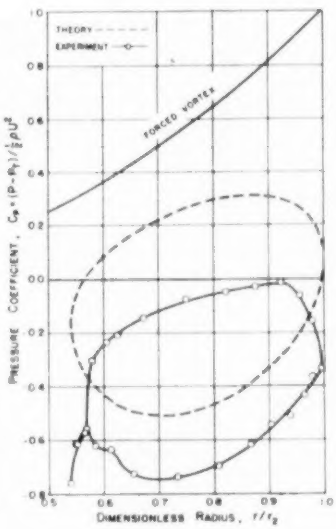

Fig. 10f. φ = 0.310

FIG. 10 EXPERIMENTAL AND THEORETICAL PRESSURE DISTRIBUTIONS AT SEVERAL FLOW RATES FOR $N = 2$

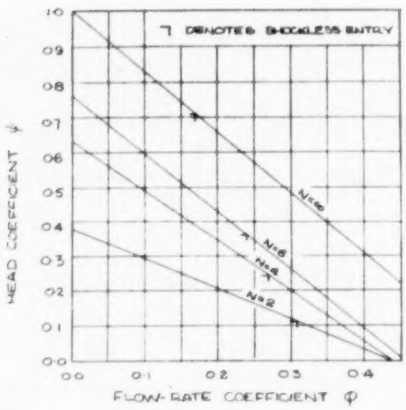

Fig. 11. Theoretical head vs. flow rate characteristics

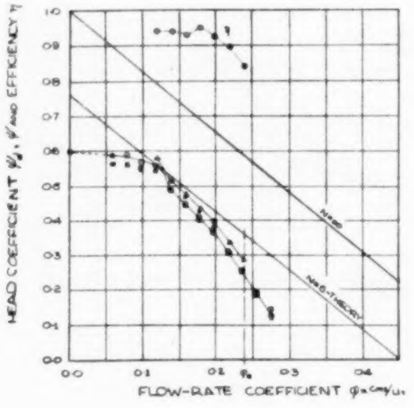

Fig. 12. Six vanes

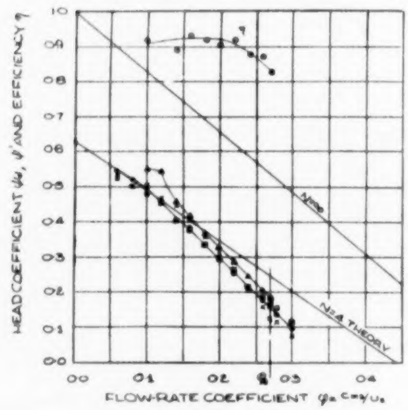

Fig. 13. Four vanes

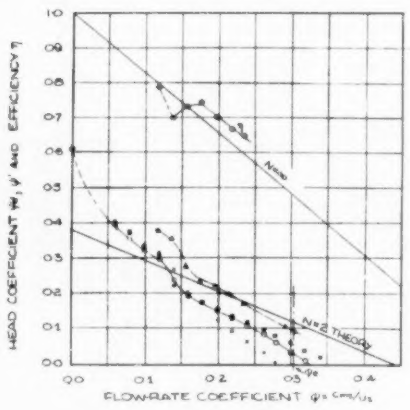

Fig. 14. Two vanes

Legend

× ψ_d—$^1/_4$ in. over bottom shroud ○ ψ_d—$^1/_2$ in. over bottom shroud
□ ψ_d—$^3/_4$ in. over bottom shroud $\Delta\psi'$—(work coefficient)

Figs. 11–14 Experimental and Theoretical Head Versus Flow-Rate Characteristics for Two-Dimensional Impellers With 30-Deg Logarithmic Spiral Vanes and a Radius Ratio of 0.54

For determination of flow patterns within the impeller passages, small, simple total head probes were installed in the impeller passages pointing into the relative flow. The tubes were formed from $^1/_{16}$-in. brass tubing about 3-in. long with a $^1/_4$-in. leg. The opening was bored out with a drill point until quite sharp and conical. Such probes are fairly insensitive to yaw (about ±20 deg) thus permitting relative total head readings to be made with a minimum of angular adjustment.

Experimental Work and Procedure.

The following experimental data were obtained on the three test impellers:

1 The head versus flow-rate relation was determined from zero flow to near-zero head.

2 Pressure distributions over a range of flow rates from shockless to approximately one half of that.

3 Internal head and static-pressure surveys were made at a passage-inlet and at a passage-outlet section for various flow rates on the six-vaned impeller. The design of the impeller-drive mechanism did not allow torque to be measured for these tests.

The tests outlined in the foregoing were run at rotative speeds from 150 to 200 rpm. The developed head was measured at three stations over the breadth of the discharge passage, namely, $^1/_4$, $^1/_2$, and $^3/_4$ in. over the bottom shroud. The head measurements were made with increasing values of flow rate; however, checks with the procedure reversed failed to show any difference.

The results of the head versus flow-rate tests are shown in Figs.

12, 13, and 14, together with the computed characteristics.

Experimental pressure distributions at the center section of the vanes were obtained for the three test impellers using the rotating manometer and the technique described in the foregoing. The manometer tubes were relatively small (5 mm) and apparently they were not all of the same size since a few of them showed capillarity differences on the order of 0.02 ft maximum. The results of these tests and computations are presented in Figs. 8, 9, and 10.

One of the principal assumptions of the theory is that the flow is the same at all stations across the breadth of the impeller. In any real impeller the flow must be turned from an axial to a radial direction during or before it enters the vane system. If in such a turn the wall curvatures are too great, the viscous properties of the fluid may result in the detachment of the main flow from the boundary and/or the growth of a region of retarded velocity. Among other things, the immediate result is that the flow scheme is different from that supposed by the theory. To investigate whether or not these phenomena actually occur, internal flow surveys were made on the $N = 6$ impeller at two radii using the probes described in the previous section. The first was taken a short distance behind the vane inlet edges ($r/r_2 = 0.646$) to determine the effect of the large curvature of the inlet shroud on the flow and to see if the vane leading edges separated. The second survey was conducted near the vane tips ($r/r_2 = 0.938$) in order to ascertain the magnitude of the losses developed within the passage. The results of these surveys are shown in Figs. 15 to 17. In order to compute the relative velocity, 0.030-in. piezometer taps were installed across the passage from one vane to the next on both the top and bottom shrouds at these radii.

Treatment of Experimental Data

(*a*) *Computation of Efficiency.* The lack of measured torques precludes the exact computation of efficiency. However, the measured pressure distributions give the normal forces exerted on the fluid, and from this information an "input" head or work coefficient ψ' can be derived. It is this quantity rather than the developed head ψ_d which should agree most closely with the theory. This coefficient is computed from the equation

$$\psi' = \frac{N}{4\pi\varphi}\int_{r_1/r_2}^{1} \Delta C_p(r/r_2)d(r/r_2) \quad [25]$$

in which ΔC_p is the measured differential pressure-loading coefficient across the vane. The work coefficient ψ' and the developed head coefficient ψ_d differ by the fluid-energy losses, and a "hydraulic" efficiency may then be written as

$$\eta = \frac{\psi_d}{\psi'} \quad [26]$$

Equation [26] may be regarded as an approximate measure of the efficiency of the impeller since ψ' represents the energy input to the flow (apart from tangential friction forces) and ψ_d the output energy. Owing to variation of the relative total head across the passage, additional mixing losses are encountered after the impeller. Such losses are not included in this computation of efficiency. For $N = 6$, this efficiency is about 95 per cent and it has a substantially flat peak in the range of flow rates $\varphi = 0.12$ to 0.20, Fig. 12. Similar results are observed on the four-bladed impeller; however, the peak efficiency for $N = 2$ is much lower, being about 80 per cent. The measured head varied somewhat from top to bottom shroud. For efficiency determination the head at the passage center was used, although at flow rates for best efficiency the head was practically constant across the passage width.

(*b*) *Computation of "Relative Head Loss."* The term "total head loss" requires some explanation when used in connection with the relative flow. The Bernoulli equation for rotating coordinates, i.e.

$$p + \frac{1}{2}\rho[W^2 - r^2\omega^2] = \text{const}$$

is rigorously true if the absolute flow (the flow observed in a stationary co-ordinate system) is incompressible, irrotational, and inviscid. If the relative flow total pressures $p + {}^1/_2\rho W^2$ are then compared at the same radius on a rotating manometer, it will be found that they are all the same since the centrifugal effects are canceled out in the tubing connecting the manometer to the total head measuring device. Thus, if the flow is a potential flow, the difference between, say, the inlet total pressure and any other total pressure as read on a rotating manometer is zero. The effect of viscosity and dissipation is to reduce the relative total head and is thus read as a loss.

Contour plots of the relative loss coefficient ζ_r for the six-vaned impeller are shown in Figs. 15 to 18. The loss coefficient is defined as

$$\zeta_r = (P_T - P_t)\Big/\frac{1}{2}\rho U_2^2$$

where P_T is the inlet total pressure and P_t is any other relative total pressure. These plots show the regions most affected by viscosity and give a good qualitative idea of the flow. By using these loss contours and the relative velocities (not shown) calculated from the flow surveys, a weighted loss coefficient may be obtained, i.e.

$$\bar{\zeta}_r = \frac{\int \zeta_r W dA}{\int W dA} \quad [27]$$

To be completely correct, each of these integrals should contain a factor $\sin \beta_f$ where β_f is the angle between the relative velocity and a normal to the radius at that point. It is quite difficult to measure this angle experimentally, so for the purposes of computation it is assumed to be constant, and as a consequence the value of $\bar{\zeta}_r$ must be low.

With the coefficient $\bar{\zeta}_r$ as defined, an order-of-magnitude check of the efficiency as computed by Equation [26] may be made. It can be shown that the energy input to the flow is given by $\psi_d + \bar{\zeta}_r/2$ hence

$$\eta = \psi_d/(\psi_d + \bar{\zeta}_r/2)$$

Evaluation of $\bar{\zeta}_r$ for $\varphi = 0.238$ gave 0.07 for the exit survey. The efficiency computed by this relation is 87 per cent, whereas Equation [26] gives 84. At $\varphi = 0.178$ the two methods agree to within 2 per cent. It is not desired to belabor this point unnecessarily but in view of the experimental accuracy this agreement is taken to mean that the "hydraulic" efficiency as computed here is probably accurate to within 2 or 3 per cent and that the method of measuring the developed total head is accurate to the same order.

Comparison of Theory and Experiment

From comparison of measured and calculated distribution of pressures afforded by Figs. 8, 9, and 10, it is immediately evident that the theoretical results do not agree satisfactorily with the actual measurements, particularly for flow rates near shockless entry. The agreement is best for the four and six-vaned impellers at flow rates of about $\varphi = 0.14$ to 0.18. The measured head coefficients, Figs. 12 to 14, also deviate considerably from the theoretically predicted ones near shockless entry but at flow rates substantially less ($\varphi = 0.18$) the disparity is 10 per cent or less. The values of the work coefficient obtained from the measured pressure distributions agree fairly well with the computed values

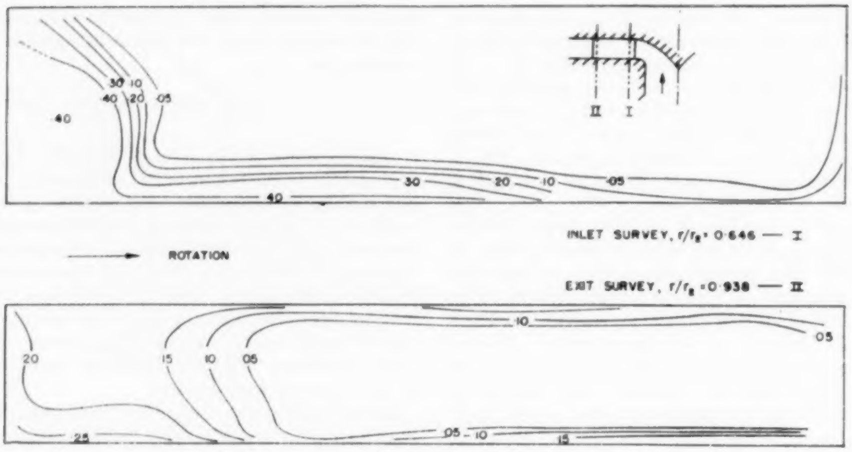

Fig. 15 Contour Plots of Loss Coefficient ζ_r
(Six vanes, φ = 0.238. Developed head = $0.50[u_2^2/g]$ Plotted on developed passage perimeter which is taken as unity in each case.)

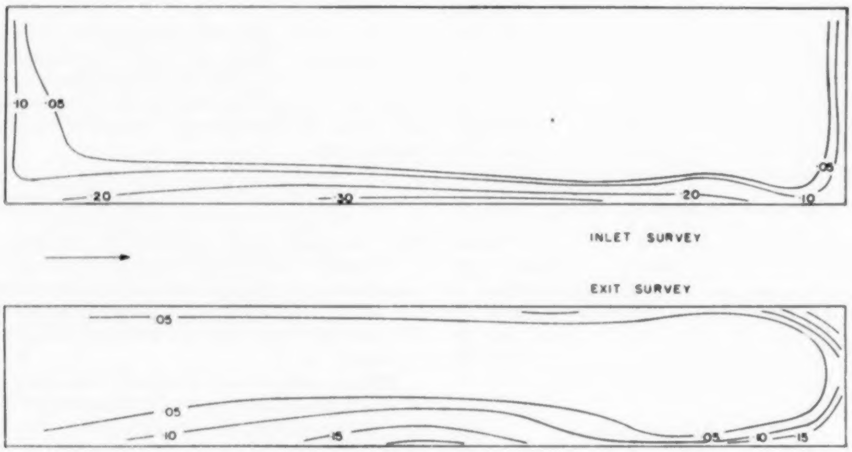

Fig. 16 Contour Plots of Loss Coefficient ζ_r
(Six vanes, φ = 0.198. Developed head = $0.70[u_2^2/2g]$.)

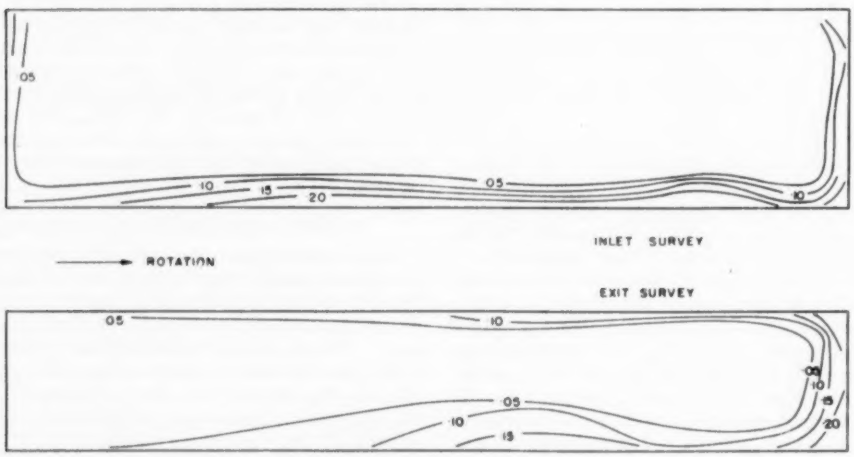

Fig. 17 Contour Plots of Loss Coefficient ζ_r
(Six vanes, φ = 0.178. Developed head = $0.80[u_2^2/2g]$.)

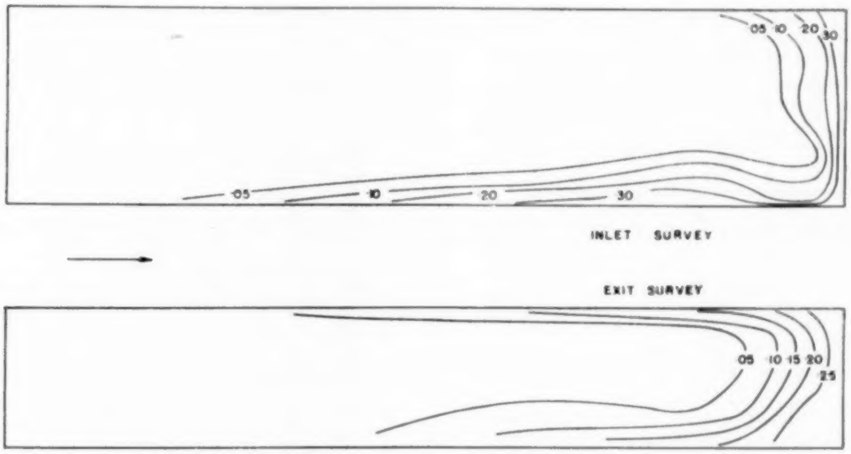

FIG. 18 CONTOUR PLOTS OF LOSS COEFFICIENT ζ_r
(Six vanes, φ = 0.140. Developed head = 0.92 $[u_2^2/2g]$.)

near φ = 0.18 for all impellers, although its slope is steeper than the predicted head versus flow-rate line.

The fact that the discrepancy between the observed and computed quantities becomes greater as shockless entry is approached is rather surprising. It is usually expected that agreement between potential flow calculations and experiment will be best when sharp velocity peaks at leading edges are avoided. The experimental fact that the pressure distributions and work coefficient are in poor agreement with the theory, here strongly suggests that phenomena not necessarily connected with the vanes alone have become important enough for these flow rates to change the flow.

The inlet surveys taken on the N = 6 impeller, Figs. 15 to 18, show that for a flow rate of $\varphi = \varphi_s$ = 0.238 the flow is scarcely potential. On the leading face of the vane (pressure side) and on the bottom shroud, substantial regions of high loss occur. These losses are diffused throughout the passage and a further increase in the boundary layer occurs as is evidenced in the exit survey. Part of the "diffusion" of the high-loss areas no doubt is due to secondary flows in the passage which originate from the nonuniformities in relative total head. Further evidence of the nonuniformities of the flow pattern is supplied by static-pressure measurements made at the inlet on the impeller shrouds. At this operating point static pressures on the top and bottom shrouds differed by 15 per cent or more midway between the vanes, whereas such differences were not observed at lower flow rates.

It is fairly clear now how the discrepancy between theory and experiment arises at this flow rate. The abrupt turn and large curvature of the approach section immediately before the bottom inlet shroud, Fig. 7, gives rise to a relatively thick boundary layer (if not local detachment) along the bottom shroud and a nonuniform velocity across the passage height. At the vane leading edge the approaching fluid is accelerated by the small radius of curvature of the bottom shroud. (Although these velocities were not measured, it is clear that high local velocities must occur there.) The immediate result is that the angle of attack is higher near the bottom shroud than at the top, and consequently the flow on the lower portion of the vane can separate prematurely. The over-all shape of the loss-contour curves indicates that such an effect occurs. At low rates of flow (much less than shockless) it would be expected, because of the higher velocity on the inlet bottom shroud, that the reverse situation should take place, i.e., the flow near the top shroud should deteriorate first.

The loss contours of Fig. 18 tend to support this argument.

The operating point designated as "shockless entry" is usually taken to be the "design" point as well since it is desired to eliminate regions of large underpressure or high local velocity for reasons of cavitation or gas evolution. With the present apparatus the inlet turn is of great importance to the over-all behavior of flow rates for which shockless entry occurs on these impellers. Consequently, it would seem appropriate to make comparisons with the theory where inlet conditions are the most favorable, even though large underpressures may still exist on the vane. Inspection of the loss distributions given in Figs. 15 to 18 shows that at a flow rate coefficient of φ = 0.178, the inlet portions of the vanes are relatively free of wakes. Typically, however, a fairly large boundary layer still remains on the bottom shroud. The agreement of both the development head, Fig. 12, and measured distributions of pressure with the computations is seen to be relatively good at this flow rate. Reasonably favorable entrance flows are found to occur in the range of about φ = 0.14 to φ = 0.20 and in this region not only are the work coefficients nearly equal to the predicted head, but the pressure distributions are fairly close.

Thus far all comparisons have been made at flow-rate coefficients based on the total discharge. Actually, the presence of boundary layers and the thickness of the vanes result in a velocity increase of the effective part of the stream. This effect may be roughly taken into account by comparing the experimental results to the theory evaluated at flow rates higher by an appropriate amount.

Such a comparison can be realistic only when the flow is not greatly disturbed by real fluid effects. Thus, in the present case, these comparisons are restricted to flow rates for which the entrance conditions are best. At a flow-rate coefficient of φ = 0.178, an approximate measure of the boundary-layer influence is provided by a plot of the relative velocity across the passage height, midway between the vanes at an entrance and an exit section, Fig. 19. The ratio of the velocity of the main flow to the average is 1.06 at the inlet. Vane thickness accounts for 7 per cent of the peripheral area at the inlet and 4 per cent at the exit. The effective flow rate is then about 10–12 per cent more than the average. Comparisons of measured and computed distributions of pressure on this basis are presented for φ = 0.178, N = 6, Fig. 20, and for φ = 0.18, N = 4, Fig. 21.

It is seen that the agreement is better than for the unadjusted

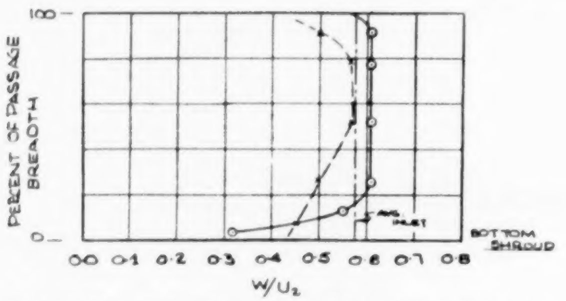

O. Inlet relative velocity $r/r_2 = 0.646$ X, Exit relative velocity $r/r = 0.938$

Fig. 19 Inlet and Exit Relative Velocity Traverse Across Passage Breadth Midway Between Vanes; $\varphi = 0.178$, $N = 6$

theory and that the corrections made are in the right direction. At a corrected value of $\varphi = 0.178$ the predicted head for $N = 6$ becomes close to the measured work coefficient, but the pressure-distribution loops are still somewhat lower than called for by the theory. Part of this discrepancy is due to inlet losses which are still present.

The actual state of affairs is certainly more complicated than the simple adjustment of flow rate might indicate. Not only is the main flow speeded up, but a boundary layer develops along the vane faces which results, essentially, in a blade profile different from that originally assumed. This fact is supported by a thick layer of high-loss fluid on the vane trailing side seen in the exit relative-flow surveys, and it is suggested by the general progressive downward shift of the experimental pressures from the calculated one. The loss contours of Figs. 15 to 17 all show substantial boundary-layer developments on the trailing faces of the vanes. Roughly speaking, this effect is to reduce the vane angle, which in turn results in a steeper head versus flow-rate line. In the region of best efficiency this effect would account for the increased slope of the work-coefficient line.

The general behavior of the two-bladed impeller followed that of the four and six-vaned ones. The discrepancy in pressure distributions is, in general, somewhat more than for the others; however, as before, the theoretical head provides a good estimate of the work coefficient. The efficiency, though, is lower than the $N = 4$ and $N = 6$ runners and has a maximum value of only 80 per cent. As in the other cases, the experimentally determined value of shockless flow rate is nearly equal to the predicted value. The high value of the developed head near shutoff is interesting since, in order to achieve heads substantially higher than the theoretical perfect fluid value, a large part of the flow must rotate like a solid body.

Effect of Number of Vanes

For a given vane angle and radius ratio the effect of vane number for a pump is similar to the effect of solidity in a two-dimensional cascade. For commonly employed impeller parameters the head developed is nearly proportional to the number of vanes if there are only a few of them, i.e., two or three. If the number becomes appreciable, say, six to eight, then the effect of mutual interference becomes important and the head developed rapidly approaches the maximum given by the infinite-vane theory. Low values of N have low values of the coefficients ψ_0 and C_r resulting in lower and flatter head versus flow-rate lines, as seen in Fig. 11. However, for low numbers of blades the pressure loading per vane is high. Since the pressure cannot exceed that of a forced vortex, the practical result is that blade static pressures for $N = 2$, 3, 4, etc., are much lower than for $N = 6$ or 8. This trend is readily seen in the plots of computed pressure distributions.

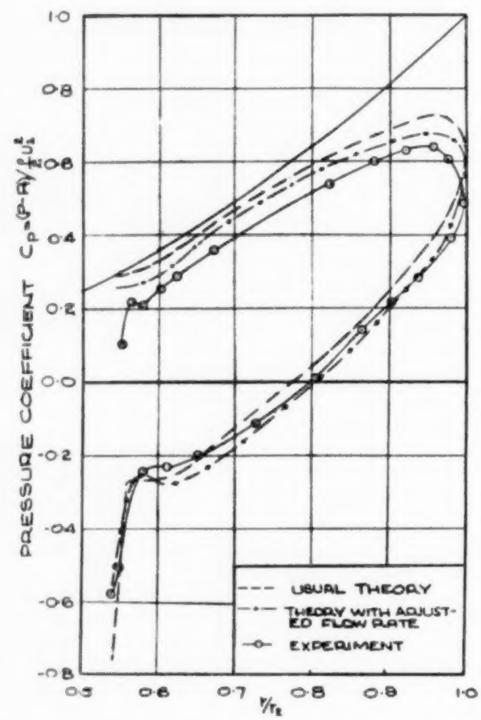

Fig. 20 Effect of Modifying Flow Rate $\varphi = 0.178$, $N = 6$

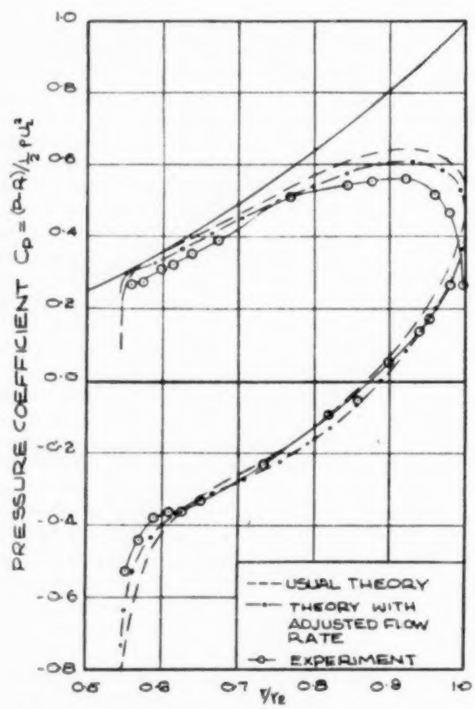

Fig. 21 Effect of Modifying Flow Rate $\varphi = 0.18$, $N = 4$

A result of having a large number of vanes is the suppression of large-scale separation or flow detachment from the vane leading edges. This effect is observed in Figs. 8(*a*), 9(*a*), and 10(*a*) wherein the progressive departure with decreasing number of vanes of the measured and calculated pressures on the trailing side of the vane is seen.

The low heads and high loadings of impellers with only two or three vanes place them at a great disadvantage. For these reasons their use is limited to very special applications.

Situations of the sort found in this work are not uncommon in the application of potential theory to problems in the flow of real fluids. Pinkerton (14), in a study of measured and calculated pressure distributions on the NACA 4412 Airfoil, observed discrepancies in lift coefficient of 20 per cent when computed by usual methods. At moderate angles of attack, measured and experimental distributions of pressure disagreed in much the same way as they were found to in this work. However, he was able to "adjust" the airfoil profile to account for the progressive development of the boundary layer in such a way as to obtain excellent agreement of the computed and measured distributions.

The flow within the passages of centrifugal-pump impellers is much more complex than that over an airfoil. The regions of fluid affected by viscosity are larger and secondary flows caused by the nonuniformities in relative total head occur. The low-aspect ratio of the passage also enables viscous effects to become more important than for the flow over airfoils. In this work it would have been possible to change the vane profile to account for some of the boundary-layer effects, as Pinkerton has done for airfoils; however, this process for a circular array of vanes is much more laborious than for a single profile. Moreover, for the cases studied, the inlet conditions were not ideal. For these reasons computations along such lines were not considered to be worth while at present.

Summary and Conclusions

The measured distributions of pressure and work coefficient were found to agree fairly well with the predicted values when the flow conditions at the inlet of the vane system were best. At flow rates near shockless entry, large deviations were observed which were traced to nonuniformities in the inlet flow arising from the abrupt inlet turn. The fact that the agreement between the potential flow calculatons and the experiments is as good as it is for flow rates much less than shockless, where pressure discontinuities still occur on the vane-inlet edges, is considered promising. Consequently, it would seem reasonable to suppose that if a highly uniform inlet flow were supplied to the impeller, then better agreement over a broader range of flow rates would result. The theory as it now stands appears to be useful for design over certain limited rates of flow. Application to wide ranges of operating conditions is still restricted since the inlet turn introduces many as yet unknown factors.

Acknowledgment

The author would like to acknowledge the support of the Office of Naval Research.

BIBLIOGRAPHY

1 "Head and Flow Observations on a High-Efficiency Free Centrifugal-Pump Impeller," by W. C. Osborne and D. A. Morelli, Trans. ASME, vol. 72, 1950, pp. 999–1007.

2 "An Analysis of Flow in Rotating Passage of Large Radial-Inlet Centrifugal Compressor at Tip Speed of 700 Feet Per Second," by V. D. Prian and D. J. Michel, NACA Technical Note 2584, December, 1951.

3 "On Potential Flow of Water Through a Centrifugal Impeller," by S. Uchimaru and S. Kito, *Journal of the Faculty of Engineering*, Tokyo Imperial University, Tokyo, Japan, vol. 19, 1931, pp. 191–223.

4 "Das Förderhöhenverhältnis radialer Kreiselpumpen mit Logarithmischspiraligen Schaufeln," by A. Busemann, *Zeitschrift für Angewandte Mathematik und Mechanik*, band 8 heft 5, 1928, pp. 372–384.

5 "Potential Flow Through Centrifugal Pumps and Turbines," by E. Sorensen, NACA Technical Memorandum 973, April, 1941.

6 "Mitteilungen des Instituts für Strömungsmachinen der Technischen Hochschule Karlsruhe," by W. Spannhake, heft I, Oldenbourg, Munich and Berlin, Germany, 1930, pp. 4–39.

7 "The Flow Through Centrifugal Compressors and Pumps," by H. E. Sheets, Trans. ASME, vol. 72, 1950, pp. 1009–1015.

8 "Two-Dimensional Compressible Flow in Centrifugal Compressors With Straight Blades," by J. D. Stanitz and G. O. Ellis, NACA Report 954, 1950.

9 "Potentialströmung durch Gitter," by E. König, *Zeitschrift für Angewandte Mathematik und Mechanik*, band 2, 1922.

10 "Partial Differential Equations of Mathematical Physics," by H. Bateman, Dover Publications, New York, N. Y., 1944, p. 243.

11 "Centrifugal and Axial Flow Pumps," by A. J. Stepanoff, John Wiley and Sons, Inc., New York, N. Y., 1948, p. 39.

12 "Measured Performance of Pump Impellers," by W. C. Osborne and D. A. Morelli, ASME Paper No. 50—A-90, 1950.

13 "A Method for Calculating Airfoil Sections From Specifications on the Pressure Distributions," by G. H. Peebles, *Journal of the Aeronautical Sciences*, vol. 14, 1947, p. 451.

14 "Calculated and Measured Pressure Distributions Over the Midspan Section of the NACA 4412 Airfoil," by R. M. Pinkerton, NACA Report No. 563, 1936.

The Kaplan Turbine—Design and Trends

By J. Fisch,[1] York, Pa.

The adjustable-blade propeller turbine, known in the hydropower industry as a Kaplan turbine, in honor of its inventor, Dr. V. Kaplan of Brunn, Czechoslovakia, was first introduced in Europe in the early 1920's and in the United States in 1928. Since then, approximately 274 units with a total output of 7,647,000 hp have been installed, or are under construction, in this country. Runner diameters vary from 30 to 292 in. and maximum operating heads for the individual units range from 7 to 105 ft. The world's most powerful Kaplan turbine is in operation at the U. S. Engineers, McNary Dam, developing a guaranteed output of 111,300 hp under a net head of 80 ft. This output will be surpassed by the Dalles units, also for the U. S. Engineers, which are rated at 123,000 hp under 81-ft head.

General Characteristics

The main feature of the Kaplan turbine is the simultaneous adjustability of its runner blades and wicket gates which, when properly synchronized for varying conditions of load, results in a very flat efficiency curve, thereby improving part-load efficiency over other reaction-type turbines by a considerable amount as shown in Fig. 1.

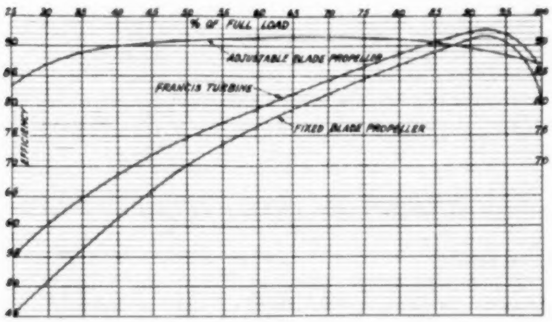

Fig. 1 Efficiency Comparison of Adjustable-Blade Propeller 164 Rpm, Fixed-Blade Propeller 150 Rpm, Francis Unit 100 Rpm, All Rated 9500 Hp at 38 Ft Head

Being essentially an infinite number of propeller runners with different blade angles built into one unit, the Kaplan turbine maintains high efficiency over a wide range of load.

Usually the normal rating corresponding with the generator capacity occurs at a blade position less than maximum open and where the efficiency is still high. The ability to go to wide-open position during periods of high tail water results in large outputs during flood seasons when water is plentiful but capacity is limited owing to reduction in head.

Fig. 2 shows a comparison of horsepower and efficiency curves for propeller and Kaplan turbines under various heads.

The high specific speed of Kaplan runners results in economy of the over-all installation due to higher speed generators which, together with the adjustable features, readily justifies selection of Kaplan turbines for heads up to 100 ft. Its flexibility, greater over-all power output, and conservation of stored water at part load have resulted in wide application in the low and medium-head field.

The high unit capacity per inch of runner diameter effects substantial savings in dimensions and cost of the powerhouse structure and excavation.

Careful studies of the over-all power output in multiunit installations based on head and flow-duration data, usually result in worth-while gains if all units are of the Kaplan type rather than a combination of Kaplan and fixed-blade-propeller units. Cost comparisons must be based on the entire development rather than on the turbines alone to obtain realistic answers. Only relatively small yearly kilowatthour output gains are necessary to pay for the increased investment in Kaplan units. Fig. 3 represents a typical study comparing the yearly kilowatthour output of three Kaplan units with three each of fixed-blade-propeller and Francis-type units.

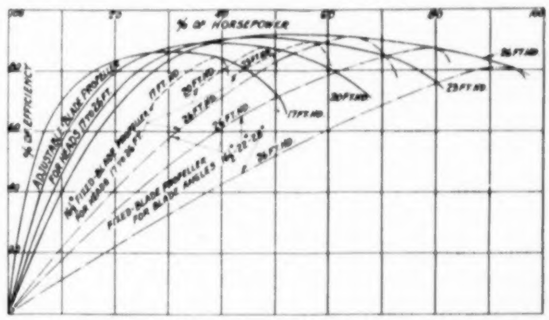

Fig. 2 Load Curves for Adjustable and Fixed-Blade Propellers Showing Comparison of Efficiencies

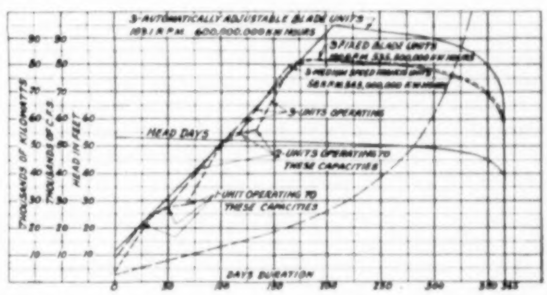

Fig. 3 Study of Yearly Output of Three Adjustable-Blade Propellers and Three Each of Fixed-Blade Propeller and Francis Turbines

Plant operation in regard to distribution of load on the units is considerably simplified in an all-Kaplan-unit installation.

Present and Future Trends

The trend today in Kaplan-turbine installations is primarily

[1] Chief Engineer, S. Morgan Smith Company. Mem. ASME.

Contributed by the Hydraulic Division and presented at the Annual Meeting, New York, N. Y., November 29–December 4, 1953, of The American Society of Mechanical Engineers.

Note: Statements and opinions advanced in papers are to be understood as individual expressions of their authors and not those of the Society. Manuscript received at ASME Headquarters, August 19, 1953. Paper No. 53—A-101.

toward higher heads into the region where Francis turbines heretofore have been the only practicable choice. Also, the development of Kaplan runners for installations under lower heads than formerly have been economically feasible continues, aided by improved methods of earth and rock removal, which is required for the relatively low setting with regard to the elevation of the tail water.

The high-head, lower specific-speed trend suggests the desirability of exploring basic changes in design. The Bort-Rhue installation in France as reported by M. Bovet,[2] with a rating of 31,800 hp under a head of 230 ft at 375 rpm, has a specific speed of 74.7. Assuming that this runner is of the orthodox Kaplan design, it necessarily would have a relatively large hub and number of blades.

The higher part-load efficiency and overload capacity obtained with the Kaplan principle coupled with the improved flow conditions in the draft tube may justify the ultimate development of this type for materially higher heads, even up to several hundred feet, provided a wide enough head range exists.

Such requirements might be met by the axial-flow or usual design, Fig. 4 (*a*), with diagonal flow, Fig. 4 (*b*), or with radial flow, Fig. 4 (*c*). The disadvantage of (*b*) and (*c*) would lie in the more complex mechanism for blade movement, involving ball joints and bell cranks.

Fig. 4 Suggested Designs for High-Head, Low-Specific-Speed Adjustable-Blade Propellers

The advantage of (*b*) and (*c*) would lie in the reduced size of hub necessary with attendant disk-friction loss, in reduced hydraulic thrust and probably reduced runaway speed owing to greater average entrance diameter. Part of the hub of (*a*) might be made stationary, but vanes or struts across the water passage would be necessary.

Extremely low-head installations call for runners with few blades, small hub diameter, and relatively deep draft tubes to permit the maximum regain of the high energy remaining in the water discharged from the runner. With only small fluctuation in head-water level, syphon settings permit the entrance to the runner to be above the maximum head-water level with possible omission of the head gates. The Vargon installation in Norway is an example of such a setting.

Runner. The Kaplan runner, the hub-tip diameter ratio of which increases with the number of blades, consists of a heavy cast-steel hub in which each blade is supported in two journal bearings. A thrust bearing is provided to take the radial centrifugal load. The forces acting on blade and shank are hydraulic thrust, torque, centrifugal force, and operating force. Linkage connections and crosshead are mounted inside of hub and cone.

Crosshead and operating rod are guided in two bearings to take care, in emergencies, of possible unbalanced crosshead-arm moments due to nonuniform distribution of blade-operating forces.

Shank bearings usually are furnished of a bronze with low coefficient of friction. Experience has shown that the wear on properly designed bearings is extremely small even though the angular motion is of the oscillating type and too slow to develop an oil film. To produce nearly uniform load distribution over the full bearing length, it is necessary either to provide diametrical clearances of only a few thousandths or to machine the two bearing surfaces eccentrically to maintain the shank center line parallel with the bearing walls, Fig. 5. The latter method is good but obviously more difficult and costly than the former. Several units with small shank-bearing clearances were overhauled after more than 20 years of operation but the bronze bearings did not require replacement. Such results amply justify the use of conservative unit bearing pressures and shank stresses that minimize deflection and thereby maintain uniform load distribution.

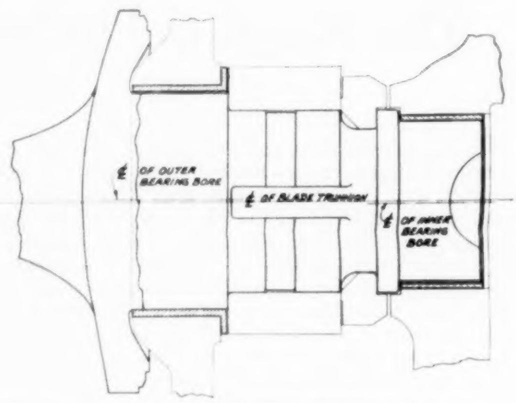

Fig. 5 Blade Trunnion Bearings With Offset Bores

Earlier designs provided shank seals, to seal the water out and the hub oil in, which were accessible only when the unit was disassembled. Although their performance generally was satisfactory, the trend is now toward seals which are adjustable and replaceable while the runner is in place. This design is being applied also to small units in so far as practicable. Water which, because of its pressure being higher than the hub oil pressure, leaked by the seals into the hub was found in a number of units. But because of the emulsion formed, no detrimental effect in regard to corrosion of internal parts or excessive bearing wear was experienced.

Large high-head units are sometimes provided with an automatically charged air-pressure tank mounted on the shaft below the blade servomotor and connected with the inside of the hub through the hollow main shaft. An air cushion is maintained in the tank at a pressure slightly higher than the maximum water pressure around the hub caused either by the resultant pressure above the blades or the back pressure under high tail water. Provisions are made to check for water in the hub either by removing a plug located in the wall of the hub above the blades on sizes that permit access between the wicket gates, or on large units by a special device located in the main shaft above the guide bearing and connected to the hollow operating rod during standstill.

Both devices lead to the bottom of the hub to permit the heavier water to escape first, forced out by the standing oil column up to the filling basin below the blade servomotor or by the pressure maintained in the air tank. The drain is closed when clear oil comes through.

All hubs are equipped with a valve or plug at the bottom for complete emptying.

Better blade-shank seals together with extensive operating experience tend toward selection of lower viscosities of hub lubricating oils. The trend is from the original recommendation of 1500 SSU at 100 F, to 1000 SSU at 100 F, (or lower) to facilitate filling and emptying through the restricted passages. The high-quality oil should contain rust and oxidation inhibitors.

[2] "Modern Trends in Hydraulic-Turbine Design in Europe," by G. A. Bovet, Trans. ASME, vol. 75, 1953, pp. 975–988.

Designs are now available which utilize antifriction bearings. The primary purpose is the reduction of operating forces and consequent smaller servomotor oil-pressure systems. Since the bearing load is essentially static, it is necessary to select bearings of adequate capacities to avoid brinelling and early failure of the races. Antifriction bearings have been used successfully in several Terry automatically adjustable-blade runners. Adequate shank seals and the use of rust-inhibited lubricating oils are expected to prevent corrosion of standard antifriction bearings.

Runner blades, usually made of cast steel, are subject during operation to cavitation pitting on the back or suction side and on the peripheral face. The elevation of the runner with respect to tail-water elevation is usually established on the basis of minimum cavitation as determined by laboratory tests. Operation above the given cavitation power limits is, however, sometimes economical in that the gain of output and revenue may be considerably in excess of the cost to repair pitted areas. The area, or pattern, of this pitting is well established from many units in service before preventive measures were applied, Fig. 6.

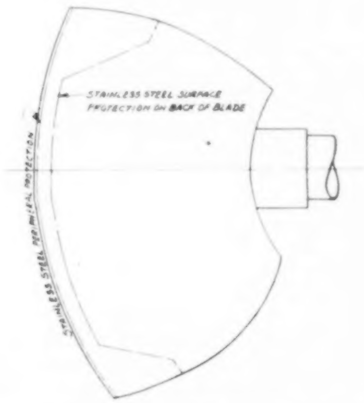

Fig. 6 Cavitation Protection on Periphery and Back of Adjustable Propeller Blade

Several methods have been in use for some years to protect the areas which may be attacked by cavitation, sometimes accelerated by corrosive agents contained in the water. The original shop-applied protection by prewelding with stainless-steel weld rods was developed from field repairs made on unprotected blades. This method still in use today, particularly on medium-size runners, utilizes 18-8 type 308 coated weld rods to overlay the areas. Owing to the fact that the first layer of beads on the cast steel picks up extra carbon and dilutes chrome and nickel in the fusion process, it is advisable to provide at least two layers of overlay to reduce dilution and more closely maintain the selected composition of the weld rod which gives best cavitation resistance.

However, this method is relatively expensive and other means have been developed in an effort to reduce cost and improve the product. The cladding method utilizes small 18-8 stainless-steel plates approximately $^3/_{16}$ in. thick and of about 15 sq in. area, either square or rectangular in shape, which are welded around the edges to form a quilt over the area to be protected. It is necessary to grind the cast-steel surface to a reasonable finish to provide a good surface for the cladding. The size of the strips, or plates, and their thickness are selected to prevent local flutter due to cavitation implosion forces. The reduced amount of welding over complete prewelding results in decreased distortion of the treated blade area.

The foregoing methods are not practicable for smaller blades because of the thin entrance and discharge edges. The blades either are entirely cast of stainless steel or cast stainless sections are welded to the cast steel.

A recent development utilizes a series-arc automatic welding apparatus mounted on a curved track to deposit the stainless overlay beads on large blades. To maintain proper space between the arc and the surface of the blade, the latter is supported on several jacks which tilt the blade automatically into correct position. The inherent light penetration of series-arc applied deposits results in low dilution of the chrome and nickel elements in the wire even in one-pass welding of $^3/_{16}$ to $^1/_4$ in. thickness.

The periphery of the blade usually is protected with stainless plates or weld overlay since repairs in place are difficult to perform. This protection is desirable even on low-head runners since wear eventually will occur as a result of the high velocity of the water passing through the clearance space.

The shape of the blade profiles is highly important for good performance and research on accurate models is continually carried on in the laboratories to improve efficiencies and cavitation characteristics.

Distributor. The wide spread of physical sizes of Kaplan distributors, Figs. 7 and 8, covering actual installations, requires adaptation of several concepts of design. The smaller sizes are more economically constructed in cast iron or cast steel, depending on the head, while the larger units are advantageously weld-fabricated of plate steel. Welded construction results in sound members with easily controlled weights and allowances for finish. Large and expensive patterns together with large molding-pit facilities are thus unnecessary; often quite extensive, inherent casting defects are avoided. Weld fabrication favors wheel cases for runner diameters of about 130 in. and larger. The advantage is even greater after the forming dies are available which may be used for a range of sizes.

Stay Ring. The stay ring is designed to span the throat outside of the wicket gates, to resist the separating forces due to the pressure in the case, and to support a superimposed load consisting of concrete, generator, hydraulic thrust, and so on. An integral structure of upper and lower crown flanges and stay vanes is preferred although the ring may have to be sectionalized to meet shipping limitations. Extra-large stay rings for comparatively low heads may be designed with separate guide vanes bolted to the two crown flanges. The inherently greater rigidity and better alignment of cast or weld-fabricated integral stay rings facilitate shop and field erection. This construction also provides greater resistance against distortion due to initial concrete embedment or subsequent working and settling.

Weld-fabricated rings such as shown in Fig. 9 are stress-relieved after welding to reduce residual strains and to maintain dimensional stability during and after machining.

Discharge Ring. It has become general practice to weld-fabricate throat rings of plate steel. Large rings are welded to the cast or formed curved bottom ring to make an integral piece as shown in Fig. 10. Most throat rings are solidly anchored and embedded in concrete to provide a rigid foundation for the distributor case. The expensive removable-type construction is rarely used today. Such a design is not warranted because damage has been reduced to a minimum by proper design and also because of the relative ease with which weld repairs of pitted areas may be made on the ring in place. The machine throat is partially curved to reduce the clearance between it and the periphery of the runner blades with resulting improved efficiency.

Head Cover. Weld fabrication also is applied extensively to head covers of larger sizes, Fig. 11. The inherent intricacy of the cover with its curved contours and necessary ribbing to pro-

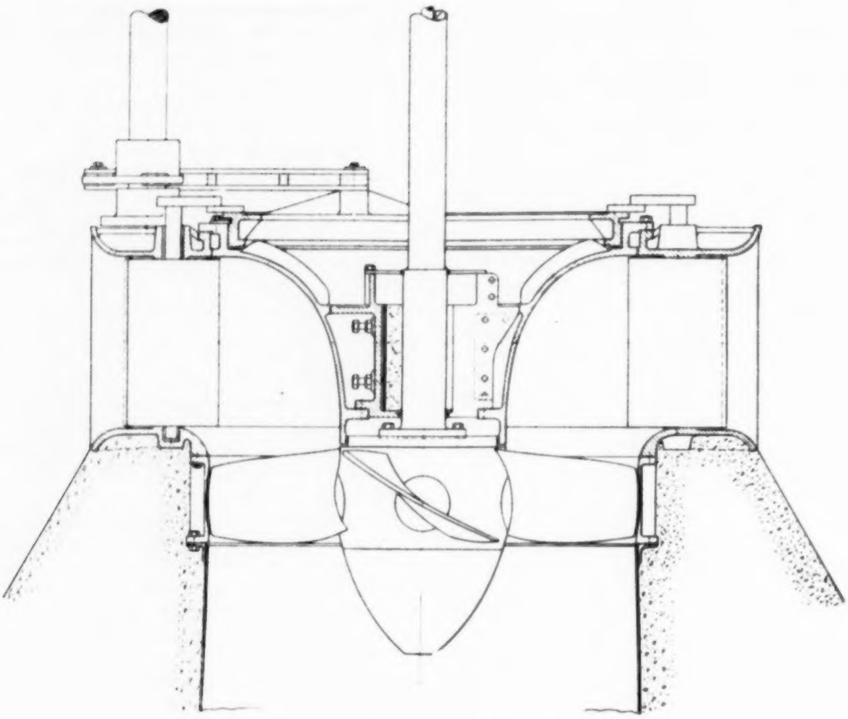

FIG. 7 DISTRIBUTOR SECTION OF A SMALL KAPLAN UNIT

vide sufficient rigidity against deflection due to water pressure and gate-servomotor reactions, and for the support of the guide bearing, makes it a risky casting. Splitting of the head cover into inner and outer rings facilitates assembly and removal of the runner without removing wicket gates. A circular joint is provided of a size that permits clearance over the runner diameter so that runner, shaft, and inner head cover will pass as a unit through the generator stator.

Wicket Gates. While, generally, wicket gates are made of cast steel, it is advantageous to fabricate smaller gates for heads up to 50 ft. The relatively large leaf is formed of plate steel and either welded or pinned to a stem of hot-rolled steel. Longitudinal sealing edges of the gates may be protected against corrosion and pitting with stainless steel. Increasing use is made of corrosion-resistant facing plates mounted on head cover and bottom ring to protect and maintain gate-end clearances. The mating gate ends may be protected against wear by weld overlay, bars, or plates of stainless steel.

Rubber seals mounted in the facing plates have been utilized on some installations to reduce leakage during shutdown or when considerable motoring will be done.

Guide Bearing. Water-lubricated shaft-guide bearings are used extensively for runner diameters up to 100 in. and sometimes for larger units. Usually of the strip, or stave, adjustable-block or shoe, or rubber-sleeve type, the bearings have performed quite successfully, particularly when the shaft journal through bearings and packing box is protected with a corrosion-resistant sleeve. The original lignum-vitae blocks are gradually being replaced by laminated phenolic plastics, first, because of the poorer quality of the former now available and secondly, because of the considerably longer life of the latter which readily offsets the greater initial cost.

The neck of the head cover which supports the bearing restricts space on smaller units to such an extent that a grease-lubricated bearing is the only alternative. Indeed, if the available lubricating water from the case, or flume, cannot be strained satisfactorily or is otherwise unsuitable and an outside source cannot be provided, this is the only practical solution. Although extensively used by European manufacturers, the grease bearing has not met with much favor in this country owing to the fact that the grease supply must, of necessity, be expendable.

While water-lubricated guide bearings for shafts of large sizes are in successful service, it is accepted practice to provide oil-lubricated bearings wherever possible. Lubrication may be furnished by an oil-circulating system or the bearing may be of the immersed self-pumping skirt type. The latter bearing is limited to larger turbine sizes because of its greater radial space requirements over conventional bearings, thereby reducing accessibility to the packing box which is located between it and the runner.

Packing boxes of the carbon seal-ring type have not as yet been installed on Kaplan turbines although they are in successful service on Francis units. There is no reason why they should not serve equally well on Kaplan types, provided the water does not contain silt. The self-adjusting feature lends itself particularly well to smaller units where access space is restricted.

Main Shaft and Blade Operator. The forged-steel shafts have reached tremendous dimensions; the diameter of the Dalles shaft is 45 in. Designs are based on stresses which are conservative, approximately 5000 psi at rating, and assure reliable service. The portion of the shaft passing through the packing box, and water-lubricated bearing, where used, is protected with corrosion-resistant replaceable sleeves.

While the tendency in Europe is toward closer coupled units

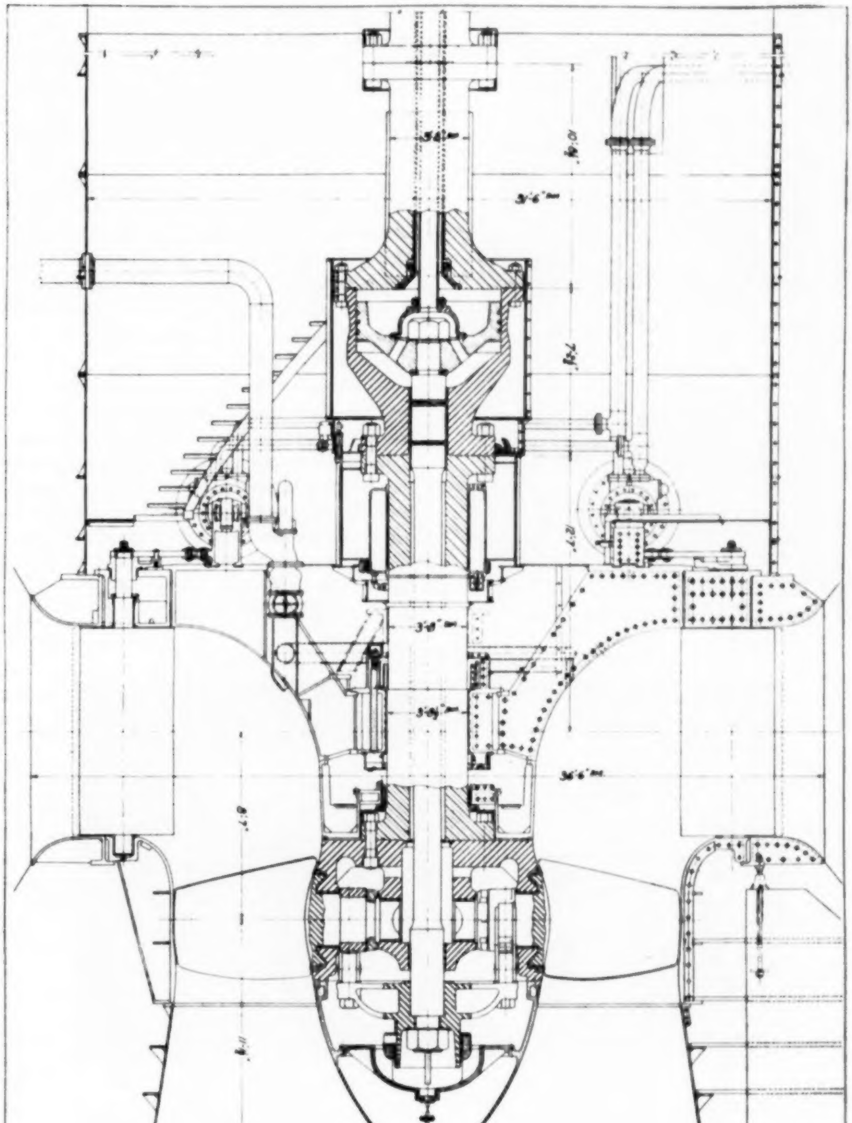

FIG. 8 DISTRIBUTOR SECTION OF A LARGE KAPLAN UNIT

with a minimum distance between turbine and generator, there is not a noticeable tendency in this direction in the United States. Judging from experience, the consulting engineers and governmental agencies who design the power plants tend to keep the generator-floor elevation relatively high with respect to the turbine, either from the standpoint of stability of the powerhouse or from a desire to keep the generator floor above maximum tail-water level, or very little below it. This usually results in ample space below the generator for the thrust bearing and for the hydraulic-blade servomotor. A practical advantage of this servomotor location is its accessibility for inspection. In this country it is considered advantageous to make this servomotor a part of the turbine, entirely separate from the generator rotor or the thrust bearing, so as not to interfere with generator design and to facilitate servicing of the thrust bearing.

In Europe, the thrust bearings are usually furnished by the turbine manufacturer whereas in the United States they are always supplied by the generator manufacturer. This tends to keep the thrust bearing apart from the turbine but, even if this were not the case, the advantage derived from having the thrust bearing mounted directly on the turbine head cover, or supported therefrom at a higher elevation, would appear questionable.

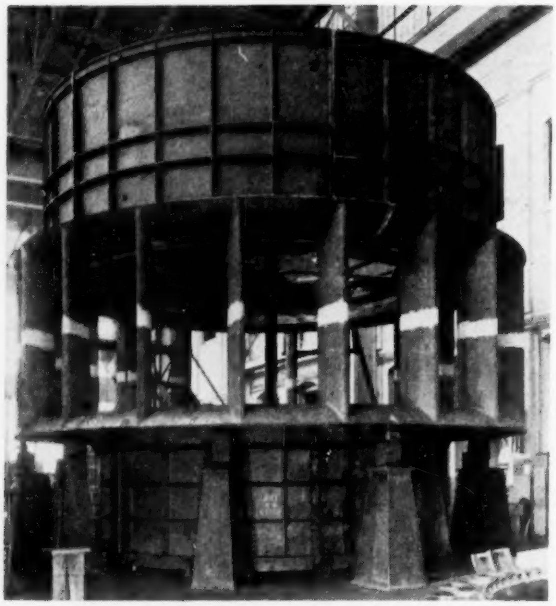

Fig. 9 Large Stay Ring of Weld-Fabrication

This statement is made from the standpoint of possible vibration and the impairment of turbine-bearing accessibility.

Depending on size and economical aspects, the servomotor cylinder is forged integrally with the turbine shaft or made a separate piece either of forged or cast steel.

The majority of Kaplan units are equipped with hydraulic servomotors to operate the blades to provide quick response when load changes call for an adjustment. Some smaller units are provided with a manually operated gear-and-screw-type mechanism which is mounted between the shaft-coupling flanges. Although the full benefit of the Kaplan feature is not realized, such a lower-cost installation may be justified when the unit is normally operated at full load corresponding to the head, and the variation of head for which the blades are manually adjusted at standstill is gradual.

Electric motor-driven operators, as large as 10 hp, also mounted between shaft flanges, have been furnished with several units, Fig. 12. This type was developed in connection with Kaplan runners which replaced existing fixed-blade runners, utilizing the old generators with solid shafts. These units operate entirely satisfactorily when tied into a system but are not suitable for close regulation because blade adjustments must, of necessity, be slow. Numerous slip rings are required for the leads to the motor and the electric transmitter for automatic positioning or remote indication of the blade setting.

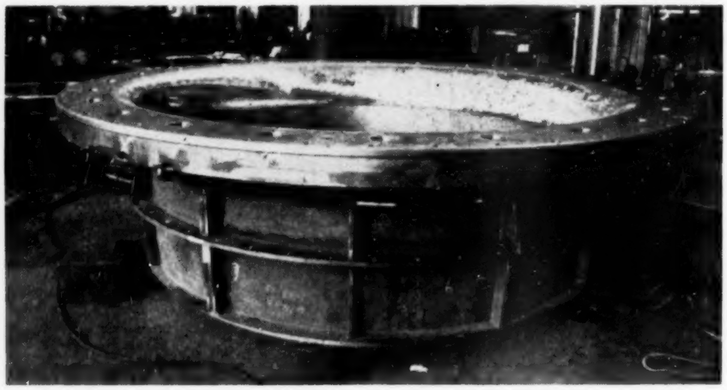

Fig. 10 Large Discharge Ring of Weld-Fabrication

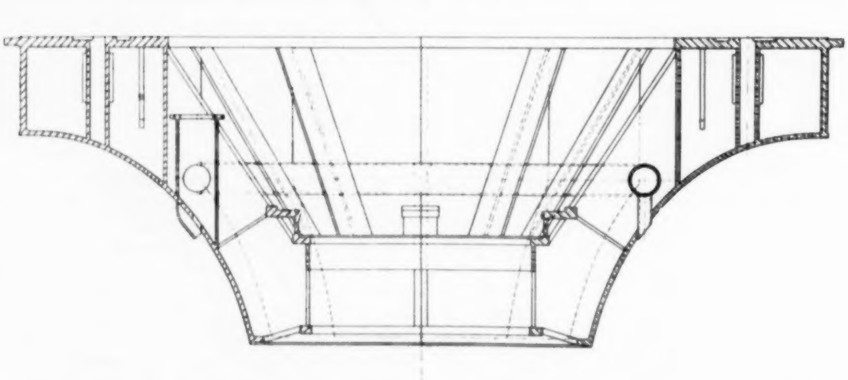

Fig. 11 Weld-Fabricated Inner Head Cover for McNary

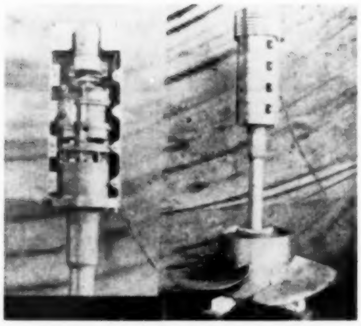

FIG. 12 EXTERNAL VIEW AND SECTION OF ELECTRICAL ADJUSTABLE-BLADE OPERATING MECHANISM

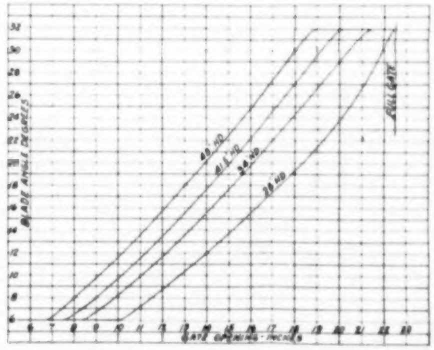

FIG. 13 CURVES SHOWING GATE OPENING-BLADE ANGLE RELATIONSHIP FOR A KAPLAN TURBINE OPERATING UNDER A HEAD RANGE OF 48–25 FT

KAPLAN CONTROLS

To produce proper synchronization of the runner-blade position with the wicket-gate opening over the full stroke, it is necessary to interconnect the four-way control valve mechanically, if the Kaplan runner blades are hydraulically operated, with the governor in such manner that correct relationship is always maintained. Fig. 13 shows a typical curve of the relationship for best performance between gate opening and runner-blade position for various heads. A cam driven by the movement of the governor is used to position the roller of the Kaplan control-valve floating lever. In the case of actuators, particularly of the cabinet type where wicket-gate servomotor and Kaplan-blade-servomotor control valves are installed in a single cabinet, the cam is mounted on a rotating shaft. The cam for separate Kaplan control valves used in combination with gate-shaft governors is usually of the sliding reciprocating type, Fig. 14.

The design of cam shapes is based on laboratory model data. Its correctness should be confirmed by field index tests.[3]

Relatively small head variations permit the use of a single cam which, because of the parallelism of the curves, Fig. 13, is shifted manually to maintain proper relationship for the respective heads. Large head ranges require several cams which can be positioned readily, to reduce compromise of the cam shape within narrow head ranges to a minimum and thereby produce best performance of the unit.

Repositioning of the Kaplan control valve to neutral is provided by a restoring mechanism which is connected rigidly to the blade-servomotor piston through the oil distributor mounted on top of the generator and the inner oil pipe located in the generator shaft.

It is the practice in this country to furnish an inner and an outer pipe located concentrically in the generator-shaft hole to supply oil pressure to the bottom or the top of the servomotor piston. Thus the generator-shaft design is simplified in that it is not necessary to make oil-tight joints in the generator which would be the case if the shaft hole were used as the outer oil conduit.

The type of connection of the oil pipes to the servomotor, as customarily furnished, requires access space at the cylinder-shaft flange coupling. Separation of the flanges by as much as 12 in. for large units is accomplished by lifting or jacking the generator rotor. Oil-distributor and exciter parts which are mounted on top of the generator cannot be designed conveniently for this lift and must be removed.

Several units have been equipped with oil pipes which are screwed into sockets in the servomotor after the cylinder and shaft

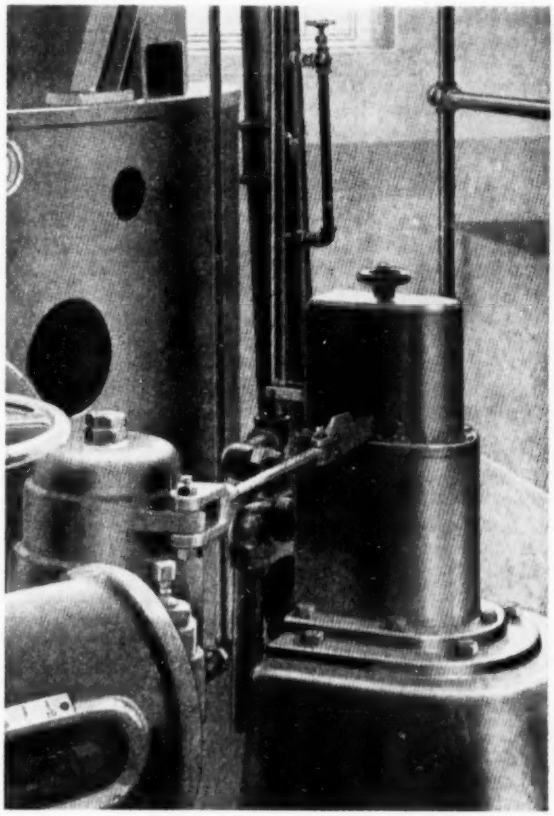

FIG. 14 KAPLAN CONTROL VALVE WITH SLIDING AND RECIPROCATING CAM

flanges are coupled. A rotor lift is, therefore, unnecessary. Extreme care must be exercised during erection to assure oil-tight joints. The units equipped with such pipes are operating entirely satisfactorily.

The timing of the blade-opening movement coincides with the governor timing for load-on to provide quick response. However, the closing time of the blades is usually increased to approximately twice the opening time to produce a lag with respect to

[3] "Index Testing of Hydraulic Turbines," by G. H. Voaden, Trans. ASME, vol. 73, 1951, pp. 481–488.

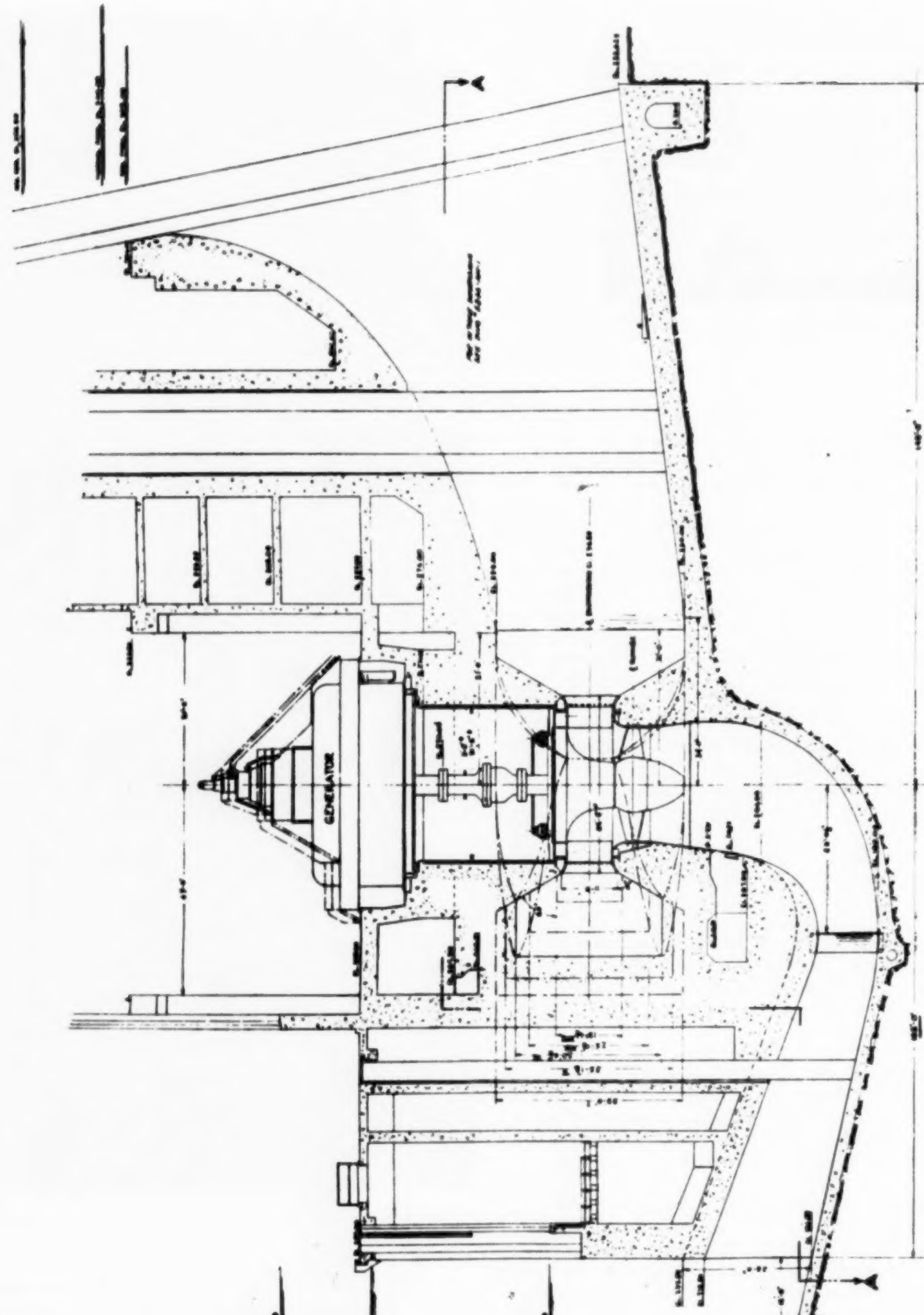

Fig. 15 Cross Section of Powerhouse and Kaplan Turbine Installed at McNary Dam, 111,300 Hp at 80 Ft Head, 85.7 Rpm

the wicket-gate movement for better regulation during quick reversals of load.

Operating pressures of the governor oil system vary from 200 to 350 psi depending on the make and type of governor. Consideration should be given to pressures of 400 to 500 psi for large units to permit reduction of the size of the pressure system.

Kaplan control valves for units provided with remote governor-starting equipment are furnished with a device that permits presetting of the blades into a fixed intermediate position to facilitate starting and synchronizing. The device is de-energized when the unit is on the line and the cam then takes over control of the blade position.

Controls for electric-blade operators usually consist of push buttons and remote electric dial indicator to set the blades from the switchboard. Positioning is done in accordance with charts giving blade angle with respect to gate opening and head. The blade-stroke time must be long, 15 sec or more, to permit the use of a reasonable size of motor and gear reduction.

Several units are in satisfactory operation with automatically adjusting electric operators. But again, because of the inherent long timing for a complete stroke this equipment is not recommended for units subject to frequent load changes.

Air Valve. Because the Kaplan runner-blade position is adjusted for various loads, it is not necessary to provide a supply of atmospheric air to the draft tube for part load, as required on other reaction-type runners. An air dump valve to break the draft-tube vacuum upon shutdown is needed, however. Usually of the balanced swing-check, or the spring-loaded poppet type, the valve opens automatically on low pressure under the head cover and closes slowly, controlled by a dashpot if such a device is provided. The valve takes its air from the turbine pit or through piping from the outside of the powerhouse. The latter is preferable because of less noise when the valve operates.

Spiral Case. The maximum operating heads used for Kaplan turbines in the United States, up to the present, suggest in the majority of installations a reinforced-concrete design of the semi-spiral type, with the powerhouse incorporated in or attached to the dam structure, Fig. 15. If penstocks are necessary, then it becomes a matter of economics to decide whether to design a full spiral case of relatively light plate-steel construction or reinforced concrete with attendant expensive forms.

Draft Tube. The large quantities of water passing through Kaplan runners require highly efficient draft tubes to recover the relatively high kinetic energy in the water at the runner discharge by decelerating its velocity to the outlet with minimum loss. Draft tubes, with few exceptions, are of the elbow type.

Cavitation characteristics of Kaplan runners require a relatively low setting of the discharge edge with respect to tail water. Therefore the bottom leg of the draft tube is usually sloped upward toward the outlet end to reduce excavation. The height of the vertical leg is important in that it must be great enough, at least two or more times the diameter of the runner, to permit sufficient deceleration of the velocity before entering the elbow portion.

Runaway Speed. The high runaway speed of Kaplan turbines, as discussed in a previous paper,[4] deserves serious consideration. Provisions to reduce it to a reasonable value should be made. But rather than adding separate braking blades as advanced by a European manufacturer, the runner blades themselves can be utilized with the same effect. The overspeed is substantially reduced when the blades are at the steeper angles and the blade pivot positions can be so located as to have a decided tendency to go open if released. A dependable device is, however, necessary to uncouple the blades from the control system and let them go open when a predetermined overspeed is reached.

[4] "Runaway Speed of Kaplan Turbines," by G. H. Voaden, Trans. ASME, vol. 74, 1952, pp. 989–997.

Discussion

W. J. Rheingans.[5] The author has presented an excellent paper on Kaplan turbines. However, the writer would like to present some additional information on the design and trends in this type of turbine, which probably was not available at the time the paper was written.

The author defines a Kaplan turbine as an adjustable-blade propeller turbine and apparently includes under that definition those with manually operated gear and screw-type mechanism, mounted between the shaft-coupling flanges. If such is the case, then Kaplan-type turbines were in operation in this country before the year 1928, mentioned in the abstract of the paper. During the years 1925 to 1927, the writer's company built twenty-three Kaplan turbines of the manually as well as electric-motor-operated types.

The author mentions the Vargan installation in Norway as an example of a syphon setting for low head. Another example a little closer to home is the Henry Ford and Son, Green Island Plant in New York, N. Y., built in 1921, consisting of four units rated 2000 hp each at 13-ft head. Normal headwater at this plant is at the center line of the distributor, with the surrounding scroll-case roof 11 ft above normal headwater elevation. This plant has given satisfactory performance during its 32 years of operation.

Mention is made in the paper of antifriction bearings, as having been used successfully in several Terry automatically adjustable-blade runners. At the Pickwick Plant of the TVA, two of the largest-size standard Kaplan runners in this country (292 in. diam) have been operating satisfactorily for more than a year with antifriction bearings. The Washington, Chelan County PUD No. 1, Rock Island Plant, has had six Kaplan units in operation for about a year with antifriction bearings in the runner. Recent inspections indicated that these bearings were giving no trouble.

The author mentions the grease-lubricated main guide bearing as being used extensively by European manufacturers. The writer's company furnished a grease-lubricated bearing in 1939, for the Kaplan service unit at Santee Cooper Power Plant. This has given 14 years of trouble-free operation. Grease-lubricated bearings also were furnished for the six Kaplan units for the Rock Island Power Plant just mentioned. These have given about a year of satisfactory operation so far.

The grease-lubricated bearings have many advantages, among them being the minimum space requirements for smaller units mentioned by the author. Other advantages over oil-lubricated bearings are accessibility of the packing box, which is located above the bearing, elimination of oil pumps and motors with their stand-by equipment, and elimination of sump pumps and stand-bys. The grease-lubricated bearing also eliminates danger of flooding the oil reservoir and wiping the bearing. These advantages outweigh the disadvantage of an expendable grease supply, which normally is less than a pound per day.

The writer's company also has been using the carbon sealing type of packing boxes on a number of Kaplan turbines successfully for several years. However, it is important that this type of packing box be supplied with silt-free water.

The author states that the closing time of the runner blades usually is increased to approximately twice the opening time to produce a lag with respect to wicket-gate movement for

[5] Hydraulics Section, Allis-Chalmers Manufacturing Company, Milwaukee, Wis. Mem. ASME.

better regulation during quick reversals of load. It is rather difficult to see just how a lag would improve regulation. Recently the writer's company furnished the governors for some Kaplan units built by the author's company, and the closing time of the runner blades was set at 60 sec, which was about twelve times the opening time. It was thought that the reason for this was to reduce the runaway speed of the unit during load rejection since the runaway speed is less with a steep tilt than a flat tilt. It would be interesting if the author would explain the necessity for such long runner-blade closing times.

T. Zowski.[6] This interesting review of Kaplan turbine-design trends includes several comments concerning the differences between American and European designs. These differences are often noticed by the writer in connection with the foreign hydroelectric plants being designed by the organization with which the writer is associated. The author's comments concerning the European tendency toward closer-coupled turbines and generators, and the lack of such tendency in American practice, are of considerable interest. The American tendency to place the generator-room floor at a relatively high level does not seem to be attributable to any one predominant design consideration. The author suggests that this tendency results from the desire to keep the generator floor high in relation to tailwater. Although the maximum tailwater level is a contributing factor, it is not always the deciding factor, as many powerhouses provide for maximum tailwater substantially above (20 to 30 ft) the generator-room floor.

In some cases it is practical to place the generator-room floor at the level of the main access to the powerhouse for operating convenience, even when this may require some lengthening of the turbine shaft.

As a rule, the provision of a turbine-room floor also results in a higher generator floor and longer shaft. The provision of a turbine-room floor is largely a matter of preference; some utilities and the Corps of Engineers usually insist on having a turbine-room floor, while others, including the TVA, do not.

In plants designed by the writer's company, it is generally preferred to provide a turbine-room floor, since there are many important advantages of having the extra floor space for plant auxiliary equipment. This results in greater operating convenience and accessibility for maintenance. We have designed powerhouses both with and without turbine-room floors, and we feel that such a floor is very desirable for large Kaplan turbines, and practicable for units of sizes down to about 100-in. runner diameter.

The provision of a turbine room usually places the generator-room floor at an elevation sufficiently high to assure ample space between the turbine and generator for proper access and for installation of the blade servomotor and thrust bearing.

In discussing the use of antifriction bearings for Kaplan-runner blades, the author mentions their successful application on several Terry-type runners. The following more recent American installations with runner blades mounted on roller bearings are also considered noteworthy:

Plant	No. of units	Rated head, ft	Runner diam, in.
Pickwick, Units 5 & 6	2	47	292
Rock Island, Wash.	6	45	225
Rochester G&E Sta. 26A	1	25	124
Hemlock Falls, Mich.	1	34	82

[6] Chief Mechanical Engineer, Harza Engineering Company, Chicago, Ill. Mem. ASME.

It is significant that the roller bearings in all of these units are of the standard carbon-steel type. According to the writer's knowledge, the bearings on one of the Terry units at Austin Dam were inspected after 13 years of operation and found to be in excellent condition. With the use of adequate blade seals and rust-inhibited oils, it does not seem necessary to use the more costly stainless-steel-type antifriction bearings.

In regard to the use of carbon-seal rings for the main-shaft packing boxes, the writer's information indicates that this type of packing is now in operation on a Kaplan unit at Drop No. 4 of the All American Canal and on six Kaplan units at Rock Island. The fourKaplan turbines being built by the Allis-Chalmers Manufacturing Company for the Box Canyon power plant, designed by the writer's company, also will have carbon-seal main-shaft packings. Clear water will be supplied to the seals for lubricating and purging purposes. The purging action is the main function of the clear water since the seals are sensitive to abrasives in the raw water.

It is believed that the seals could operate dry for a considerable time without damage to the shaft of overheating, although actual data for such operation are not known to the writer. A simple rubber sealing device operated by compressed air is provided below the main packings to facilitate replacement of the carbon rings.

The use of grease-lubricated main bearings with carbon-ring end seals on the Rock Island and Box Canyon turbines is another noteworthy feature of these large Kaplan turbines.

Author's Closure

The discussers have presented interesting supplementary information which enhances the value of the paper.

Mr. Rheingans' reference to the inclusion of manual and electromechanical operation under Kaplan turbines is well taken. The author's company also furnished numerous units with such blade operation; however, they were not included in the total number of Kaplan turbines listed since they do not make use of the full Kaplan principle, namely, the simultaneous adjustment of gates and blades under all conditions. Although some units equipped with electro-mechanical blade operators were tried under automatic control, the results were unsatisfactory because of the slow stroking speed. The information was added to explain the various available methods of operating the blades, but the author was amiss in not making it clear that units so controlled are not considered to be called Kaplan turbines.

The blade-closing time of the installation to which Mr. Rheingans refers has been materially reduced from the sixty seconds for which the Kaplan control valve was set during initial trials. The long timing was precautionary for the trial runs to keep the blades at the largest possible angle during checking of load rejection until all the control devices were properly adjusted. While unimportant on units with normally fixed load, we consider it desirable (on regulating units) to make the timing for the closing stroke longer than for the opening stroke. If the load drops and comes back on immediately then the blades have closed only partially and require less travel for restoration to the original position.

Mr. Zowski's remarks on floor elevations are enlightening. It is gratifying to learn that the several installations cited operate successfully with standard antifriction bearings and that carbon rings are in actual use on shaft seals for Kaplan turbines.

The author wishes to express his sincere appreciation for the comments offered by Messrs. Rheingans and Zowski.

Grand Coulee Model-Pump Investigation of Transient Pressures and Methods for Their Reduction

By E. LINDROS,[1] LOS ANGELES, CALIF.

In May, 1951, when the first of six pumps ordered for the Grand Coulee Dam was put in service, a defect of major concern was discovered. This unfavorable condition embodied objectionable discharge-line vibration. Investigation revealed that this was caused by transient pressure variation in the pump, and remedial measures incorporating reinforcement of the discharge lines were taken to minimize this condition. No previous investigation had been made of the offending transient pressure variation. This paper describes such an investigation, the test setup used, and reveals the difficulty encountered in applying instrumentation to obtain necessary data.

Introduction

When the first of six pumps, furnished to the United States Bureau of Reclamation by the Pelton Water Wheel Company, San Francisco, and Byron Jackson Co., Los Angeles, was started at Grand Coulee in May, 1951, a condition was discovered which resulted in a continuing program of investigation and alterations covering a period of more than 2 years. This condition, a transient pressure variation in the pump discharge, resulted in objectionable discharge-line vibration as described in a recent paper by Parmakian.[2] Reinforcement of the discharge lines by the addition of numerous stiffener rings, and prototype alterations resulting from extensive model and prototype tests eventually reduced the discharge-line vibrations to acceptable limits.

Comprehensive and exacting model tests, witnessed by the USBR and leading to a final model for the prototype, were performed on the contractor's model pump in accordance with specifications. A complete description of this testing program was published in January, 1950.[3] However, the offending transient pressures were neither investigated, nor was their presence observed or suspected. As described,[3] the model tests were performed at field heads, requiring high-speed operation. The presence of transient pressures within the pump casings and at their discharge was first discovered in the prototype operating at its relatively slow speed of 200 rpm.

Remote location, time and expense of alterations due to size, and lack of power for extensive experimental testing dictated that the major part of the experimentation be done with models. Since water hammer was believed to be involved in the problem, it was considered essential that all operation be at field heads to duplicate prototype conditions as nearly as possible. The salient objection to this high-speed operation was the extreme difficulty encountered in accurately recording transient pressures at frequencies of from 300 to 1820 cycles per sec (cps).

Soon after the initial start-up of Unit P-1 in May, 1951, investigation by Bureau personnel revealed the existence of sizable pressure transients within the pump casing and lesser ones with the same basic frequency in the discharge line. Temporary alterations were made to this pump to permit operation with the unreinforced pipe line. Unit P-2 was started in July, 1951, after having been altered in a slightly different manner. Since neither of the altered units was considered to be entirely satisfactory from a transient-pressure standpoint, additional investigation was indicated. The original contractor's model was set up in the laboratory of the author's company, and testing was started in early September, 1951.

Test Setup

The test setup differed slightly from that in the Hydrodynamics Laboratory of the California Institute of Technology previously described[3] and shown in Figs. 1 and 2. Suction pressure was supplied by a vertical booster pump and the tank containing the intake transition (duplicating that at the dam), Fig. 2, was omitted. However, the model suction elbow and long discharge diffuser, being considered a part of the pump, were included. For convenience in piping, the pump casing was rotated 90 deg from its former vertical position to discharge horizontally. Also, the suction elbow was placed in a horizontal position. Suction pressure was measured by a mercury column, and discharge pressure by calibrated Bourdon gage. Flow was obtained by a calibrated venturi meter in the suction line.

To minimize transient disturbances from throttling, the discharge was manifolded to a number of pipes of various sizes in parallel, each containing a nest of smaller pipes to increase wetted surface. Each of these pipes was designed to dissipate the entire head produced by the pump at a specified flow rate. By use of various combinations in parallel, it was possible to obtain seven points in the desired operating range without resorting to throttling by valves. The model, $^1/_{13}$th prototype size, was driven at 13 times prototype speed, or 2600 rpm, to duplicate water velocities and heads. Power was supplied by a 400-hp d-c dynamometer with accurate speed control.

Time did not permit an exhaustive search for a suitable gage to respond to the transient pressures produced by the model. Because of the frequencies involved, the pickup had to be located in or very near the wall of the pipe in which transients were being measured. The first recordings were made using a pickup designed for recording pressures in cylinders of internal-combustion engines. This pickup utilized a small piston in its face, transmitting pressure to a quartz crystal. The assembly was sealed by copper gaskets. No prolonged runs with this equipment were possible, since even minute quantities of moisture, virtually im-

[1] Assistant Chief Engineer, Byron Jackson Co. Assoc. Mem. ASME.

[2] "Vibration of the Grand Coulee Pump-Discharge Lines," by J. Parmakian, published in this issue, pp. 783–790.

[3] "Development of the Hydraulic Design for the Grand Coulee Pumps," by Carl Blom, Trans. ASME, vol. 72, 1950, pp. 52–70.

Contributed by the Hydraulic Division and presented at the Annual Meeting, New York, N. Y., November 29–December 4, 1953, of The American Society of Mechanical Engineers.

 Manuscript received at ASME Headquarters, October 5, 1953. Paper No. 53—A-213.

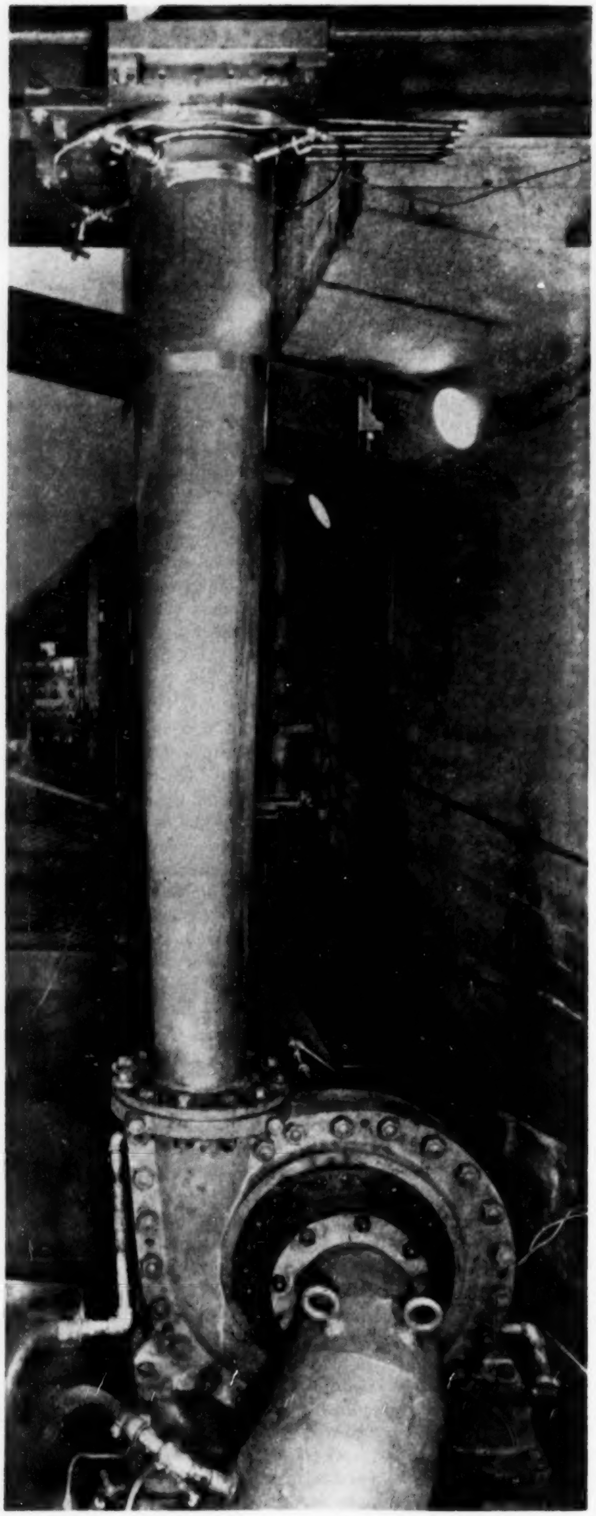

FIG. 1 GRAND COULEE MODEL PUMP INSTALLED IN CAL TECH LAB

FIG. 2 MODEL OF INLET TRASH RACK

possible to exclude, made it inoperative. Also, it was necessary to amplify the output of the piezoelectric quartz crystal a thousand times in order to drive the galvanometers in the oscillograph. An additional drawback, discovered during the initial phases of the program, was the susceptibility of the pickup to vibration. The combined mass of crystal and piston was such that, under some conditions, two thirds of the resultant signal was produced by vibration of the pipe wall and pickup.

Eventually, a pressure pickup, avoiding or minimizing these several disadvantages, was developed. This new pickup utilized a piezoelectric ceramic disk (barium titanate) 0.5 in. diam by 0.1 in. thick, silver-plated on both faces. The body of this instrument was made of type-303 stainless steel. A thin, spun-brass cup at the pressure end of the body contained the $BaTiO_3$ disk, the outside diameter of the disk being insulated from the cup by a thin cylinder of polystyrene. An O-ring in a groove in the body effectively sealed out moisture. A specially constructed and formed beryllium-copper spring, shouldered at the end of the pickup body, maintained pressure on the brass cup and disk. A polystyrene plug, screwed into the terminal end of the pickup, completed the assembly. This plug was faced with brass where it contacted the $BaTiO_3$ disk and contained a center contact for the amplifier. The body of the pickup, contacting the lower face of the disk through the spring and brass cup, formed the second contact.

The greatly reduced mass of the sensitive element in this pickup resulted in fewer disturbances from vibration. Its sensitivity, about 100 times that of the quartz crystal, greatly simplified the problem of recording. Furthermore, if dampness made it inoperative, it could be cleaned and dried quite simply and im-

mediately put back into service. Because the pressure pickups used are sensitive only to changes of pressure, it was necessary to produce a known pressure variation for calibration purposes. To accomplish this, a small eccentric flywheel, mounted on ball bearings, was clamped securely to the piston of a Crosby deadweight tester and the pickup was connected to the pressure chamber. With the air bled from the tester the natural frequency of the calibration setup was recorded by tapping the piston lightly. The flywheel was then started, spinning freely, and recordings were made of the signals produced. The piston was rotating in its cylinder during all recording. With the exact weight and eccentricity of the flywheel known and the rotating speed obtainable from the recordings, it was possible to determine the load applied to the pickup. Displacement was measured directly on the recordings, and sensitivity in inches per psi was calculated. Natural frequency of the system was considered in sensitivity calculations. A typical recording of free oscillations, for natural-frequency calculations, is shown in Fig. 3. Fig. 4 shows a typical calibration run. Timing lines are spaced at $^1/_{100}$-sec intervals.

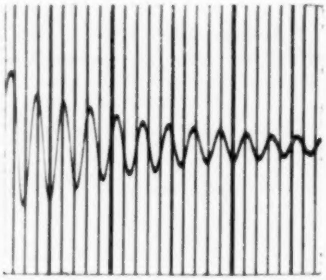

Fig. 3 Recording of Free Oscillations of Pickup and Tester

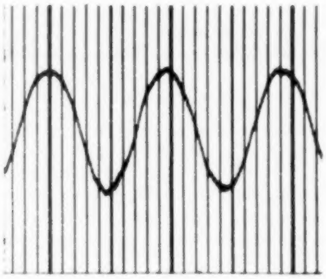

Fig. 4 Recording of Pickup Calibration

Calibration Runs

Calibration recordings were made with the same amplifiers and on the same oscillograph channels used during test runs. Recordings of a known 60-cycle voltage were made before and after each calibrating run and each test run. This voltage (approximately 0.025 volt) was applied at the input side of the preamplifier and afforded a quantitative check of the entire electrical system including the oscillograph galvanometers and optical system. Fig. 5 is a typical recording made prior to a gage-calibration run.

Pressure transients were recorded in the suction pipe near the pressure-piezometer connections and in the discharge diffuser at points corresponding to prototype distances of 22 ft and 96 ft from its center line. An unsuccessful effort was made to install the pickup in the wall of the pump case between diffuser vanes.

In excess of 100 tests were run on the model during this period, checking the effects of minor alterations to both the diffuser casing and the impeller. As may be seen[2] extensive alterations were ruled out due to structural considerations and the necessity of complying with rigid performance requirements.

As previously explained,[3] a dividing rib had been added to the original model to improve velocity distribution, Fig. 6. During

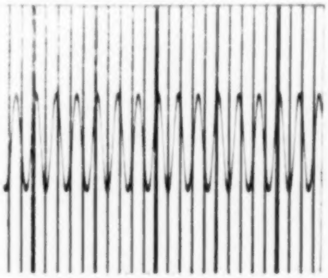

Fig. 5 Recording of Standard Reference Voltage

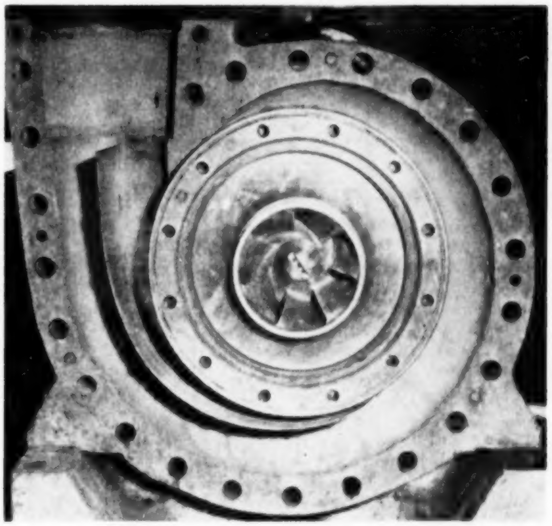

Fig. 6 Grand Coulee Model Pump With Half of Casing Removed Showing Impeller, Diffuser Ring, and Separating Rib

this investigation, transient pressures were recorded at field heads on the original model with this dividing rib in place and with it removed. Both these tests and those on the prototype confirmed the existence of stronger transients in the final discharge with the rib in place than when removed. This fact, coupled with the inability of the rib structurally to withstand the effects of the transient pressures encountered, led to its eventual removal from all prototypes. Though this relatively thin membrane was not considered to be a stress-carrying part from an average pressure standpoint, it was subjected alternately to relatively strong transient pressures which ultimately would have led to its destruction. No decrease in efficiency of the prototype was noted on removal of this rib.

Numerous alterations were made to impellers and diffuser vanes. One diffuser was altered in a manner which logically could be expected to increase the amplitude of pressure transients.

This was done deliberately, and confirmation, at the time, was most gratifying.

Model test results obtained in late November and early December, 1951, indicated that a solution had been found which would result in substantial reductions in transient pressures under all operating conditions. This alteration was the end result of successive cutting back of the inner tips of the diffuser vanes in varying amounts. It was decided to make similar alterations to one of the prototypes in an attempt to obtain comparable results.

TABLE 1 ANGLES IN DEGREES BETWEEN DIFFUSER-VANE TIPS AT INLET
(Grand Coulee Pump No. P-1)

Angle (see Fig. 7)	Test number 1	2	3
y	10.25	6.50	2.00
a	63.45	64.07	66.57
b	59.29	62.44	63.95
c	59.22	60.82[a]	61.31
d	61.31	59.18	58.69
e	59.81	57.56	56.05
f	56.92	55.93	53.43

[a] A section was added to tip of vane D during this alteration.

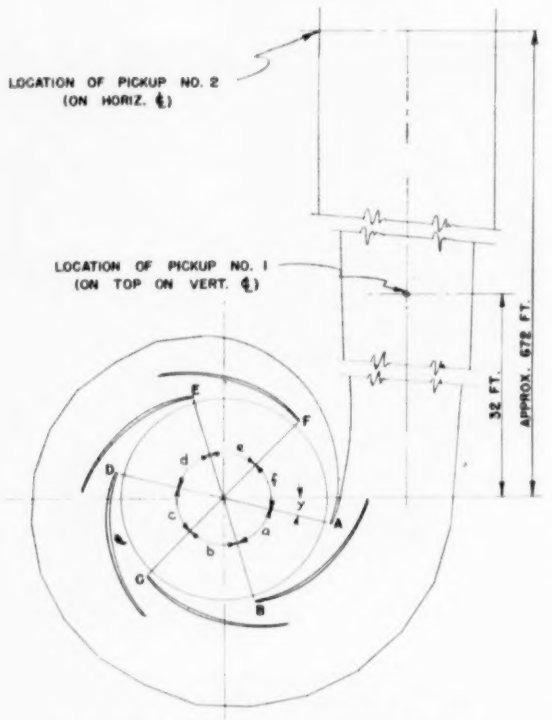

FIG. 7 TRIAL ALTERATIONS TO PROTOTYPE DIFFUSER

Column 1, Table 1, lists the angles between inlet tips of the diffuser ring for the first test in this series. It will be noted from Fig. 7 and Table 1 that the separator rib previously had been removed, as well as a piece of about $3^1/_2$ deg from vane A. Column 2, Table 1, lists the angles resulting from the first alteration and column 3 lists the angles after a second alteration. Transient pressures in the discharge line at roughly equal discharge capacities are shown on recordings 1–3, 2–3, and 3–3, Fig. 8. Efficiency was not significantly affected by these changes.

On the basis of model tests, a greater reduction in the strength of transients had been expected in Test 3 of this series. Although

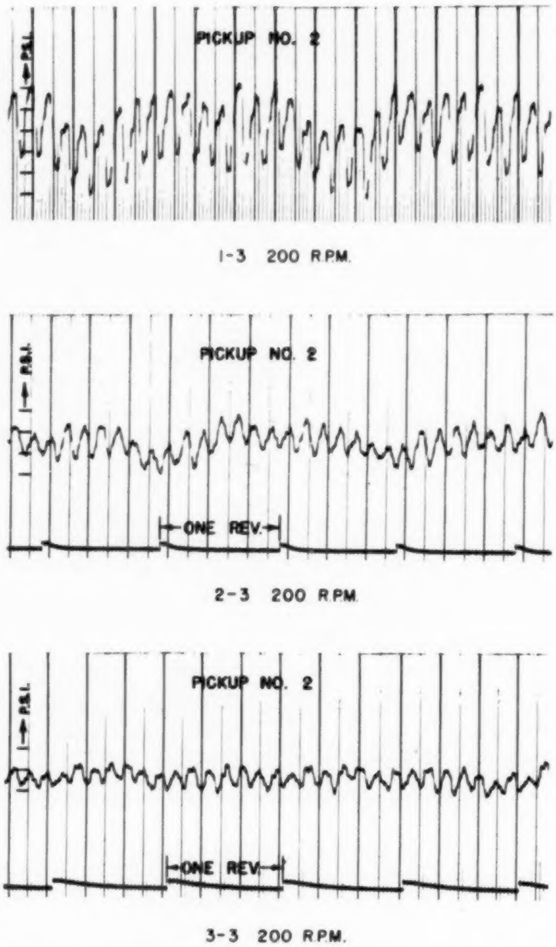

FIG. 8 RECORDINGS OF TRANSIENTS DURING TRIAL-ALTERATION PROGRAM

a sizable reduction had been realized in the transient pressures produced by the pump, as the results were not the same, they were not considered to represent a final solution to the problem, and model testing was resumed.

The model discharge piping had been dismantled during the lull for the prototype testing and had to be reconnected for the resumption of model testing. Though the next test was run without changes to the model, it at once became apparent that previous encouraging results could not be duplicated. Numerous extensive changes were made to the discharge line, each resulting in some change in the strength of recorded transients. The suction supply was altered in various ways to remove disturbances from this source, two boosters were used in parallel in place of the one previously used, and impellers in these were changed twice. The supply was piped to a large tank containing an air cushion and thence to the pump. Results obtained in November, 1951, could not be duplicated.

ADDITIONAL ALTERATIONS

Additional alterations were made to the several diffuser rings and impellers. One impeller was trimmed in successive small increments without reducing transients significantly. A slot

was cut in the final vane A, Fig. 7, but this only increased capacity and reduced efficiency. Also, during and after this program, numerous alterations to the prototypes were suggested and some were tried. Some vane tips were shortened and some were lengthened, and at one time air was introduced into the diffuser. The area of one diffuser section was reduced by a baffle plate to reduce hydraulic losses. None of these alterations resulted in material reductions in the strength of transient pressures.

Figs. 9 through 25 illustrate a few of the recordings made on the model discharge line at a point corresponding to 96 ft from the prototype center line. Figs. 9, 10, and 11 show the effect of trimming one vane, A, Fig. 7, on one experimental diffuser. Gage sensitivity for recordings shown in Figs. 12 through 25 was $^1/_{10}$ in. per psi except where otherwise noted. Fig. 13 shows results obtained with an alteration expected to increase magnitude of transient pressures. Recordings shown in Figs. 14, 15, and 16 were interpreted optimistically as representing a solution to the problem and led to the series of prototype alterations outlined in Table 1. However, as has been explained, and may be seen in Fig. 8, results were not comparable from model to prototype.

Figs. 17 through 25, all made with a gage sensitivity of $^1/_{10}$ in. per psi, illustrate the effect of impeller trimmings on the strength of transient pressures. These tests show no significant decrease in strength of transient pressures although the clearance between impeller and diffuser vanes was increased by 67 per cent between run 71 and run 77.

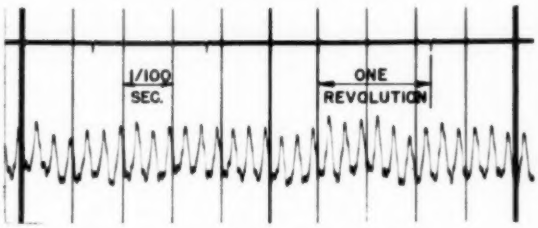

Fig. 9 Original Design Less Rib, 4070 Gpm

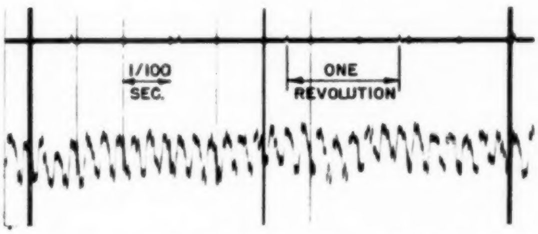

Fig. 10 Same as Fig. 9, Except That Vane A Was Cut Back $^1/_2$ In., 4070 Gpm

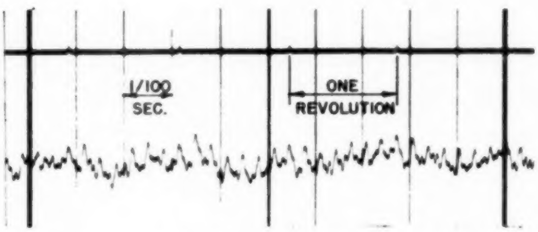

Fig. 11 Same as Fig. 9, Except That Vane A Was Cut Back 1 In., 4060 Gpm

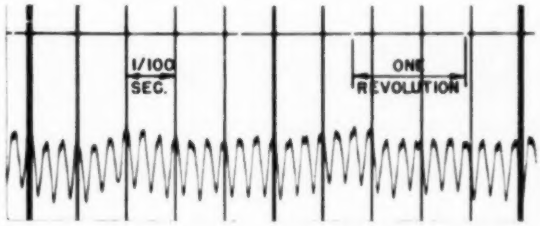

Fig. 12 Run 48-2, Original Design, Less Rib, Recorded With New Design Pressure Pickup, 4030 Gpm

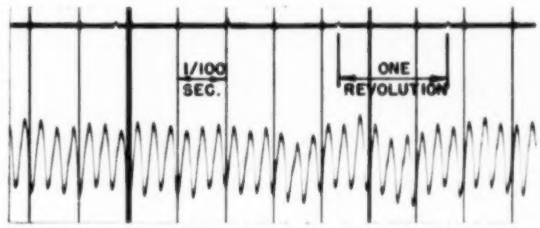

Fig. 13 Run 50-2, Diffuser Altered to Provide Maximum Opening Between Vanes F and A, 4040 Gpm

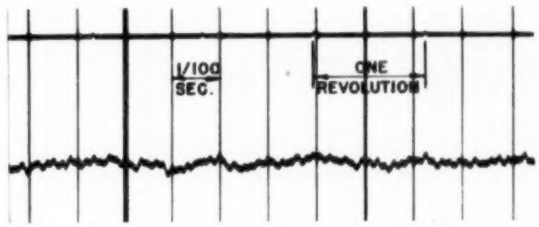

Fig. 14 Run 51-2, Diffuser Altered to Provide Maximum Opening Between Vanes A and B, Gradually Decreasing to FA, 4040 Gpm

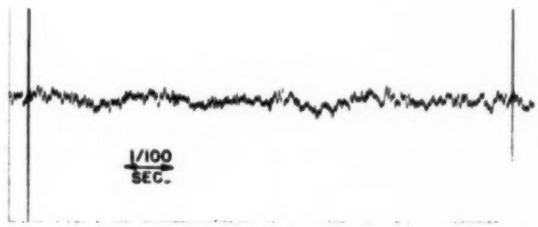

Fig. 15 Run 52-2, Same as Run 51-2 Except That Sensitivity Increased to $^1/_4$ In. Per Psi

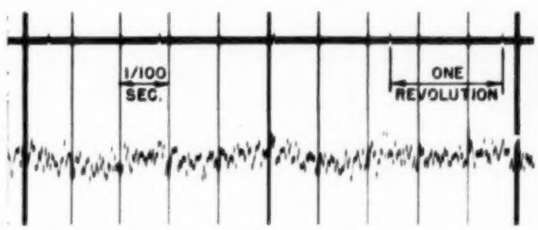

Fig. 16 Run 56-2, Same as Run 52-2 Except That Separator Rib Was in Place, Same Sensitivity

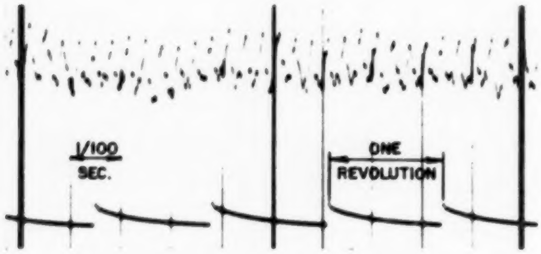

Fig. 17 Original Design Less Rib, Impeller No. 3, Diffuser No. 1, Run 71-2, 4220 Gpm

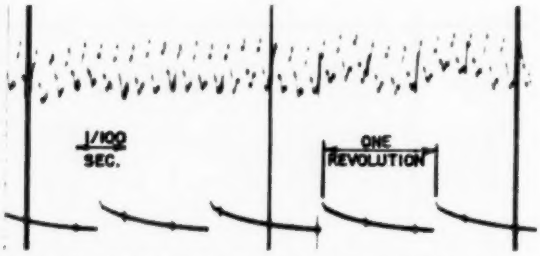

Fig. 18 Run 72-2, Same as 71-2 Except That One Vane of Impeller Was Trimmed $^{1}/_{16}$ In. on OD, 4220 Gpm

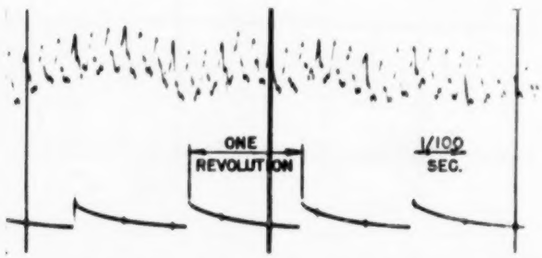

Fig. 19 Run 73-2, Same as 71-2 Except That Three of Impeller Vanes Were Trimmed $^{1}/_{16}$ In. on OD, 4180 Gpm

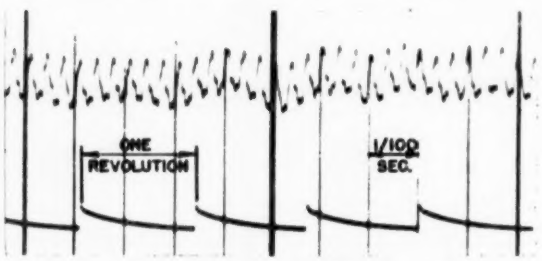

Fig. 20 Run 74-2, Same as 71-2 Except That All Vanes of Impeller Were Trimmed $^{1}/_{8}$ In. on Diameter, 4170 Gpm

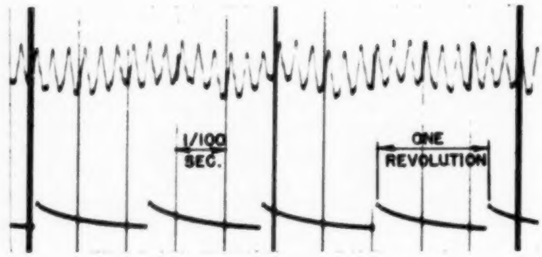

Fig. 21 Run 75-2, Same as 74-2 Except That Impeller Vanes Were Underfiled to Knife Edge, 4240 Gpm

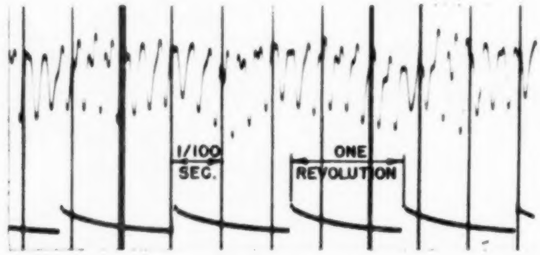

Fig. 22 Run 76-2, Same as 75-2 Except That Impeller Vanes Were Trimmed Additional $^{1}/_{8}$ In. on Diameter ($12^{5}/_{8}$), 4210 Gpm

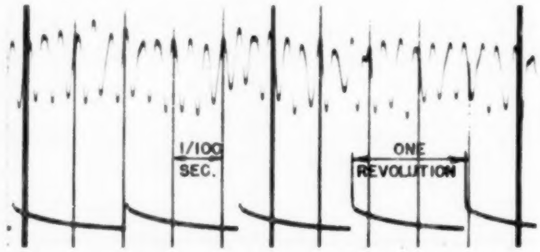

Fig. 23 Run 77-2, Same as 76-2 Except Impeller Vanes Were Trimmed Additional $^{1}/_{8}$ In. on Diameter ($12^{1}/_{2}$), 4130 Gpm

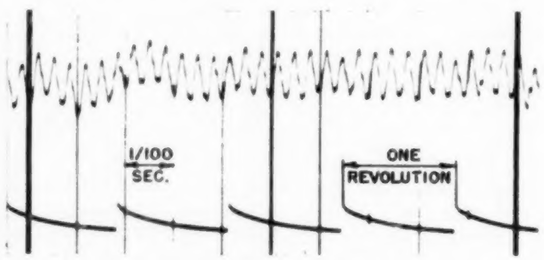

Fig. 24 Run 78-2, Same as 77-2 Except That Impeller Vanes Were Underfiled to Knife Edge, 4170 Gpm

Figs. 26 and 27 are recordings made at the discharge of pumps installed on the Colorado River Aqueduct. Operating speed was 400 rpm. Though impellers are different diameters, the pump casings are duplicates.

A final series of prototype tests and alterations, in the fall of 1952, pointed the way toward the alterations decided upon and described.[3]

Conclusions

In the foregoing chronological description of the investigation of transient pressures and their reduction, an effort has been made to describe the difficulties of instrumentation, some of the measures taken to overcome them, and the shortcomings of an experimental setup to represent the prototype accurately. It is evident, from the tests concluded, that accurate quantitative measurements of transient pressures, comparable to those occurring in a prototype, cannot be observed in a model, unless suction and discharge lines also are modeled accurately and flow condition duplicated. Qualitative agreement may be obtained if reasonable care is used to avoid extraneous disturbances.

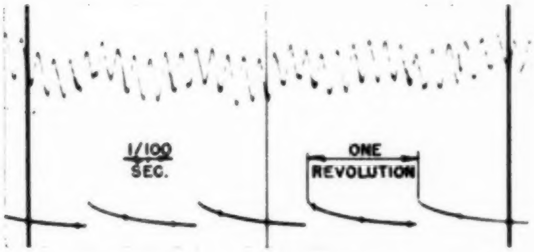

FIG. 25 RUN 79-2, SAME AS 78-2 EXCEPT THAT IMPELLER SHROUDS WERE TRIMMED FROM 12 7/8 IN. DIAM TO VANE DIAMETER, 12 1/2 IN., 4165 GPM

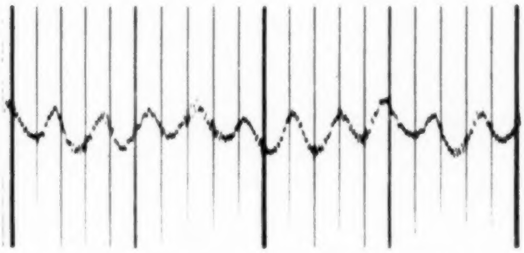

FIG. 26 DISCHARGE-PRESSURE TRANSIENTS IN 44-IN. SINGLE-VOLUTE PUMP INTAKE STATION, COLORADO RIVER AQUEDUCT
(Capacity, 200 cfs; impeller diameter, 76 in.)

It should be pointed out that transient pressures encountered in this installation are, in a measure, a result of the abnormal pump design dictated by the operating conditions. These conditions include normal operation (over 80 per cent of total) at overcapacity and lowest head with ample suction head, maximum efficiency at a higher head due to reduced suction head, and maximum head (135 per cent of the minimum) with a minimum suction head which determined suction design to avoid cavitation at a quite abnormal minimum flow. Obviously, as previously described,[3] this required a compromise design. Furthermore, the operating heads and size of these pumps excluded the use of single or double-volute design with the massive ribbing required, and made only the adopted fixed-vane-diffuser design economically feasible. All of the foregoing design requirements contributed to the strength of transient pressures produced.

This paper would not be complete without pointing out the reason that transient pressures, even though minor, were significant. The size of the unit, and consequent low operating speed of 200 rpm, resulted in transient pressure frequencies within the

FIG. 27 DISCHARGE-PRESSURE TRANSIENTS IN 44-IN. SINGLE-VOLUTE PUMP GENE STATION, COLORADO RIVER AQUEDUCT
(Capacity, 200 cfs; impeller diameter, 78 in.)

range of the natural frequencies of the thin-walled discharge line, particularly near its upper end. For these lines it is not the strength, but the stiffness that is important. The effect of vacuum, present in the uppermost sections of the discharge lines, contributes to the initiation of vibration. The strength of transient pressures descreases but little in the length of the line, but as the absolute pressure is very low, the fluctuations become of the same order.

Even before any alterations were made, these fluctuations were only 9 per cent of the total pressure at the discharge nozzle, but resulted in accelerations of the ribbed pipe line equivalent to 13.5 g's. After more than 2 years of experimentation, the pressure transients were reduced to approximately 3.9 per cent of the total pressure at the pump discharge at minimum operating head. These transients, weakened only slightly by transmission through a little more than 800 ft of pipe and two elbows, result in discharge-pipe accelerations equivalent to about 3.5 g's.

Evidently a further study of this problem is indicated, particularly for large pumps of low rpm (frequency) with large thin-walled discharge lines.

ACKNOWLEDGMENT

The author wishes to compliment John Parmakian, USBR, on his presentation of the facts regarding discharge-line vibrations,[2] and to express appreciation for the co-operation and helpful suggestions of Mr. L. N. McClellan, Mr. I. A. Winter, and Mr. Parmakian of the U. S. Bureau of Reclamation, Denver, Col., throughout this program. The design of the gages and electronic equipment was most ably accomplished by Haskell Shapiro, California Institute of Technology.

A special note of appreciation is due Messrs. I. M. White, Pelton Water Wheel Company, and Carl Blom and A. Hollander, Byron Jackson Co., for their assistance during the alteration program.

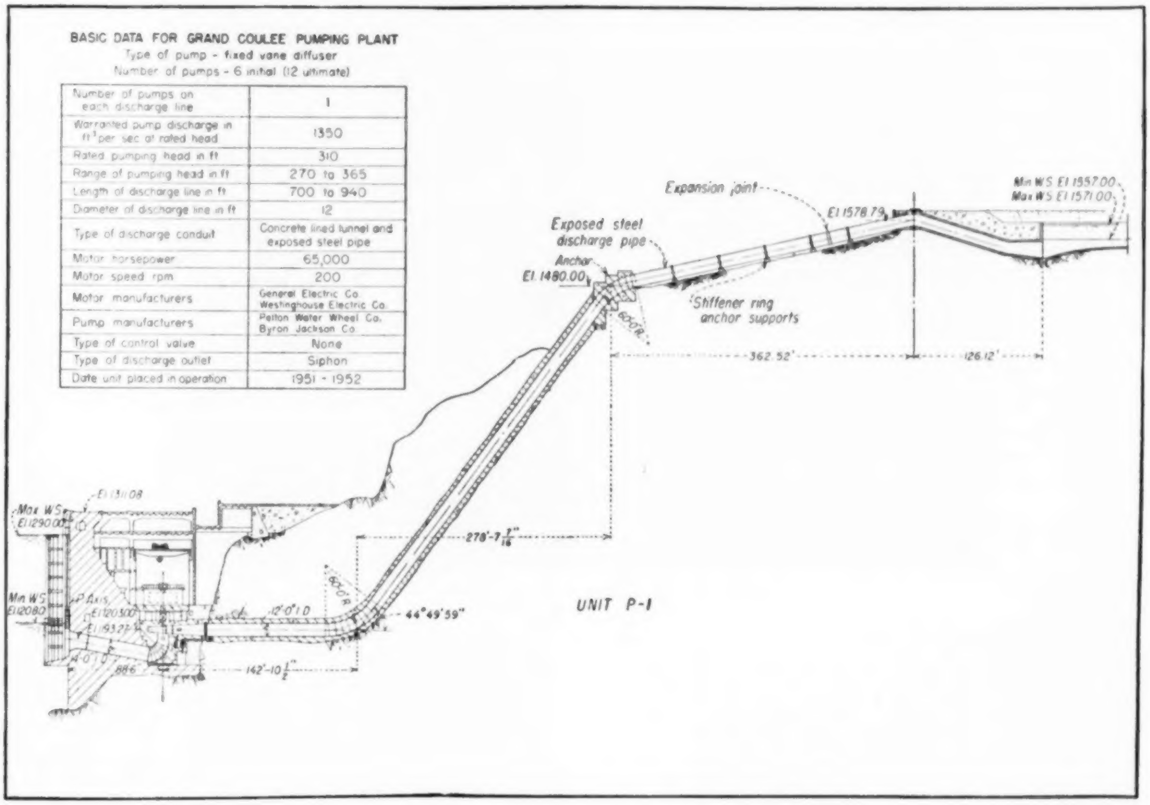

FIG. 1 TYPICAL SECTION THROUGH GRAND COULEE PUMPING PLANT AND DISCHARGE PIPE

Vibration of the Grand Coulee Pump-Discharge Lines

BY JOHN PARMAKIAN,[1] DENVER, COLO.

This paper describes a program of field tests, analyses, and modifications at the Grand Coulee Pumping Plant which were made to reduce the periodic vibration of the exposed sections of the pump-discharge lines. The source of the discharge-line vibration was traced to pressure oscillations originating in the pump. The vibration of the discharge lines subsequently was reduced to acceptable limits by a series of modifications of the pumps and discharge lines.

[1] Engineer, Design and Construction, Bureau of Reclamation, U. S. Department of the Interior. Mem. ASME.

[2] "Development of the Hydraulic Design for the Grand Coulee Pumps," by Carl Blom, Trans. ASME, vol. 72, 1950, pp. 53–70.

Contributed by the Hydraulic Division and presented at the Annual Meeting, New York, N. Y., November 29–December 4, 1953, of THE AMERICAN SOCIETY OF MECHANICAL ENGINEERS.

NOTE: Statements and opinions advanced in papers are to be understood as individual expressions of their authors and not those of the Society. Manuscript received at ASME Headquarters, July 27, 1953. Paper No. 53—A-50.

INTRODUCTION

GRAND Coulee Pumping Plant is located on the Columbia Basin Project and has its intake in the reservoir formed by the Grand Coulee Dam. The physical characteristics of this pumping plant and the general arrangement of a typical pumping unit are shown in Fig. 1, and the exposed sections of the twelve pump-discharge lines are shown in Fig. 2. The six initial pumps for this pumping plant were furnished by the Pelton Water Wheel Company and the Byron Jackson Co.[2] The steel pump-discharge lines were built by the Consolidated Western Steel Corporation in accordance with Bureau of Reclamation designs.

DISCHARGE-LINE VIBRATION

The first unit in this pumping plant was started in May, 1951, when the intake-water surface was at its highest level near 1290-ft elevation, and the pumping head was about 270 ft. During this initial operation, severe vibration of the exposed sections of the

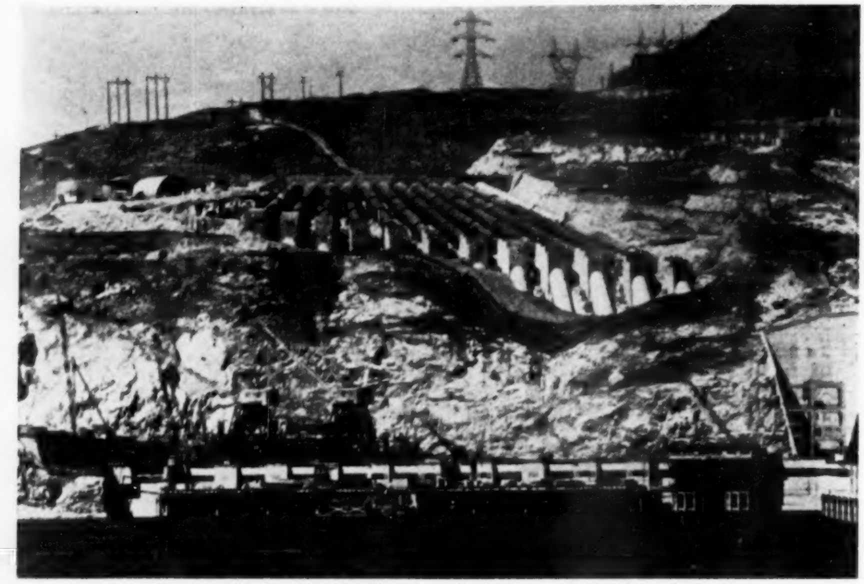

Fig. 2 Grand Coulee Pumping Plant and Discharge Lines

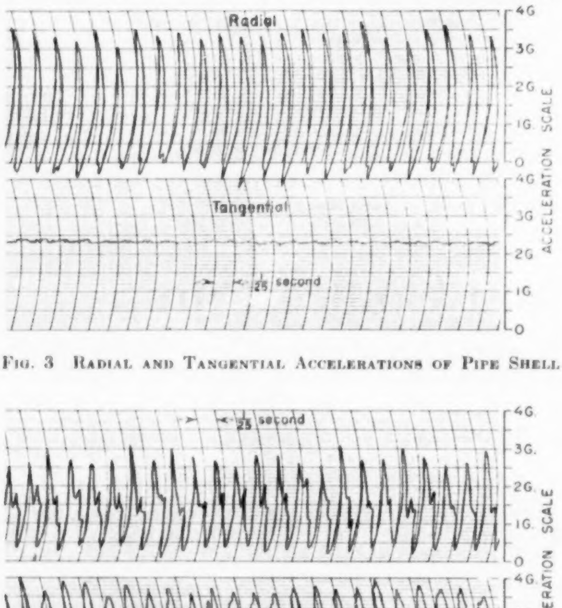

Fig. 3 Radial and Tangential Accelerations of Pipe Shell

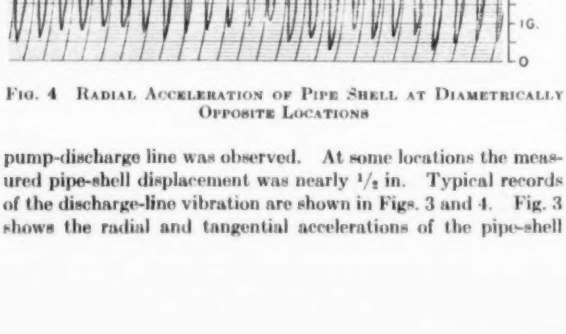

Fig. 4 Radial Acceleration of Pipe Shell at Diametrically Opposite Locations

pump-discharge line was observed. At some locations the measured pipe-shell displacement was nearly $^1/_2$ in. Typical records of the discharge-line vibration are shown in Figs. 3 and 4. Fig. 3 shows the radial and tangential accelerations of the pipe-shell

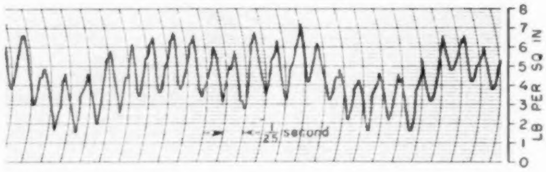

Fig. 5 Pressure Pulsations at Exposed Sections of Pump-Discharge Line

vibration, and Fig. 4 shows the simultaneous recording of the radial acceleration of the pipe shell at diametrically opposite points. Fig. 5 shows the water-pressure pulsations inside the pipe at the exposed sections of the discharge line.

These records indicated that the periodic pipe-shell vibration and the water-pressure pulsations in the discharge line had a basic frequency of $23^1/_3$ cycles per sec (cps). This frequency was traced directly to the pump. The pump speed is 200 rpm, and there are seven vanes on the impeller. Therefore the frequency at which the seven vanes of the impeller pass a fixed point in the pump casing is $200 \times 7/60 = 23^1/_3$ times per sec. In order to reduce the vibration of the pump-discharge line to acceptable limits, it was decided to reduce the magnitude of the pressure pulsations originating in the pump and also to stiffen the exposed sections of the pump-discharge line to better withstand the internal-pressure pulsations.

Pump Modifications

Since a satisfactory explanation for the presence of periodic pressure pulsations in the pump-discharge line was not available, the modifications of the pumps for the purpose of reducing these pressure pulsations were determined from a test program in the field. The extent of these modifications was limited by the strength requirements of the pump casing. The final pump modifications, as shown in Fig. 6, were as follows:

(*a*) Remove the splitter from the vane opposite the tongue of the pump.

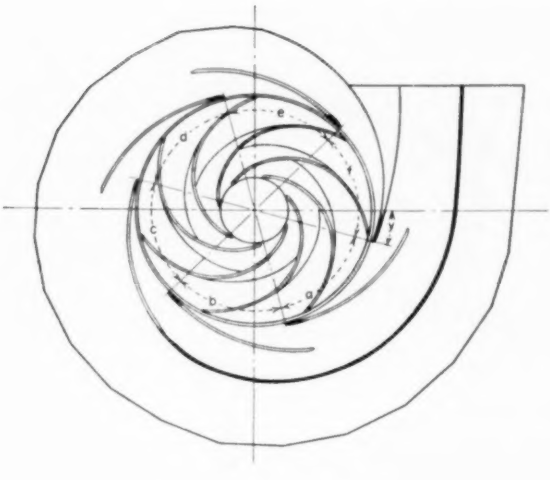

Angle y = 15.00° and angles a, b, c, d, e, and f = 60.00° in original design.
Shaded area indicates the location and amount of material removed by the modifications.

Fig. 6 Modification of Pump P-4 to Reduce Pressure Pulsations

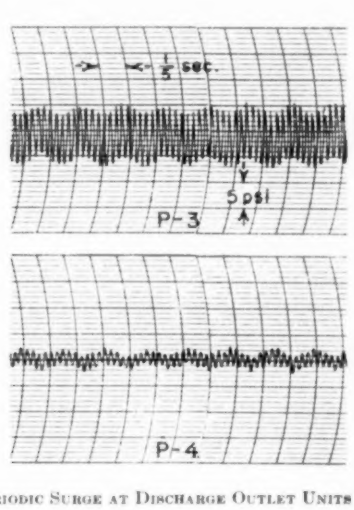

Fig. 7 Periodic Surge at Discharge Outlet Units P-3 and P-4

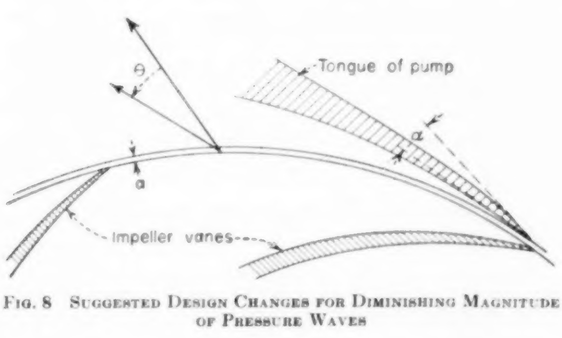

Fig. 8 Suggested Design Changes for Diminishing Magnitude of Pressure Waves

(*b*) Remove approximately 12 in. from the leading edge of the five diffuser vanes and 20 in. from the tongue of the pump.

(*c*) Remove $^3/_4$ in. radially from each of the seven impeller vanes.

The reduction in pressure pulsations at the pump which resulted from these modifications is shown in Fig. 7. This illustration shows a simultaneous record of the pressure pulsations at the discharge side of pump units P-3 and P-4. Pump P-3 was an unmodified pump and pump P-4 was modified in the manner just described. In addition to reducing the pressure pulsations, these modifications also increased the pump discharge and efficiency for the low pumping head at which the pump is used most of the time.

Source of Pressure Pulsations

The phenomena which produce pressure pulsations at a fixed-vane centrifugal pump are not understood completely at present. However, according to one analysis[3] the tongue of the pump is considered to be the producer of the pressure waves which are felt in the discharge line. Briefly, when pressure pulsations are transmitted from the pump to the discharge line, a possible explanation is as follows:

The total energy of the fluid at all points in the pump impeller is not distributed between pressure and kinetic energy in the same proportion. As a result, the velocity distribution at the exit of the pump impeller is not uniform. As this nonuniform flow passes the tongue or a fixed vane of the pump casing, an abrupt change in the direction of the impeller-exit-velocity vector occurs at the proximity of the fixed vanes. This produces positive pressure waves at the pressure face and negative pressure waves on the back face of each fixed vane. The magnitude of these pressure waves is proportional to C times θ, where C is the average absolute water velocity at the exit of the impeller, and θ is the angular change in the velocity vector in the proximity of the fixed vanes. Because of the nature of the water paths in the casing, the only fixed vane at which the positive and negative pressure waves do not nullify each other before reaching the discharge line is the tongue of the pump. From this location the positive pressure waves travel directly up the discharge line, while the negative pressure waves travel completely around the pump casing before reaching the discharge line. These positive pressure pulsations have a frequency equal to the product of the pump speed and number of blades in the impeller as was observed at the Grand Coulee Pumping Plant.

Suggested Design Changes for Diminishing Pressure Waves

The suggested design changes[3] for diminishing the magnitude of the pressure waves at a pump are explained as follows by referring to Fig. 8:

(*a*) Position the tongue and guide vanes of the casing so that the average direction of the vanes lines up with the direction of the average velocity vector at the impeller exit.

(*b*) Make the entrance angle α of the tongue and guide vanes larger than the change in angle θ of the velocity vector at the impeller exit.

(*c*) Increase the radial distance a between the impeller and the guide vanes of the casing to the maximum value consistent with the head-discharge requirements.

The Grand Coulee pumps were designed and built for a rated pumping head of 310 ft. However, excessive vibration of the

[3] "Pressure Oscillations in a Centrifugal Pump and the Analytical Determination of Pump Characteristics," by M. I. I. Rashed, Doctor's thesis in German, Eidgenossischen Technischen Hochschule, Zurich, Switzerland, 1951.

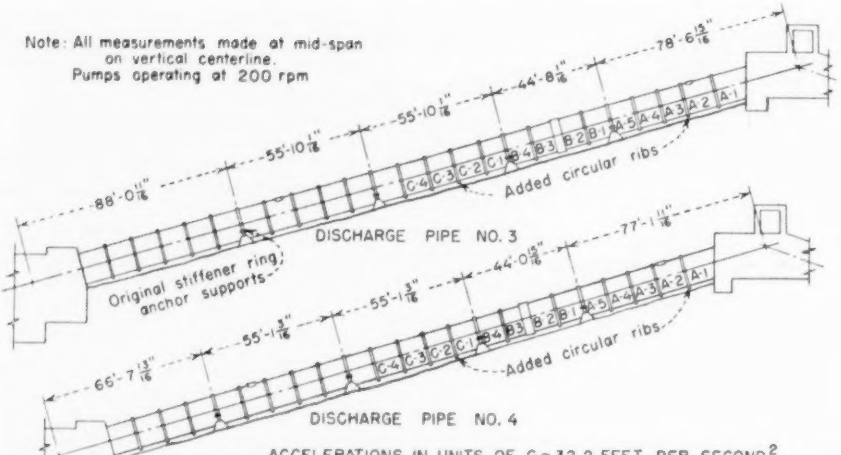

ACCELERATIONS IN UNITS OF G = 32.2 FEET PER SECOND^2

Location	A-1	A-2	A-3	A-4	A-5	B-1	B-2	B-3	B-4	C-1	C-2	C-3	C-4
Unit P-3	13.0	8.5	4.5	3.4	2.7	2.4	1.5	4.0	3.2	5.6	6.6	5.4	7.4
Unit P-4	3.5	1.5	0.7	0.6	1.1	1.0	0.9	1.0	1.0	1.0	1.0	1.4	1.2

FIG. 9 VIBRATION ACCELERATION OF PUMP-DISCHARGE LINES P-3 AND P-4

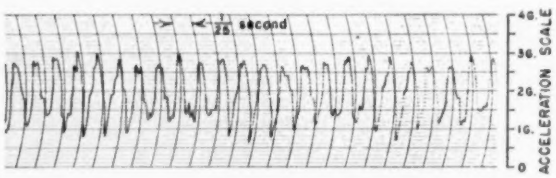

FIG. 10 VIBRATION OF UPPER MID-SPAN P-2 PUMP-DISCHARGE LINE WITH NO INTERMEDIATE STIFFENER RINGS

pump-discharge lines occurred when the pumps were delivering maximum discharge at a pumping head of 270 ft. For this condition of operation, C times θ is a maximum, and hence the pressure pulsations at the pump could be expected to attain maximum values according to the foregoing criteria. Since the pumps already had been built with a fixed position for the tongue and guide vanes, the only change which could be made to reduce the magnitude of the pressure waves, according to the three factors previously listed, was to increase the radial distance a between the impeller and the guide vanes of the casing and to steepen the entrance angle α of the tongue and guide vanes. This is essentially what was accomplished by the final modifications of the Grand Coulee pumps.

MODIFICATION OF PUMP-DISCHARGE LINES

The exposed sections of the pump-discharge lines originally were installed with stiffener-ring anchor supports at approximately 55-ft intervals, as shown in Fig. 9. Increased stiffening of the discharge lines was accomplished by the use of circular ribs, which first were bolted to the pipe shell between the existing stiffener-ring anchor supports and later welded securely to the pipe shell. These circular ribs were fabricated from 8-in. H-bearing pile sections. The most advantageous spacing of these ribs was determined by experimentation in the field on several spans of the actual discharge line. These tests indicated that a spacing of approximately 12 ft was the minimum practicable spacing for the ribs. Typical acceleration records which show the reduction in vibration because of the addition of the circular ribs in a span are shown in Figs. 10, 11, and 12.

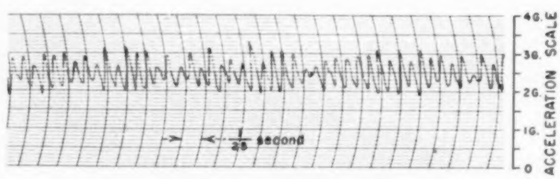

FIG. 11 VIBRATION OF UPPER MID-SPAN P-2 PUMP-DISCHARGE LINE WITH TWO INTERMEDIATE STIFFENER RINGS

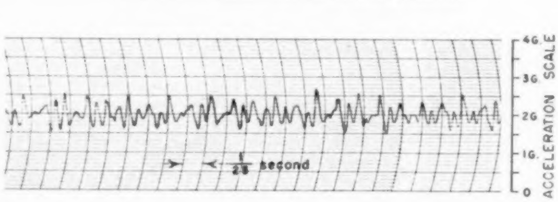

FIG. 12 VIBRATION OF UPPER MID-SPAN P-2 PUMP DISCHARGE LINE WITH FOUR INTERMEDIATE STIFFENER RINGS

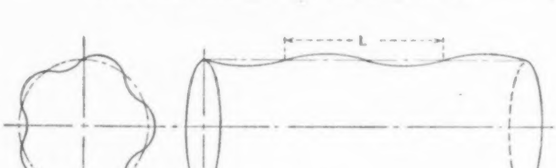

FIG. 13 PIPE-SHELL DEFORMATION WAVES CAUSED BY DISCHARGE-LINE VIBRATION

ANALYSIS OF DISCHARGE-LINE VIBRATION

A theoretical analysis[4] of the discharge-line vibration due to

[4] "Analysis of Pipe Vibrations With Internal Fluid Flow," by Che-Min Cheng, California Institute of Technology, January 20, 1952, Report submitted to the Byron Jackson Co.

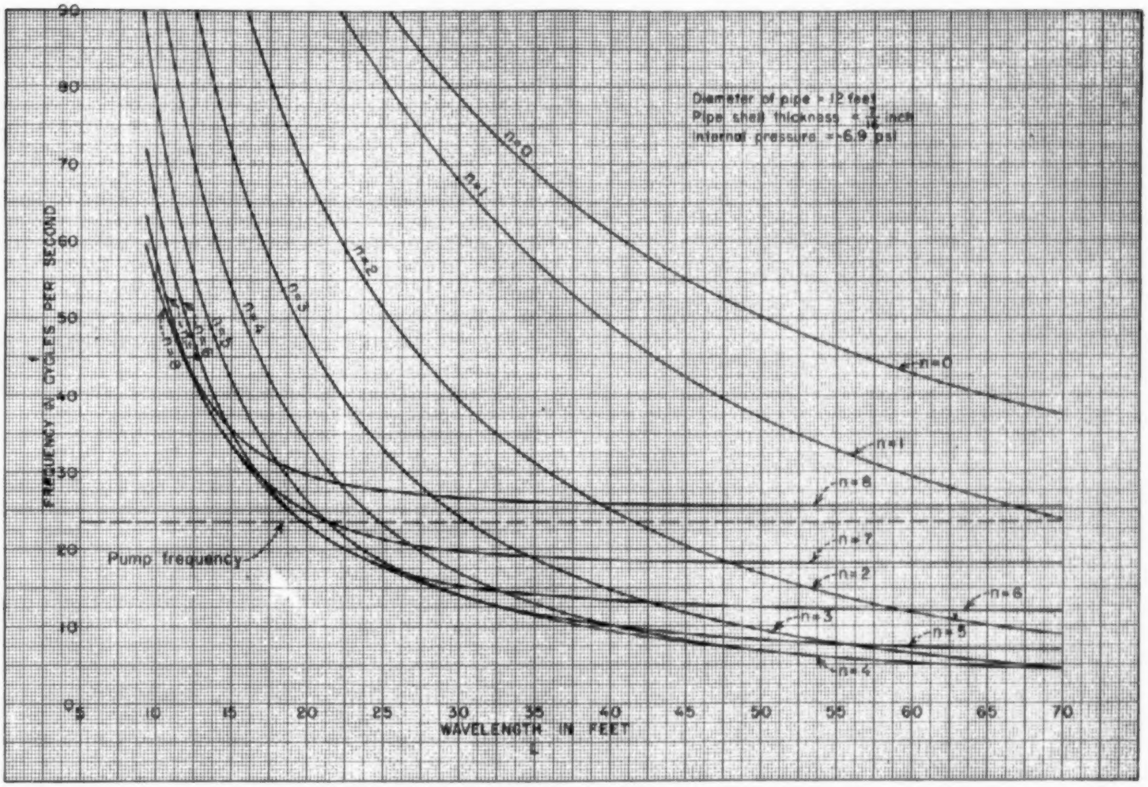

FIG. 14 LONGITUDINAL WAVE LENGTH L PLOTTED AGAINST NATURAL FREQUENCY VIBRATION f FOR VARIOUS CIRCUMFERENTIAL MODES OF VIBRATION n

periodic pressure pulsations in the water also was made at a later date. The type of vibration investigated is one which occurs in two modes simultaneously; that is, the pipe shell deforms into waves along the axis of the pipe, while the circumference is subdivided into $2n$ half waves as shown in Fig. 13. The results of this analysis are given in Fig. 14. This illustration shows the longitudinal wave length L plotted against the natural frequency of vibration f for various circumferential modes of vibration n. This graph is applicable for the uppermost portion of the exposed discharge line near the siphon outlet where the internal pressure is subatmospheric. Fig. 14 indicates that with a longitudinal wave length L of 20 ft or more, the pipe shell can vibrate with a frequency of $23^1/_3$ cps at one or more circumferential modes of vibration. In order to avoid a vibration-resonance phenomenon, the natural frequency of the span was increased by a reduction in the longitudinal wave length. This was accomplished in the actual installation by the use of circular ribs placed between the existing anchor-stiffener rings. The circular ribs were effective in increasing the natural frequency of a span by reducing the longitudinal wave length, by suppressing the circumferential modes of vibration of the pipe shell at the ribs, and by preventing the radial-deflection pattern of the pipe-shell vibration from carrying over from one span to the next.

REDUCTION IN VIBRATION DUE TO PUMP MODIFICATIONS

Fig. 9 shows the location of the circular ribs which were installed on the exposed portions of the P-3 and P-4 pump-discharge lines. After the rings were welded to the pipe shell, additional vibration measurements were taken on these two discharge lines to determine the effect of the pump modifications. Pump P-3 was an unmodified pump, and pump P-4 had been modified in the manner described previously. The measured pipe-shell vibration of the upper portion of these two discharge lines is shown by the table in Fig. 9. From this table it is seen that the measured vibration of the P-3 discharge line with an unmodified pump is much greater than the vibration at corresponding locations of the P-4 discharge line. With the exception of the uppermost span, the vibration acceleration of the P-4 discharge line with a modified pump has been reduced to less than $2G$. Subsequent to these tests the vibration at this span has been reduced further by the installation of one more circular rib at the middle of this span.

FIELD PERFORMANCE

Two of the Grand Coulee pump-discharge lines already have completed two years of operation and are currently in their third year of operation. During the first two years of operation, the pumps and discharge lines were undergoing modifications. For example, in 1951, after some modifications had been made on the pumps, the discharge lines were operated without the circular ribs but with the pumps operating at a reduced speed of 190 rpm. Later in the year the pump speed was returned to normal after further modifications were made on the pumps and after a number of circular ribs had been bolted to the pipe shell between the existing anchor-support rings. Prior to the start of the 1952 pumping season, circular ribs were welded to the pipe shell of the six discharge lines at a spacing of not more than 12 ft. The final modifications of the six pumps were not completed until after the 1952 pumping season had been completed. During the first two years of opera-

tion, two pumps delivered over 1,000,000 acre-ft of water, and one of the discharge lines withstood nearly a half-billion pressure pulsations without signs of distress in the pipe shell.

Conclusions

A reduction in the vibration of the Grand Coulee pump-discharge lines was obtained by an experimental modification program in the field. The source of vibration was traced directly to periodic pressure pulsations originating in the pump. These pressure pulsations could not be eliminated but were reduced by modifications of the pump. Additional stiffening of the exposed portions of the discharge line with circular ribs also was required before the vibration of the discharge lines could be reduced to acceptable limits.

Acknowledgment

A reduction in the vibration of the Grand Coulee pump-discharge lines was obtained as a result of a co-operative test program in which both the pump manufacturers and the Bureau of Reclamation participated. I. A. Winter, Chief of the Hydraulic Machinery Branch, was in charge of the pump-modification program for the Division of Design and Construction of the Bureau. Others from this division who participated in the analyses, modifications, and field tests were F. E. Cornwell, F. E. Swain, W. E. Evans, C. C. Crawford, R. H. Williams, and the author. N. G. Holmdahl, D. D. McGregor, W. H. Clumpner, and F. O. Ruud from the Coulee Dam Field Division of the Bureau, participated in the field vibration tests. For the pump manufacturers, Carl Blom, E. E. Lindros, and Carlo Bartelero of Byron Jackson Co., I. M. White of the Pelton Water Wheel Company, and Prof. A. Hollander of the California Institute of Technology, participated in the pump-modification program. Mr. Lindros was in charge of the pump-modification program for the pump manufacturers. The modification of the discharge lines and the vibration tests of the pumps and discharge lines in the field were under the direction of the author. The illustrations in this paper were prepared by R. H. Williams.

Discussion

C. E. Crede.[5] The methods described by the author for reducing the magnitude of the vibration in the pump-discharge lines are quite interesting. It is noted that the paper does not include an explanation of a rather unexpected characteristic of the test results. In Fig. 10, for example, the vibration is predominantly at a frequency of approximately 23 cps with some indication of higher frequencies being present. The vibration depicted in Figs. 11 and 12 is at a frequency of approximately 46 cps, with some indication of lower frequencies.

Inasmuch as the operating condition is one of forced vibration and the driving force from the pump has not been modified appreciably, the change in the predominant frequency resulting from stiffening of the pipe is rather unusual. A lower amplitude at the same frequency would be expected as a result of the addition of stiffeners to the pipe. One possible explanation of the result is that the unstiffened pipe represented by Fig. 10 has a natural frequency of approximately 23 cps. Stiffening of the pipe might change the spectrum of its natural frequencies so that one of the natural frequencies then coincides with the second harmonic of the driving force, or 46 cps.

It would be interesting to know whether the author feels that the change in the frequency of vibration is a result of tuning the discharge pipe to the second harmonic by the addition of stiffening rings, whereas it was tuned initially to the fundamental.

[5] Chief Engineer, The Barry Corporation, Watertown, Mass.

A. Hollander.[6] This thorough report with the companion paper of Mr. Lindros[7] are worth-while additions to the former papers of Messrs. Blom,[8] Moses,[9] and White,[10] because with their discussions they constitute a full disclosure of this greatest pumping plant ever attempted, in reference to the hydraulic plant and pump design from model to prototype and its construction, as well as the troubles encountered in the field and the corrective measure taken to obviate them.

This novel attitude in telling the whole story by the user, who was simultaneously the designer of the plant and penstocks and the manufacturer of the hydraulic machinery, adds one more "first" in the host of others of this grand project. To point out the main firsts and how they were arrived at:

1 A pumping plant with an initial installation of 390,000 hp and a final of 780,000 hp will stand for a long time as a monument of engineering vision.

2 The preliminary model experiments of the Bureau at the California Institute of Technology[11,12,13,14] through about $2^1/_2$ years, to enable them to work out the specifications for bid indicate the foresight in preparation.

3 As a result of this preliminary work it was possible to prescribe a very simple, light, and therefore, inexpensive design with stationary guide vanes which give a high efficiency through the whole operating range between a minimum operating head of 270 ft and a maximum head of 365 ft at a constant speed.

4 This operating speed was raised from the originally contemplated one by 33 per cent reducing the weight units by 50 per cent.

5 Further model experiments by a novel approach of the successful bidder, making the diffusion vanes as short as permissible by strength requirement, and leaving further diffusion to the volute of a circular arc section, permitting light plate fabrication, made another weight reduction of similar order possible, without impairing the efficiency.

6 The result of these steps is a pump of clean, simple design built under strict specifications to the highest standards. Subject to a hydrostatic test pressure of 315 psi, the total weight of one pump, including suction elbow and the shaft between pump and motor, is about 325,000 lb, or about 5 lb per hp; and the price, less erection of about $3.50 per hp, including the contractors' model experiments, figures unsurpassed in an economical sense, at the 1951 price level.

7 Equally daring for units of this magnitude was the elimination of the discharge valve, with its regulatory control.

8 As a result of this, a novel starting procedure had to be adopted, namely, a start of the turbogenerator without excita-

[6] Professor Emeritus, California Institute of Technology, Pasadena, Calif. Consulting Engineer, Byron Jackson Co., Los Angeles, Calif. Fellow ASME.

[7] "Grand Coulee Model Pump Investigation of Transient Pressures and Methods for Their Reduction," by Ernest Lindros, published in this issue, pp. 775–782.

[8] "Development of the Hydraulic Design for the Grand Coulee Pumps," by Carl Blom, Trans. ASME, vol. 72, 1950, pp. 53–70.

[9] "History and Development of the Grand Coulee Pumping Plant," by E. B. Moses, *Mechanical Engineering*, vol. 71, 1949, p. 729.

[10] "The Mechanical Design and Construction of the Grand Coulee Pumps," by Ira Morgan White, *Mechanical Engineering*, vol. 71, 1949, p. 686.

[11] "Cavitation Characteristics of Centrifugal Pumps Described by Similarity Consideration," by G. F. Wislicenus, R. M. Watson, and I. J. Karassik, Trans. ASME, vol. 61, 1939, pp. 17–24.

[12] "A Theory of Cavitation Flow in Centrifugal-Pump Impellers," by A. Gongwer, Trans. ASME, vol. 63, 1941, pp. 29–40.

[13] "Centrifugal-Pump Performance as Affected by Design Features," by R. T. Knapp, Trans. ASME, vol. 63, 1941, pp. 251–260.

[14] "Test Characteristics of a Combined Pump-Turbine Model With Wicket Gates," by R. V. Terry and F. E. Jaski, Trans. ASME vol. 64, 1942, pp. 731–744.

tion, the electrical coupling of a turbogenerator, and a motor pump, which are brought up to speed together, after applying excitation to the generator field; and thereafter when synchronized, the motor is put on the system, thus eliminating very expensive starting devices.

9 Similarly, the cutting out of a unit by simply opening a circuit breaker and by breaking the vacuum of the syphon and letting the water run back and the pump slow down, stop and reverse, and at low speed, stopping by hydraulic brakes, constitutes the simplest method without noticeable shock to the electrical system, which is about 45 times larger than a single pump power.

10 Finally, the very size of this installation resulted in many additional problems, civil, electrical, and mechanical, which were solved in a similar manner by the simplest and most economical manner.

No wonder that the Bureau and the manufacturers are equally proud of this unique installation.

With so many innovations there were minor troubles encountered as described by the authors of this and the companion paper.[11] These were approached with the aim to learn everything possible from them and tell fully so that others may avoid them. They point out that further study of transient pressures, how they are influenced by the pump design and the penstock system, will be needed to clarify this problem. They are to be congratulated for their successful efforts in this direction.

H. L. Ross.[15] This paper confirms the fact that the design and building of large hydraulic machines very often brings up problems which simply cannot be predicted on the basis of model testing as normally conducted. The author has done a very good job of presenting the problem and analyzing the steps necessary to obtain acceptable operation.

It is difficult to understand why the original pump produced a vibration of $23^1/_3$ cps. The pump as designed with the splitter in place can be considered practically a double-volute pump and it would seem that we should consider the impeller as passing two major fixed points and that therefore we would expect the frequency to be

$$\frac{200 \times 7 \times 2}{60} = 46^2/_3 \text{ cps}$$

The author's reasoning that the guide vanes permit equalizing at the ends and do not act as fixed points may be sound, but we certainly would have expected the splitter vane to have a great deal of effect, perhaps the major effect. Perhaps this vane was acting as the major offender in the original tests and the casing tongue had only a secondary effect. Then when the vane was cut out the major effect was transferred to the casing tongue.

It is difficult to reconcile the statement that the modifications to the pump increased the discharge and efficiency at low heads with the curves and data shown in footnote 2 of the paper on the original design of the pump. This paper shows a comparison curve of the 6-vane diffuser, with and without the splitter, showing the splitter to have increased the pump efficiency nearly 2 per cent at the lower heads. It would seem therefore that other modifications must have contributed to the increase of the efficiency more than offsetting the reduction that would be obtained by removal of the splitter unless the original tests were in error.

Were these efficiency tests with and without the splitter conducted on the prototype or were they rerun on the model? Our own experience would indicate that we should not expect a decrease in efficiency with the removal of a splitter since essentially this is transforming the pump from a double-volute pump to a single-volute pump and, in pumps of smaller sizes, we usually have a slight reduction in efficiency with a double-volute pump. In a pump of this size we probably would expect the efficiency to be about the same.

It would be interesting to have the author comment on the actual field efficiency obtained as compared to the model-pump efficiency.

We wonder if it was possible to test the prototype under a range of operating heads and whether the intensity of the vibrations was still maintained at the higher heads, that is, at near the best efficiency point. We certainly would expect less disturbance when operating at this point than at the reduced heads where the angles of the casing tongue and guide vanes do not correspond to the impeller-discharge angles.

It was disappointing that the alterations made on the model which seemed so satisfactory did not show the same improvement in the prototype. It shows that there is a lot to be learned about the modeling of these transient phenomena.

[15] Chief Engineer, Centrifugal Pump Section, Power Department, Allis-Chalmers Manufacturing Company, Milwaukee, Wis. Mem. ASME.

G. F. Wislicenus.[16] The author as well as the office and the manufacturers who collaborated with him deserve the wholehearted thanks of all hydraulic engineers for this frank disclosure of an important type of difficulty encountered with the world's largest pumps. The existence of this kind of difficulty is in itself not too surprising, considering the pioneering character of this installation not only regarding its size, but also with respect to several of its design characteristics. With the information made here available, future installations of comparable dimensions or characteristics can be undertaken with increased confidence, particularly if a thorough-going analysis of this information can achieve an improved understanding of the hydrodynamic and mechanical processes involved. It is with this end in mind that the writer would like to raise a few specific questions, although he has not read reference (3) of the paper which may contain some of the answers.

Referring to the section Source of Pressure Pulsations in the paper, it would be of interest to learn more about the reason why "The magnitude of these pressure waves is proportional to C times θ" (as defined there). This relationship suggests the existence of a water-hammer type of pulsation, since in this case pressure changes are known to be proportional to the product of the fluid velocity C, and the acoustic velocity. Otherwise, pressure variations due to changes θ in the angle of attack are of course proportional to C^2. A water-hammer type of pressure change further invites the question whether this phenomenon is assumed (or known) to be connected with cavitation at the diffuser vane tips.

Turning to the next section, Suggested Design Changes . . ., the writer would like to qualify the statement that the product C times θ is a maximum at reduced pump head and therefore increased rate of flow. Only the *relative* velocity increases, whereas the absolute velocity of the fluid leaving the impeller (with backward-bent vanes) is indeed *reduced* about proportionally to the pump head (strictly, its peripheral component is proportional to the runner head at constant rpm). Furthermore, it is not obvious that the flow leaving the impeller has increased fluctuations θ of its direction under low-head conditions. However, the fact that at increased rate of flow the mean velocities in the diffuser must increase according to the condition of continuity obviously produces a mismatching between the diffuser and the impeller-discharge velocities, leading to irregularities in the flow at the diffuser inlet which may indeed produce the pressure

[16] Chairman, Mechanical Engineering Department, The Johns Hopkins University, Baltimore, Md. Mem. ASME.

fluctuations observed. However, such irregularities also could be produced by a rate of flow well below the design point, as it may not be the increase of C as such (as implied in the paper) but its departure from the design value that causes the objectionable pressure fluctuations observed.

It should not be thought that the writer wishes to make a definite statement in regard to the last point, as the flow conditions under off-design conditions are altogether too involved to permit today any general predictions as to their nature or effects. The only practical reason for the considerations mentioned is the desire to avoid unwarranted detailed conclusions to be drawn from this paper that may tend to spoil in some future instances the great practical value of this contribution.

Author's Closure

The author wishes to thank Messrs. Crede, Hollander, Ross, and Wislicenus for their discussions.

Mr. Crede offers a possible explanation for the change in the discharge-line vibration frequency resulting from the additional stiffener rings. The increase in the natural frequency of the pipe shell due to the added stiffener rings is obtainable from Fig. 14 of the paper. For a stiffener-ring spacing of 12 ft the lowest natural frequency of the pipe shell for several of the possible modes of vibration is about 45 cycles per second (cps).

Professor Hollander's discussion includes an informative summary of some of the novel features of the Grand Coulee Pumping Plant. The author agrees with Professor Hollander on the need for further study of transient pressures due to various pump and discharge-line designs.

In answer to the questions raised by Mr. Ross, the observed frequency of the pressure pulsations was predominantly $23^1/_2$ cps at the pump both with and without the splitter rib. It is possible that if this rib had been more rigid, stronger pressure pulsations of double this frequency might have been present. The field tests indicated stronger transients in the discharge line with the rib in place than when removed. This fact, coupled with the inability of the rib to withstand the effects of the pressure pulsations, led to its removal from all prototypes. The field-performance tests indicated no decrease in efficiency of the prototype because of removing the rib. The pump performance based on the field tests of the modified prototype pumps and the anticipated performance based on the model tests with the rib are shown in Fig. 15 of this closure. A gradual decrease in the discharge-line vibration was observed as the pumping head was progressively increased.

Professor Wislicenus has suggested another possible explanation for the source of the pressure waves at the pump. The existence of the water-hammer type of propulsion was obtained from hydrodynamic considerations in Rashed's thesis.[3] According to this thesis the pressure pulsations are due primarily to the periodic velocity fluctuations in the water delivered along the circumference of the impeller-exit circle. Such an irregular flow produces pressure waves in the guide channel of the pump with a magnitude proportional to the velocity fluctuation. These velocity fluctuations are further influenced by the size, number, and alignment of the fixed guide channels of the casing. Similar pressure pulsations and objectionable vibrations of a buried discharge line have been observed at another smaller installation where the water was supplied by a single-volute pump with no diffuser vanes.

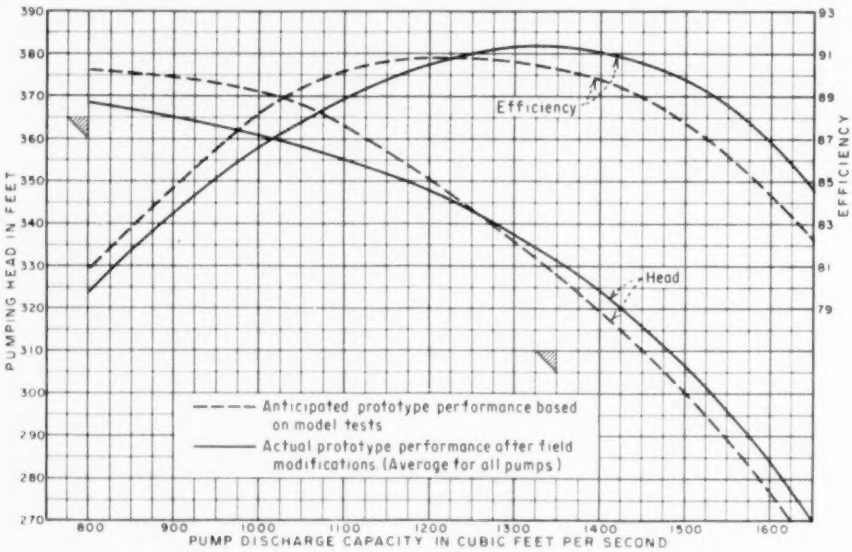

Fig. 15 Performance of Grand Coulee Pumps

Mechanical Features of the Tandem Helicopter Drive System

By W. F. PLUME,[1] MORTON, PA.

In the shaft-driven helicopter, drive-system reliability plays a large part in the safety of the helicopter. Drive-system reliability is established by extensive development testing and is maintained by quality control and production load runs. This paper describes in detail the transmissions and clutches of two types of tandem-rotor helicopters and the methods used for testing.

Introduction

The development of the helicopter has opened up an entirely new concept of flight and its application to military and civilian uses, but at the same time has introduced mechanical problems not encountered in any other type of machine. The low-speed rotors on vertical shafts are driven by engines buried in the fuselage requiring not only high-ratio gearing but also angular drives and long connecting shafting. The high inertia of the rotors also requires a clutch which will permit starting the engine without load. After warm-up the rotors are started with the engine turning at idling speed. In addition to these requirements, there must be an overrunning clutch in the system so that in the event of engine failure the rotors will continue to turn freely to permit an autorotative landing.

All Piasecki helicopters in production use the tandem-rotor arrangement. One tandem-rotor configuration is illustrated in Fig. 1 which shows an HUP helicopter in service. The forward and aft rotors are equal in size and rotate in opposite directions. The drag torques counteract each other and both rotors share the lift. The HUP has a rear pylon as shown with the plane of the aft rotor above and parallel to the plane of the forward rotor and the rotor disks overlap. This configuration makes the helicopter very compact for easy handling and storage on board ship.

Fig. 2 shows an HRP-2 helicopter in service. This type has both rotor disks in one plane with no overlap. Instead of using a rear pylon, the fuselage is carried up to the aft rotor. When proper blade-droop clearance is provided at the center, the fuselage assumes the typical "flying-banana" shape as shown.

Fig. 3 shows the H-21 helicopter. This is similar to the HRP-2 in size and configuration but has about twice the power. The drive system is also similar to that in the HRP-2 except that components are larger to transmit the increased power.

Fig. 1 HUP Helicopter in Service

Fig. 2 HRP-2 Helicopter in Service

Fig. 3 H-21 Helicopter in Flight

Drive-System Requirements

The drive systems in the HUP and HRP-2 single-engine tandem-rotor helicopters have the following general requirements:

The engine is located within the fuselage so that a special cooling system for engine cylinders and oil coolers is required. The engine-output shaft, turning at crankshaft speed, has a fan mounted on it. This fan consists of a large-diameter disk with axial-flow blades mounted on the periphery. The cooling air is driven over the cylinders and through the engine and transmission-oil coolers by this fan which also acts as a flywheel. The rotor inertia cannot be used for flywheel effect at the engine because of the long elastic connecting shafting and the clutch.

[1] Design Staff Engineer, Preliminary Design Division, Piasecki Helicopter Corporation.

Contributed by the Aviation Division of the ASME and the Society of Automotive Engineers and presented at the Annual Meeting, New York, N. Y., November 29–December 4, 1953, of The American Society of Mechanical Engineers.

 Manuscript received by ASME Headquarters, Oct. 8, 1953. Paper No. 53—A-214.

A section of flexibly coupled shafting connects the engine shaft to the clutch shaft. The clutch has three functions:

(*a*) It has a friction element which permits starting the large-inertia rotors while the engine idles at about 1000 to 1500 rpm.

(*b*) When the clutch shafts have synchronized (in about 10 to 20 sec) a positive-drive dog clutch is engaged and the friction plates disengage. Then full engine torque can be applied to bring the rotors up to full speed.

(*c*) The dog clutch is of the saw-tooth design so that it drives in one direction only. If the engine slows down or stops in flight, the dog clutch overruns and permits the rotors to continue turning, still geared together by the synchronizing shaft, and the helicopter can be landed safely by use of autorotation.

The output from the clutch connects to the main transmission system. This consists of a combined planetary and spiral bevel-gear transmission at each rotor with a long high-speed synchronizing shaft connecting the two rotor transmissions. In designs where the rotor disks overlap, the rotors must be synchronized so that the blades intermesh. The rotors must be synchronized also for control reasons even when the rotor disks do not overlap. The total gear ratio is between 8 and 10 to 1.

Except during a power-off autorotational descent, continued flight of a helicopter depends on the continuous transmission of power from the engine to the rotors. The safety-of-flight feature of the helicopter-drive system is the most important single philosophy in both design and manufacture. Design stresses must not exceed stresses that have been proved to be safe. Extensive development testing must be done on all new designs. Every production transmission is given a short-load run before being installed in the helicopter and elaborate quality control is maintained at all stages of manufacture.

HUP Drive System

Fig. 4 shows a cutaway view of the HUP drive system. The engine has a take-off rating of 550 hp and at 2400 rpm for the HUP-2 model. The screened-air intake for engine cooling is shown in the pylon. The engine drive shaft goes to the clutch in the aft transmission. This transmission drives both the aft-rotor shaft and the synchronizing shaft. The synchronizing shaft has two intermediate supporting bearings and flexible couplings. The forward transmission has a much shorter rotor shaft. The rotor shafts are parallel and inclined forward when the synchronizing shaft is horizontal.

Fig. 5 shows an external view of the HUP forward transmission. The drum on the input shaft is a combined rotor parking brake and Thomas coupling adapter. The parking brake is an external-band-type brake operated by mechanical controls. It is

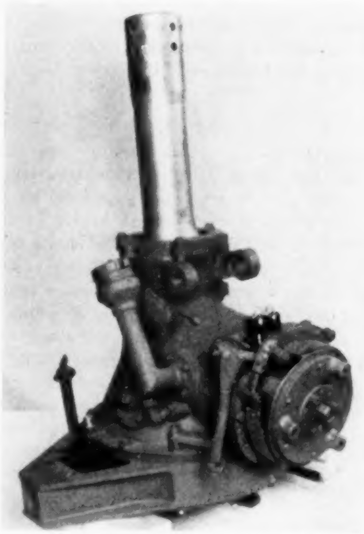

Fig. 5 External View of HUP Forward Transmission

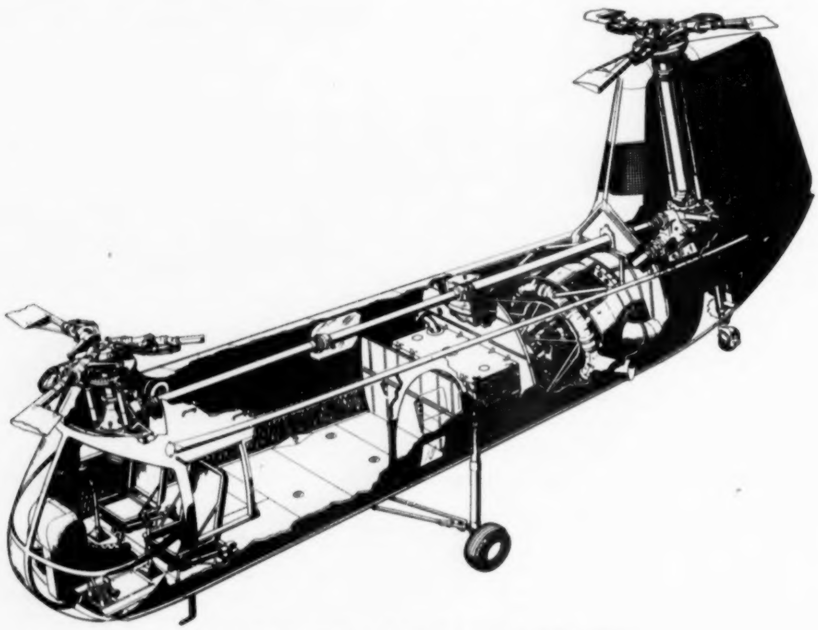

Fig. 4 Cutaway View Showing HUP Drive System

used to prevent the rotors from "windmilling" while the helicopter is parked or being loaded, serviced, or inspected. The oil-filler neck is to the left of the parking brake. The bayonet-type oil-level gage is to the left rear of the transmission. The main support member at the bottom of the transmission carries rotor loads into the fuselage structure through supporting pins.

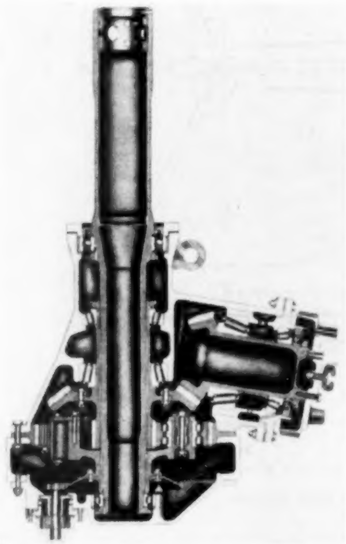

FIG. 6 SECTION THROUGH HUP FORWARD TRANSMISSION

Fig. 6 is a section through the HUP forward transmission. The input shaft drives a spiral bevel pinion at 2000 rpm. The spiral bevel gear drives the sun gear of the planetary set. The planet gears are mounted in a rigid carrier which is splined to the rotor shaft at the bottom. The rotor shaft goes up through the sun gear. The rotor-shaft thrust bearing is at the top of the case and the radial bearing at the bottom. This provides a wide span to take out side loads and moments from the rotor. This inverted arrangement results in a compact design with the input-shaft center line high enough so that the drive shaft will not interfere with headroom in the fuselage.

The spiral bevel pinion and gear are each mounted on a pair of tapered roller bearings with "indirect" mounting to provide a long effective span. These bearings are preloaded by shimming to provide adequate rigidity. Other shims are used to adjust the spiral bevel gears for proper backlash and tooth pattern. The pinion shim is under the cover flange. The gear shim is at the gear-ring flange.

The planet gears are mounted on pairs of cylindrical roller bearings. The gear itself acts as the outer race of the bearing. This design was found to provide the greatest capacity for the limited space available.

The lubricating pump is driven by a spur gear mounted on the rotor shaft. The pump is the "gerotor" type and has proved very reliable. The pump circulates the entire oil supply for the transmission approximately three times per minute. The pump suction is protected by a screen. The pump discharge goes through a pressure-relief valve, micronic filter, and a cooler before it reaches the jets which spray it on gears and bearings. Since the cooling air for the oil cooler is supplied by the engine fan, the oil must be circulated practically the full length of the helicopter to the oil cooler aft of the engine and back again.

Fig. 7 is an outside view of the HUP aft transmission and

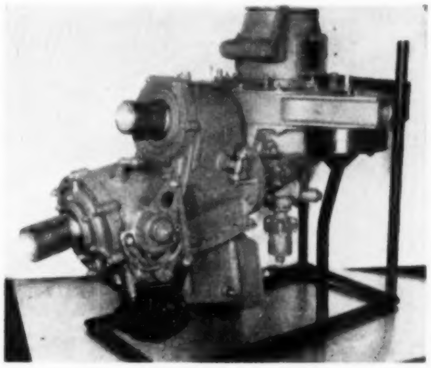

FIG. 7 EXTERNAL VIEW OF HUP AFT TRANSMISSION AND CLUTCH

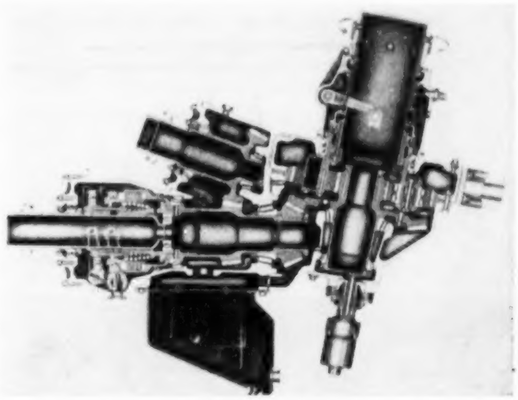

FIG. 8 SECTION THROUGH HUP AFT TRANSMISSION AND CLUTCH

clutch. The clutch is operated by an actuator shown in black mounted just below the clutch. The two clutch yokes are operated by the external cam connected to the actuator by a link.

Fig. 8 is a section through the aft transmission. As explained before, there are two phases of clutch engagement: With the engine idling and with rotors stationary, the actuator turns the clutch cam through part of a turn and stops. This engages the friction plates shown in Fig. 8. The static torque of the friction plates is adjusted to about 15 per cent of the full take-off torque of the engine. When the tachometers indicate that the shaft speeds are synchronized, the pilot engages the actuator again. The cam then turns through the remainder of its travel. In doing so, it engages the saw-tooth dog clutch and at the very end of its stroke releases the friction element. The top half of the clutch section in Fig. 8 shows the dog clutch in the released position. The bottom half shows it engaged. If an engine failure occurs in flight, the overrunning of the clutch will permit the pilot to go into autorotation immediately. On the clutch-release cycle, the friction element does not engage.

The spiral bevel pinions and gears are all mounted on tapered roller bearings. The planetary-gear set is the same as in the forward transmission except for different mounting of the sun gear and planet carrier. The pump and tachometer are driven by an internal gear in the bottom end of the sun-gear shaft.

Above the planetary gearing is the dephasing device, a hand-operated splined clutch. When the rotor blades are folded to take up less space in the hangar, one blade of each rotor remains

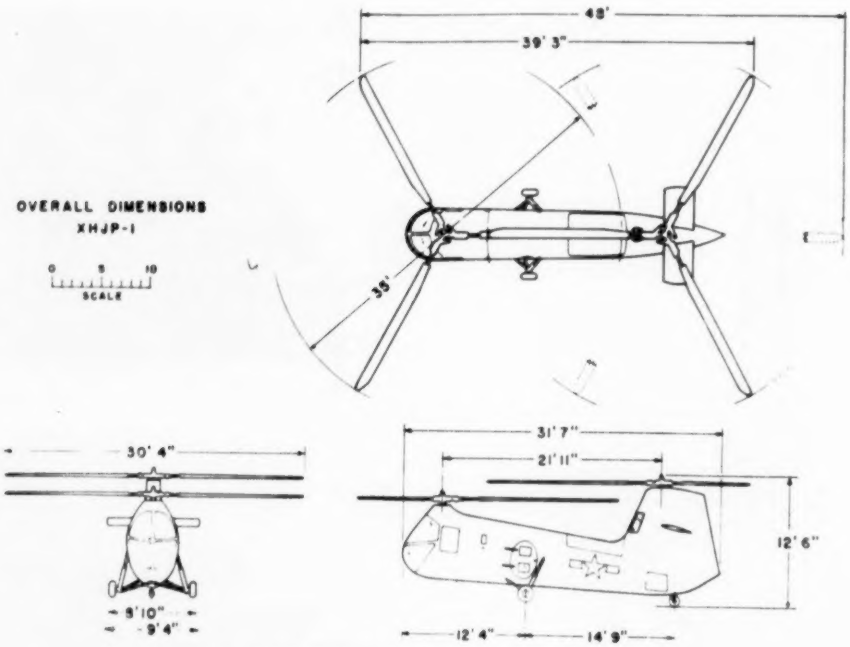

Fig. 9 XHJP With Blades Dephased but Not Folded

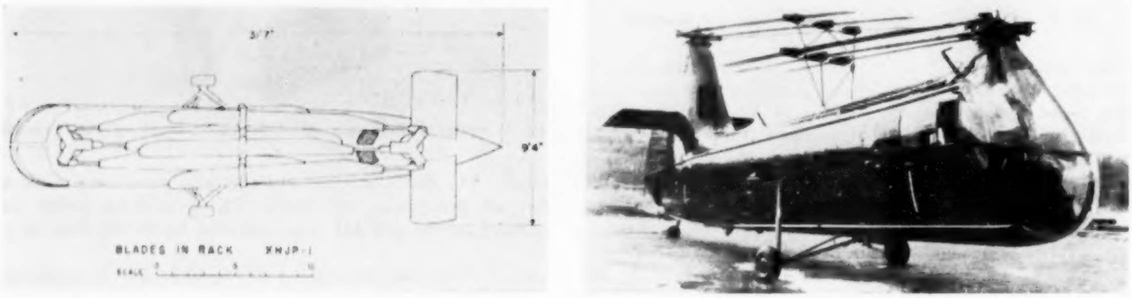

Fig. 10 XHJP With Blades Dephased and Folded

pinned in its regular position, and the other two are unpinned and swung around parallel to it. The dephasing device disconnects the splined shaft and permits both sets of folded blades to be brought in over the fuselage.

Fig. 9 shows the XHJP helicopter with blades dephased but not folded. One rotor has been rotated 60 deg relative to the other so that the over-all length of the ship over blade tips is reduced from 48 ft to 39 ft 3 in.

Fig. 10 shows the blades dephased and folded. The helicopters can be stored in a very small space with folded blades. The dephasing device also acts as a flexible connection for the aft-rotor shaft. The spline at the lower end of the shaft in the dephasing device takes out radial reactions and also transmits the torque. The thrust bearing at the top of the pylon takes thrust and radial loads.

HRP-2 Drive System

The HRP-2 with its flying-banana configuration has a slightly different drive system. Fig. 11 shows a cutaway section of this helicopter. The engine has a take-off rating of 600 hp at 2250 rpm. The engine shaft extends forward and connects to the clutch of a central transmission. The drive to the forward rotor is directly through the transmission-input shaft. The drive to the aft rotor is through gearing which brings the shaft out at an angle relative to the forward drive shaft and at the same speed. Each rotor transmission is identical except for the direction of rotation of the input shaft and the corresponding change in hand of the spiral bevel gears. Clutch operation and other general features are similar to those for the HUP.

Fig. 12 shows a cutaway section of the HRP-2 rotor transmission. The input pinion is straddle-mounted on angular-contact ball bearings and cylindrical roller bearings. The planetary gears are similar to those in the HUP except that they are above the spiral bevel gears in both rotor transmissions. The rotor shaft still passes through the sun gear for greater bearing span in a small space but the thrust bearing is located at the bottom. The encircled detail shows the oil pump and drive gear which is mounted on the lower end of the rotor shaft.

Fig. 13 shows a cut away section of the HRP-2 central transmission and clutch. The clutch details and operation are prac-

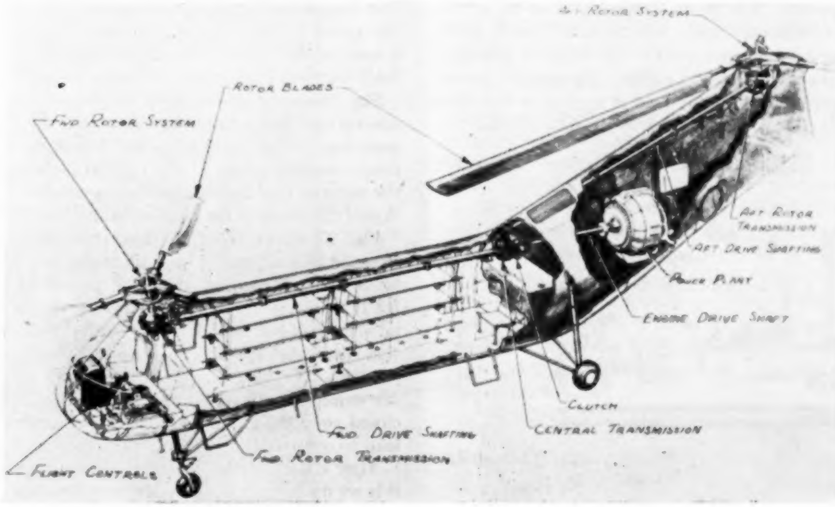

Fig 11 Cutaway View Showing HRP-2 Drive System

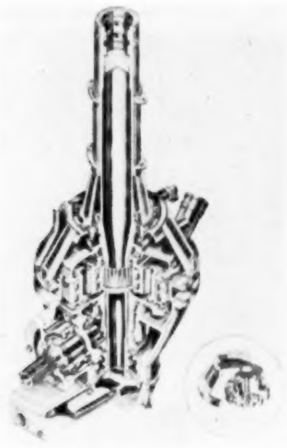

Fig. 12 Cutaway Section of HRP-2 Rotor Transmission

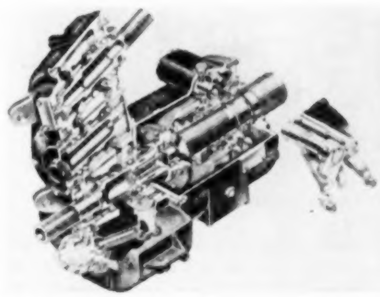

Fig. 13 Cutaway Section of HRP-2 Central Transmission and Clutch

tically the same as for the HUP transmission. The spiral bevel pinion drives a gear through an idler to obtain the proper rotation to the aft transmission. The forward transmission drive is directly through the shaft. The central-transmission gears transmit power only for the aft rotor.

The pump is shown below the drive shaft and is driven by a gear meshing directly with the main pinion. All three gears are straddle-mounted on ball and cylindrical roller bearings.

In the HRP drive system, dephasing is done by disconnecting a pin drive in the connecting shafting.

Materials and Design Details

All main power-transmission gears for all models are made of 9310 steel with carburized and hardened teeth. When 9310 steel is not available, 3310 steel is used as a substitute. The teeth of all spur and spiral bevel gears are ground except in a few cases where flange interference or grinding-machine capacity prevents grinding. The spur gears have full-radius fillets with either 25 or $27^1/_2$-deg pressure-angle, full-depth form. Practically all of the main transmission housings are made of cast magnesium. Some covers and highly stressed members are aluminum. The connecting drive shafting is aluminum tubing riveted to either aluminum or steel adapters at the ends. The friction-clutch plates are made of alternate plain-steel plates and steel plates bonded to sintered-bronze coatings. All splined connections including clutch plates are 30-deg involute splines.

Transmission lubricating oil is ANA specification MIL-0-6082 grade 1065. This is a straight mineral oil without extreme pressure additives. The Saybolt viscosity is approximately 65 sec at 210 F.

Load-Run Testing

When a new design is developed or when a major dynamic part is changed in a transmission, the transmission must be run through a qualification endurance test. The endurance testing is divided into two phases. The first phase is done in a test stand in which a static torque can be applied through a closed circuit of shafts and gear units. The driving motor then is used only to overcome the

friction in the system. The second phase is done in a "tie-down." This is a helicopter which has the same rotors, shafts, and all parts of the dynamic system as in the complete helicopter but which is tied to the ground by cables. The cables prevent take-off of the helicopter when the load is applied to the drive system by increasing the collective pitch of the rotor blades.

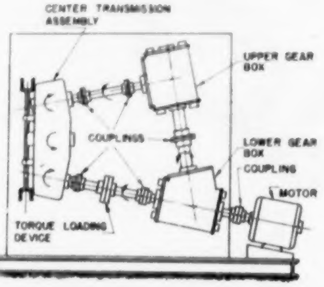

Fig. 14 Schematic Drawing of HRP Central-Transmission Load-Test Stand

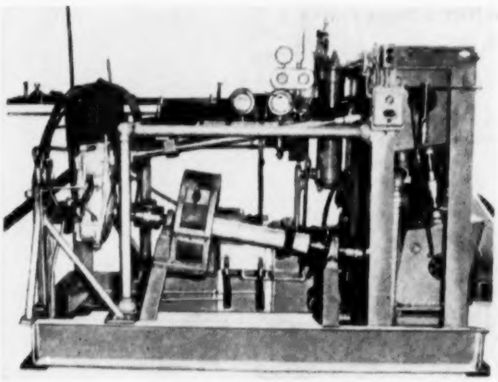

Fig. 15 HRP Central-Transmission Load-Test Stand

Fig. 14 shows a schematic drawing of the HRP central transmission-load test stand. The helicopter transmission is at the left. The upper and lower shafts turn at the same speed in the directions shown. The upper and lower test-stand gear boxes are designed to form a closed circuit in which proper shaft rotations are maintained. The shaft of the lower test-stand gearbox is extended to a motor drive. In the lower shaft of the closed circuit is a torque-loading device. This consists of a worm and gear mounted in bearings in an enclosed housing. The worm and housing are connected to the shafting on one side. The worm gear is connected to the shafting on the other side. With the shafts at rest, the worm is turned with a wrench to wind up one part of the shaft relative to the other. This wind-up results in a locked-in torque in the closed circuit. The magnitude of the torque is measured either with a mechanically actuated gage or an electrical strain gage.

After the desired torque is reached, the wrench is removed and the motor started. The shafts, worm, worm gear, and housing rotate as a unit. All gears in the closed system thus are operating at high torque and full speed. The motor operates at full speed but the only torque load is the total friction torque in the closed system plus acceleration torque when starting. In this stand, a 40-hp motor is used to test transmissions up to about 400 hp.

Fig. 15 shows the HRP central-transmission load-test stand. The torque-loading device is covered by a guard. The hole in the guard is for torquing-wrench clearance. The lubrication system of the central transmission in the test stand consists of flexible-rubber hose connected to the jets and pump.

Fig. 16 shows a schematic drawing of the HRP rotor-transmission load-test stand. In this stand, the upper gearbox has a gear ratio equal to that in the helicopter transmission. The torque-loading device in the vertical high-speed shaft is exactly the same as that in the central-transmission test stand. Operation of this stand is the same as for the central transmission.

Fig. 17 shows the HRP rotor-transmission load-test stand. Because of a difference in shaft angles and speeds and different transmission mounting, the HRP test stand cannot be used for HUP transmissions. Fig. 18 shows the HUP forward-transmission load-test stand. Fig. 19 shows the HUP aft-transmission load-test stand. This transmission has three shaft extensions. To load all three shafts, two closed-torque circuits are required. A separate torque-loading device is used in each closed circuit. The drive motor still has only the total friction load to overcome.

After a transmission is newly assembled for an endurance test, it is set up in the test stand and run for a few minutes at no load

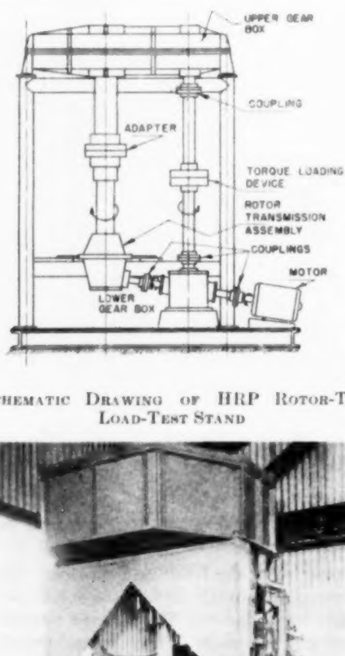

Fig. 16 Schematic Drawing of HRP Rotor-Transmission Load-Test Stand

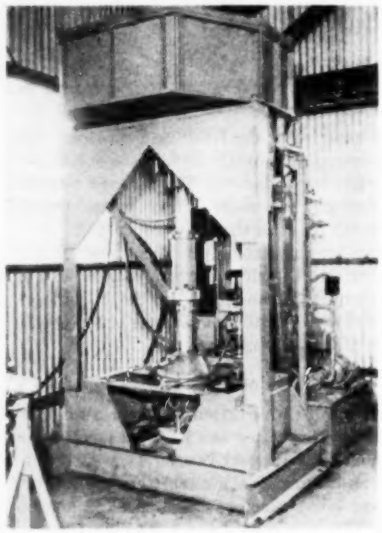

Fig. 17 HRP Rotor-Transmission Load-Test Stand

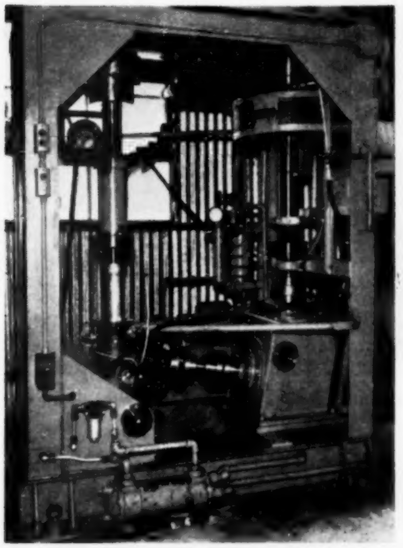

FIG 18 HUP FORWARD-TRANSMISSION LOAD-TEST STAND

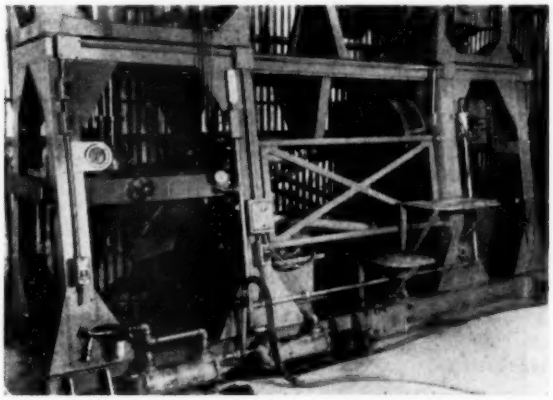

FIG. 19 HUP AFT-TRANSMISSION LOAD-TEST STAND

to check the oil pressure. If the oil pressure is not within limits, the hole size in one or two jets is changed as required. After the oil pressure is correct, the transmission is run at no load for approximately 1/2 hr to check for smooth operation and for temperature. If this test is satisfactory, load is applied in increments up to full take-off load. The load endurance run usually lasts several hundred hours. Several inspections take place during the load run. The first occurs after 1/2 hr at about 75 per cent load to check spiral bevel-gear-contact patterns. If any pattern is not within limits, the gears are reshimmed, run for another 1/2 hr, and reinspected. Thereafter, inspections take place at about 25 to 50-hr intervals to check gear teeth, bearings, and other dynamic parts.

The tie-down test then is run. In the tie-down the torsional vibrations of the actual ship are simulated. In this test normal rated power is used for most of the time.

After the transmission design is qualified, every new transmission made to those specifications is load-run in the load-test stand before installation in a helicopter. These production load runs usually consists of no-torque, half-torque, and full-torque runs. This permits proper adjustment of oil pressure, check of spiral bevel-gear patterns, oil-temperature check, and general noise and performance check.

CHECKING, TESTING, AND TROUBLE SHOOTING

During assembly, every transmission goes through a predetermined procedure of checks and adjustments. One of these is preload adjustment on all tapered roller bearings. The shims are adjusted, shaft assembled in the case, and the preload checked. Fig. 20 shows the method of checking preload in the vertical bevel-gear shaft of the HUP aft transmission using a special adapter and standard torque wrench. After preloads are adjusted, the spiral bevel-gear sets are checked and shimmed for correct no-load contact pattern. When the correct pattern is obtained, the backlash is checked by the method shown in Fig. 21. This figure shows the HUP forward transmission with a special adapter mounted on the input shaft. An arm on the adapter has a mark at exactly twice the pitch radius of the pinion. The dial indicator set on this mark will read twice the backlash, since the linear movement is twice that at the pitch radius of the teeth inside the transmission.

FIG. 20 BEARING PRELOAD CHECK ON HUP AFT BEVEL-GEAR SHAFT

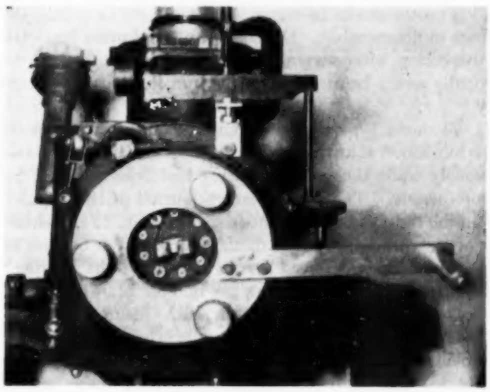

FIG. 21 BACKLASH CHECK ON HUP FORWARD SPIRAL BEVEL PINION

Before the planet-gear assembly is installed, the concentricity of sun gear and internal gear are checked in the case. Next, the planet-gear assembly is installed with a special cover which has large openings. The rotor shaft is locked and a small torque applied to the input shaft. The backlash of each planet is then checked through the openings in the special cover. In many cases, all four planets are in contact and show zero backlash.

In some cases, one or two of the planets show a small amount of backlash. An increase in torque will remove all backlash. This backlash check is a composite check of all errors which affect load distribution between planets. These checks indicate that at full load there is nearly perfect load division.

Fig. 22 shows the method of setting the static torque of the friction element in the clutch in the HUP aft transmission. The upper torque arm locks the synchronizing-shaft extension. The lower torque arm supports a weight giving the specified torque. This same stand is used to overrun the dog clutch. The upper

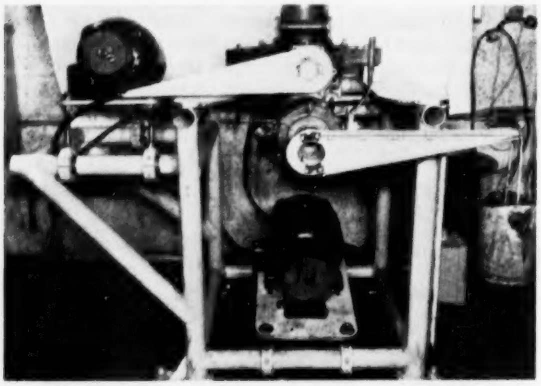

Fig. 22 Clutch-Torque Adjustment on HUP Aft Transmission

motor drives the synchronizing shaft at full speed by means of a V-belt drive. The lower motor drives the clutch shaft at reduced speed. The speed differential causes the clutch to overrun.

A considerable amount of development testing is usually required to get all the "bugs" out of a transmission. On the HUP, the transmission bearings in some locations were mounted with light fits on the shafts to eliminate any danger of damage to the bearings in disassembly. Others had normal press fits. On the first inspection, after several hours of load run in the test stands, practically every bearing had turned on its shaft and scored it badly.

Fig. 23 shows typical scored journals. The aft planet carrier on the left shows that the top bearing of the duplex set had scored excessively while the bottom bearing had practically no indication of turning. The lower bearing journal of the spiral bevel gear on the right shows moderate scoring. Fig. 23 also shows the form of the saw-tooth overrunning clutch at the bottom of the shaft. Some shafts showed severe fretting at the bearing fillet together with moderate scoring, as in Fig. 24. The fits of all tapered roller bearings were then revised to insure adequate press fits. Repeated tests showed that the bearings still could be disassembled safely with this press fit. Higher surface hardness of bearing journals also was called for. Under these conditions, slight creep did not damage the shaft and the scoring troubles were practically eliminated.

During endurance-load-testing of an HUP transmission, a number of the rollers developed banded areas with a frosted appearance, as shown in Fig. 25. The races were not damaged or marked. Sections checked with the microscope showed that, in the frosted areas, metal had been removed to a depth of about 0.0002 in. This same trouble then showed up in several other transmissions at overhaul. In one endurance run on the test stand, the transmission was run at take-off power with the frosted bearings installed to see how long bearings in this condition could be run. After 300 hr, one bearing had failed as shown in Fig. 26. Some of the rollers had pitted severely and one half of the

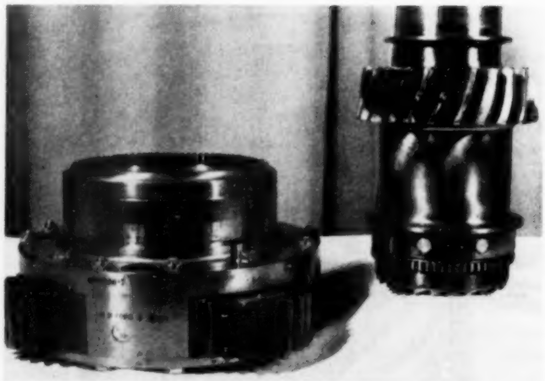

Fig. 23 Bearing-Journal Scoring on HUP Planet Carrier and Spiral Bevel Gear

Fig. 24 Fretting at Bearing Fillet in HUP Forward Spiral Bevel Pinion

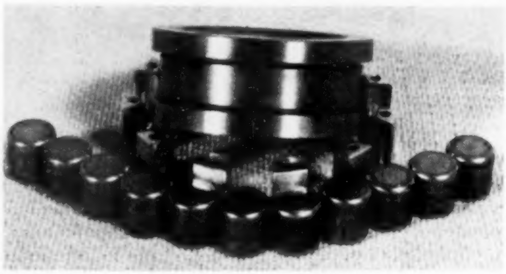

Fig. 25 HUP Planet-Bearing Failure

inner race was completely destroyed. In the planet bearing the load is stationary relative to the inner race so that only one half of the race was loaded. Fig. 27 shows what happened to the outer race of this bearing. Apparently, pieces of the damaged inner race were carried by the rollers and brinelled into the outer race.

Extensive checks of microstructure, surface finish, dimensions, hardness, and lubrication could not determine a definite cause for this condition. The shallow depth of roller failure indicated that it was not a normal fatigue failure due to load. Later, other bearings went through the tests with no signs of failure. The trouble did not reoccur when the size and number of rollers were

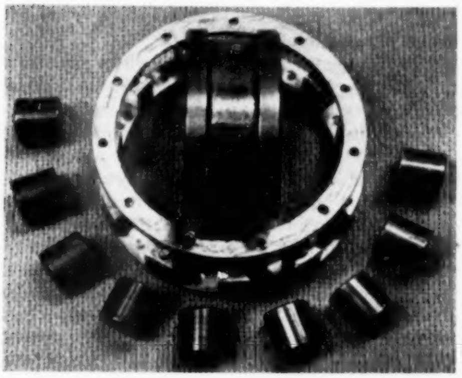

FIG. 26 PITTED ROLLERS AND SPALLED INNER RACE OF HUP PLANET BEARING

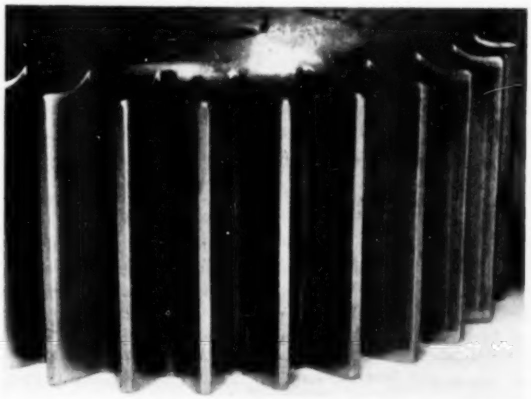

FIG. 28 PITTED HUP SUN GEAR

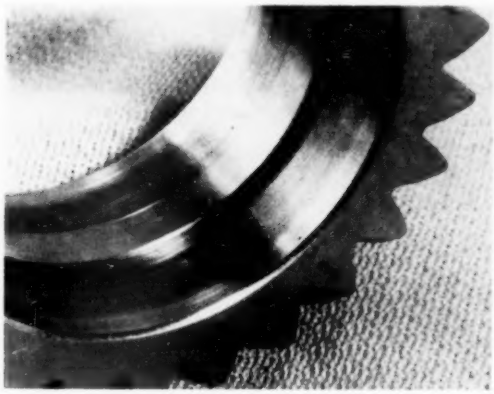

FIG. 27 BRINELLED BEARING RACE IN HUP PLANET GEAR

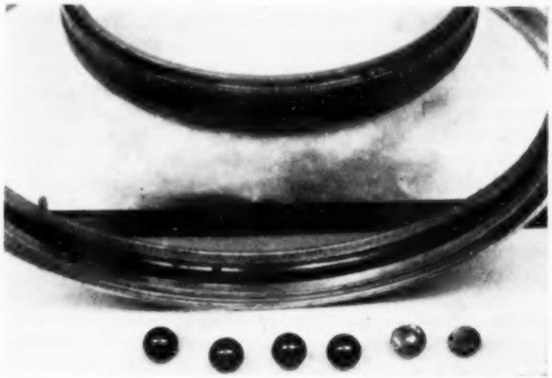

FIG. 29 DAMAGED HUP DRIVE-SHAFT BEARING

later increased for a higher horsepower transmission. It was suggested that a surface-finishing process may have affected the rollers of some of the bearings but no definite conclusions could be reached from the investigation.

The planetary gears in the XHJP, the prototype of the HUP, were 20-deg pressure-angle spurs in which the internal gears were case-hardened and ground and the sun gears and planets shaved, hardened, and lapped. The teeth had a flat root form with standard fillets. When the HUP model was develo[illegible] was decided to improve the tooth form and processing to reduce stresses and facilitate quality control.

First, the pressure angle was increased to increase beam strength as well as surface durability. The flat roots were changed to full-fillet roots to reduce stress concentration. Grinding was specified for all gears to improve tooth form, spacing, and concentricity. This would reduce dynamic stresses and improve load division between teeth and between planets. Generous rounding of the ends of the teeth was called for to reduce the danger of chipping. Then shot peening of all teeth was added to improve fatigue strength by putting the surface material into compression. Finally, the face width was increased slightly.

During the development testing of these new gears, the sun gears and some of the planet gears pitted and flaked excessively at the pitch line and near the tip. This pitting had started at the first inspection and reached a peak before half the test was completed. At the height of the pitting, involute checks were made. The sun-gear involute chart showed a dip at the pitch line up to 0.003 in. below the remainder of the tooth.

Fig. 28 shows one of these sun gears with pitted teeth. This was a disappointing result after incorporating so many improvements.

During the development program, checks were made on tooth hardness, microstructure, and load-test-stand calibration, all of which were according to specifications. Various oil-jet arrangements were tried with no improvement. Finally the shot peening was omitted on one set of gears. The pitting and distortion stopped. Thereafter the shot peening process was removed with good results.

Fig. 29 shows a damaged drive-shaft bearing. The race was badly pitted in spots. One ball was fractured and the cage was completely destroyed. This was the worst of several drive-shaft-bearing failures which were attributed to insufficient internal clearance. The bearing is a very light section ball bearing which had been originally designed with no cage and a full complement of balls for torque-tube applications. The manufacturer rebuilt this bearing for high-speed continuous operation by omitting some of the balls and adding a phenolic cage. The bearing was mounted on the shaft with a light press fit and in some cases was slightly preloaded. The shaft was made of aluminum and the differential expansion plus the initial press fit caused high preloads at operating temperature. After increasing the internal clearance, the bearings gave satisfactory service.

The foregoing examples are only a few of the typical develop-

ment problems encountered. The load-test stand has been a great help in finding the answers. It costs considerably less per hour to run than a helicopter. The transmissions can be set up for running in a minimum of time, and full take-off load can be applied 24 hr per day without endangering a costly helicopter and without overloading the engine.

Conclusions

There is not always a simple obvious solution to the design of a drive system for a new helicopter configuration. Design features that consistently give trouble in engine gears may work well in helicopter drives. Tooth forms or processes that work well in industrial gear drives may give trouble when applied to helicopter drives. With the obviously limited knowledge of the true fundamentals of transmission design in its present state of development, the designer must be careful not to reject all design features that have failed in other application. Different conditions of speed, temperature, lubrication, or rigidity may give entirely different results.

Endurance testing combined with previous experience with similar designs is a valuable tool for development of a successful helicopter-drive system. Once the endurance testing is completed successfully the design can be considered frozen by economic considerations. If it is discovered at a later date that weight and production cost can be reduced by a change in design, the saving in future production must be compared with the costs of endurance testing in addition to engineering and other costs.

The experience at Piasecki has been that development testing is considered essential and has proved the reliability of a number of novel and previously untried design features in addition to checking conventional configurations. Such testing is expensive but in the long run has been the major factor in establishing and maintaining the present high level of reliability of the helicopter-drive system.

Characteristics of a Vaporizing Combustor for Aviation Gas Turbines

By W. D. POUCHOT[1] and J. R. HAMM,[2] PHILADELPHIA, PA.

An annular vaporizing-type combustor for an aviation gas turbine is described and its performance and operational characteristics are given. Test results show that the level of combustion efficiency at high altitudes is high and nearly constant over a wide range of fuel-air ratios. The other performance and the operational characteristics of the combustor have been found to be satisfactory. The outstanding advantage of the vaporizing combustor was its short length relative to a liquid-injection combustor developed for the same application.

Nomenclature

The following nomenclature is used in the paper:

A = combustor annulus area between casings at upstream end of flame tube, sq ft
F/A = fuel/air ratio
g = gravitational constant
K = ratio of specific heats
L = combustor annular width at upstream end of flame tube, ft
N_M = combustor-inlet Mach number, $\dfrac{Wa\sqrt{RT_{T3}}}{AP_{T3}\sqrt{gK}}$
N_R = combustor-inlet Reynolds number, $\dfrac{WaL}{A\mu}$
P_{T3} = compressor-outlet total pressure, psia
P_{T4} = combustor-outlet total pressure, psia
ΔP_B = combustor total pressure loss $(P_{T3} - P_{T4})$, psi
R = gas constant, ft/deg R
T_{T3} = compressor-outlet temperature, deg R
T_{T4} = combustor-outlet temperature, deg R
ΔT_B = combustor temperature rise $(T_{T4} - T_{T3})$, deg F
ΔT_{max} = maximum obtainable temperature rise, deg F
Wa = combustor total air flow, lb/sec
μ = absolute viscosity, lb/ft-sec

Introduction

The vaporization of liquid fuel prior to its introduction into the burning space has been used in many kinds of combustion chambers and was an attractive possibility from the beginning for aircraft gas-turbine use. However, most attempts to use such a method were beset with difficulties and abandoned in favor of liquid-fuel injection.

This paper presents the tested characteristics of a vaporizing combustion chamber which has been developed to the point where it has met satisfactorily the requirements of the modern jet engine and is being used in field service. The requirements may be stated quite simply: It should be highly efficient, stable, and capable of ignition over a wide range of operating conditions, light in weight, small in size, durable, require a minimum of maintenance, and have no harmful effect on other components. Easy to say, sometimes more difficult to accomplish.

We have found this vaporizing combustor to have the following desirable qualities: (*a*) It can be of very short length and still maintain good efficiency and stability because of the removal of the time for vaporization from the combustion time; (*b*) it is clean burning using a wide range of fuels which results in low wall deposits and low luminosity of the flame, thereby reducing wall temperatures; and (*c*) it can use extremely low fuel pressure without performance penalty. Its chief virtue in our eyes is a 40 per cent saving in burning length over a comparable liquid-injection burner which was developed for the same application.

During the starting cycle, the vaporizing combustor requires auxiliary liquid fuel-injection nozzles. The use of these nozzles insures prompt ignition and good starting by eliminating the reluctance to ignite and the tendency to torching on the bottom half of the burner which is characteristic of the vaporizing combustor before its vaporizer elements have reached operating temperature. The auxiliary nozzles operate only during the starting cycle. After the vaporizer elements reach operating temperature, the combustor's response to fuel-rate changes is excellent.

We had anticipated heavy vaporizer surface deposits particularly when using fuels with high gum content. However, these deposits have failed to materialize even when using fuels with a gum content considerably in excess of that allowable under present-day aviation jet-fuel specifications.

In respect to evenness of outlet-temperature distribution, the burner has proved neither better nor worse than comparable liquid-injection chambers.

The observed characteristics of the combustor are arranged in two general categories in the subsequent discussion, (*a*) performance and (*b*) operational. These will be discussed in detail after a description of the combustor and its operation.

Description of Vaporizing Combustor

The vaporizing combustor is an annular-type burner shown schematically in Fig. 1. It is made up of the following basic parts:

1 The diffuser whose main function is to direct the air from the compressor to the combustor and to divide it into the proper proportions for combustion air (the air required for the burning process) and diluent air (the air required to cool the products of combustion down to a temperature usable in the turbine).

2 The ignition system which consists of two spark plugs and six to eight auxiliary fuel nozzles located in the first cylindrical section of the outer liner.

3 The upstream plate which holds the vaporizing tubes and secondary-air admission ports.

4 The vaporizing tubes which are immersed in the flame tube and whose main function is to vaporize the liquid fuel which is supplied by the fuel tube and to mix it with a portion of the air needed for combustion called the primary combustion air.

5 The secondary-air ports which supply the remainder of the air needed for combustion.

---

[1] Supervising Engineer, Westinghouse Aviation Gas Turbine Division.

[2] Design Engineer, Westinghouse Aviation Gas Turbine Division.

Contributed by the Aviation Division and the Society of Automotive Engineers and presented at the Annual Meeting, New York, N. Y., November 29–December 4, 1953, of The American Society of Mechanical Engineers.

Note: Statements and opinions advanced in papers are to be understood as individual expressions of their authors and not those of the Society. Manuscript received at ASME Headquarters, September 10, 1953. Paper No. 53—A-182.

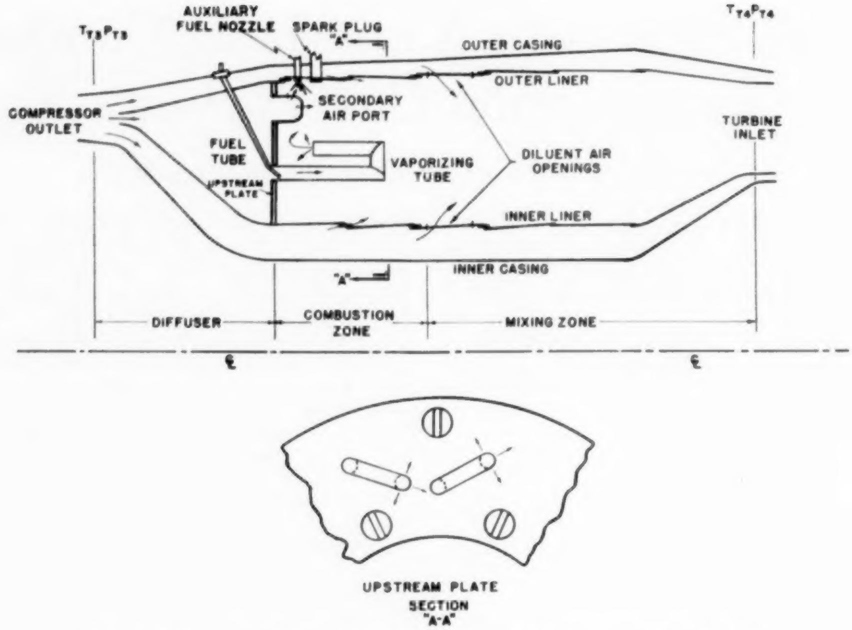

FIG. 1 SCHEMATIC OF VAPORIZING COMBUSTOR WITH ANNULAR-TYPE BURNER

6 The inner and outer liner walls which define the combustion space and provide the diluent-air openings for the air necessary to cool the combustion gases down to a temperature which the turbine can utilize.

OPERATION

Burning is initiated in the combustor by the previously mentioned ignition system. Fuel is admitted through both the auxiliary fuel nozzles and the vaporizing tubes to give a fuel-air mixture which is ignited by the spark plugs. When the flame is spread completely around the annulus and the vaporizing process is well established, the auxiliary fuel nozzles and the spark plugs are turned off.

The steady-state operation of the vaporizing combustor may be divided into the following steps: Vaporization of the liquid fuel and the addition and mixing of the air needed for the combustion process, the combustion process, and the admission and mixing of the diluent air.

The fuel-vaporization process is accomplished by directing liquid fuel into the upstream end of the vaporizing tube. An amount of air sufficient to give a minimum air/fuel ratio within the tube of about 4/1 over the range of operating conditions of the combustor is added along with the fuel. The vaporizing tube itself is shaped somewhat like a "candy cane" or "walking stick" and is immersed in the flame of the combustor. Sufficient heat is transferred through the walls of the tube to vaporize the liquid fuel. Cracking of the fuel on the walls of the tube with consequent coke formation is prevented since the vaporization process is accomplished in an atmosphere of air and, therefore, the temperature required to vaporize the fuel is relatively low. The rich air/fuel mixture is discharged toward the upstream plate and is mixed with sufficient air from the secondary-air ports to form a burnable mixture which burns in the combustion zone of the combustor.

The diluent air is added through ports in the inner and outer liner walls and is mixed with the combustion gases in the mixing zone of the burner.

The vaporizing combustion chamber has a combustion zone about 40 per cent shorter than a corresponding atomizing-type combustor. This length saving is possible since the fuel is delivered to the upstream end of the combustion zone in a gaseous state premixed with a portion of the air that is needed for burning.

PERFORMANCE CHARACTERISTICS

The performance of a combustion chamber is determined by the combustion efficiency, the combustion stability, and the combustion-chamber pressure loss.

Combustion Efficiency. The characteristic relationship between combustion efficiency and over-all fuel-air ratio for a vaporizing combustor is shown plotted in Fig. 2. This plot shows that the peak efficiency occurs on the lean side of the fuel-air-ratio range and that the rate of decrease of efficiency with increasing fuel-air ratio becomes greater as the inlet-pressure level diminishes. However, except at the very low pressure levels, the efficiency level does not vary greatly over a wide range of fuel-air ratio. This characteristic shape of the efficiency curve for the vaporizing combustor is markedly different from the efficiency curve of the typical atomizing combustor, which generally peaks in the high fuel-air-ratio range and drops appreciably at lower fuel-air ratios. The same efficiency data is shown plotted in Fig. 3 as a function of combustion-chamber temperature rise. This plot shows that the variation in combustion efficiency is not great over a wide range of temperature rise except at the 10-in-Hg inlet-pressure level where a maximum obtainable temperature rise was reached and a very abrupt change in efficiency level resulted. However, this pressure level is generally outside the range of interest in aviation gas turbines.

Fig. 4 shows the effect of combustor inlet-air temperature on combustion efficiency. Increasing the inlet temperature improves the combustion efficiency at a diminishing rate up to a temperature level of about 300 F where the effect of temperature increase becomes zero. The effect is substantially independent of fuel-air ratio. A direct-fired preheater was used to vary the

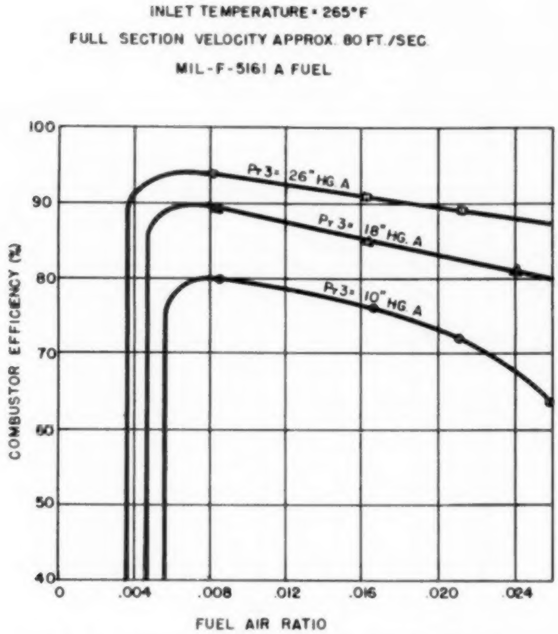

FIG. 2 EFFECT OF FUEL-AIR RATIO ON EFFICIENCY

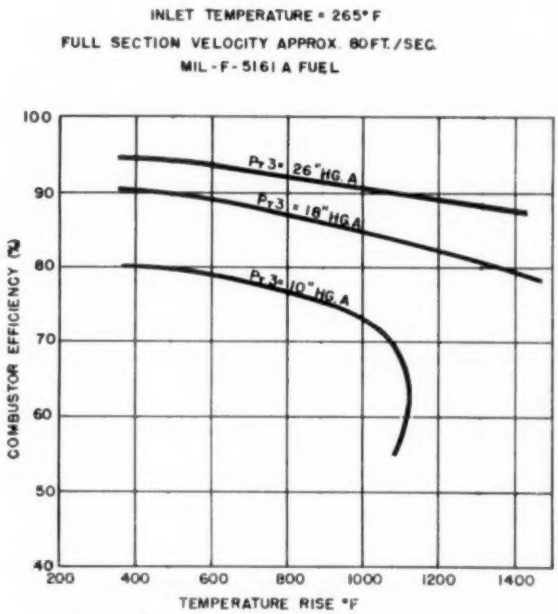

FIG. 3 EFFECT OF TEMPERATURE RISE ON EFFICIENCY

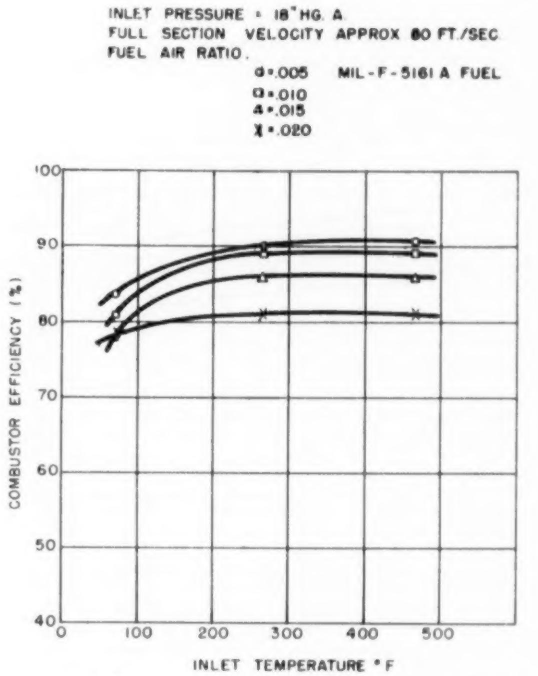

FIG. 4 EFFECT OF COMBUSTOR-INLET TEMPERATURE ON EFFICIENCY

inlet-air temperatures; therefore these results are clouded somewhat by vitiation of the combustion air.

The effect of combustor full-section velocity[3] on combustion efficiency is shown in Fig. 5. Increasing the full-section velocity causes the combustion efficiency to decrease at an increasing rate. The effect is substantially independent of fuel-air ratio.

The effect of combustor-inlet pressure is shown in Fig. 6. Increasing the inlet pressure causes the combustion efficiency to improve at a decreasing rate. The data indicate that the efficiency would continue to improve up to a pressure level of about 35 in. Hg. Here again, the effect is substantially independent of fuel-air ratio.

Combustion Stability. In an academic sense the range of stability of a combustor extends from the lean-mixture blowout point to the rich-mixture blowout point. In a practical sense, however, the range of stability extends from the lean-mixture blowout point to the point of maximum obtainable temperature rise. Most engine controls become unstable if the slope of the temperature rise versus fuel-air-ratio curve becomes negative. In some instances the point of maximum obtainable temperature rise and the point of rich-mixture blowout are coincident. However, in the majority of cases the maximum obtainable temperature rise occurs at a fuel-air-ratio value appreciably lower than that at which the rich-mixture blowout occurs.

The effect of combustor-inlet pressure on the lean-mixture stability limits of a vaporizing combustor is shown in Fig. 7. The air-fuel ratio at which the lean-mixture blowout occurs increases with pressure at an accelerating rate in this range of pressures. It is unreasonable to expect this increase in stability limits to continue indefinitely. However, the point at which the lean limits stop improving has not been determined yet.

Fig. 8 shows the effect of combustor-inlet temperature on lean-mixture stability limits. The air-fuel ratio at which blowout occurs does not vary appreciably over a wide range of inlet temperature.

The effect of combustor full-section velocity on the lean-mixture stability limits is shown in Fig. 9. The effect is negligible at velocities up to 100 fps. At velocities above 100 fps the air-fuel

[3] Full-section velocity is based on the compressor-outlet temperature, pressure, and air flow and the annular area between the inner and outer casings.

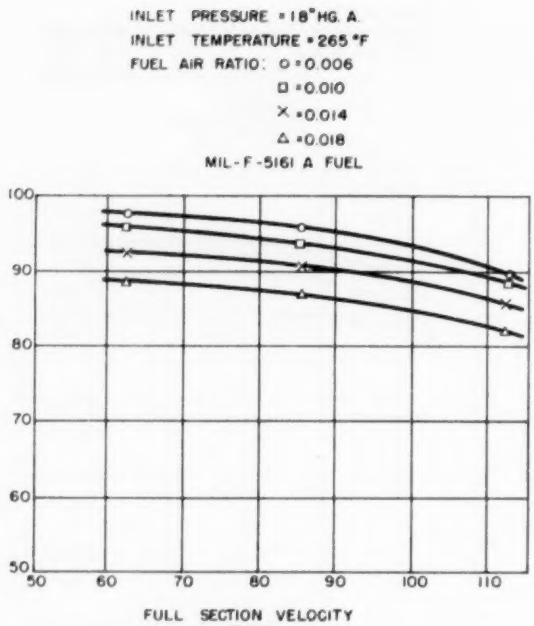

Fig. 5 Effect of Full-Section Velocity on Efficiency

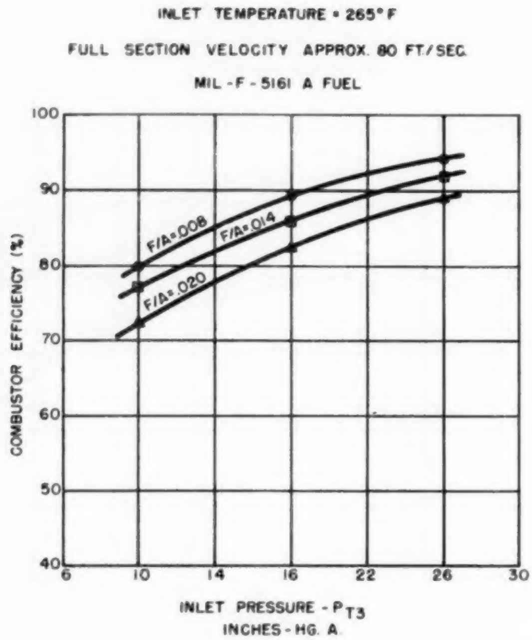

Fig. 6 Effect of Pressure on Efficiency

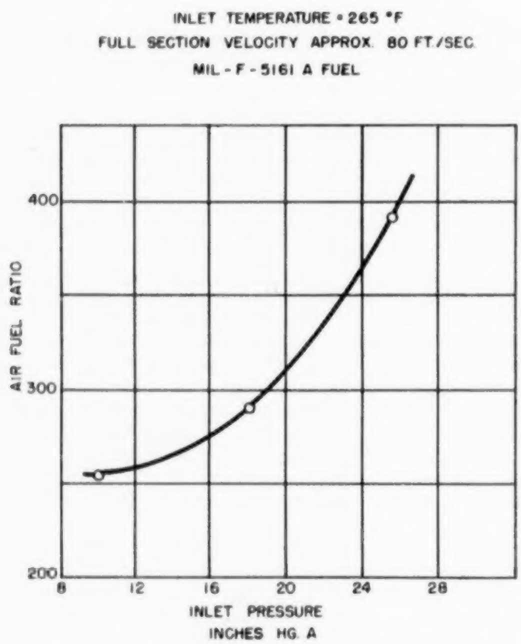

Fig. 7 Effect of Inlet Pressure on Lean-Mixture Stability

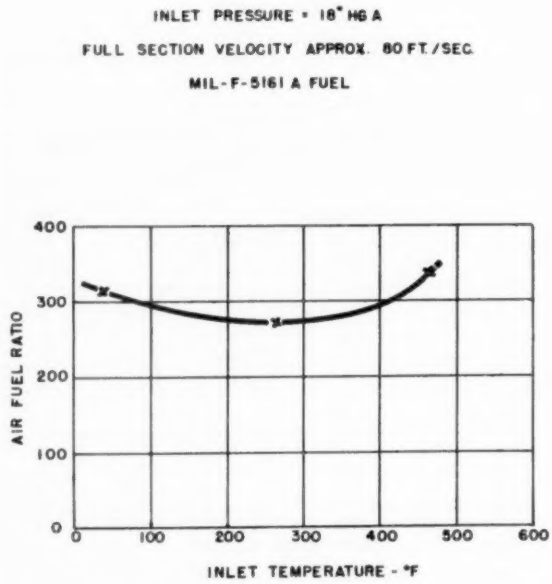

Fig. 8 Effect of Inlet Temperature on Lean-Mixture Stability

ratio at which blowout occurs decreases rapidly with increasing velocity.

The plots in Figs. 7, 8, and 9 were made from data taken on different combustor configurations. Therefore the limiting air-fuel rates at the common condition of 80 fps, 265 F, and 18 in. Hg are somewhat different. However, these plots give typical relationships between lean-mixture stability limits and pressure, velocity, and temperature.

The following correlation of maximum obtainable temperature-rise data has been obtained

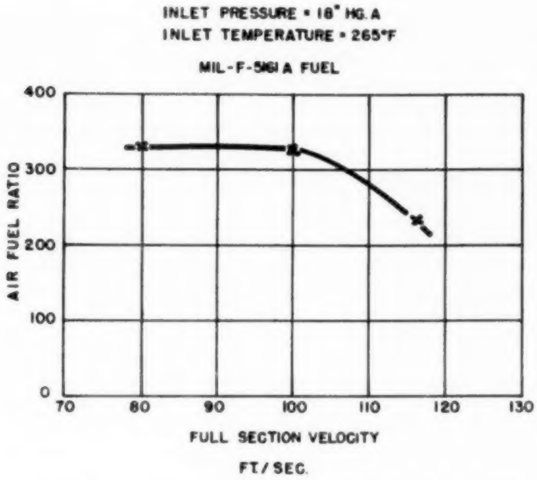

FIG. 9 EFFECT OF VELOCITY ON LEAN-MIXTURE STABILITY

$$\frac{\Delta T_{max}}{T_{T3}} = f(N_R, N_M)$$

That is, the ratio of combustor maximum obtainable temperature rise to the combustor inlet-air temperature is a function of the combustor-inlet Mach and Reynolds numbers based on the combustor-inlet pressure and temperature and the combustor total area at the upstream end of the flame tube.

Typical maximum obtainable temperature-rise characteristics of the vaporizing combustor are shown correlated on this basis in Fig. 10. This correlation shows that the maximum obtainable temperature rise is very sensitive to combustor-inlet Mach number and that it is appreciably affected by combustor-inlet Reynolds number.

Combustor Pressure Loss. Typical pressure-loss data for the vaporizing combustor are shown plotted in Fig. 11. This plot shows that the combustor pressure loss is very sensitive to the combustor-inlet Mach number and is affected relatively little by the combustor temperature rise.

OPERATIONAL CHARACTERISTICS OF A VAPORIZING COMBUSTOR

In addition to the pyrogenic performance discussed in the foregoing section, the evaluation of an aviation gas-turbine combustor depends on the following operational characteristics: (1) Good durability and structural stability; (2) small size and light weight; (3) minimum complexity; (4) good ignition; (5) good radial and circumferential temperature distribution at the inlet to the turbine; (6) minimum carbon deposit and smoking tendencies.

In the annular vaporizing combustor, good durability has been achieved by using heat and corrosion-resistant materials with small amounts of cooling or insulating air injected at frequent intervals along all surfaces which are exposed to the flame.

The vaporizing tubes are cooled by promoting turbulence in the air-fuel mixture passing through them. This gives adequate durability to the tubes, insures a high degree of vaporization of the liquid fuel, and thoroughly mixes the vaporized fuel with the air passing through the tubes.

Particularly in the design of larger-diameter burners of the annular type, the structural stability of the outer burner wall becomes very important. Since a pressure drop exists across the burner wall, some stiffening of the outer shell is necessary to prevent buckling. Circumferential stiffeners at intervals along

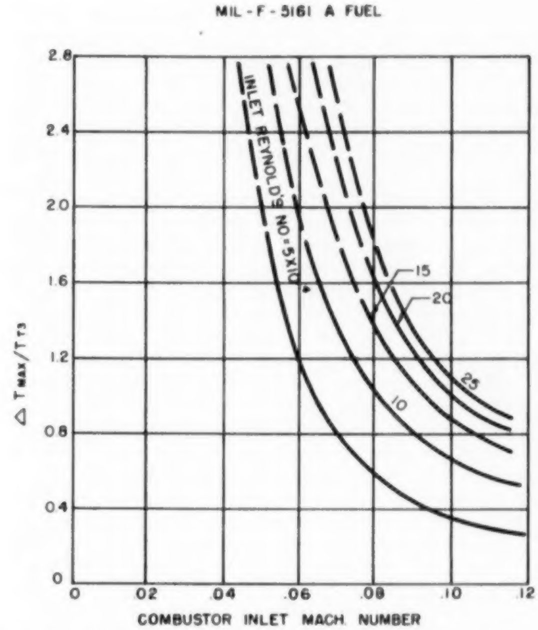

FIG. 10 MAXIMUM OBTAINABLE TEMPERATURE-RISE CHARACTERISTICS

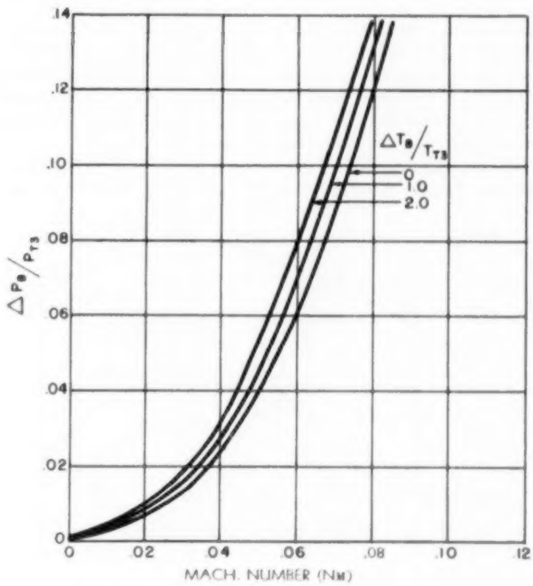

FIG. 11 PRESSURE-LOSS CHARACTERISTICS

the outer liner wall have overcome this problem successfully.

This vaporizing combustor has a shorter over-all length than most conventional combustors owing to its smaller primary-combustion volume. However, the vaporizer is no lighter than its counterpart—the atomizing combustor—because of the vaporizing tubes and fuel lines which are necessary. Its decreased over-all length, however, makes substantial engine and aircraft-structure weight savings possible.

The complexity of the annular vaporizing combustor is about equal to that of the more complicated annular atomizing combustors. The liner, casing, and diffuser construction is the same as that used on atomizing combustors. While no fuel nozzles or dual fuel-distribution lines are required for the basic combustor, the number of fuel lines and vaporizing tubes is relatively large, and auxiliary fuel nozzles and controls are required for the ignition system.

One of the advantages of the vaporizing combustor is that the fuel pressures required are low and are set not by the combustor but by the necessary drops to operate the gas-turbine-engine controls. The maximum pressure used with this combustor is 380 psig. This results in a saving in pumping power over a comparable liquid fuel-injection burner operating at a maximum pressure of 460 psig. The time cycle for igniting the vaporizer and the range of operating conditions where it will ignite are comparable with other type burners. High-energy spark-discharge systems are better suited for this application than the high-voltage types.

In all combustors for gas-turbine engines, the temperature distribution of the gases which are delivered to the turbine is of prime importance to the life of the turbine. The detail shape of the temperature-distribution curve which is required is dictated by the material properties and the physical design of the turbine. In a typical gas-turbine-engine application of the vaporizing combustor under discussion, a radial temperature distribution of the general shape shown in Fig. 12 is desired. A circumferential variation of no more than ±200 deg F at a given radial location is desired to minimize vibrational stresses set up by unequal loading of the rotating turbine blades, and a plus variation of no more than 200 deg F is desired to obtain adequate turbine-nozzle life. The vaporizing combustor has proved capable of producing the desired radial temperature distribution with little circumferential variation as shown in Fig. 12. These properties enable substantial weight savings to be realized in the design of the turbine.

Analysis of the gases from this combustor with a von Brand filter-type smoke analyzer have shown that the exhaust gases do not contain a measurable amount of smoke.

Coke or, more generally, the deposits which may form within a burner during the combustion process can affect the performance and operational characteristics. These deposits may affect the vaporization of the fuel seriously if they occur on the vaporizing tubes. If deposits occur on the upstream plate or on the liner walls, the mixing of the fuel and air may be affected so as to cause poor efficiency and circumferential temperature maldistribution. Deposits which break off and pass through the turbine have caused no damage.

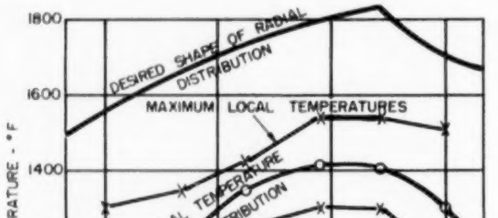

Fig. 12 Combustor Outlet-Temperature Distribution

Two methods are used to prevent the formation of deposits within the burner: (1) The injection of a blanket of air, which also is used to improve durability, and (2) running the metal surfaces hot enough to prevent any deposits from forming. The anticoking air blanket is used on the walls and upstream plate since running these parts hot generally results in poor durability. The air blanketing has been very successful and only very small amounts of coke have been found within the burner. The temperature at which the vaporizing tubes operate prevents the accumulation of any large deposits on the tubes. No deposits of any consequence have occurred on the inside of the vaporizing tubes with fuels intended for aircraft use.

Conclusion

The annular vaporizing combustor possesses, to a high degree, the operational and performance qualities needed for a good gas-turbine combustor. Compared with a typical annular liquid-injection combustor, its efficiency varies less with fuel-air ratio and it is appreciably shorter in length. Future development can be expected to make its position even more outstanding for aviation gas-turbine application.

Acknowledgments

The authors wish to acknowledge the following companies and individuals: Armstrong-Siddeley Motors, from whom most of the basic ideas for this burner came; the Westinghouse Electric Corporation, which carried out the development; and Messrs. E. P. Walsh, W. L. Christensen, and others who played a large part in the development and aided in the preparation of this paper.

Discussion

A. Shaffer,[4] S. Suciu,[4] and H. A. Fremont.[5] The vaporizing combustor, while well known to British designers, is fairly new to American practice. This paper is therefore of great interest in bringing out some of the design problems and advantages associated with this type of fuel-injection system. The vaporizing burner offers greatest advantages at low operating pressures, and this is the region the authors have chosen to study.

The vaporizing burner in the past has presented two main design difficulties:

1 An auxiliary fuel-injection system is needed for starting.

2 The vaporizing tube is susceptible to carbon deposition and overheating.

The second problem seems to be absent in the configuration described by the authors. Solution of the first is needed to eliminate weight penalties to the combustion system and complexities in the control system.

We should like to point out that caution must be exercised in interpreting combustion-chamber data for a specific configuration over a limited range of operating conditions. This is of importance, since other components of the aircraft gas-turbine engine place definite limitations on combustor-design conditions. For example, all of the authors' data show maximum combustion efficiency at fuel-air ratios considerably lower than representative

[4] Aircraft Gas Turbine Division, General Electric Company, Cincinnati, Ohio. Assoc. Mem. ASME.

[5] Aircraft Gas Turbine Division, General Electric Company

of normal engine operation. The desirable combustor should, if possible, show increased efficiency at higher fuel-air ratios, since at these ratios efficiency has a considerably greater effect upon engine fuel consumption and hence upon aircraft range.

In this connection, the drop off of efficiency with increasing inlet velocity tends to limit the combustor and engine to low air flows per unit frontal area.

The 40 per cent saving in burning volume quoted by the authors is not reflected in a corresponding decrease in combustor length, since appreciable space in the combustor is required to cool the combustion gases to allowable temperatures.

The authors claim that the vaporizing combustor affords the use of "extremely" low fuel pressures. This is not quite correct, since in current and probably future engine designs the fuel pressure is dictated largely by combustor operating pressures and by some extent to fuel-line and vaporizer losses. The figure of 380 psig for fuel pressure is not an appreciable reduction from the 460-psig figure quoted for a liquid-injection burner. In any case, pumping losses per se in an aircraft gas-turbine cycle are minor.

Finally, the authors use the term "combustion stability" to refer only to blowout conditions. A complete treatment of burner stability requires consideration of burner pulsations.

Authors' Closure

The authors agree with the discussers of this paper that it is difficult to consider adequately a combustor apart from the engine to which it is attached and that it can sometimes be misleading to do so. In this connection two questions have been raised.

The first has to do with the combustion efficiency as a function of fuel-air ratio. It is our conviction that a high constant level of efficiency over a wide range of fuel-air ratios is the most desirable because the jet engine must operate over a variety of thrust ranges from low cruise to military power. This calls for good efficiency at both high and low fuel-air ratios. This vaporizing combustor comes close to accomplishing this down to about 18 in. Hg abs which is the lower-pressure limit of steady-state operation at which it is required to serve.

On the second question raised, to the authors' knowledge all combustors exhibit this tendency for the combustion efficiency to fall with increasing air velocity. This vaporizer is quite comparable in respect to its velocity tolerance with other combustors now in production.

On the balance of the discussion, we have no comment to make with the exception of some remarks about our definition of "combustion stability." We have defined the stable operating range of the combustor as that between the lean blowout limit and the maximum attainable temperature rise and the objection is made that a full treatment of combustion stability requires consideration of burner pulsations. Since we were not bothered by burner pulsations with this combustor, we rather pleasantly forgot that such things can exist and apologize for our oversight.

In conclusion the authors would like to thank Messrs. Shaffer, Suciu, and Fremont for their interesting and worthwhile discussion of this paper.

Thermal Conductivity of Gases

By F. G. Keyes,[1] Cambridge, Mass.

This paper is a continuation of earlier reported work in connection with two of the fundamental properties required for understanding and designing heat-transfer equipment. New measurements of heat conductivity are presented along with values for viscosity obtained by correlation of all available data found in the literature. The simplest substance from the point of view of theory is the monatomic gas. The results of a study of the five rare gases are included.

Introduction

The earlier papers (1, 2, 3)[2] dealt with measurements of thermal conductivity of the diatomic gases, mixtures of nitrogen and carbon dioxide, and a few triatomic gases. Measurements have now been extended to neon, argon, hydrogen, nitrous oxide (N_2O), methane (CH_4), ammonia (NH_3), ethane (C_2H_6), ethylene (C_2H_4), ethyl chloride (C_2H_5Cl), Freon 12 (CCl_2F_2), and Freon 114 $(CCl_2F_2)_2$. In addition, pressure coefficients have been formulated from the observed data for ten substances.

The facilities available now cover three temperature ranges, as follows: The first apparatus was designed for the range 0 to 400 C and has been in use continuously for several years. The need for verification of lower temperature values of conductivity prompted the design and construction of the equipment now in use over the range 0 to —190 C, and lower but for the lack of thermocouple information. The third range, 400 to perhaps 900 C, has involved the solution of grave difficulties which appear now to have been surmounted. Trial operations using air and argon have provided satisfying results.

The older conductivity apparatus has been described fully in a paper of 1950 for steam and nitrogen (4). The low-temperature facility makes use of a conductivity cell of much the same annular type used for steam, but the method of maintaining low temperatures is probably novel and permits measurements at any selected temperature between 30 and —190 C as just stated.

Equipment for Low-Temperature Measurements

The requirement of a steady state in the present method employed must be met at low temperatures by refrigeration which will absorb the heat generated in the axis of the emitter and compensate for the heat flowing into the system from the surroundings. The refrigeration must be applied uniformly over the surface of the receiver, and to insure this condition it was decided to use a heavy copper cylinder into which the conductivity-cell case fitted closely. The problem of delivering refrigeration to this massive copper refrigeration jacket was solved as follows:

The outer surface of the cylinder was provided with an eight-start square-thread system. This required that each thread start on a right section 45 deg from the preceding thread and using a $^1/_{32}$-in. wide, $^1/_{32}$-in. deep thread, each completing 2 turns per inch of cylinder length. After completion of the thread system, a 16-gage copper sleeve about 0.003-in. less in inner diameter than the outer diameter of the threaded cylinder was prepared. The sleeve was heated and the cylinder cooled in order to unite the two and secure good thermal contact between sleeve and thread tops. The sleeve was left long enough to provide a chamber below the closed bottom of the cylinder into which liquid could be introduced for rapid preliminary cooling when circumstances required. The top of the thread system was closed with a circular hollow header into which a connection lead was attached for introducing expanded gas from the Joule-Thomson-Siemens interchanger (G, Fig. 1) in a manner now to be described.

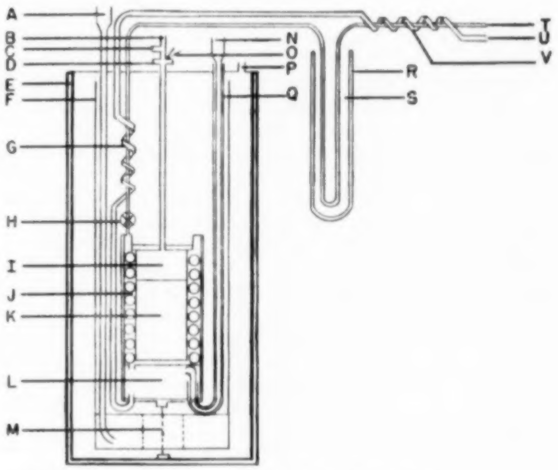

A, liquid N_2 loading tube to shield reservoir
B, cell-charging cock
C, vacuum connection to cell
D, teflon pressure seal from cell
E, vacuum-tight brass container
F, radiation shield
G, Joule-Thomson-Siemens heat interchanger
H, Joule-Thomson expansion valve
I, heat station
J, refrigerating jacket
K, cell
L, liquid reservoir
M, red fiber support
N, filler tube
O, electric leads
P, vacuum connection
Q, outer jacket of loading means to provide for gas escape
R, Dewar tube
S, solid CO_2 and alcohol (N_2 precooling) or liquid N_2 (H_2 precooling)
T, gas-tank connection N_2 or H_2
U, exhaust N_2 or H_2
V, heat exchanger

Fig. 1 Diagram of Means for Maintaining Low Temperatures During Heat-Conductivity Measurements

The source of refrigeration chosen was that derivable from nitrogen or hydrogen expanded from a suitable pressure through a throttle or Joule-Thomson effect valve designed for sensitive regulation with respect to the amount of gas flow per unit of time. The amount of refrigeration per unit weight of gas for a gas below the inversion temperature is a function of the pressure difference before and after the valve, as well as the temperature of the gas before the expansion valve. Accordingly it becomes possible by controlling the fore-pressure and temperature of the gas in conjunction with the setting of the throttle valve to obtain, even with hand regulation, a quite delicate control of temperature of the outer surface of the refrigerating jacket.

In the event that the expanded gas carries a proportion of liq-

[1] Department of Chemistry, Massachusetts Institute of Technology. Mem. ASME.

[2] Numbers in parentheses refer to Bibliography at end of paper.

This research was conducted under the auspices of Project Squid, jointly sponsored by the Office of Naval Research, the Office of Scientific Research (Air Force), and the Office of Ordnance Research (Army) under Contract No. N5ori-105 Task Order III, NR 098-038.

Contributed by the Heat Transfer Division and presented at the Annual Meeting, New York, N. Y., November 29–December 4, 1953, of The American Society of Mechanical Engineers.

 Manuscript received at ASME Headquarters, July 28, 1953. Paper No. 53—A-58.

uid phase, this will be deposited in the chamber at the bottom of the jacket, J. However, this is not desirable for present purposes because the condition of liquid-phase formation marks a limit of temperature of the expanded-gas phase. To attain temperatures below the liquefaction point of nitrogen it is best to turn to hydrogen for the jacket temperature control using solid CO_2 and liquid nitrogen in successive stages for precooling before expansion. In this way it is possible to attain working temperatures approaching the boiling point of hydrogen.

The copper radiation shield chamber F in Fig. 1 should be kept filled with liquid nitrogen when working temperatures descend to −100 C and lower. Aluminum foil in multilayers was used generously to surround the Joule-Thomson-Siemens interchanger G, the jacket J, and the radiation shield F. A vacuum of 10^{-5} mm of mercury is maintained at all times in the apparatus case E, by suitable trap and pumps connected at P.

The refrigeration obtainable using N_2 may be illustrated by considering the case where solid CO_2 is used for precooling. Assuming the fore-pressure to be 100 atm and the temperature −78 C, there will be available 16.8 cal per gram of N_2 expanded to atmospheric pressure. The total weight of the cell, cell case, and refrigerating jacket is 5071 grams, or 1 cal communicated to the system will change its temperature by about 0.002 C. The amount of refrigeration, 16.8 cal, for example, may be diminished to zero by any gradation desired by regulation of the throttle valve to diminish the time rate of flow to zero.

It is of course desired to maintain a constant temperature at the outer surface of the cell receiver with constant energy input to the emitter. A thermocouple is placed in a well in the receiver for measuring its temperature relative to 0 C. It serves also as an indicator of the steady state or the condition where a balance has been attained between energy input to the emitter and absorption of this energy through refrigeration applied to the jacket J. There is also a thermocouple attached to the refrigeration jacket. In practice, however, the preferred guide for controlling the refrigeration applied appears to be the trend in the readings of the receiver thermocouple. The sensitivity of the potentiometer permits the recognition of a change of 0.001 C and by establishing an approximately favorable relation by trial between fore-pressure and Joule-Thomson (J-T) valve setting, subsequent control may be realized by variation of the fore-pressure using a hand-operated sensitive needle valve and pressure gage. The operator reading the potentiometer indications of all thermocouples in a run of observations notes the drift on a 1 or 2-min schedule and reports up or down for the receiver couple, and the operator at the refrigeration control soon locates the limits of pressure which cause an "up" or a "down." In this way it is possible to hold the steady state indicated by the invariability of the temperature drop in the fluid annulus of the cell. By taking observations over a range of energy inputs (multiple observations procedure) it is possible to obtain by graphical means the ratio of energy input to temperature drop for infinitely small energy input.

There are two sets of three couples in series at different depths of well (2.5 cm and 5.7 cm) in the receiver-emitter system. By this arrangement variation in the temperature drop relative to position along the length of the cell can be noted.

The design of the cell was changed after some use by embedding the thermocouples in Apiezon wax, and later in ceresine wax[3] in vacuo, and each thermocouple lead was brought through a modified heat station whose form was as follows: The new heat station is, in principle, a continuation section of the cell proper with a separate heater. Passages are provided in the heat-station receiver for all thermocouple leads having junctions in the cell receiver. Likewise, passages are formed in the heat-station central portion for the cell-emitter thermocouple leads and the four heater leads.

[3] The ceresine wax was heated to 100 C for some 12 hrs in a vacuum of 10^{-6} mm Hg, in the course of which a small amount of volatile material was released.

$\partial E/\partial t$ for Copper-Constantan Thermocouples

A brass cell was used for the thermocouple calibration similar to that employed for conductivity measurements, except that the metal cases of the resistance thermometers were inserted into well-fitting holes, each to the same depth, 7.6 cm, in the emitter and the receiver. Two thermocouples were inserted adjacent to each platinum thermometer boring at different depths, one at 5.7 cm and the second near the top level of the winding at 2.5 cm.

The procedure for measurements consisted in supplying current to the emitter heater to produce a temperature difference of 3 to 5 deg C between receiver and emitter with air at atmospheric pressure within the cell. When a steady state was secured the resistances of the thermometers were read every 1 or 2 min over a period of some 10 to 20 min. The arithmetic average of the temperatures of the resistance thermometer of the emitter and receiver was assigned as the temperature of $\Delta E/\Delta t$ where ΔE is the couple electromotive force corresponding to the temperature difference indicated by the resistance thermometers.

The values of $\Delta E/\Delta t$ deduced from the prior calibration of the resistance thermometers differ from the values employing the postmeasurements calibration, the prior results exceeding the post results as indicated by the mean ratios: 1.0026 at 29 to 33 C, the greatest ratio being 1.0047, the smallest 1.0007. In the range −111.7 to −176.5, the mean ratio is 1.0079 with the greatest ratio 1.015 and the smallest 1.0037. The mean of both post and prior results is represented by the following equation: Fig. 2 gives a graphical impression of the results

$$\partial E/\partial t = 3.78 + 0.1667T \times 10^{-4.5\cdot10^{-4}T} \qquad [1]$$

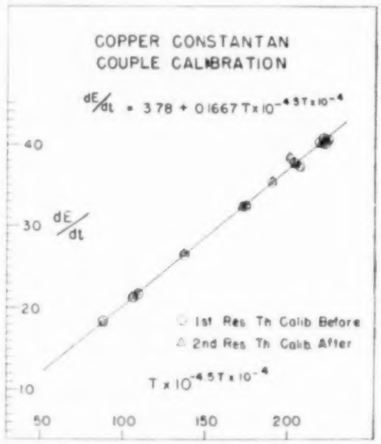

Fig. 2

A satisfactory survey of the relation of the present $\partial E/\partial t$ data and published integral values is obtained by integrating Equation [1]. The integral is as follows

$$E - E_0 = \Delta E = 3.78T - 160.881 \times 10^{-4.5\cdot10^{-4}T}(T + 965.093) - 149071.5 \qquad [2]$$

Fig. 3 gives a graphical impression of differences between temperatures given by Equation [2] and those of the standard tables of Southard and Andrews.

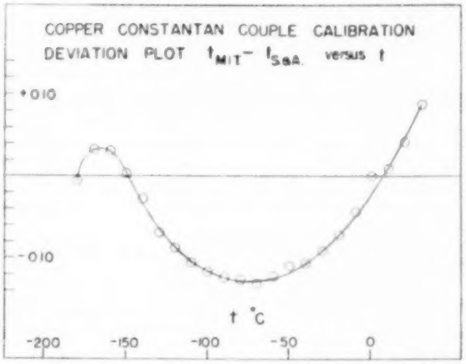

FIG. 3

Because of the drop in magnitude of $\partial E/\partial t$ with falling temperature, three junctions in series were used in the cell assembly for conductivity measurements. The potentiometer permits the estimation of less than 0.1 microvolt resulting in 0.0009 C sensitivity at 0 C, and 0.0022 C at −200 C. Nominally, therefore, temperature differences between emitter and receiver may be as small as 1 C at ordinary temperatures and 2.4 C at −200 C. This relation of sensitivity favors obtaining the conductivity of the liquid phase as well as the gaseous phase, without inconveniently large energy input. In view of the fundamental role of the conductivity of the monatomic or rare gases in the kinetic theory of transport properties, it is hoped to complete measurements for all of the rare gases that can be procured, not alone in the low-temperature range but also at high temperatures. The case of hydrogen is important because of its small moment of inertia which causes a rapid decline of its rotational energy contribution, bringing the molecule into a state of virtual monatomic characteristics at −180 C. Considerable data have been obtained from room temperature upward and lower temperature results will now be forthcoming. In general low-temperature results for as many diatomic and polyatomic molecules are sought for the practical bearing the results have upon the interpretation of the interplay of translational, rotational, and vibrational energy in the transport process.

Equipment for High-Temperature Measurements

The difficulties of measurement increase rapidly above 500 C. The more important items relate to the increasing importance of radiation from the surfaces of the conductivity cell with rising temperature and its control, and the selection of materials of the cell which must be nonvolatile, inert chemically, and of low emissivity. The heat-insulating materials and electrical insulating qualities of materials are items of special importance for thermocouples, for indeed any means of measuring temperatures electrically will depend on the availability of insulating materials of high resistance.

Of course the vital element in thermal-conductivity measurements is the reliability of temperature differences, and after considering all factors it appeared that the platinum-rhodium couple (Pt-10 per cent Rh) offered the best compromise. This couple has been universally and extensively employed, and accordingly, much data is available from many reliable sources particularly in the range 600 to 1063 C (melting point of gold). The vapor pressure of each metal of this couple is extremely low at 1000 C, both are chemically stable, resist oxidation, are reproducible in quality, and readily procurable. There is a disadvantage owing to the ease with which they alloy with all other metals. The 10 per cent by weight Rh alloy is the composition about which most information is available. The proposed limiting temperature of use in heat conductivity is about 1000 C.

Constant-Temperature Air Bath. The furnace has been constructed with a central vertical tube of porcelain ($1^1/_8$ in. OD, $^7/_8$ in. ID) wound with three sections of platinum ribbon; a long middle section with adjacent short windings. The three independent sections allow a distribution of heating current to offset the normal parabolic temperature gradient along the heated zone of the porcelain tube when a single uniform winding is employed. By manual adjustment of the current supplying each of the three windings it becomes possible to realize uniformity of temperature for a finite distance along the heated zone.

One of the difficulties of maintaining constancy of temperature at any point along the heated zone is related to preserving a steady temperature gradient radially through the insulation surrounding the heated tube. As a means of providing a constant temperature over the exterior surface of the insulation, a double-walled cylindrical brass case was prepared in which the porcelain tube was centered in insulation of magnesium oxide and asbestos. By placing water in the interspace of the hollow case and providing a condenser open to the atmosphere, the surrounding temperature of the furnace remains sensibly 100 C. The water is kept boiling when the temperature of the hot zone of the porcelain tube is 500 C.

The cell comprises a platinum-10 per cent rhodium tube 11 mm OD and 10.4 mm ID, 127.0 mm in length. The emitter of platinum is 2.5 mm OD, 2.2 mm ID, and 152 mm long. The alloy is of the same composition as the wire used for thermocouples. Three Pt-Rh couples are welded to the receiver at the mid-point and at each end of a 5 cm mid-section. Two thermocouples are welded to the emitter, opposite those on the receiver. In addition, couples are welded to the emitter 1.25 cm above and below the ends of the 5-cm mid-section for the purpose of detecting a temperature gradient along the emitter between the potential leads.

The heating of the emitter is accomplished by mounting a platinum-rhodium wire in the axis of the emitter using as support close-fitting porcelain cylinders having a 0.4-mm central hole and an eccentric 0.2-mm hole. The potential leads of Pt-10 per cent Rh are gold-soldered at each end of the 5-cm mid-section of wire and pass upward in the porcelain eccentric channel in the case of the top lead, and downward in the eccentric channel in the case of the lower potential lead. The effective cell length is about 5 times the diameter. However, with uniformity of temperature exceeding the effective cell length, no end errors because of axial conduction are present, and the potential leads enable the radial energy flow per unit length to be determined accurately. The foregoing arrangement is in process of modification and will be described in detail at a later time.

New Measurements

Table 1 gives the measured values of the heat conductivities for the substances listed in the Introduction. It will be noted that the conductivity has been measured under pressure, and the pressure coefficients have been treated in accordance with the indications of the theory of the pressure effect assuming a van der Waals type of intermolecular field. A list of the equations for the pressure effect is given in Table 2.

The Classical Ratio $\lambda/C_v\eta$ for the Rare Gases

General Statement. The monatomic gases are of special interest in relation to transport properties because they are the simplest entities available for consideration by the methods of the kinetic theory or statistical mechanics. In the gaseous phase at low pressures, and making use of simplified concepts of intermolecular

TABLE 1 NEW DATA

	p atm	$10^5\lambda$	t° C
Neon	0.67	4.87[a]	—182.1
	0.74	6.41[a]	—144.8
	0.78	7.95[a]	—101.2
	0.81	9.48[a]	— 52.0
	0.82	10.91[a]	0
Argon	0	4.95	90
	12.4	5.11	90
	19.5	5.16	90
	0	6.13	200
	11.1	6.25	200
	17	6.27	200
	0	7.13	300
	12	7.33	300
	17	7.29	300
	1	7.48[a]	350
Hydrogen	0	49.71	85
	15.6	50.58	85
	32.6	51.30	85
	56.2	52.01	85
	98.4	52.64	85
	144.8	53.17	85
	0	57.56	150
	21.0	58.58	150
	37.3	59.65	150
	57.3	59.93	150
	80.1	60.59	150
	1	65.86[a]	250
Nitrous oxide	0	4.56	50
	8.3	4.64	50
	15.8	4.84	50
	28.2	5.16	50
	40.5	5.60	50
	52.7	6.10	50
Methane	0	8.81	50
	18.4	9.04	50
	32.4	9.51	50
	46.3	9.62	50
	60.5	10.09	50
	0	12.68	150
	4.9	12.84	150
	6.6	12.79	150
	11.0	13.01	150
	24.7	13.34	150
	38.6	13.34	150
	0	17.35	250
	5.6	17.57	250
	13.1	18.01	250
	16.3	18.11	250
	0	19.83	300
	7.8	20.08	300
	12.5	19.98	300
	20.0	20.12	300
Ammonia	0	6.46	50
	5.3	6.74	50
	8.5	6.96	50
	0	9.68	150
	4.9	9.85	150
	9.0	10.13	150
	0	13.71	250
	5.4	13.84	250
	9.0	14.06	250
Ethane	0	5.99	51.9
	9.8	6.21	51.9
	17.0	6.42	51.9
	24.7	6.66	51.9
	32.0	7.18	51.9
	39.4	7.66	51.9
	1	13.89[a]	249.2
Ethylene	0	6.37	72.2
	10.4	6.54	72.2
	15.5	6.71	72.2
	0	9.33	152.5
	4.9	9.40	152.5
	8.9	9.52	152.5
Ethyl chloride	1	3.38[a]	54.4
	1	4.18[a]	98.7
	1	5.43[a]	151.7
Freon 12	0	2.68	50
	6.9	2.81	50
	0	3.17	100
	4.1	3.27	100
	6.1	3.32	100
	0	3.83	150
	3.3	3.94	150
Freon 114	1	2.77[a]	50
	1	3.42[a]	100
	1	4.20[a]	150

[a] Provisional

TABLE 2 PRESSURE-COEFFICIENT EQUATIONS

Argon	$\lambda = \lambda_0 (1 + 0.75\ p\tau)$	: (1-20)[a]
Hydrogen	$\lambda = \lambda_0 (1 + 0.44\ p\tau \times 10^{-p\tau})$	: (1-145)
Nitrogen	$\lambda = \lambda_0 (1 + 0.49\ p\tau \times 10^{0.3p\tau})$	: (1-200)
Carbon dioxide	$\lambda = \lambda_0 (1 + 1.14\ p\tau \times 10^{p\tau})$	: (1-60)
Nitrous oxide	$\lambda = \lambda_0 (1 + 1.0\ p\tau \times 10^{3p\tau})$	: (1-53)
Ammonia	$\lambda = \lambda_0 (1 + 1.16\ p\tau \times 10^{15p\tau})$	: (1-9)
Methane	$\lambda = \lambda_0 (1 + 0.72\ p\tau)$	: (1-61)
Ethane	$\lambda = \lambda_0 (1 + 0.98\ p\tau \times 10^{3p\tau})$	: (1-40)
Ethylene	$\lambda = \lambda_0 (1 + 0.76\ p\tau \times 10^{p\tau})$	: (1-16)
Freon 12	$\lambda = \lambda_0 (1 + 2.46\ p\tau)$	: (1-7)

$\tau \equiv T^{-1}$

[a] The numbers in parentheses mark the limits of the experimental pressure range upon which the formulation is based.

action, the theory predicts properties which correspond well with observed properties. The specific heat, internal energy, p-v-T properties, and other equilibrium properties are examples of successful prediction. The nonequilibrium properties of mass diffusion, viscosity, and heat conduction also have been predicted and the correspondence with the facts is satisfactory, but for the case of heat conductivity only for the monatomic gases which have no intramolecular energy in the sense of diatomic or polyatomic molecules. Indeed, the theory of internal-energy transport or thermal conduction for molecular rotation and intramolecular vibrations has not been developed at present.

It has been noted that the ratio of the standard specific heats C_p to C_v or γ as determined by the velocity of sound $[(\text{vel})^2 \times M/RT = \gamma]$ is a function of the frequency of the sound wave propagated by the gas for molecules whose vibrational energy is excited. The quantity C_p is most conveniently measured in the static state and with the measurement of γ by sound, access is had to the value of C_v. The results prove that for C_v for air or oxygen, for example, from the velocity of sound, values at 100 to 1000 C are smaller than C_v-values by calorimetric methods. Carbon dioxide shows a similar effect.

It has been estimated that vibrational energy interchange requires periods of time for equilibrium not less than the order of 0.02 sec. The rotational energy interchange, however, comes into equilibrium much more rapidly.

It is evident from the foregoing brief reference to the facts pertaining to the polyatomic molecules that the monatomic gases present features of relatively extreme simplicity with respect to transport properties. It is therefore important to be assured about the degree of correspondence in properties with the predictions of the kinetic theory, and accordingly, all relevant data on transport properties have been assembled. The viscosity and heat-conduction data have been considered critically over as great a temperature range as measurements permit for each of the rare gases.

A fundamental relationship given by the kinetic theory is the following

$$\lambda = FC_v\eta$$

where λ, C_v, and η denote, respectively, the heat conductivity, the constant-volume specific heat, and the viscosity. The quantity F is a magnitude which theory predicts to be in the neighborhood of 2.5 for the monatomic gases, and for the classical model independent of temperature.[4] F is 2.522 for rigid elastic spheres, for smooth field-free spherically symmetrical molecules, 2.50. The data are briefly discussed for each rare gas in what follows, and a graphical survey is given of the resulting values of F.

The Helium Viscosity Data. There is an abundance of viscosity data for helium gas at low pressures over the temperature

[4] In Chapman and Cowling's treatise on nonuniform gases, page 241, it is stated that if "molecular attractions are taken into account, a slight variation of F with temperature is found."

range 1.64 to 10.88 K. There is, however, a gap in the measurements in the temperature range between about 20 and 80 K, reference to which will be made in some detail.

An earlier report to Project Squid of April 1, 1952 (Technical Report No. 37) (5), gave in Table 2 three viscosity correlation equations for helium gas; one for the ranges 1.64 to 20 K, one for 20 to 140 K, and the third for the range 140 to 373 K. Another review has now been completed for all the data found, the results of which will be described with the aid of Figs. 4 and 5.

Fig. 4 was prepared by using as ordinates the differences, beginning with the highest temperatures, between the observed and calculated viscosities using Equation [3] which appears later. It will be noted that the higher temperature data of Trautz and Zink (6) and Wobser and Müller (7) are self-consistent. The data of Trautz and Zink as reported are relative to their selected values of air recorded in the same paper. These air-viscosity values are, however, smaller than similar values which have been obtained from a correlative consideration of all reported air-viscosity values. The Trautz and Zink values for helium accordingly have been multiplied by the ratios of our correlations for air viscosity to the viscosity for air assigned by Trautz and Zink. The air viscosities were calculated for each temperature of the helium measurements from the equation constants appearing in Squid Report No. 37, Table 2. The Trautz and Zimmerman values (8) are relative to the viscosity of air at 0 C, namely, $17.09 \cdot 10^{-5}$, which is now known to be too low. The Squid Report No. 37 (5) correlation value is $17.22 \cdot 10^{-5}$.

In the data of Wobser and Müller (7), whose reported values were obtained with a "falling-ball" type of viscosimeter and are relative to air assigned at 20 C, the viscosity value $18.15 \cdot 10^{-5}$, the helium-viscosity data, have been increased in the ratio 18.20/18.15, or 1.00275. The range of the values is 20 to 100 C.

The oscillating-disk method for measuring helium viscosities was employed by Johnston and Grilly (9) for the temperature range 80 to 300 K. The values reported are absolute values in the sense that they depend upon the geometry of the disk system and the constants of the suspension. The relation of the various groups of data to one another is made evident in Fig. 4. The Trautz and Zink (6) group at higher temperatures, as already noted, is remarkably consistent with the Wobser and Müller data (7). However, the Johnston and Grilly (9) helium viscosities, while satisfyingly consistent as a group, cannot easily be reconciled correlatively with the data of Onnes, Dorsman, and Weber; Vogel; Ishida; Gille; van Itterbeek and van Paemel; and van Itterbeek, van Paemel, and van Lierde (10, 11, 12, 13, 14, 15), respectively. The datum of States (16) at about room temperature and that of others seem consistent.

Helium is a gas whose atoms exhibit an exceptionally small mutual attractive field. One consequence of this fact is that at high temperatures the properties of a helium assembly using classical mechanics may be represented with tolerable accuracy on the basis of repulsive force only[5] (17*a* and *b*). In the case of viscosity this leads to the expression

$$\eta = C_0 T^s$$

where s is related to the index of the repulsive force ν or

$$s = {}^1/_2 + \frac{2}{(\nu - 1)}$$

The helium viscosities related to the straight line in Fig. 4 are given by the equation

$$\log \eta \times 10^6 = 9.6246 - 10 + 0.67615 \log T, \quad (100 \text{ to } 1000\ \text{K}) \ldots [3]$$

It will be observed from Fig. 4 that there are no data represented from about 100 to 20 K, but data are available from 20 to 1.64 K. The data in this latter range can be represented by the type formula suitable for substances whose attractive field is large, as, for example, nitrogen or carbon dioxide. The reason for this change in behavior is largely related on the classical view to the fact that at low temperatures the atom velocities are sufficiently small to bring about (relative to high temperatures) large distances of approach of atom centers, thereby diminishing the repulsion and bringing into action an increasing proportion of attractive force. Quantum considerations also are increasingly significant as very low temperatures are approached. The equation previously given (Squid Report No. 37, reference 5) as correlating the data in the range 1.64 to 20 K is retained, namely

$$10^5 \eta = \frac{0.848\sqrt{T}}{(1 + 1.5937\tau)}, \quad (1.64 \text{ to } 20\ \text{K}) \ldots\ldots\ldots\ldots [4]$$

[5] Massey and Mohr in two articles discuss the viscosity of helium using (*a*) the assumption of field free atoms, and (*b*) the inclusion of the field given for helium by J. C. Slater. The accord with observation for the first treatment is about 7 per cent while the second leads to the conclusion that the Slater potential is inexact.

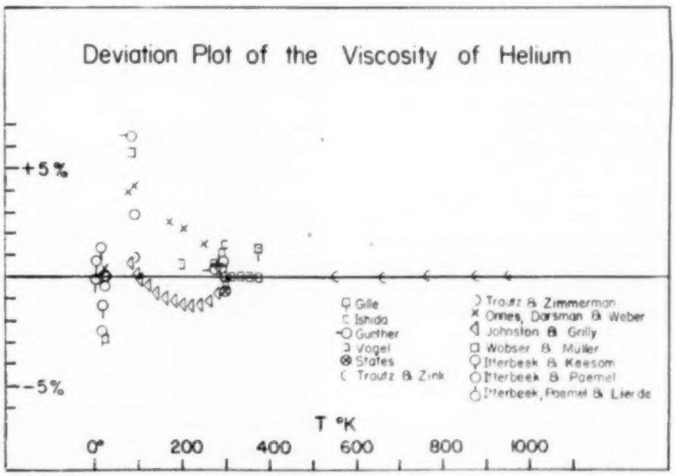

Fig. 4

Equation [3] does not represent the low-temperature data.

The Heat-Conductivity Data. The most recent and comprehensive group of measurements of heat conductivity for gaseous helium is due to Johnston and Grilly (18) who reported eighteen values from 80 to 376 K; Eucken; Weber; Dickins; Kannuluik and Martin; Ubbink and de Haas; and more recently Kannuluik and Carman (1952) (19, 20, 21, 22, 23, 24), respectively, have supplied data for six temperatures from 90 to 579 K. The results of measurements made to date at M.I.T. also are included.

The difficulty experienced in correlating the viscosity data using a single equation over the whole range of temperature is reflected in attempting to correlate the conductivity data. A possible procedure is to form the ratio $\lambda/C_v\eta = F$. Upon assembling the data graphically in relation to the corresponding temperatures a linear relation was disclosed with $\partial F/\partial T$ negative. Fig. 5 gives a survey of the relationship based on the use of the classical value of C_v (2.98 IT cal per mole) for a monatomic gas. The linear relationship can be used to compute smoothed values of λ, the thermal conductivity.

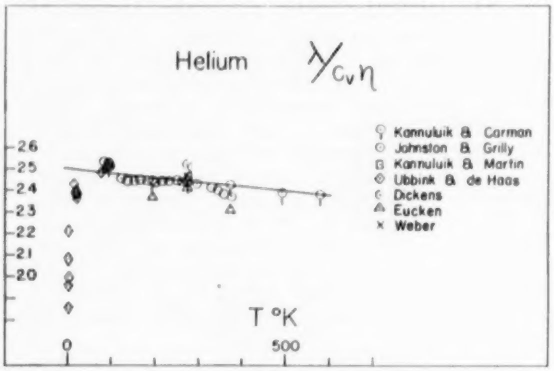

Fig. 5

The drop in value of F for the lowest temperatures may be brought about by the use of the classical value of C_v. This quantity, because of quantum effects and subject to the Fermi-Dirac theory of a monatomic gas, leads to the conclusion that C_v would be linear in T and zero for $T = 0$. Experimental values of $C_v{}^0$ derived from velocity of sound measurements do indicate a decline from the classical value 2.98 cal per mole at 3.86 K, but not nearly enough to explain the low value of F shown in Fig. 5. It appears therefore that the major factor causing the fall in F must be ascribed to quantum effects in one or the other, or perhaps both of the transport quantities λ and η.

The Neon-Viscosity Data. The amount of data for neon is relatively small compared with the case of helium, although the temperature range extends from about 20 to 1100 K. The attempt to represent the viscosity data with a single analytical form has met with as little success as was encountered with helium. Neon, like helium, has a small attractive field and the higher temperature data, 300 to 1100 K, is representable by a log η:log T relationship. The range 160–370 K conforms to the form

$$10^5\eta = \frac{a_0\sqrt{T}}{1 + a\tau \times 10^{a_1\tau}}$$

while below 160 K, extending to 80 K, a Sutherland form appears to be satisfactory. By the use of these formulations, interpolations can be made which are faithful to the reported numerical data. The actual equations follow

$$\left.\begin{aligned} (A)\quad 80\text{–}160\ \text{K} : 10^5\eta &= \frac{1.975\sqrt{T}}{1 + 37.7\tau} \\ (B)\quad 160\text{–}370\ \text{K} : 10^5\eta &= \frac{2.356\sqrt{T}}{1 + 98.9\tau \times 10^{-18\tau}} \\ (C)\quad 370\text{–}1100\ \text{K} : \log 10^5\eta &= -0.0705 + 0.636 \log T \ldots \end{aligned}\right\} \ldots [5]$$

The data reported by Trautz and Zimmerman (8), Trautz and Binkele (25), Trautz and Zink (6) have been adjusted to values of the viscosity of air given in Report No. 37 (5), Table 2. The data of Wobser and Müller (7) also were multiplied by the factor 1.00275 representing the air value of viscosity, 18.20 × 10^6 at 20 C, divided by the value originally employed, namely, 18.15 × 10^6. Fig. 6 gives an impression of the deviations from Equation [5].

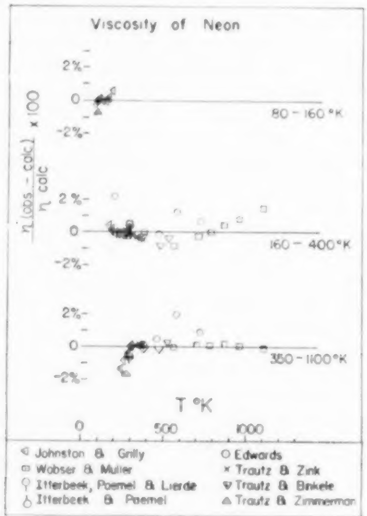

Fig. 6

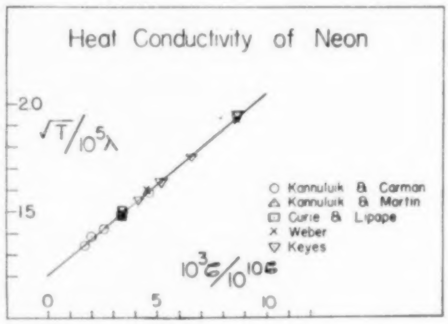

Fig. 7

The Thermal Conductivity of Neon. There is a total of ten observations recorded in the literature of the conductivity for neon over the temperature range 90 to 579 K. Six of the ensemble of data are by Kannuluik and Carman (24) reported in 1952. The consistency of the entire list of data may be inferred from Fig. 7 wherein $\sqrt{T}/\lambda$ has been employed as ordinates and $\tau \times 10^{-10\tau}$ as abscissas, leading to the constants 10^6C_0, 0.83; C, 70.5.

For each observed value of the conductivity λ, the viscosity η has been computed for the corresponding temperature. Em-

ploying the classical value of C_v (2.98 cal per mole) the quantity F has been formed. A survey of the values of F in relation to temperature is given in Fig. 8. A negative slope of F is indicated similar to the case of helium, and the dots represent computed F-values employing Equations [5] and the foregoing equation constants.

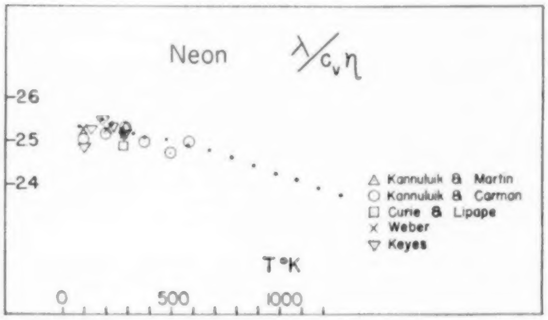

FIG. 8

The Argon Viscosity Data. A considerable volume of data is available over a wide range of temperatures, namely, 55 to 1866 K. The various investigators differ considerably. For example, the most recent data of Johnston and Grilly (9) are taken in the range 80 to 300 K and are consistent and well represented by the following formula

$$\eta \times 10^5 = \frac{2.173\sqrt{T}}{1 + 218.4\tau \times 10^{-14\tau}} \quad \text{[6]}$$

The deviations of the Johnston and Grilly data from the computed viscosities differ on average by 1 part in 550. However, van Itterbeek and van Paemel (26),[6] also using the oscillating-disk method, and for the temperature range 55 to 293.5 K, show deviations from the equation representing Johnston and Grilly's results which average 1 part in 62. Again, Vasilesco (27) whose results are in the range 273 to 1866 K, while agreeing with Johnston and Grilly at 273.1 K (2100.5, J and G; 2105, Vasilesco; 2099.2 eq), are increasingly less than the J and G equation extrapolation values to the extent of 8.5 per cent at 1866 K. In the case of air the correlating equation based on the Johnston and McCloskey data (28) proved to represent satisfactorily the body of data of all observers to 1873 K (1) (Squid Report No. 37, reference 5). However, the Vasilesco data are represented by the following equation

$$\eta \times 10^5 = \frac{1.910\sqrt{T}}{1 + 136.6\tau} \quad \text{[7]}$$

The data of Wobser and Müller (7) (293 to 371 K) are represented by Equation [6] based on Johnston and Grilly's results to an average of 1 part in 560.

The Thermal Conductivity. Data are available from Eucken; Weber; Dickins; Kannuluik and Martin; Kannuluik and Carman (19, 20, 21, 22, 24), respectively, and the recent M.I.T. work from 362 to 613 K; eighteen determinations in total. The mutual relation of the results may be sensed from Fig. 9 wherein $\sqrt{T}/\lambda$ is related to $\tau \times 10^{-10\tau}$. A full complement of low-temperature results will follow from the M.I.T. investigation in progress.

The equation for λ follows

[6] Van Itterbeek and van Paemel report measurements from 55 to 90 K with an isolated point at 293.5 K. They report also unpublished measurements by Kopsch using a transpiration method contained in Halle Dissertation of 1909. The Kopsch data are contained in a paper by K. Schmitt, *Ann. d. Phy.*, vol. 10, 1909, p. 393.

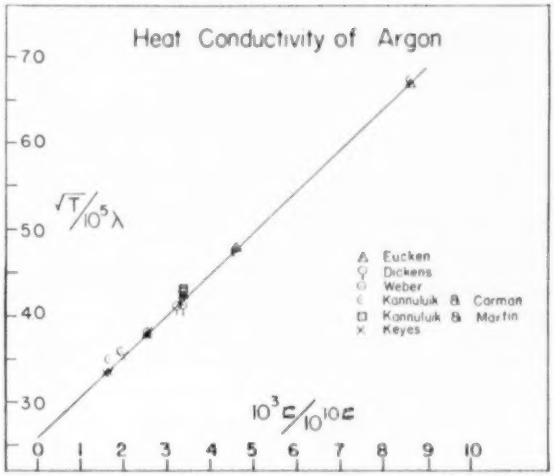

FIG. 9

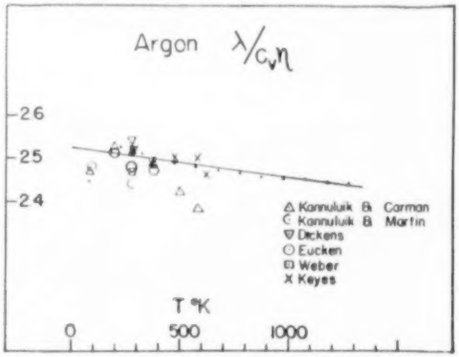

FIG. 10

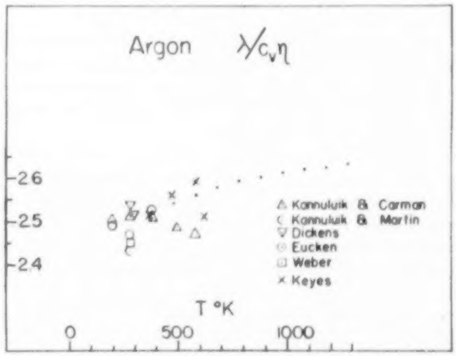

FIG. 11

$$\lambda \times 10^5 = \frac{0.3883\sqrt{T}}{1 + 186.7\tau \times 10^{-10\tau}} \quad \text{[8]}$$

The Value of F. The smoothed viscosity, Equation [7], thermal conductivity, and specific heat data have been united to form the classical relation $\lambda/C_v\eta = F$. A representation is given in Figs. 10 and 11.

In Fig. 10 the experimentally reported thermal conductivities

have been divided by the viscosities computed from Equation [6], multiplied by the specific heat. The dots represent the ratio F computed from Equation [8] for λ and Equation [6] for η. The drawn line assumed to represent the trend is of negative slope and indicates a value of F, 2.52 at 0 K by extrapolation.

Fig. 11 is similar to Fig. 10 except that the smoothing equation based on Vasilesco's data (27) has been used with the observed thermal conductivities while again the dots mark the ratio F compiled from Equation [8] for λ and the viscosity equation based upon Vasilesco. The trend is positive and accordingly differs radically from the cases of helium and neon.

Krypton and Xenon. The viscosity and heat-conductivity data are not numerous for these gases. However, F-values for the existing data have been assembled, and the results are shown in Figs. 12 and 13. The new heat-conductivity measurements are in progress and will be reported at a later time.

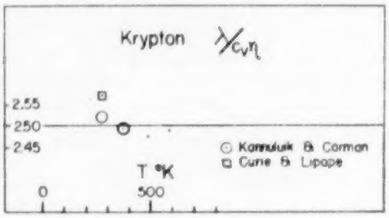

Fig. 12

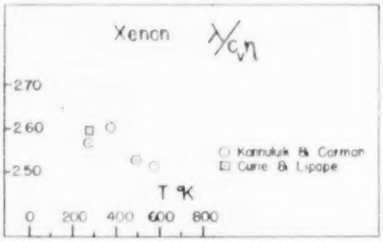

Fig. 13

Acknowledgment

It is a pleasure to acknowledge the financial assistance in this investigation of The American Society of Mechanical Engineers, the Permanent Science Fund of the American Academy of Arts and Sciences, and Project Squid acting for the United States Navy, Air Force, and Army.

The Linde Air Products Division of Union Carbide and Carbon Corporation has been more than generous in supplying facilities without which progress would have been very difficult. In particular, thanks are due for generous supplies of the rare gases.

The author acknowledges with deep thanks the unstinted assistance received in the new measurements and in the calculations incident to the preparation of this paper from the following coworkers: Miss Ruth Crimmins, Miss Elizabeth Vander Pol, B. G. Humphrey, Jr., and W. T. Lindsay, Jr.

BIBLIOGRAPHY

1 "A Summary of Viscosity and Heat Conduction Data for He, A, H_2, O_2, N_2, CO, CO_2, H_2O, and Air," by F. G. Keyes, Trans. ASME, vol. 73, 1951, p. 589–596.

2 "Measurements of the Heat Conductivity of Nitrogen-Carbon Dioxide Mixtures," by F. G. Keyes, Trans. ASME, vol. 73, 1951, pp. 597–603.

3 "Additional Measurements of Heat Conductivity of Nitrogen, Carbon Dioxide, and Mixtures," by F. G. Keyes, Trans. ASME, vol. 74, 1952, p. 1303.

4 "New Measurements of the Heat Conductivity of Steam and Nitrogen," by F. G. Keyes and D. J. Sandell, Jr., Trans. ASME, vol. 72, 1950, p 767.

5 "The Heat Conductivity, Viscosity, Specific Heat and Prandtl Numbers for Thirteen Gases," by F. G. Keyes, Project Squid Technical Report No. 37, April 1, 1952.

6 "Die Reibung, Wärmeleitung und Diffusion von Gasmischungen," by M. Trautz and R. Zink, *Annalen der Physik* [5], vol. 7, 1930, p. 427.

7 "Die Innere Reibung von Gasen und Dämpfen und ihre Messung im Höppler Viskosimeter," by R. Wobser and Fr. Müller, *Kolloid Beihefte*, vol. 52, 1941, p. 165.

8 "Die Reibung, Wärmeleitung und Diffusion von Gasmischungen," by M. Trautz and H. Zimmerman, *Annalen der Physik*, vol. 22, 1935, p. 189.

9 "Viscosities of Carbon Monoxide, Helium, Neon and Argon Between 80 and 300 K. Coefficients of Viscosity," by H. L. Johnston and E. R. Grilly, *Journal of Physical Chemistry*, vol. 46, 1942, p. 948.

10 "The Internal Friction of Gases at Low Temperatures. I. Hydrogen. II. Helium," by H. K. Onnes, C. Dorsman, and S. Weber, *Verslag Koniklijke Nederlandse Akademie Wetenschappen*, vol. 21, 1913, pp. 1375 and 1385.

11 "Über die Viskosität einiger Gase und ihre Temperaturabhängigkeit bei tiefen Temperaturen," by H. Vogel, *Annalen der Physik*, vol. 43, 1914, p. 1235.

12 "Determination of Viscosities and of the Stokes-Millikan Law Constant by the Oil-Drop Method," by Y. Ishida, *Physical Review*, vol. 21, 1923, p. 550.

13 "Die Koeffizienten der inneren Reibung bei Gemischen von Helium und Wasserstoff," by A. Gille, *Annalen der Physik*, vol. 48, 1915, p. 799.

14 "Measurements on the Viscosity of Neon, Hydrogen, Deuterium and Helium as a Function of the Temperature, Between Room Temperature and Liquid Hydrogen Temperature," by A. van Itterbeek and O. van Paemel, *Physica*, vol. 7, 1940, p. 265.

15 "Measurements on the Viscosity of Gas Mixtures," by A. van Itterbeek, O. van Paemel, and J. van Lierde, *Physica*, vol. 13, 1947, p. 88.

16 "The Coefficient of the Viscosity of Helium and the Coefficients of Slip of Helium and Oxygen by the Constant Deflection Method," by M. N. States, *Physical Review*, vol. 21, 1923, p. 662.

17 "Free Paths and Transport Phenomena in Gases and the Quantum Theory of Collisions. I. The Rigid Sphere Model," by H. S. W. Massey and C. B. O. Mohr, Proceedings of the Royal Society, London, England, vol. 141, 1933, p. 434.

"Free Paths and Transport Phenomena in Gases and the Quantum Theory of Collisions. II. The Determination of the Laws of Force Between Atoms and Molecules," by H. S. W. Massey and C. B. O. Mohr, Proceedings of the Royal Society, London, England, vol. 144, 1934, p. 188.

18 "The Thermal Conductivities of Eight Common Gases Between 80 and 380 K," by H. L. Johnston and E. R. Grilly, *Journal of Chemical Physics*, vol. 14, 1946, p. 233.

19 "Über die Temperaturabhängigkeit der Wärmeleitfähigkeit einiger Gase," by A. Eucken, *Physikalische Zeitschrift*, vol. 12, 1911, p. 1101.

20 "The Heat Conductivity of Gas Mixtures," by S. Weber, *Annalen der Physik*, vol. 54, 1917, p. 437.

21 "The Effect of Accommodation on Heat Conduction Through Gases," by B. G. Dickins, Proceedings of the Royal Society, London, England, series A, vol. 143, 1934, p. 517.

22 "The Thermal Conductivity of Some Gases at 0 C," by W. G. Kannuluik and L. H. Martin, Proceedings of the Royal Society, London, England, series A, vol. 144, 1934, p. 496.

23 "Thermal Conductivity of Gaseous Helium," by J. B. Ubbink and W. J. de Haas, *Physica*, vol. 10, 1943, p. 465.

24 "The Thermal Conductivity of Rare Gases," by W. G. Kannuluik and E. H. Carman, Proceedings of the Physical Society, vol. B65, 1952, p. 701.

25 "Die Reibung, Wärmeleitung und Diffusion in Gasmischungen," by M. Trautz and H. E. Binkele, *Annalen der Physik* [5], vol. 5, 1930, p. 561.

26 "Measurements on the Viscosity of Argon Gas at Room Temperature and Between 90 and 55 K," by A. van Itterbeek and O. van Paemel, *Physica*, vol. 5, 1938, p. 1009.

27 "Recherches Expérimentales sur la Viscosité des Gaz aux Températures Elevées," by V. Vasilesco, *Annales de physique*, vol. 20, 1945, p. 292.

28 "Viscosities of Several Common Gases Between 90 K and Room Temperature," by H. L. Johnston and K. E. McCloskey, *Journal of Physical Chemistry*, vol. 44, 1940, p. 1038.

Thermal Conductivity of Some Industrial Liquids From 0 to 100 C

By H. L. Mason,[1] Washington, D. C.

Because of discrepancies among published values for thermal conductivity of liquids, the Iowa Engineering Experiment Station undertook a series of thermal-conductivity measurements on a number of nonmetallic, noncorrosive, lower viscosity liquids, with the results reported in this paper.

Introduction

Among published values for the thermal conductivity of liquids, considerable discrepancies and omissions may be noted. For some technically important liquids, the results at room temperature as given by different experimenters disagree by anywhere from 3 to 20 per cent. For many liquids the data are not available over a range of temperatures, and for others no tests whatever have been reported. The Iowa Engineering Experiment Station therefore undertook to build apparatus and make thermal-conductivity measurements on a number of nonmetallic, noncorrosive, not too viscous liquids in the temperature range from 0 to 100 C.

Liquids were chosen for test for one of the following reasons: (*a*) seriously discordant values reported by different observers; (*b*) no data for liquids commercially available; (*c*) lack of sufficient data on which to base a temperature coefficient. However, it is obvious that these categories have by no means been exhausted, and this must be considered only a progress report.

Apparatus

An earlier paper (10)[2] gave a detailed description of the apparatus, compared it with that used by other experimenters in the last three decades, and noted the summaries of earlier work which were prepared by Jakob (7) 1920, Smith (13) 1930, Eucken (5) 1940, and Riedel (12) 1940, 1949. The present author's test cell, Fig. 1, consisted of two concentric vertical copper cylinders 2 and 3, the inner one being heated electrically by a measured wattage, the outer serving as a constant-temperature heat sink. The test liquid filled the cylindrical annular space 1 between them, 0.017 in. wide × 5 in. long × 0.391 in. mean diam. Closure, centering, and support were provided by Teflon disks 0.005 in. thick. Four pairs of thermojunctions in wells 20 and 21 averaged the temperature difference (of the order of 0.500 deg C) across the liquid layer. Thermal conductivity was computed from the relation

$$q = \frac{2\pi Lk(\Delta T)}{\ln r_o/r_i}$$

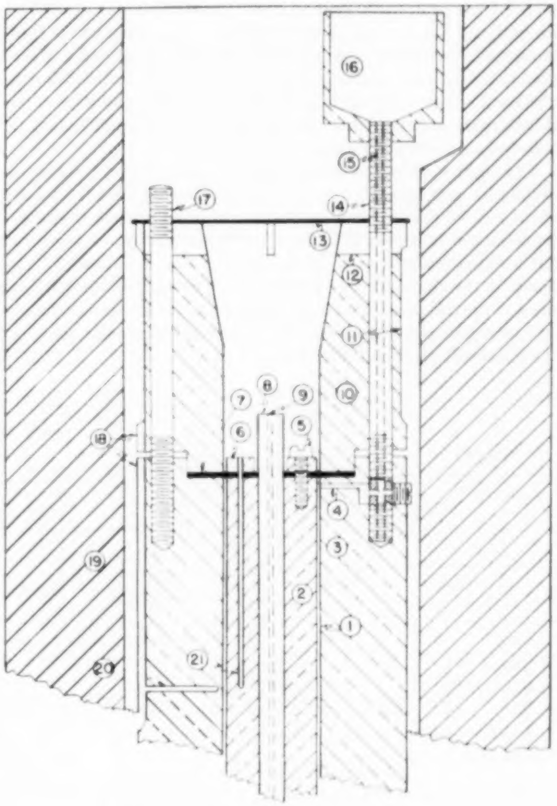

Fig. 1 Upper End of Test Cell

where

q = heat flux to inner cylinder, cal/sec
k = conductivity, cal/(sec)(cm²)(deg C per cm)
L = axial length, cm
r_o, r_i = outer and inner radii of annulus, cm
ΔT = temperature difference between r_o and r_i, deg C

The values of L, r_o, and r_i depend on the geometry. Inner cylinder 2 has a diameter of 0.3743 in. measured at 21 points with an estimated accuracy of five digits in the fifth place and a range from 0.3740 to 0.3749 in. Its length is 4.995 in., measured at four points with an estimated accuracy of 0.0003 in. and a range from 4.990 to 5.000 in. Outer cylinder 3 has a bore of 0.4084 in. diam measured at 24 points with an estimated accuracy of 0.0001 in. and a range from 0.4077 to 0.4107 in. The length in contact with liquid is 5.0003 in., measured at four points with an estimated accuracy of 0.0005 in. and a range from 5.0002 to 5.0005 in. The concentricity of 2 in 3 depends on the accuracy of the machining operations on OD and shoulders of 2, bore and countersinks of 3, and concentricity and accuracy of Teflon-disk diame-

[1] Now with the Office of Basic Instrumentation, National Bureau of Standards. Mem. ASME. The work described was done while the author was Professor of Mechanical Engineering at Iowa State College, Ames, Iowa.

[2] Numbers in parentheses refer to the Bibliography at the end of the paper.

Contributed by the Heat Transfer Division and presented at the Annual Meeting, New York, N. Y., November 29–December 4, 1953, of The American Society of Mechanical Engineers.

Note: Statements and opinions advanced in papers are to be understood as individual expressions of their authors and not those of the Society. Manuscript received at ASME Headquarters, July 8, 1953. Paper No. 53—A-40.

ters. At the ends of the 5-in. length, where the eccentricity can be estimated under a binocular microscope, it was judged less than 0.001 in. Even at twice this figure, the conductivity of the liquid under test would be only about 0.7 per cent too small, according to a computation by Enos E. Jones.[3]

The value ΔT depends primarily on the temperature-emf relation of the copper-constantan thermocouples. This was measured for two standard multistrand couples made up from the same spools of wire as the working couples. These two agreed with 0.1 per cent, calibrated at 30.65 and 60.35 deg C against an ice bath, for the average of five readings, using a resistance thermometer, a Mueller bridge readable to 0.0001 ohm, and a White double potentiometer readable to 0.01 microvolt. Another calibration point was a steam bath at 99.15 C. Differentiation of the third-degree polynomial evaluated by least squares gave a slope believed accurate to four significant figures per deg C.

The eight working junctions, tested in place in the cell but individually connected to a potentiometer, showed a maximum deviation of 0.3 per cent among themselves when reading a nominal temperature difference of 90 deg C. This deviation was averaged out automatically by the connections in Fig. 2. Also, ΔT depends on the elimination of spurious emf's in the working arrangement. Special precautions were taken to provide wiping contacts and to equalize the temperatures of possibly dissimilar joints in the microvolt circuits of Fig. 2.

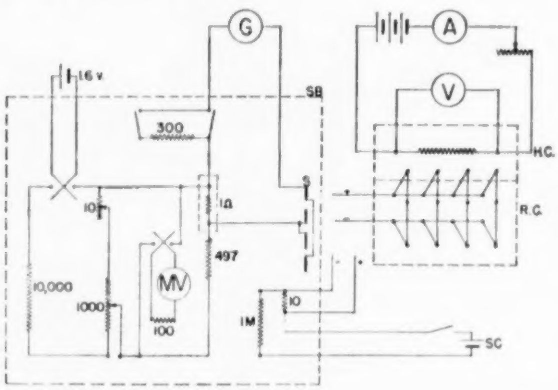

Fig. 2 Circuits for Heating and Temperature Difference

Further, one must consider accuracy of the multiplier resistors, reading errors for calibrated millivoltmeter MV, and observation of null on galvanometer G. Each ΔT-value used was the average of six readings, with emf applied to switchbox SB first in one direction and then in the other. Readings of MV could be estimated to 0.0005 deg C, and of G to 0.001 deg C. Everything considered, the temperature differences used in computing k were probably accurate to better than 0.005 deg C. They were corrected to allow for the drop across the copper wall between a hot junction and the inner boundary of the liquid layer, amounting to 0.004 deg C for water and about 0.001 deg C for most of the liquids reported.

The value q depends primarily on the readings of calibrated ammeter A and voltmeter V in Fig. 2, which were made to three significant figures. Corrections to the input q were needed to give q conducted through the test liquid. A major advantage of the cell design is that thermal leakages are believed reduced to 0.5 per cent or less, so that computed corrections can be applied with confidence. One reason is the long thin test layer, another the 0.0045-in. diam wires used for thermocouple and heater leads, another the Teflon closure disks 7. As stated previously (10) the heat conducted through one disk was computed to be 1.2 milliwatts, and that through four lead wires was 0.6 milliwatt, while radiation and convective transfer were negligible.

Results

Table 1 lists in chronological order for each liquid the values of conductivity and its temperature coefficient as reported by experimenters using absolute methods. It omits all secondary sources, such as the relative determinations of Stankevic, Goldschmidt, Kardos, and Davis, and the undocumented recommendations of Barratt and Nettleton, Marks, and Lange. The two sets of values reported as the present author's work are taken from a least-squares straight line, there being no evident tendency to curvature indicated by the individual determinations listed under Remarks.

Each line involves three or more independent fillings of the cell, some being several months apart. The standard error of estimate reported is relative to this line. Before the cell was filled with fresh liquid, the old sample was blown out with dried air, and the cell was first flushed with the new liquid and then evacuated for several minutes. Contamination of samples by water was scrupulously avoided; for low-temperature determinations in humid weather, a continuous stream of dried air was fed into the cap (not shown) of lag cylinder 19. Test temperatures were read from a mercury thermometer in the thermostatted bath; a thermocouple check at 90 deg C showed the cell to be about 1 deg cooler than this bath. Temperature variation at 90 deg C as a result of on-off action of the thermostat amounted to about 0.06 deg in the bath, about 0.01 deg in the air surrounding the test cell, and was negligible in the cell itself.

Sufficient details of the author's work have been given to enable the interested reader to judge its precision for himself. Its accuracy or inaccuracy will be determined finally by a consensus of values, both past and future, reported by other workers.

[3] Research Associate, Engineering Experiment Station, Iowa State College, Ames, Iowa.

TABLE 1 VALUES OF CONDUCTIVITY AND TEMPERATURE COEFFICIENTS

Reference[a]	Conductivity,[b] 10^6k	at °C	Temp coeff.,[b] $10^6\,\Delta k/°C$	Remarks
Acetone				
Bridgman, 1923; under pressure	429	30	−0.58	30, 75 C observed
Riedel, 1940	384	20		
Hutchinson, 1945	407	18		
van der Held, 1948	453	16.1		
Riedel, 1949	387	20	−0.93	1.5, 20, 50 C
Riedel, 1951	383	20	−1.0	−50, −20, 20, 40 C
Author, ±5.4[e]	385.2	20	−1.201	404, 414, 409 at 0 C; 380, 381 at 19.6 C; 385, 385 at 20 C; 369, 363, 354, 356 at 40 C; Allied Chem. and Dye reagent grade
iso-Amyl acetate				
Riedel, 1940	312	20		Pure
Author, ±2.8	310.1	20	−0.523	321, 326, 315 at 0 C; 310, 310, 309 at 19.7 C; 294, 295, 296 at 50.3 C; 273, 273 at 90 C; Eastman #P298
n-Amyl acetate				
Weber, 1885	302	9–15		$C_7H_{14}O_2$ (n-?)
Author, ±5.3	329.0	20	−0.535	348, 345, 343 at 0 C; 320, 323, 325, 325 at 20 C; 311, 311 at 60 C; 288, 287 at 90 C; 288, 289, 290 at 100 C; Eastman #2360
n-Butyl acetate				
Author, ±7.4	327.1	20	−0.488	335, 329, 332 at 0 C; 328, 328, 326 at 30 C; 306, 304 at 60 C; 275, 284, 283 at 100 C; Eastman #710
Carbon tetrachloride				
Weber, 1885	252	9–15		
Rice, 1924	287	0		
Bates, 1941	380[d]	20	−1.2	20 to 50 C
Hutchinson, 1945	380	18		
van der Held, 1948	256	14		
Riedel, 1949	250	20	−0.53	1.5, 20, 50 C
Riedel, 1951	248	20	−0.58	−20, 20, 50 C
Author, ±2.3	245.7	20	−0.334	248, 244 at 20 C; 238, 237 at 40 C; 229, 233 at 65 C; Merck CP grade
p-Chlorotoluene				
Author, ±1.9	310.1	40	−0.510	291, 288 at 40 C; 276, 274 at 71 C; 260, 257 at 100 C; Eastman #74
Chloroform				
Weber, 1885	289	9–15		
Riedel, 1940	278	20		
Bates, 1941	310[d]	20	−1.2	20 to 50 C
Hutchinson, 1945	318	18		
van der Held, 1948	289	15.9		
Author, ±2.2	278	30	−0.60	274, 279, 279 at 31.7 C; 260, 259, 261 at 50 C; USP grade, General Chem. Corp.
Cresol				
Riedel, 1951	358	20	−0.18	Meta; 20, 80 C
Author, std. dev. ±2.8	345	20.1		Para; Merck S4394, USP
Cumene (isopropyl benzene)				
Author, ±5.4	298.2	20	−0.470	308, 306 at 0 C; 292, 291 at 35 C; 276, 277 at 70 C; 261, 258 at 100 C; redistilled, Na-filtered
iso-Dipropyl ether (isopropyl ether)				
Author, ±1.3	262.4	20	−0.521	261, 264 at 20 C; 252, 251 at 40 C; 245, 244 at 55 C; Eastman practical grade
Ethylene dichloride (1, 2 dichloroethane)				
Riedel, 1940	322	20		Technical grade
Riedel, 1940	272	20		Pure grade
Bates, 1941	340[d]	20	−0.9	20 to 50 C
Author, ±0.7	302	20	−0.60	302, 303 at 20 C; 291, 290 at 40 C; Eastman chemical grade
Ethyl acetate				
Weber, 1885	348	9–15		
Author, ±4.7	349.6	20	−0.866	369, 374 at 0 C; 339, 344 at 19.8 C; 331, 332 at 40 C; 325, 324 at 50 C; 316, 316 at 60 C; anhydrous
Ethyl alcohol				
Weber, 1885	424	9–15		
Lees, 1898	430	25	−2.3	25, 51 C
Bridgman, 1923	430	30	−0.31	
Smith, 1930	435	30	−0.38	99.8%
Daniloff, 1932	433	30		99.8%
Bates, 1938	430	20	−2.32	10 to 60 C
Hutchinson, 1945	436	18		
Riedel, 1951	400	20	−0.7	99.8%; −30 to 60 C
Author, ±5.1	392	20	−1.308	396, 393, 388, 390 at 19.8 C; 388, 389 at 29.8 C; 367, 363 at 40 C; 337, 336 at 60 C; absolute grade
Ethyl ether (diethyl ether)				
Weber 1885	303	9–15		$C_4H_{10}O$
Bridgman 1923	329	30	−0.155	"Ether"
Riedel 1951	311	20	−1.0	−80, 20 C
Author, ±3.6	307.4	20	−1.180	332, 330 at 0 C; 307, 305, 300 at 20 C; 297, 296 at 30 C; anhydrous
Glycerol				
Weber, 1885	670	9–15		
Lees, 1898	682	25	−2.76	25, 48 C
Weber, 1903	656	29–34		
Rice, 1924	789	0	−3.0	
Kaye, 1928	680	20	+0.36	97.7%, 0 to 140 C
Bates, 1936	680[d]	20	Zero	10 to 80 C
Eucken, 1938	690	0		
Hutchinson, 1945	672	18		
Author, ±4.9	703.0	20	+0.502	705, 711 at 26 C; 704, 708 at 27 C; 711, 723 at 39 C; 724, 715, 713 at 40 C; 729, 723, 719 at 60 C; 734, 737, 729 at 80 C; 745, 744, 736, 749, 746, 745 at 100 C; USP dehydrated
Linseed oil				
Author, ±2.7	393.1	30	−0.500	396, 392, 390 at 30 C; 386, 385, 383, 382 at 50 C; 375, 370 at 70 C; bodied Alinco #25M, from V. W. Uhl, Lehigh University

(TABLE 1 *continued on following page*)

TABLE 1 (*continued*)

Reference[a]	Conductivity,[b] 10^4k	at °C	Temp coeff,[b] $10^6\ \Delta k/°C$	Remarks
Methyl alcohol				
Weber, 1885	495	9–15		
Lees, 1898	480	25	−1.36	25, 47 C
Bridgman, 1923	503	30	−0.22	
Bates, 1938	510	20	−1.02	10 to 50 C
van der Held, 1948	475	15.1		
Riedel, 1951	483	20	−0.74	99.7%; −30 to 50 C
Author, ±2.7	482	30	−0.3	479, 484 at 29 C; 480, 482 at 50 C; absolute grade
iso-Propyl acetate				
Weber, 1885	326	9–15		$C_5H_{10}O_2$(n-?)
Author, ±4.6	320.8	20	−0.714	334, 347 at 0 C; 306, 310, 313, 314 at 30 C; 302, 301, 292, 292 at 50 C; 299, 298, 294, 291, 290, 289 at 60 C; 284, 282 at 70 C; 280, 287 at 80 C; Eastman practical grade
s-Tetrachlorethane				
Bates, 1941	320[d]	20	−0.9	20 to 50 C
Author, ±1.5	272.1	20	−0.440	279, 281 at 0 C; 266, 263 at 40 C; 250, 249 at 70 C; 237, 236 at 100 C; Eastman #241
Tetrachlorethylene (perchlorethylene)				
Riedel, 1940	261	20		
Bates, 1941	390[d]	20	−1.3	20 to 50 C
Author, ±3.9	268.1	20	−0.628	288, 279, 280 at 0 C; 254, 255 at 35 C; 237, 235 at 70 C; 222, 219 at 100 C; Dupont technical grade
Trichlorethylene				
Riedel, 1940	272	20		
Bates, 1941	330[d]	20	−0.9	20 to 50 C
Riedel, 1951	278	20	−0.59	−60, 20 C
Author, ±3.7	285.4	20	−0.951	309, 302, 302 at 0 C; 266 at 35 C; 266 at 40 C; 240, 240 at 70 C; technical grade, redistilled

[a] See bibliography appended.
[b] k and Δk in g-cal/(sec-cm-° C).
[c] Standard error of estimate, 10^6 g-cal/(sec-cm-° C)

$$= \sqrt{\Sigma_1^n\,(10^6k_{obs} - 10^6k_{calc})^2/(n-2)} \text{ for } n \text{ observations.}$$

[d] Last two digits rounded off; original source gives only five decimal places.

BIBLIOGRAPHY

1 "Thermal Conductivity of Liquids; Binary Mixtures of Water and Glycerol," by O. K. Bates, et al., *Industrial and Engineering Chemistry*, vol. 28, 1936, pp. 494–498.

"Thermal Conductivity of Liquids; Binary Mixtures of Water-Methyl Alcohol and Water-Ethyl Alcohol," by O. K. Bates, et al.; *Industrial and Engineering Chemistry*, Analytical Edition, vol. 10, 1938, pp. 314–318.

"Thermal Conductivity of Liquids; Twelve Industrial Chlorinated Hydrocarbons," by O. K. Bates, et al., *Industrial and Engineering Chemistry*, vol. 33, 1941, pp. 375–376.

2 "The Thermal Conductivity of Liquids Under Pressure," by P. W. Bridgman, Proceedings of the American Academy of Arts and Sciences, vol. 59, 1923, pp. 141–169.

3 "Thermal Conductivity of the Normal Primary Saturated Alcohols," by M. Daniloff, *Journal of the American Chemical Society*, vol. 54, 1932, pp. 1328–1332.

4 "Die Experimentelle Bestimmung des Wärmeleitvermögens einiger verfestigter Gase und Flüssigkeiten," by A. Eucken and H. Englert, *Zeits. für die gesamte Kälte-Industrie*, vol. 45, 1938, pp. 109–118.

5 "Allgemeine Gesetzmässigkeiten für das Wärmeleitvermögen verschiedener Stoffarten und Aggregatzustände," by A. Eucken, *Forschung auf dem Gebiete des Ingenieurwesens*, vol. 11, 1940, pp. 6–20.

6 "On the Measurement of the Thermal Conductivity of Liquids," by E. Hutchinson, Transactions of the Faraday Society, vol. 41, 1945, pp. 87–90.

7 "Bestimmung der Wärmeleitfähigkeit des Wassers in Bereich von 0 bis 80°," by M. Jakob, *Annalen der Physik*, vol. 63, 1920, pp. 537–570.

8 "The Thermal Conductivities of Certain Liquids," by G. W. C. Kaye and W. F. Higgins, Proceedings of the Royal Society of London, England, series A, vol. 117, 1928, pp. 459–470.

9 "On the Thermal Conductivities of Single and Mixed Solids and Liquids and Their Variation With Temperature," by C. H. Lees, Philosophical Transactions of the Royal Society of London, England, series A, vol. 191, 1898, pp. 399–440.

10 "Apparatus for Measuring Thermal Conductivity of Liquids," by H. L. Mason, *Instruments*, vol. 26, 1953 pp. 266–268.

11 "Free and Forced Convection of Heat in Gases and Liquids. II," (abstract of a G.E. Research Laboratory report), by C. W. Rice, *Physical Review*, series 2, vol. 23, 1924, pp. 306–307.

12 "Messung der Wärmeleitfähigkeit von organischen Flüssigkeiten, insbesondere von Kältemitteln," by L. Riedel, *Forschung auf dem Gebiete des Ingenieurwesens*, vol. 11, 1940, pp. 340–347.

"Wärmeleitfähigkeitsmessungen an Zuckerlösungen, Fruchtsäften und Milch," by L. Riedel, *Chemie-Ingenieur-Technik* vol. 21, 1949, pp. 340–341 and 355.

"Neue Wärmeleitfähigkeitsmessungen an organischen Flüssigkeiten," by L. Riedel, *Chemie-Ingenieur-Technik*, vol. 23, 1951, pp. 321–324.

"Wärmeleitfähigkeitsmessungen an Mischungen verschiedener organischer Verbindungen mit Wasser," by L. Riedel, *Chemie-Ingenieur-Technik*, vol. 23, 1951, pp. 465–469.

13 "Thermal Conductivity of Liquids," by J. F. D. Smith, *Industrial and Engineering Chemistry*, vol. 22, 1930, pp. 1246–1251.

"The Thermal Conductivity of Liquids," by J. F. D. Smith, Trans. ASME, vol. 58, 1936, pp. 719–725.

14 "The Measurement of the Thermal Conductivity of Liquids, Based on a Warming-Up Process," by E. F. M. van der Held and F. G. van Drunen, Proceedings of the 7th International Congress for Applied Mechanics, vol. 3, 1948, pp. 79–90.

"A Method of Measuring the Thermal Conductivity of Liquids," by E. F. M. van der Held and F. G. van Drunen, *Physica*, vol. 15, 1949, pp. 865–881.

15 "Das Wärmeleitungsvermögen der tropfbaren Flüssigkeiten," by H. F. Weber, *Berliner Berichte*, vol. 2, 1885, pp. 809–815.

"Das Wärmeleitungsvermögen der tropfbaren Flüssigkeiten," by H. F. Weber, *Repertorium der Physik*, vol. 22, 1886, pp. 116–122.

16 "Wärmeleitung in Flüssigkeiten," by R. Weber, *Annalen der Physik*, vol. 11, 1903, pp. 1047–1070.

Discussion

J. F. Downie Smith.[4] The determination of the thermal conductivity of liquids is not easy. It requires careful experimentation and considerable skill in the measurement of temperature. Many different schemes have been used for the proper evaluation of thermal conductivity and it was only after a careful investigation of the entire field that the author decided to concentrate on what really amounts to a modification of the original proposal by Dr. P. W. Bridgman. Some short time after Professor Bridgman built and used his equipment, I borrowed it myself and determined the thermal conductivities of several liquids; so that I know, firsthand, the difficulties that are involved.

When discussing the matter with the author while he was beginning this project at Iowa State College, he analyzed the

[4] Dean, Engineering School, Iowa State College, Ames, Iowa. Fellow ASME.

equipment used by Dr. Bridgman and the writer and he thought that he could perhaps improve the accuracy by changing the design of the cylindrical copper cell, and particularly, by modifying the end conditions. The amount of heat conduction through the German-silver disks at each end of the cylinders built by Bridgman could be reduced by the substitution of a plastic disk. This was done by the author and calculations would seem to indicate that the accuracy of the equipment has been improved. While these determinations were under way I was quite impressed by the steadiness of the readings and I believe that I can recommend these values by the author as among the most accurate in the literature.

The equipment is still available at Iowa State College and we have a competent investigator who is familiar with the equipment and who could be persuaded to determine some additional conductivities. However, because of circumstances beyond our control, such experimentation must be on a self-supporting basis. But this can frequently be justified by industry. We are also willing to co-operate with our colleagues in the various colleges and universities in completing their projects.

The Thermal Conductivity of Fluids[1]

By A. F. SCHMIDT[3] and B. H. SPURLOCK, JR.,[2] BOULDER, COLO.

In this paper an apparatus is developed which is capable of measuring the thermal conductivity of gases, vapors, and liquids over a wide range of temperatures. A compensating-type hot-wire apparatus was employed to make absolute thermal-conductivity determinations of various fluids; in particular, air was used to check the agreement of experimental results between previous investigations and the present one. In addition, the thermal conductivities of furfural vapor and liquid were measured in order to supplement existing data in the field of heat conduction with results of considerable industrial importance.

Introduction

During the past 25 years, a considerable degree of advancement has taken place in the field of heat conductivity, but the critical demand for fresh data has always exceeded the supply. Hawkins concluded his review and bibliography of the thermal conductivity and viscosity of gases by stating:

"Before World War II, the engineers to a large extent relied on the basic research work of the European institutions to provide data on the thermal conductivity and viscosity of gases and vapors. The data from these organizations will in all probability not be forthcoming in the immediate future at the same rate as in the past; hence every effort should be made to encourage engineers and scientists in this country to pursue research work dealing with these properties" (1).[4]

Previous investigations of the thermal conductivities of gases and vapors have been confined mainly to modifications of two principal methods: (*a*) The parallel-plate method; (*b*) the hot-wire method. Both have certain significant advantages and limitations and they will be considered briefly in the order of their development.

(*a*) The parallel-plate method was first used by Todd (2) and later by Hercus and Laby (3). In this method a known quantity of thermal energy was conducted from the upper plate of the apparatus, through a horizontal lamina of the gas under investigation, to the lower plate. A series of thermocouples were used to measure the surface temperatures of both plates, and from these data and the dimensions of the apparatus the thermal conductivity could be calculated. Since the upper plate was the hotter of the two, convective losses virtually were eliminated by this design. Also, any temperature discontinuity at the surface of the plates was of slight magnitude, because the temperature gradient could be made quite small. However, maintaining the temperature at a constant value over the surface of the plates was a serious problem, as was the loss of heat by conduction through the plate supports. These investigations also were limited in value because the work could be done only at one pressure and one temperature gradient. Hercus and Sutherland (4) used this method with slight mechanical changes in more recent years.

(*b*) The hot-wire method was first used by Schleiermacher (5) to give an absolute value for the thermal conductivity. In this method a concentric cylinder arrangement was maintained, the inner cylinder (hot wire) serving as both a heat source and a resistance thermometer. The gas or vapor to be investigated was admitted to the annular space between the wire and the external cylinder wall, and the wire and the wall were heated to any desirable temperatures by supplying an electric current to the wire and immersing the cylinder in a thermostat; this provided the necessary temperature gradient across the test fluid for conductivity calculations. Using a long thin wire in his experiments, Schleiermacher measured the resistance of the central (constant-temperature) portion of the wire by means of two fine potential leads which were passed through the tube wall, thus accounting for the loss of heat by conduction through the end segments of the wire to the thermostat.

Weber (6) modified this method by applying an arrangement used by Goldschmidt (7) in his work on the thermal conductivity of liquids. In this case the heat-conduction loss along the lead wires was accounted for experimentally by the inclusion of a similar but shorter tube in the experimental system. The differential measurements then referred to a central portion of the longer tube where radial-flow conditions existed.

Later work by Gregory, et al. (8 to 13), greatly increased the popularity of such a method, and a considerable flow of heat-conductivity data was established from the English laboratories at that time (14 to 19). Further hot-wire refinements occurred in Russia (20 to 22) during the period 1935–1940, extending the temperature and pressure ranges established in previous investigations. This work invalidated extrapolations of older data obtained from limited-range research, and the need for actual experimental values was indicated. In more recent years, well-known American experimenters, engineers, and scientists such as Taylor and Johnston (23), Boelter and Sharp (24), and Keyes (25 to 28) have made significant advances in the art of thermal-conductivity measurement.

Determination of the thermal conductivity of liquids may be approached in much the same manner as that of gases and vapors. Perhaps the most noteworthy contributions to the liquid thermal-conductivity field were made by means of (*a*) the column method; (*b*) the coaxial-cylinder method; (*c*) the parallel-plate method; (*d*) the hot-wire method.

(*a*) R. Weber (29) surrounded a column of liquid with a guard ring and heated the top of the column with an electrically heated oil bath contained in a suitable vessel; the lower end of the column was maintained at a lower temperature by the use of an ice-cooled copper plate. Thermocouples facilitated the necessary temperature measurements at points 1 cm apart (vertically) in the test fluid.

(*b*) The coaxial-cylinder method was used successfully by Bridgman (30) and more recently by Smith (31, 32) to determine the conductivity of liquids. The fluid was contained between two concentric cylinders in much the same manner as in the hot-wire method; however, the inner cylinder, which also acted as the heating element, was much larger than a conventional hot wire, and the annular space was much narrower. Also, a small tem-

[1] Based on a master's thesis, University of Colorado, Boulder, Colo., 1953, by one of the authors.[2]

[2] Mechanical Engineer, NBS Cryogenic Engineering Laboratory. Assoc. Mem. ASME.

[3] Associate Professor of Mechanical Engineering, University of Colorado. Mem. ASME.

[4] Numbers in parentheses refer to the Bibliography at the end of the paper.

Contributed by the Heat Transfer Division and presented at the Annual Meeting, New York, N. Y., November 29–December 4, 1953, of The American Society of Mechanical Engineers.

 Manuscript received by ASME Headquarters, September 2, 1953. Paper No. 53—A-184.

perature gradient was retained across the fluid to minimize convection currents. The primary drawback in such a system was the degree of accuracy necessary in the measurements of film thickness and temperatures of the bounding surfaces to obtain good results.

(*c*) The parallel-plate method of Bates (33, 34) was based primarily on a modification of Lees' (35) disk apparatus and was similar in principle to the parallel-plate method previously discussed. The careful design of the apparatus indicated a good degree of accuracy in the results, but the excessive length of time necessary to attain a steady state, together with the complicated details of construction, tended to offset the more desirable features.

(*d*) The hot-wire method, which first was applied to liquids in the double-wire differential form by Goldschmidt (7) and later used by Davis (36) for the same purpose, was revived in recent years by Hutchinson (37) and used as a single, noncompensating-tube system in determinations concerning organic liquids. Convection appeared to be absent when temperature gradients of the order of 1 deg C were maintained. Simplicity of the apparatus was the predominant feature in this case, as was the ease involved in making required measurements for the conductivity calculations.

Hot-Wire Method

The ideal hot-wire method implies a radial flow of heat from wire to tube wall; however, in the actual system, heat also may be lost from the wire by 1, convection, 2, radiation, 3, conduction through the current leads, 4, conduction through the potential leads. In addition to this, it also may be necessary to make an allowance for 5, the temperature discontinuity between the test fluid and the solid (wire or tube-wall) surfaces, caused by the imperfect interchange of energy between the fluid molecules and the solid surfaces.

1 Convective losses were assumed to be reduced to a minimum by (*a*) making the internal diameter of the cells small (a condition deemed necessary by previous research); (*b*) placing the tubes in a vertical position; (*c*) making the fluid-inlet connection at the lower end of the tubes.

2 The correction applied for the emission of heat by radiation from a wire maintained at a desired temperature to a coaxial surface maintained at a lower temperature was not of serious importance in this method, owing to the small dimensions of the wires used. An exact determination is one of considerable difficulty; however, such an investigation was carried out by Milverton (16) with respect to radiation from bright platinum, and his results were expressed by the formula $\phi = 5.88(T_1^{3.82} - T_2^{3.82})10^{-13}$ cal/sec/cm² of wire surface, in which T_1 and T_2 refer to the absolute temperatures (deg K) of the wire and the wall.

The foregoing expression was employed to calculate the correction applied to the results in the present work.

3, 4 Experimental compensation by the short conductivity cell accounted for conduction through the current and potential leads; therefore a lead correction was unnecessary in this case.

5 Although methods are available for determining the corrections for temperature drop and accommodation of gases, these methods are invalid for vapors, owing to the departure from a linear relationship obtained by plotting isothermals for $1/I^2$ against $1/p$ in accordance with the method set forth by Gregory (13) as related by Milverton (17). Also, according to Gregory (38) the proper choice of hot-wire size (6 mils or greater) tends to make this correction negligible. Hence the wire dimension for the present work was chosen as a compromise between two conditions; it was made large enough to be of value in the elimination of the temperature discontinuity and small enough to minimize the heat transmission by radiation. Finally, the test pressure was of sufficient magnitude to reduce the correction to an insignificant quantity.

6 Since the conductivity calculations involved the temperature of the inner cell wall, an additional correction was necessary to determine this temperature. If the temperatures of the internal and external surfaces are represented by t_2 and t_3, then t_2 can be found from the relation

$$t_2 = t_3 + 3.413EI\,\frac{\ln(r_3/r_2)}{2\pi k_g L}$$

where k_g is the thermal conductivity of the glass at an average temperature $(t_2 + t_3)/2$. Stephens (39) showed that the conductivity of pyrex glass could be represented accurately over a temperature range from —182 to 250 C by the expression

$$k_g = 0.00245 \log T - 0.00352$$

where

T = average absolute temperature, deg K
k_g = mean thermal conductivity of pyrex glass, cal/cm sec deg C

If an electrically heated wire is transmitting heat by conduction and radiation in a radial direction only, across an annular volume of fluid, to a coaxial cylindrical surface, the thermal conductivity of the enclosed fluid may be calculated from the relation

$$3.413EI = \frac{2\pi kL(t_1 - t_2)}{\ln(r_2/r_1)} + q_r$$

or, solving for k

$$k = \frac{1}{2\pi}\ln(r_2/r_1)\,\frac{3.413EI - q_r}{L(t_1 - t_2)}$$

For the double-tube compensating system, the measurements are understood to refer to effective quantities; thus

$$k = \frac{1}{2\pi}\ln(r_2/r_1)\,\frac{3.413E_eI - q_{r_e}}{L_e(t_e - t_2)}$$

where

k = mean thermal conductivity of fluid, Btu/hr ft deg F
r_1 = radius of hot wire, in.
r_2 = internal radius of pyrex tube, in.
I = electric current through hot wire, amp
E_e = effective potential drop across effective length of hot wire, volts
L_e = effective length of hot wire, ft
= length of long hot wire between potential leads minus length of short hot wire between potential leads
q_r = net rate of heat transfer by radiation from effective length of hot wire to pyrex tube, Btu/hr
t_1 = temperature of effective length of hot wire, deg F
t_2 = temperature of internal surface of pyrex tubes, deg F

Experimental Apparatus

Conductivity Cells. Two lengths of precision-bore pyrex glass tubing (4 in. and 10 in., respectively), having an internal diameter of 0.2497 in. ± 0.0003 in. and an external diameter of 0.338 in., were placed in gaseous connection with each other by means of a pyrex glass tee which led to the main body of the apparatus.

The hot wires were cut from a length of chemically pure 0.011-in. platinum wire and annealed for 1 hr at 750 F; the wires were measured to the nearest 0.001 in. with a hand micrometer, as was the external diameter of the precision-bore tubing. Two lengths

of the platinum resistance wire were fused to 0.020-in. platinum springs and carefully mounted along the axes of the tubes.

Because of the difficulty encountered in centering the measuring wires accurately in the tubes, an apparatus was devised to aid in setting up and constructing the cells. This device consisted of a piece of quarter-round wood held on each end by a sturdy metal standard. The wood provided a sliding surface for two adjustable tube clamps in the central portion, flanked by two adjustable wire holders. As each tube was to be developed, the cell wire was first fused to a platinum spring on one end and fastened tautly between the wire holders of the cell-building apparatus. Potential lead wires of 0.006-in. chemically pure platinum wire were then wound twice around the hot wire at appropriate points, and a satisfactory contact was made by applying a slight tension during the winding. Glass sleeves were melted around all potential and current leads for the purpose of providing an insulating surface between the wires; this procedure also simplified the fabrication of glass-to-platinum seals on both ends of each cell.

After accomplishing this, one end of the wire was released from its holder, and the respective length of precision-bore tubing was put into place around it. The tubing was secured by the tube clamps, and the loose end of the wire was fastened once again to the wire holder. In this manner, with both wire and tubing firmly held by one apparatus, slight adjustments could be made at each wire holder until the cell wire was visibly centered in the tube and supplied with the correct amount of tension at the spring to compensate for the heating and subsequent lengthening of the wire in relation to the pyrex-glass containing wall. The pyrex-glass-to-platinum seal was made easily after adjustment of the wire holders was completed.

Upon completion of the double conductivity-cell arrangement, it was checked carefully for imperfections, alignment, and so on, and then fused to the auxiliary glass apparatus (described in the following section). The current and potential leads were attached to 18-gage copper wires insulated from each other by means of heavy pyrex capillary tubing and bound together in compact tube bundles.

Auxilary Apparatus in Connection With Conductivity Cells. Fig. 1 indicates the details of the pyrex-glass apparatus which was in direct gaseous or liquid connection with the conductivity cells. The glass tee joining the two cells led to the bottom of the large U-tube which also contained test fluid. Upper extremities of the U were opened or closed independently of each other by means of individual stopcocks. One end was fitted with a ground-glass joint above the stopcock, making a vacuum-tight connection between the cells and an external liquid supply; plain glass tubing extended above the stopcock on the other end, facilitating vacuum-pump connections.

The center tube, which was connected to one leg of the U-tube, served a dual purpose; it acted as an overflow well when the conductivity cells were filled with liquid (an operation which partially filled the U to a point below the center-tube connection); it also served as a liquid reservoir when a vapor was to be tested, since a small amount of liquid could be admitted to this tube from above (prior to the evacuation of the apparatus) from which the vapor was released upon subsequent heating of the thermostat surrounding the tubes.

The upper end of the center tube was attached to a three-way stopcock which functioned as a selective control capable of (*a*) closing off the upper end of the center tube completely; (*b*) joining the center tube to an external liquid source; (*c*) providing a path between the center tube and the liquid air trap located directly above the stopcock.

Operation (*a*) was utilized almost continuously, with the following exceptions: (*b*) was used to admit a small amount of liquid into

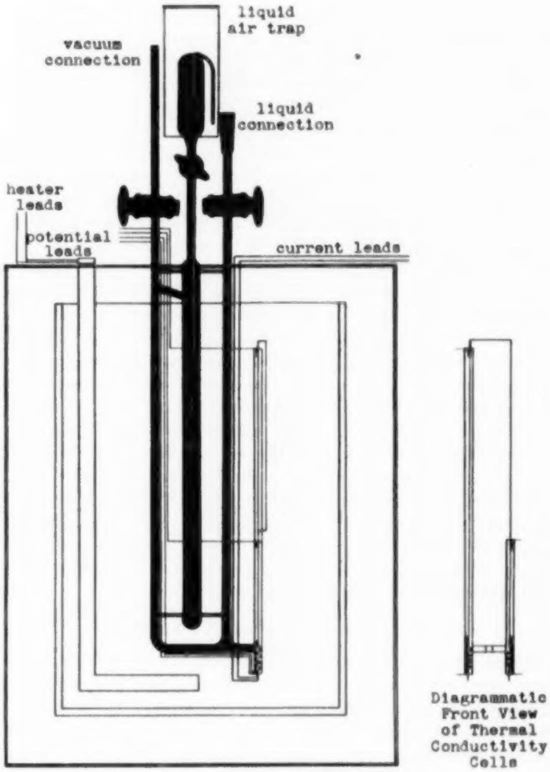

Fig. 1 Sectional View of Hot-Wire Thermal-Conductivity Apparatus

the center tube prior to the conductivity tests on vapors; (*c*) was active immediately before each conductivity measurement in order to relieve excessive pressure in the apparatus caused by the expansion of vapor as a result of heating.

An air trap was included in the construction to provide a means of equalizing pressure within the system with atmospheric conditions (approximately 24.8 in. Hg in Boulder, Colo.) without permitting an influx of contaminating air. This was accomplished by making the sealing liquid in the trap identical with that being tested. Since the temperature was always increased during the actual conductivity tests, the displacement through the trap was always of a positive nature, resulting in proper operation of this part of the system.

Thermostat. In order to regulate the outer tube-wall temperature of the conductivity cells, an oil thermostat was designed to provide the desired degree of temperature control. This consisted of an uncovered 3-gal pyrex-glass tank centrally located within an 8-gal metal tank. The large tank was fitted with a permanent cover after thermal insulation had been stuffed into the cavity between the tanks; a $2^1/_2$-in. $\times$ 4-in. rectangular section was cut from the center of the cover to facilitate the disposition of cells and auxiliary apparatus within the thermostat.

Thermostatic fluid was obtained from the Carbide and Carbon Chemicals Corporation under the "Ucon" brand designation; the presence of an oxidation stabilizer resulted in flash and fire-point temperatures of 500 and 600 F, respectively, which was considered high enough for the present series of tests.

The heating element was a 38-in., 750-watt tubular heater controlled by a Variac voltage regulator. Agitation of the oil was

accomplished by means of a stirrer equipped with an induction-type, nonsparking motor capable of continuous operation at a full-load speed of 1525 rpm. Oil-level control was considered essential to prevent an overflow caused by expansion of the oil upon heating; therefore a full-siphon arrangement was set up to be operated manually at intervals throughout each test run.

Electrical System. Electric current was supplied to the hot-wire circuit by a 6-volt, three-cell storage battery, and adequate current control was maintained by two variable wire-wound rheostats. Also included in series with the hot wire was a 1-ohm standard resistance coil certified to be accurate within 0.2 per cent of 1 ohm.

Switching was accomplished by means of Leeds and Northrup pinch-type, double-pole, double-throw switches; one was used as a selective potential-measurement switch between the long and the short conductivity cells; one was used as a selective switch between the 1-ohm standard resistance and the switch connection to the potential leads of the conductivity cells.

Potential measurements across the hot wires and standard resistance were made with a Leeds and Northrup type K-2 potentiometer with an external Leeds and Northrup No. 2420B lamp and scale-type galvanometer as the null instrument. Two d-c ammeters were connected to the hot-wire and potentiometer circuits to indicate the approximate line-current magnitude. All wiring, with the exception of the platinum-fitted conductivity cells, was done with 18-gage copper wire.

Calibration and Test Procedure

An accurate calibration of the platinum hot wires in terms of resistance versus temperature involved measurements of the resistance of the wires (within the tubes) immersed in the oil thermostat. Readings were taken at 10-deg-F intervals over the entire test range from room temperature to 450 F with a current of approximately 0.012 amp flowing through the wires. It has been found in work concerning platinum-resistance thermometry that current of such a magnitude has a negligible heating effect upon wires of the size used here; therefore true resistance determinations were easily and quickly made in the present case. Large-scale plots were made of these temperature-resistance data for the purpose of quick reference values during the test runs and for the final conductivity calculations at the end of each test. Graphs were made for both the effective resistance-versus-temperature relationship used for gases and vapors and the long-wire resistance-versus-temperature relationship used for liquids.

Spot calibration checks were made prior to and succeeding each conductivity run in order to insure proper functioning of the apparatus at all times; these checks indicated that the hot-wire resistance remained constant for a given temperature over the entire test range.

The experimental procedure employed in the actual thermal-conductivity determinations was similar to that used in the calibration tests with the following exception: A larger current was used in the conductivity runs to provide the necessary temperature difference between hot wire and tube wall. Measurement of the oil-thermostat temperature was in all cases quickly and precisely accomplished by means of a series of calibrated mercury-in-glass thermometers certified by the National Bureau of Standards and by the manufacturer to be accurate within 0.1 deg C.

Prior to filling the conductivity cells with test fluid, the apparatus was evacuated to a few millimeters of mercury with a vacuum pump. The fluid was then permitted to enter the cells, increasing the pressure to atmospheric conditions, and the process was repeated, insuring a pure test sample. All tests were conducted at prevailing atmospheric pressure, since temperature was to be the only variable under consideration. As determined from previous research in which pressure was a variable factor, the change in conductivity due to a pressure deviation of 5 in. Hg from standard conditions was negligible; therefore all results tabulated here may be assumed valid for standard conditions.

Discussion of Results

In order to check the accuracy of the apparatus, clean dry air was introduced into the conductivity cells on three separate occasions in the manner previously described. For each run the entire test range was covered. It was found that for certain portions of each of the first two test runs, equilibrium conditions were unattainable, therefore necessitating a third run (each run occurring on a separate date). The reason for such discrepancies finally was traced to open overhead laboratory windows which, on the two days in question, permitted short outdoor temperature variations, due to (*a*) a sudden rainstorm and (*b*) a shift of cold wind, measurably to affect the extremely sensitive measuring instrumentation. The third run was made with a suspicion of these conditions in mind, and when the temperature in the laboratory was again noticeably varied from the outside, erratic behavior was immediately observed as before, thus verifying the earlier suspicion. Equilibrium of the system was restored by closing the windows. Data given in Table 1, for which the graphical representation is made in Fig. 2, constitute the results obtained from these tests and indicate the almost absolute agreement of experimental results between the author and Taylor and Johnston (23); good agreement also is established with regard to the high-temperature work of Suspanov (20).

Reproducibility of results is quite markedly illustrated by the fact that the tabulated and graphical presentations are composed of data obtained on three different dates from three separate tests conducted with three fresh samples of test air. More accurately, all data collected at one temperature are from one test, but a change from one temperature group to another usually indicates a change of test run as well as temperature. The linear distribution of data obtained in the foregoing manner, as indicated by Fig. 2, combined with the agreement of previous research with the present work, would seem to reflect quite favorably upon the method and design of apparatus employed here.

Since the design of the apparatus encompassed all types of fluids, it seemed advisable and extremely worth while to determine the thermal conductivity of a liquid and a vapor of industrial importance for which conductivity measurements had not as yet been made. Furfural was such a fluid, being highly valued as a selective solvent in the lubricating-oil and wood-rosin industries (40–43).

Pure furfural was obtained from the Department of Chemistry at the University of Colorado, and it was tested in both the liquid and vapor phases by the method described previously.

Concerning the vapor phase, a small amount of liquid furfural was admitted to the center tube of the auxiliary glass apparatus, and the system was pumped down to a few millimeters of mercury. The external oil thermostat was then heated, and as the vacuum was slowly lost because of the formation of vapor from the warm furfural at reduced pressure, the vacuum pump was allowed to cut in and the system was once again pumped down. This process was repeated occasionally while the liquid was still at relatively low temperatures, insuring a pure vapor sample when the boiling point was reached at atmospheric pressure. Since all boiling took place in the center tube, the cell wires were never in contact with the agitated liquid, and the axiality and balance of the wires was at no time disturbed. Results of this test are given in Table 2 with the graphical representation made in Fig. 3. The grouping at each temperature is seen to be at least as good as that obtained with air, and a linearity may well be established for the short temperature range covered here.

TABLE 1 THERMAL CONDUCTIVITY OF AIR DATA

t_1 (°F)	t_2 (°F)	t_{av} (°F)	I (amp)	E_{eff} (volt)	R_{eff} (ohm)	q_t (Btu)/(hr.)	q_r (Btu)/(hr.)	q_c (Btu)/(hr.)	k (Btu)/(hr.ft.°F)
149.5	103.6	126.6	0.78603	0.27061	0.3443	0.727	0.013	0.714	0.0156
149.4	103.3	126.4	0.78965	0.27180	0.3442	0.733	0.013	0.720	0.0157
148.5	103.1	125.8	0.79035	0.27165	0.3437	0.717	0.013	0.704	0.0155
170.8	125.1	148.0	0.78770	0.28103	0.3568	0.756	0.014	0.742	0.0163
171.0	125.1	148.1	0.78780	0.28117	0.3569	0.757	0.014	0.743	0.0162
171.0	125.1	148.1	0.78810	0.28130	0.3569	0.758	0.014	0.744	0.0162
171.0	125.1	148.1	0.78810	0.28131	0.3569	0.758	0.014	0.744	0.0162
219.6	179.2	199.4	0.73519	0.28310	0.3851	0.711	0.016	0.695	0.0172
219.6	179.4	199.5	0.73509	0.28310	0.3851	0.711	0.016	0.695	0.0173
219.4	179.4	199.4	0.73497	0.28299	0.3850	0.711	0.016	0.695	0.0174
219.6	179.4	199.5	0.73497	0.28304	0.3851	0.711	0.016	0.695	0.0173
260.8	221.2	241.0	0.72775	0.29790	0.4093	0.741	0.018	0.723	0.0182
306.7	264.9	285.8	0.74429	0.32456	0.4361	0.825	0.023	0.802	0.0192
306.7	265.1	285.9	0.74430	0.32459	0.4361	0.826	0.023	0.803	0.0193
306.9	265.1	286.0	0.74430	0.32465	0.4362	0.826	0.023	0.803	0.0192
306.9	265.1	286.0	0.74415	0.32460	0.4362	0.825	0.023	0.802	0.0192
356.7	309.2	333.0	0.78965	0.36747	0.4654	0.992	0.031	0.961	0.0207
356.7	309.2	333.0	0.79003	0.36766	0.4654	0.993	0.031	0.962	0.0203
356.7	309.2	333.0	0.79018	0.36771	0.4654	0.993	0.031	0.962	0.0203
356.9	309.4	333.2	0.79020	0.36781	0.4655	0.993	0.031	0.962	0.0203
406.2	356.9	381.6	0.80360	0.39695	0.4940	1.090	0.038	1.052	0.0213
406.0	356.9	381.5	0.80340	0.39676	0.4939	1.089	0.038	1.051	0.0214
406.0	356.9	381.5	0.80350	0.39687	0.4939	1.090	0.038	1.052	0.0214

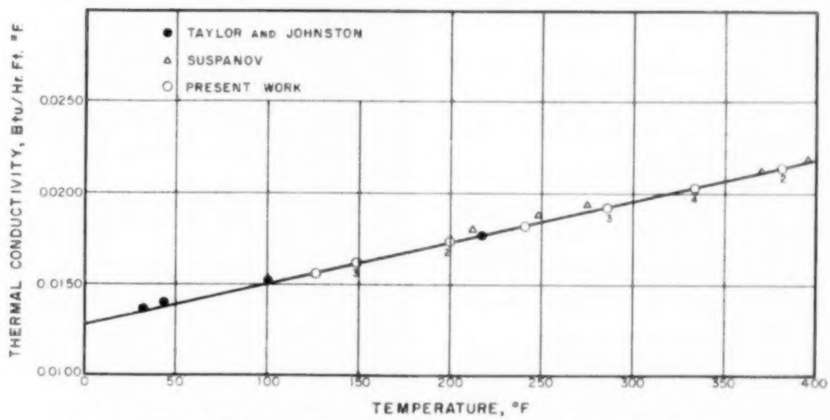

Fig. 2 Thermal Conductivity of Air Versus Temperature
(Numbers near data-point symbols represent number of measurements for which identical data were recorded.)

The liquid-phase run presented a slight problem in the method of filling the conductivity cells to the top, since an introduction of the liquid to the system in a normal manner necessarily would have entrapped a small but appreciable amount of air or vapor above the liquid in the upper portions of the cells. Designing the cells with the tee-shaped inlet connection at the upper part would have eliminated this difficulty, but the problem of convection currents then would have arisen in work with gases and vapors. Therefore it became necessary to remove the entire glass apparatus from the oil thermostat during the filling operation in order to be able to tip it in the proper direction for complete elimination of the air and vapor entrapment. When this had been accomplished, it was again placed in the thermostat in readiness for the forthcoming tests.

Since it is well understood that in the case of liquids, convection currents are easily set up in an apparatus such as this, temperature differences of less than 10 deg F generally were maintained throughout the liquid tests. Also, since such a small gradient was employed, the need for the small compensating cell was minimized, and it seemed advisable to use the long cell without compensation for end effects since such effects would be negligible for small temperature gradients. A radiation correction was not made for liquid furfural because of the small temperature differences held during the testing; another reason for such a decision was based upon the knowledge that furfural absorbs radiation in the infrared portion of the spectrum, making a correction for this effect extremely difficult. The same condition probably applied to the testing of furfural vapor as well; however, a correction in this in-

TABLE 2 THERMAL CONDUCTIVITY OF FURFURAL-VAPOR DATA

t_1 (°F)	t_2 (°F)	t_{av} (°F)	I (amp)	E_{eff} (volt)	R_{eff} (ohm)	q_t (Btu/hr.)	q_r (Btu/hr.)	q_c (Btu/hr.)	k (Btu/hr.ft.°F)
349.0	306.0	327.5	0.77339	0.35648	0.4609	0.942	0.028	0.914	0.0212
349.2	306.1	327.7	0.77368	0.35665	0.4610	0.943	0.028	0.915	0.0212
349.3	306.1	327.7	0.77411	0.35691	0.4611	0.944	0.028	0.916	0.0212
349.3	306.3	327.8	0.77417	0.35693	0.4611	0.944	0.028	0.916	0.0212
349.5	306.5	328.0	0.77459	0.35727	0.4612	0.946	0.028	0.918	0.0213
349.9	306.7	328.3	0.77469	0.35748	0.4614	0.946	0.028	0.918	0.0212
364.3	320.2	342.3	0.78169	0.36720	0.4698	0.980	0.030	0.950	0.0215
364.5	320.4	342.5	0.78255	0.36770	0.4699	0.984	0.030	0.954	0.0216
364.8	320.5	342.7	0.78251	0.36785	0.4701	0.984	0.030	0.954	0.0215
364.8	320.5	342.7	0.78248	0.36781	0.4701	0.984	0.030	0.954	0.0215
364.6	320.5	342.6	0.78255	0.36777	0.4700	0.984	0.030	0.954	0.0215
365.0	320.5	342.8	0.78257	0.36796	0.4702	0.984	0.030	0.954	0.0215
389.3	342.5	365.9	0.80220	0.38842	0.4842	1.057	0.036	1.021	0.0220
389.3	342.5	365.9	0.80225	0.38844	0.4842	1.057	0.036	1.021	0.0220

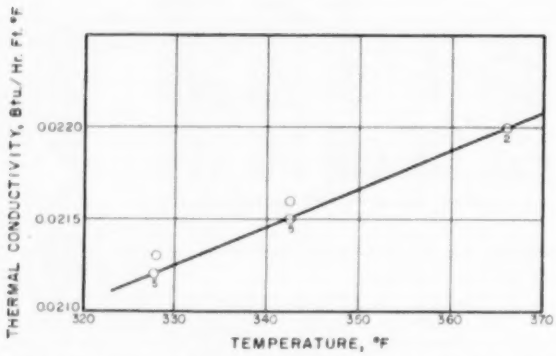

FIG. 3 THERMAL CONDUCTIVITY OF FURFURAL VAPOR VERSUS TEMPERATURE

(Numbers near data-point symbols represent number of measurements for which identical data were recorded.)

stance, made with the usual assumption of a nonabsorbing test medium, was deemed advisable in view of the large temperature gradients employed. Tabulated and graphical results for this test are presented in Table 3 and in Fig. 4; again, a linear distribution of data is illustrated.

Owing to the fact that equilibrium conditions could not be maintained in the vicinity of the boiling point of furfural, there was necessarily a short range for which no data were obtainable. However, there is no reason to believe that a linear extrapolation of existing data could not be made toward the boiling point from the established curves of both the liquid and the vapor phases. In all probability, the immediate vicinity of the vaporization point would contain a curve of approximately infinite slope, providing the over-all (vapor and liquid) furfural curve with a finite discontinuity in the phase-change region. At standard conditions, furfural boils at 323 F. However, since the normal barometric pressure in Boulder, Colo., is 24.8 in. Hg, the liquid boils at a lower temperature, and the 323 F point was easily approached in the vapor phase. Recalling a previous statement, the variation between standard atmospheric pressure and Boulder barometric pressure should have no measurable effect upon thermal conductivity; therefore all data presented here should be valid for standard pressure conditions.

ACKNOWLEDGMENT

The authors wish to acknowledge gratefully the research fellowship given by the Texas Company to carry out the present research work. Acknowledgment is also due to Mr. Hans L. Landay of the Scientific Glass Laboratory in Boulder, for the skill and patience applied to the fabrication of the thermal-conductivity cells and the auxiliary glass apparatus.

BIBLIOGRAPHY

1 "Brief Review of Available Data on the Dynamic Viscosity and Thermal Conductivity for Twelve Gases," by G. A. Hawkins, Trans. ASME, vol. 70, 1948, pp. 655–659.

2 "Thermal Conductivity of Air and Other Gases," by G. W. Todd, Proceedings of the Royal Society of London, England, series A, vol. 83, 1909, pp. 19–39.

3 "The Thermal Conductivity of Air," by E. O. Hercus and T. H. Laby, Proceedings of the Royal Society of London, England, series A, vol. 95, 1919, pp. 190–210.

4 "The Thermal Conductivity of Air by a Parallel Plate Method," by E. O. Hercus and D. M. Sutherland, Proceedings of the Royal Society of London, England, series A, vol. 145, 1934, pp. 599–611.

5 "Über die Wärmeleitung der Gase," by A. Schleiermacher, *Annalen der Physik und Chemie*, band 34, heft 8a, 1888, pp. 623–646.

6 "Experimentelle Untersuchungen über die Wärmeleitfähigkeit," by S. Weber, *Annalen der Physik*, folge 4, band 54, heft 21, 1917, pp. 325–356.

7 "Über Wärmeleitfähigkeit von Flüssigkeiten," by R. Goldschmidt, *Physikalische Zeitschrift*, band 12, heft 11, 1911, pp. 417–424.

8 "Experimental Determination of the Thermal Conductivities of Gases," by H. S. Gregory and C. T. Archer, Proceedings of the Royal Society of London, England, series A, vol. 110, 1926, pp. 91–122.

9 "The Variation of the Thermal Conductivity of Gases With Pressure," by H. S. Gregory and C. T. Archer, *Philosophical Magazine and Journal of Science*, series 7, vol. 1, 1926, pp. 593–606.

10 "The Thermal Conductivity of Carbon Dioxide," by H. S. Gregory and S. Marshall, Proceedings of the Royal Society of London, England, series A, vol. 114, 1927, pp. 354–366.

11 "The Thermal Conductivities of Oxygen and Nitrogen," by H. S. Gregory and S. Marshall, Proceedings of the Royal Society of London, England, series A, vol. 118, 1928, pp. 594–607.

12 "The Thermal Conductivities of Carbon Monoxide and Nitrous Oxide," by H. S. Gregory and C. T. Archer, Proceedings of the Royal Society of London, England, series A, vol. 121, 1928, pp. 285–293.

13 "The Thermal Conductivity of Air," by H. S. Gregory and C. T. Archer, *Philosophical Magazine and Journal of Science*, series 7, vol. 15, 1933, pp. 301–309.

14 "The Thermal Conductivities of the Saturated Hydrocarbons in the Gaseous State," by W. B. Mann and B. G. Dickens, Proceedings of the Royal Society of London, England, series A, vol. 134, 1931, pp. 77–96.

15 "The Effect of Accommodation on Heat Conduction Through Gases," by B. G. Dickens, Proceedings of the Royal Society of London, England, series A, vol. 143, 1934, pp. 517–540.

TABLE 3 THERMAL CONDUCTIVITY OF LIQUID-FURFURAL DATA

t_1 (°F)	t_2 (°F)	t_{av} (°F)	I (amp)	E_{long} (volt)	R_{long} (ohm)	q_t (Btu/hr.)	k (Btu/hr.ft.°F)
108.7	100.8	104.8	0.82880	0.37132	0.4480	1.051	0.0946
108.5	100.6	104.6	0.82996	0.37171	0.4479	1.054	0.0949
108.5	100.6	104.6	0.82988	0.37171	0.4479	1.054	0.0949
108.3	100.4	104.4	0.83013	0.37169	0.4477	1.054	0.0949
158.0	149.7	153.9	0.83098	0.40617	0.4888	1.153	0.0992
158.0	149.7	153.9	0.83072	0.40607	0.4888	1.153	0.0992
158.0	149.7	153.9	0.83047	0.40593	0.4888	1.152	0.0992
158.0	149.7	153.9	0.83018	0.40591	0.4889	1.151	0.0992
202.6	194.4	198.5	0.81798	0.42989	0.5256	1.202	0.104
202.6	194.4	198.5	0.81814	0.42997	0.5256	1.202	0.104
202.8	194.5	198.7	0.81833	0.43025	0.5258	1.203	0.102
203.0	194.7	198.9	0.81777	0.43006	0.5259	1.202	0.103
203.0	194.7	198.9	0.81800	0.43022	0.5259	1.202	0.103
238.3	230.0	234.2	0.80607	0.44717	0.5548	1.232	0.107
238.3	230.0	234.2	0.80580	0.44713	0.5549	1.231	0.106
238.3	230.0	234.2	0.80285	0.44540	0.5548	1.222	0.106
238.3	230.0	234.2	0.80256	0.44533	0.5549	1.221	0.106
238.3	230.0	234.2	0.80197	0.44488	0.5547	1.219	0.107

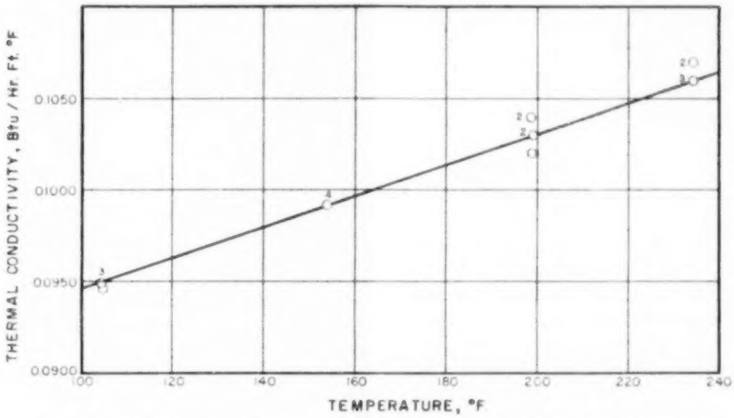

FIG. 4 THERMAL CONDUCTIVITY OF LIQUID FURFURAL VERSUS TEMPERATURE
(Numbers near data-point symbols represent number of measurements for which identical data were recorded.)

16 "An Experimental Determination of the Thermal Conductivity of Air Between 0° and 100° C," by S. W. Milverton, *Philosophical Magazine and Journal of Science*, series 7, vol. 17, 1934, pp. 397–422.

17 "An Experimental Determination of the Thermal Conduction Through Vapours," by S. W. Milverton, Proceedings of the Royal Society of London, England, series A, vol. 150, 1935, pp. 287–308.

18 "The Thermal Conductivity of Some Gases at 0° C," by W. G. Kannuluik and S. H. Martin, Proceedings of the Royal Society of London, England, series A, vol. 144, 1934, pp. 496–513.

19 "A Hot Wire Method for the Thermal Conductivities of Gases," by G. G. Sherratt and E. Griffiths, *Philosophical Magazine and Journal of Science*, series 7, vol. 27, 1939, pp. 68–75.

20 "Heat Conductivity of Gases at High Temperatures," by P. Suspanov, *Zhurnal eksperimental noi i teoreticheskoi fiziki*, vol. 5, 1935, pp. 870–889.

21 "The Dependence of Thermal Conductivity of Gases and Vapors on the Pressure," by N. Vargaftik, *Technical Physics of USSR*, vol. 4, 1937, pp. 341–360.

22 "The Thermal Conductivity and Viscosity of Steam at High Temperatures and Pressures," by D. L. Timroth and N. B. Vargaftik, *Journal of Physics* (USSR), vol. 2, no. 2, 1940, pp. 101–111.

23 "An Improved Hot Wire Cell for Accurate Measurement of Thermal Conductivities of Gases Over a Wide Temperature Range," by W. J. Taylor and H. L. Johnston, *Journal of Chemical Physics*, vol. 14, 1946, pp. 219–233.

24 "An Investigation of Aircraft Heaters XXXII—Measurement of Thermal Conductivity of Air and of Exhaust Gases Between 50° and 900° F," by L. M. K. Boelter and W. H. Sharp, NACA Technical Note 1912, July, 1949.

25 "New Measurements of the Heat Conductivity of Steam and N_2," by F. G. Keyes and D. J. Sandell, Jr., Trans. ASME, vol. 72, 1950, pp. 767–778.

26 "Measurements of the Heat Conductivity of N_2-CO_2 Mixtures," by F. G. Keyes, Trans. ASME, vol. 73, 1951, pp. 597–603.

27 "A Summary of Heat-Conduction Data for He, A, H_2, O_2, N_2, CO, CO_2, H_2O, and Air," by F. G. Keyes, Trans. ASME, vol. 73, 1951, pp. 589–596.

28 "Additional Measurements of Heat Conductivity of N_2, CO_2, and Mixtures," by F. G. Keyes, Trans. ASME, vol. 74, 1952, pp. 1303–1306.

29 "Wärmeleitung in Flüssigkeiten," by R. Weber, *Annalen der Physik*, folge 4, band 11, heft 8, 1903, pp. 1047–1070.

30 P. W. Bridgman, Proceedings of the American Academy of Arts and Sciences, vol. 59, 1923, p. 141.

31 "Thermal Conductivity of Liquids," by J. F. D. Smith, *Industrial and Engineering Chemistry*, vol. 22, 1930, pp. 1246–1251.

32 "The Thermal Conductivity of Liquids," by J. F. D. Smith, Trans. ASME, vol. 58, 1936, pp. 719–725.

33 "Thermal Conductivity of Liquids," by O. K. Bates, *Industrial and Engineering Chemistry*, vol. 25, 1933, pp. 431–437.

34 "Thermal Conductivity of Liquids," by O. K. Bates, G. Hazzard, and G. Palmer, *Industrial and Engineering Chemistry*, vol. 33, 1941, pp. 375–376.

35 "On the Thermal Conductivity of Single and Mixed Solids and Liquids and Their Variation With Temperature," by C. H. Lees, Philosophical Transactions of the Royal Society of London, England, series A, vol. 191, 1898, pp. 399–440.

36 "Convective Cooling in Liquids—Some Thermal Conductivity Data," by A. H. Davis, *Philosophical Magazine and Journal of Science*, series 6, vol. 47, 1924, pp. 927–975.

37 "On the Measurement of the Thermal Conductivity of Liquids," by E. Hutchinson, Transactions of the Faraday Society, vol. 41, February, 1945, pp. 87–90.

38 "The Determination of the Coefficient of Accommodation From Aspects of the Temperature Drop Effect," by H. S. Gregory, *Philosophical Magazine and Journal of Science*, series 7, vol. 22, 1936, pp. 257–265.

39 "The Temperature Variation of the Thermal Conductivity of Pyrex Glass," by R. W. B. Stephens, *Philosophical Magazine and Journal of Science*, series 7, vol. 14, 1932, pp. 897–914.

40 "Furfural and Other Furan Compounds," by H. R. Duffey, *Encyclopedia of Chemical Technology*, vol. 6, The Interscience Encyclopedia, Inc., New York, N. Y., 1951.

41 "Thermal Stability of Furfural," by A. P. Dunlop and F. N. Peters, *Industrial and Engineering Chemistry*, vol. 32, 1940, pp. 1639–1641.

42 "Autoxidation of Furfural," by A. P. Dunlop, P. R. Stout, and S. Swadesh, *Industrial and Engineering Chemistry*, vol. 38, 146, pp. 705–708.

43 "Furfural Formation and Behavior," by A. P. Dunlop, *Industrial and Engineering Chemistry*, vol. 40, 1948, pp. 204–209.

The Thermal Conductivities of Some Organic Liquids[1]

By M. F. DICK[2] and D. W. McCREADY[3]

A horizontal parallel plate apparatus was designed and constructed for the measurement of thermal conductivities of liquids. The liquid was held as a thin circular disk while the heat flux was downward through the liquid disk. The thickness of the liquid can be varied so the effect of thickness can be studied. The precision of the instrument is such that the results are within 1 per cent of the mean value. The thermal conductivities of nineteen liquid organic compounds were determined at 20 and 60 C. The compounds included isomeric ethers of varying structure, some esters of varying structure, and a hydrocarbon. All theoretical equations and empirical correlations for the prediction of the thermal conductivities of liquids were tested using the thermal conductivities of the nineteen liquids. The only available physical characteristic which would correlate the experimental results was the ASTM viscosity slope, and compounds containing rings did not correlate in this case. The experimental results were found to correlate best with the number of atoms in the longest chain. Corrections can be made for the effects of side chains and rings.

Introduction

Empirical equations relating thermal conductivities to other physical properties were reported as early as 1880. Bridgman, in 1923, measured the thermal conductivities of a series of liquids which varied widely in physical properties and proposed a theory for the conduction of heat through liquids. Bridgman's equation, based upon his theory, represents his data well considering the simplicity of the equation and wide variation of the physical properties of the liquids.

Since Bridgman proposed his equation, other theoretical and numerous empirical equations have been proposed. The main criticism of the theoretical equations has been that while they predict the order of magnitude of the thermal conductivity of the liquid, the actual agreement with observation is poor.

It is believed that the structure of the molecule has a considerable effect on the thermal conductivities of liquids and that the physical properties used in existing correlations may not reflect the effect of structure.

A group of liquid organic compounds of nearly constant molecular weight but varying considerably in structure was made available for study. The thermal conductivities of these compounds were measured and the effects of structure upon the thermal conductivity were investigated.

Construction of Apparatus

The apparatus constructed for the measurement of the thermal conductivities of liquids is a modification of the device first described by Jakob (4).[4] Fig. 1 is a diagram of the apparatus.

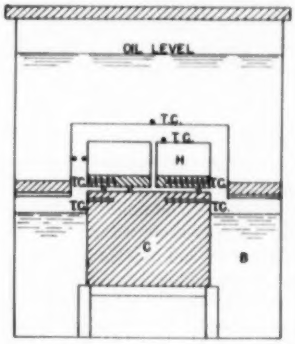

Fig. 1 Thermal-Conductivity Apparatus

The liquid under test was in the form of a thin disk between two horizontal cylindrical plates separated by three glass spacers of uniform thickness. The liquid was held in place by capillary forces at the edges. The heat flux was in the vertical direction downward so that convection effects were reduced. The top copper plate was the bottom of the test heater, H. The bottom plate, maintained at constant temperature, was a cylindrical copper block, C, which extended into the constant-temperature bath, B. Temperature difference across the liquid was measured by thermocouples inserted in the copper block and heater. The actual temperature drop across the liquid disk was obtained by subtracting the calculated temperature drop through the copper between the thermocouples and liquid-solid interface from that measured by the thermocouples.

The copper block, C, was $4^3/_4$ in. diam and 4 in. high. The top surface of the block was lapped to a flat surface and chromium-plated to prevent corrosion.

The test heater, H, was a hollow copper shell $4^3/_4$ in. diam and $1^1/_2$ in. high, which contained a resistance wire, wound in a flat spiral, as the heating element. The bottom of the heating shell was fabricated from $^3/_8$-in-thick copper bar and given the same surface treatment as the copper block. The heater shell was constructed of thin copper sheet. A $^1/_8$-in. hole was drilled through the bottom of the heater shell to use for filling the space between the heater and block with the liquid to be tested. The heater coil, 20 ft of 18-gage chromel-A wire with glass-braid insulation, was wrapped into a flat spiral, saturated with silicone insulating varnish, and baked for 8 hr at 400 F. The resulting heater, backed by a thin disk of transite, fitted snugly into the copper

[1] Based on a thesis submitted by M. F. Dick to the Graduate School, University of Michigan, in partial fulfillment of the requirements for the degree of Doctor of Philosophy in Chemical Engineering.

[2] Research Engineer, E. I. du Pont de Nemours & Company, Waynesboro, Va.

[3] Associate Professor of Chemical Engineering, University of Michigan, Ann Arbor, Mich.

Contributed by the Heat Transfer Division and presented at the Annual Meeting, New York, N. Y., November 29–December 4, 1953, of The American Society of Mechanical Engineers.

Note: Statements and opinions advanced in papers are to be understood as individual expressions of their authors and not those of the Society. Manuscript received at ASME Headquarters, September 2, 1953. Paper No. 53—A-187.

[4] Numbers in parentheses refer to the Bibliography at the end of the paper.

heater shell. A small amount of glycerol was added to the heater shell so that the heater wires would have good thermal contact with the bottom of the shell. The electrical resistance of the completed heater coil was about 7 ohms.

The glass spacers, which provide the space for the liquid under test, were cut from glass plates of uniform thickness. The thickness of each spacer was measured by means of a lightwave micrometer with the anvil pressure adjusted so that the spacer would be under the same pressure as during operation. Spacers were selected when thickness measurements agreed to within 0.0001 in. Three sets of spacers were used ranging from 0.087 to 0.023 in. in thickness with each spacer about 0.125 in. square.

The copper block, C, was immersed to within about 1 in. of the test surface in a constant-temperature oil bath. The bath was fabricated from $^1/_8$-in. copper sheet and was insulated with glass wool. A pump circulated oil around the copper block.

Temperatures were measured by copper-constantan thermocouples constructed of B&S 30-gage duplex wire with glass-braid insulation. The couples were silver-soldered, insulated with several coats of silicone varnish, and were calibrated against precision thermometers having National Bureau of Standards certificates.

The thermocouples were placed in positions in the blocks, as shown in Fig. 1, so that temperature gradients across the copper surfaces could be detected. All thermocouple holes were at least $1^1/_2$ in. deep in order to minimize the effect of possible heat losses along the thermocouple wires. The developed emf were measured by a Leeds and Northrup type K-2 potentiometer equipped with a lamp-and-scale-type galvanometer.

The power input to the heater was determined by measuring the current flow through the heater and the voltage drop across the heater. Current flow was measured by the voltage drop across a standard shunt connected in series with the test heater. The voltage drop across the test heater was measured by the potentiometer using a volt box.

Operation of Apparatus

The equipment just described was operated as follows: The thermoregulator in the bottom bath was set at about 2 to 3 deg C below the desired mean temperature of the liquid under test and the bath was brought to constant temperature. The regulator in the top bath was set at about 2 to 3 deg C above the mean temperature of the test liquid. The top surface of the bottom plate was cleaned with petroleum ether to remove any oil film remaining from previous experiments. The surface was then wiped dry with lint-free paper. The bottom surface of the test heater was given the same treatment.

The three glass spacers of the desired thickness were placed upon the bottom surface and the test heater was placed upon the spacers. Electrical connections to the test heater were made and the thermocouples were inserted. The test heater was then aligned with the copper block so that the thin disk of liquid would be cylindrical in shape. The liquid samples were heated to a temperature slightly above that of the test so that dissolved air was expelled and the viscosity was lowered for ease in filling the apparatus. The space between the plates was filled with the liquid to be tested through the filling tube, using a medicine dropper drawn out to a fine capillary. The filling process continued until the liquid had a flat meniscus between the plates. The thin disk of liquid was examined for air bubbles by shining a bright light through it from different directions. The top bath was put in place and brought to constant temperature. Heater current was adjusted by a resistance box and slide-wire resistor until the heater was the same temperature as the copper surface of the bath surrounding the heater. This was verified by thermocouples placed on the heater and on the bottom surface of the bath. A period of 2 to 3 hr was required to obtain this adjustment and to achieve steady temperatures. Thermocouple readings and readings of current and voltage were taken every 15 min until thermocouple readings indicated a change of temperature of no more than 0.01 deg C over a period of 1 hr. A period of from 3 to 4 hr was required to complete the observations necessary to calculate the thermal conductivity of the fluid under investigation.

The thermal conductivity was calculated from the following equation for heat conduction

$$q = \frac{-kA\,\Delta t}{\Delta L} \qquad [1]$$

where

q = heat transferred through liquid disk per unit of time
k = thermal conductivity of liquid
A = cross-sectional area of liquid disk
Δt = difference in temperature between surfaces of liquid
ΔL = thickness of liquid disk

Proof of Apparatus

In order that the values of thermal conductivities obtained by this apparatus could be considered absolute, it was necessary to consider carefully the determination of each of the terms in the heat-conduction equation.

The heat transferred through the glass spacers, the heat losses from the heater to the copper bath, and the heat losses resulting from evaporation of the test liquid were small and could be considered in the calculations. However, the heat loss from the test heater vertically through the air gap surrounding the heater to the oil bath below could not be calculated accurately and was too large to neglect in the calculations. This loss is a function of the temperature difference between the two baths and is a constant for a given ΔT regardless of the liquid thickness. Values of thermal conductivity were observed for two or three liquid thicknesses at constant ΔT and the results were plotted against the liquid thickness. A line drawn through the points and extrapolated to zero thickness, where the vertical heat loss is negligible, gives the true thermal conductivity as its intercept.

Fig. 2 illustrates this for several liquids. Also, by extrapolat-

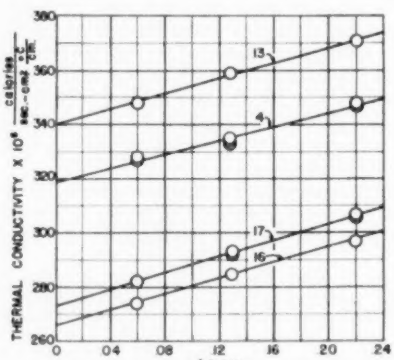

Fig. 2 Thermal Conductivity Versus Thickness of Liquid Layer at 60 Deg C

ing the data to zero thickness the effects of convection could be eliminated. Calculations using the correlation of Kraussold (5) indicate, however, that the effects of convection are negligible at the liquid thicknesses studied.

The thickness of the liquid disk was considered the same as

that of the glass spacers and electrical capacitance measurements verified this.

The temperature drop through the copper between the thermocouples and the liquid surface was calculated and was subtracted from the measured ΔT to obtain the actual ΔT across the liquid.

Precision and Accuracy of Measurements

The precision of the instrument was checked by making nine runs on the same compound. The deviations from the mean value for nine runs were less than 1 per cent. The data reported, however, result from the extrapolation of a line drawn through the experimental points, so that the precision of the extrapolated points may be considered to be about 2 per cent.

The accuracy of the determination made with the instrument may be estimated by taking into consideration the errors in the measurement of each quantity entering the heat-conduction equation. The maximum error obtained this way was found to be ± 1.75 per cent. A further check of the accuracy of the instrument was made by comparing the thermal-conductivity value for water found in the literature with that measured by this instrument. The values in the literature range from 0.001470 to 0.001590 with most of the data between 0.001555 and 0.001570 calories/(sec) (cm)^2 (°C/cm). The result found by the instrument was 0.001570 at 60 C.

Experimental Results

The series of compounds studied was synthesized as a part of a research program in which many other physical properties were evaluated. The compounds were synthesized by the usual methods and were purified by distillation. On the basis of carbon-hydrogen analyses the purity of the compounds is estimated to be greater than 98 per cent.

The thermal conductivities of the compounds were measured at 20 and 60 C and are listed in Table 1 with the structural formulas of the compounds. The hydrogen atoms have not been included in the structural formulas.

The first series of compounds include seven isomeric ethers. These ethers were used to study the effect of length and position of side chain upon thermal conductivity. A series of esters and a hydrocarbon were used to determine the effect of functional group. The remaining compounds are ethers and esters containing aromatic and naphthenic rings.

Tests of Theoretical and Empirical Correlations

The theoretical and empirical correlations were tested using the data obtained in this research to see if any existing correlation or equation would represent the data satisfactorily.

Bridgman's Equation. Bridgman (1) developed an equation relating the speed of sound in the liquid to the thermal conductivity

$$k = \frac{2\,au}{d^2} \qquad [2]$$

where

a = gas constant

u = velocity of sound in liquid

d = mean distance of separation of centers of molecules, assuming a cubicle arrangement on the average, and calculating d by the formula $d = (m/\rho)^{1/3}$, where m is the absolute weight in grams of 1 molecule of liquid

Thermal-conductivity data obtained for the high molecular weight compounds used in this research are compared in Table 2 with values calculated by Bridgman's equation. The results obtained were found to be consistently higher than the values of thermal-conductivity calculated from the equation.

Rao's Equation. Rao (6) has proposed a theory for thermal conduction through liquids which is based on the belief that the liquid state approaches more nearly the solid state than the gaseous state. On this basis he has derived the following equation for the thermal conductivity at the melting point

$$k = 2.096 \times 10^{6}\,\frac{T_s^{1/2}}{MV_s^{4/3}} \qquad [3]$$

where

T_s = absolute melting temperature

M = molecular weight

V_s = molecular volume at the melting point

Thermal-conductivity data obtained for the high-molecular-weight compounds used in this research are compared in Table 2 with values calculated by Rao's equation. The values of thermal conductivity used were extrapolated to the freezing point from 20 C. The calculated results are consistently higher than the observed values by a factor of about 2. The constant in Rao's equation could be modified to improve the situation but differences would still be present well beyond the experimental error, notably in the cases of compounds Nos. 6 and 11.

Weber's Equation. The earliest relation connecting thermal conductivity with other properties is that of Weber (9). His empirical equation was first given by: $k/(C_p\rho)$ = const and later modified to

$$k = 0.00359\, C_p\rho\,(\rho/M^{1/3}) \qquad [4]$$

where

k = thermal conductivity, calories/(sec) (cm)^2 (°C/cm)

C_p = specific heat, calories/(gm) (°C)

M = weight in grams of 1 molecule

ρ = density in grams per cu cm

Smith (8) in a review of various empirical and theoretical equations has compared values calculated by the foregoing equation with observed experimental results. Smith found that for the liquids compared, better agreement could be obtained by changing the constant of Equation [4] so that the modified equation is

$$k = 0.0043\, C_p\rho\,(\rho/M)^{1/3} \qquad [5]$$

Thermal-conductivity values observed in this research are compared with values calculated from Weber's modified equation and are given in Table 3. The calculated values are about 25 per cent lower than the observed. The agreement could be improved by modifying the constant further but the equation would still not take into account deviations noted for several compounds, for example, compounds Nos. 8 and 16.

Smith's Empirical Equations. In 1930 Smith (7) suggested an entirely empirical equation

$$k_{\text{at 30 C}} = \frac{8.1 \times 10^{-4}\,\rho^{2.15}\,C_p^{1.86}\,M^{0.192}}{\mu^{0.11}} \qquad [6]$$

where μ = viscosity in centipoises.

Smith found that this equation satisfied all the liquids for which data were available, in all fifteen liquids, with reasonable variation in physical properties. The agreement with experiment for every liquid except two oils was closer than 4.5 per cent. The oils gave errors of 3 and 20 per cent, respectively. Smith tested this equation with additional data obtained in 1936 and found that the agreement with the new data was poor.

TABLE 1 EXPERIMENTAL DATA

No.	Compound	Thermal Conductivity $k \times 10^6$ calories / (sec)(cm)^2(^oC/cm) 20°C	60°C	Thermal Conductivity B.T.U. / (Hr.)(Ft)^2 (^oF/Ft) 68°F	140°F
	Ether Isomers				
1	2, 5-Di-(2-ethylhexoxy) hexane 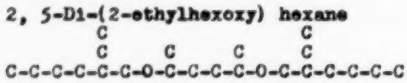	307	287	.0744	.0695
2	1, 6-Di-(n-octoxy) hexane C-C-C-C-C-C-C-C-O-C-C-C-C-C-C-O-C-C-C-C-C-C-C-C	360	339	.0872	.0821
4	1,6-Di-(2-ethylhexoxy) hexane 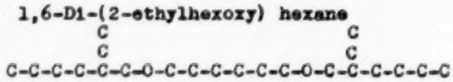	333	319	.0806	.0772
13	1, 4-Di-(n-nonoxy) butane C-C-C-C-C-C-C-C-C-O-C-C-C-C-O-C-C-C-C-C-C-C-C-C	362	340	.0877	.0824
14	1, 10-Di-(1-ethylbutoxy) decane 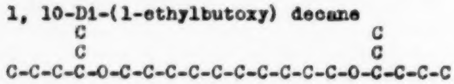	343	325	.0830	.0787
16	1, 4-Di-(3,5, 5-trimethylhexoxy) butane 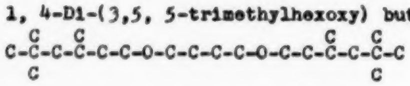	273	266	.0661	.0644
19	1, 6-Di-(1-methylheptoxy) hexane 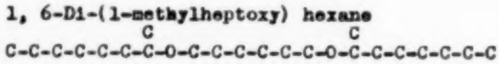	322	310	.0780	.0751
6	1,4-Di-(2-ethylhexoxy) benzene 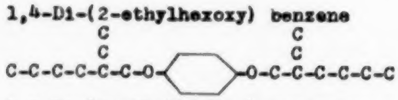	354	323	.0857	.0782
12	1,2-Di-(2-ethylhexoxy) benzene 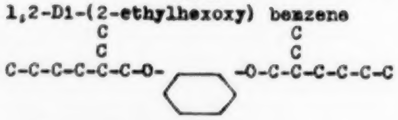	310	293	.0750	.0710
	Miscellaneous Ethers				
8	1,10-Di-(2-ethylhexoxy) decane 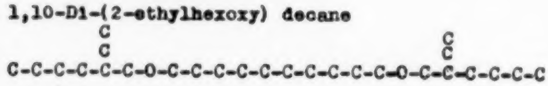	351	332	.0850	.0804
15	1,5-Di-(n-nonoxy) pentane C-C-C-C-C-C-C-C-C-O-C-C-C-C-C-O-C-C-C-C-C-C-C-C-C	361	340	.0874	.0824
24	1,6-Di-(2-butyloctoxy) hexane 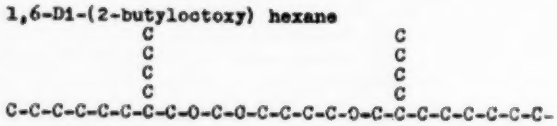	347	324	.0840	.0785
	Esters				
3	2, 5-Hexamethylene glycol di-(2-ethylhexanoate) 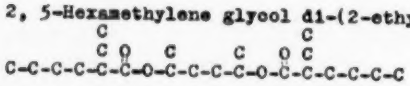	302	289	.0731	.0700

TABLE 1 EXPERIMENTAL DATA (*Continued*)

11	Di-(2-ethylhexyl)adipate 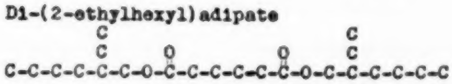	343	324	.0831	.0784
23	Di-(3, 5, 5-trimethylhexyl)adipate 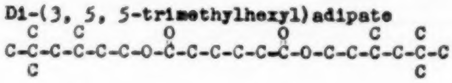	294	280	.0712	.0679
	Ethers with cyclohexyl groups				
7	1, 6-Di-(cyclohexoxy) hexane 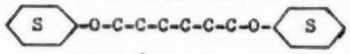	302	285	.0730	.0690
17	2, 5-Di-(β -cyclohexylethoxy) hexane 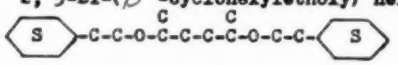	279	273	.0675	.0661
	Ester with Cyclohexyl Groups				
21	Hexamethylene glycol di-(β -cyclohexylethanoate) 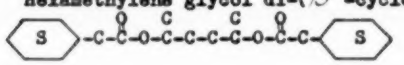	289	279	.0700	.0676
	Hydrocarbon				
20	5,14-Diethyloctadecane 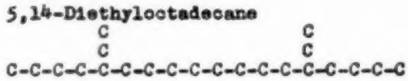	338	317	.0819	.0767

Equation [6] was tested with data obtained in this research and results are listed in Table 4. The calculated values of thermal conductivity are consistently higher than the observed values. The agreement could be improved by modification of the constant but then larger differences would be observed in Smith's comparison for other compounds.

Smith could see little chance of changing the exponents of Equation [6] to satisfy all liquids so he tried a different method. By taking variations from approximate mean values he found that

$$k_{\text{at 30 C}} = 0.000361 + \frac{(C_p - 0.45)^3}{155} + \frac{(\rho/M)^{1/3} - 0.20}{800} + \frac{\mu^{1/9} - 1}{10{,}000} \quad \text{[7]}$$

or

$$k_{\text{at 30 C}} = 0.000011 + \frac{(C_p - 0.45)^3}{155} + \frac{(\rho/M)^{1/3}}{800} + \frac{\mu^{1/9}}{10{,}000} \quad \text{[8]}$$

Smith found that the average error of the calculated values for a large number of compounds was about 7 per cent, so he considered this equation to be satisfactory for engineering use.

This equation also gives values of thermal conductivities which are in good agreement with the observed values for the high-molecular-weight compounds studied in this research. Table 4 compares observed values with calculated values. Agreement is such that the equation would seem to be satisfactory for engineering use for compounds of high molecular weight as well. This is surprising since the compounds for which the equation was devised are in general of much lower molecular weight. The equation, however, does not account for all the variation of thermal conductivity observed in the high-molecular-weight compounds.

Cragoe's Equation. A special equation applicable to hydrocarbon oils has been proposed by Cragoe (3)

$$k = \frac{0.813}{d}\,[1 - 0.0003\,(t - 32)]$$

d = specific gravity at 60 F

t = deg F

k = thermal conductivity, Btu/(hr) (ft)² (°F/in.)

Smith tested this equation on a series of oils and found the average error of the formula to be 12.4 per cent with a maximum error of 39 per cent. In addition, he found that if a constant value for the thermal conductivity of the oils of 0.000327 calories/(sec) (cm)² (°C/cm) at 30 C is taken, the average error is 6 per cent; the maximum error is plus or minus 13 per cent. Therefore he recommends the use of the constant value for hydrocarbon oils at 30 C.

Cragoe's equation was tested using the values of thermal conductivity determined in this research. The comparison of calculated values with observed values is made in Table 3. The maximum error is 21 per cent which is slightly better than Smith found for the oils he compared. If the constant value 0.000327 recommended by Smith is used the maximum error is reduced to 19 per cent.

Correlation of Data With Physical Properties

It has been observed in the evaluation of the empirical and theoretical equations that the groups of physical properties involved do not account for variations in thermal conductivity

TABLE 2 COMPARISON OF OBSERVED THERMAL CONDUCTIVITIES OF LIQUIDS WITH THOSE COMPUTED FROM BRIDGMAN'S EQUATION [2] AND RAO'S EQUATION [3]

Thermal conductivity $\times 10^6$ cal/(sec) (cm)^2 (°C/cm)

		Bridgman's Equation		Rao's Equation		
No.	Compound	k_{obs} at 25°C	k_{cal} at / k_{obs} 25°C	Freezing Point °K	k_{obs} at F.P.	k_{cal} at / k_{obs} F.P.
1	2, 5-Di-(2-ethylhexoxy) hexane C C C C C C C-C-C-C-C-C-O-C-C-C-C-O-C-C-C-C-C	304	.65	208	349	2.12
2	1, 6-Di-(n-octoxy) hexane C-C-C-C-C-C-C-C-O-C-C-C-C-C-C-O-C-C-C-C-C-C-C-C	358	.56	239	364	2.24
4	1, 6-Di-(2-ethylhexoxy) hexane C C C C C-C-C-C-C-C-O-C-C-C-C-C-C-O-C-C-C-C-C-C	331	.61	240	351	2.33
6	1,4-Di-(2-ethylhexoxy) benzene C C C C C-C-C-C-C-C-O- -O-C-C-C-C-C-C	350	.55	284	361	2.49
11	Di-(2-ethylhexyl) adipate C C C O O C C-C-C-C-C-C-O-C-C-C-C-C-C-O-C-C-C-C-C-C	341	.52	208	383	2.01
12	1,2-Di-(2-ethylhexoxy) benzene C C C C C-C-C-C-C-C-O- -O-C-C-C-C-C-C	308	.64	208	346	2.34
14	1, 10-Di-(1-ethylbutoxy) decane C C C C C-C-C-C-O-C-C-C-C-C-C-C-C-C-C-O-C-C-C-C	341	.52	216	378	1.98
17	2, 5-Di-(β-cyclohexylethoxy) hexane C C S -C-C-O-C-C-C-C-O-C-C- S	279	.72			
19	1, 6-Di-(1-methylheptoxy) hexane C C C-C-C-C-C-C-C-O-C-C-C-C-C-C-O-C-C-C-C-C-C-C	320	.55			
20	5,14-Diethyloctadecane C C C C C-C-C-C-C-C-C-C-C-C-C-C-C-C-C-C-C-C	335	.58			

observed. A thorough study of the effect of each physical property alone upon thermal conductivity was made before any new empirical correlation was attempted. However, correlation of the data with such properties as molecular weight, intermolecular distance, isothermal compressibility, freezing temperature, and viscosity proved fruitless.

The ASTM slope of the kinematic viscosity-temperature curve was then plotted instead of viscosity alone. The ASTM slope is an empirical number which is the slope of the kinematic viscosity-temperature curve for a liquid when plotted on co-ordinate paper standardized by the American Society for Testing Materials.

The thermal conductivity at 60 C is plotted against ASTM slope in Fig. 3. The numbers correspond with the compounds listed in Table 1. It will be noted that the data correlate with the ASTM slope except for the compounds represented on the plot by squares, which are much different in structure. Compounds Nos. 6 and 12 both contain an aromatic ring in the center of the longest chain while Nos. 7, 17, and 21 all contain cyclohexyl groups at the ends of the longest straight chain. Apparently the isobutyl groups act in somewhat the same way as the cyclohexyl groups at the end positions.

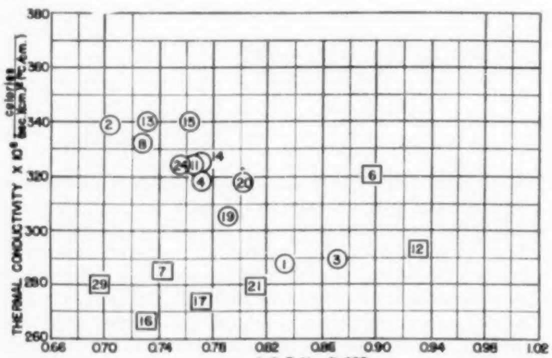

Fig. 3 Thermal Conductivity Versus ASTM Slope

TABLE 3 COMPARISON OF OBSERVED THERMAL CONDUCTIVITIES OF LIQUIDS WITH THOSE COMPUTED FROM WEBER'S MODIFIED EQUATION [5] AND CRAGOE'S EQUATION [9]

Temperature = 20 C. Thermal conductivity × 10^6 cal/(sec) (cm)^2 (°C/cm)

No.	Compound	k_{obs} at 20°C	(Weber) k_{cal}/k_{obs}	(Cragoe) k_{cal}/k_{obs}
1	2, 5-Di-(2-ethylhexoxy) hexane 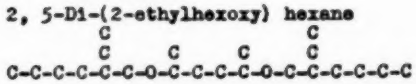	307	.80	1.08
3	2, 5-Hexamethylene glycol di-(2-ethylhexanoate) 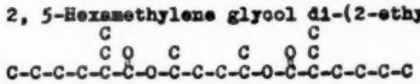	302	.85	1.01
4	1, 6-Di-(2-ethylhexoxy) hexane 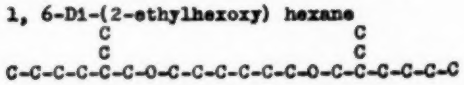	333	.72	1.01
6	1,4-Di-(2-ethylhexoxy) benzene 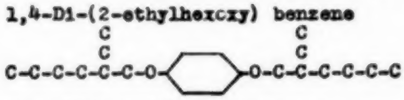	354	.75	.86
7	1, 6-Di-(cyclohexoxy) hexane 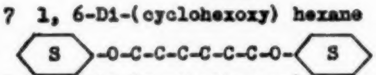	302	.87	.99
8	1,10-Di-(2-ethylhexoxy) decane 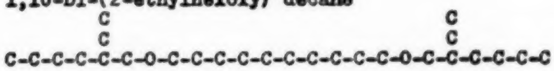	351	.64	.94
14	1, 10-Di-(1-ethylbutoxy) decane 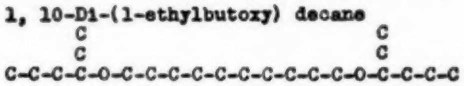	343	.73	1.04
16	1, 4-Di-(3,5, 5-trimethylhexoxy) butane 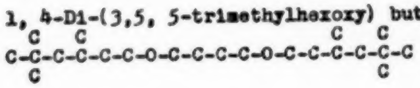	275	.92	1.21

Effect of Structure Upon Thermal Conductivity

The correlation found between the ASTM slope and thermal conductivity indicates that molecular structure does play an important part in heat conduction through liquids. Bried (2), in a study of the viscosity of a group of diesters, found that, in general, ASTM slope increased with increased branching and the slope decreased with increasing chain length. A study of the effect of chain length upon thermal conductivity as indicated in Fig. 4 reveals that there is a trend toward higher conductivities at longer chain lengths. However, wide variations from this trend were observed. Chain length as employed here is defined as the number of atoms in the longest chain in the molecule. Oxygen atoms were counted as being the same as carbon atoms. The presence of side chains on many of the compounds probably has some relationship to the deviations noted.

Smith's data on the thermal conductivity of straight-chain hydrocarbon shows that thermal conductivity increases with increasing chain length. It is believed, therefore, that the data in Fig. 4 can be correlated with chain length if suitable corrections for side chains are made. Arbitrary assignments were made for each functional group. Compounds Nos. 2, 13, and 15 can be plotted directly in Fig. 5 since these compounds have no side chains. The effect of each group is listed in Table 5. For example, a methyl group will reduce the thermal conductivity in a straight chain diether by 12 × 10^{-6} calories/(sec) (cm)^2 (°C/cm).

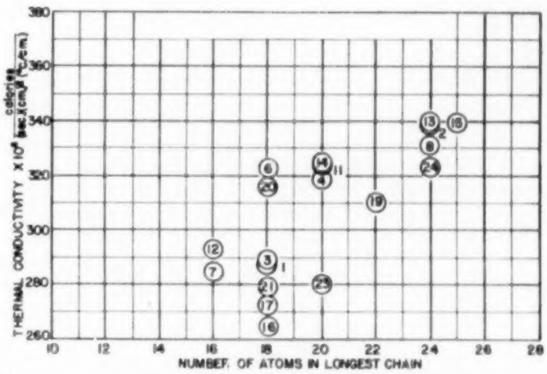

Fig. 4 Thermal Conductivity Versus Chain Length

In the case of compounds containing cyclohexyl groups on each end of the chain, the data correlate well if each ring is considered as 1 carbon atom. The compounds containing an aromatic ring in the center of the chain do not fit the correlation. Compound No. 6 is considered as having four carbons of the ring in the chain and compound No. 12 is considered as having 2 carbon atoms of the ring in the chain. An interesting point brought out by this

TABLE 4 COMPARISON OF OBSERVED THERMAL CONDUCTIVITIES OF LIQUIDS WITH THOSE COMPUTED FROM SMITH'S EQUATIONS [6] AND [8]

Temperature = 30 C. Thermal conductivity × 10^6 cal/(sec) (cm)^2 (°C/cm)

No.	Compound	k_{obs} at 30°C	Eq.(6) k_{cal}/k_{obs}	Eq.(8) k_{cal}/k_{obs}
1	2, 5-Di-(2-ethylhexoxy) hexane C-C-C-C-C-C-O-C-C-C-C-O-C-C-C-C-C-C	302	1.54	1.00
3	2, 5-Hexamethylene glycol di-(2-ethylhexanoate) C-C-C-C-C-C-O-C-C-C-C-O-C-C-C-C-C-C	299	1.64	1.04
4	1, 6-Di-(2-ethylhexoxy) hexane C-C-C-C-C-C-O-C-C-C-C-C-C-O-C-C-C-C-C-C	330	1.36	.93
6	1,4-Di-(2-ethylhexoxy) benzene C-C-C-C-C-C-O-⟨ring⟩-O-C-C-C-C-C-C	346	1.22	.93
7	1, 6-Di-(cyclohexoxy) hexane ⟨S⟩-O-C-C-C-C-C-C-O-⟨S⟩	298	1.39	1.11
8	1,10-Di-(2-ethylhexoxy) decane C-C-C-C-C-C-O-C-C-C-C-C-C-C-C-C-C-O-C-C-C-C-C-C	346	1.22	.87
14	1, 10-Di-(1-ethylbutoxy) decane C-C-C-C-O-C-C-C-C-C-C-C-C-C-C-O-C-C-C-C	339	1.40	.90
16	1, 4-Di-(3,5, 5-trimethylhexoxy) butane C-C-C-C-C-C-O-C-C-C-C-O-C-C-C-C-C-C	271	1.75	1.14

TABLE 5 THERMAL-CONDUCTIVITY INCREMENTS FOR FUNCTIONAL GROUPS

Functional group	Thermal-conductivity increment calories/(sec) (cm)^2 (°C/cm)
Methyl group	-12×10^{-6}
Ethyl group	-3×10^{-6}
Butyl group	-6×10^{-6}
C, —C—, C (quaternary carbon)	-12×10^{-6}
Carbonyl oxygen	2×10^{-6}

correlation is that the methyl group has a greater effect upon thermal conductivity than the other longer chains. Position of the group on the side chain has not been considered. The compounds available indicate that this has but a small effect. Further investigation of the ring compounds is also necessary to determine the effect of the ring, saturated or unsaturated, and its position in the chain. The available data show that the terminal rings act as a unit, not much different in effect from an atom in the chain.

Conclusions

An apparatus was designed and constructed for the measurement of the thermal conductivities of liquids. The instrument has been found to have considerable flexibility. Thermal conductivity can be measured over a range of temperature, the temperature difference across the liquid can be varied, and the thickness of the liquid layer can be varied. The precision of the instrument is sufficient to reproduce data to within 1 per cent of the mean values. The accuracy of the values obtained by the apparatus is considered to be within 2 per cent of the absolute values.

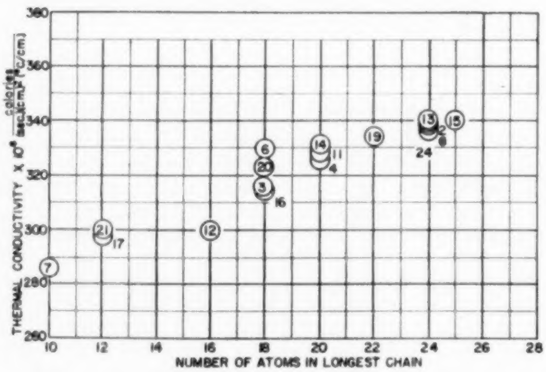

FIG. 5 CORRECTED THERMAL CONDUCTIVITY VERSUS CHAIN LENGTH

The theoretical equations which have been derived to relate thermal conductivity to other physical properties do not predict satisfactorily the thermal conductivity of the liquids studied in this research. In one case the calculated value was twice as large as the observed value and in the other case one half as large as the observed value. The theoretical equations do predict the order of magnitude of the thermal conductivities of liquids of lower molecular weight reported in the literature. But as the molecules become more complex and of higher molecular weight, the deviations from the idealized liquid described in the derivations become greater.

The empirical correlations reported in the literature predict the thermal conductivities of the liquids investigated much better than do the theoretical correlations. The latest of Smith's empirical correlations satisfies the observed results well enough for engineering use. It does not predict the deviations of thermal conductivity observed among the liquids which may be due to differences in molecular structure.

The available physical properties were studied with attempts at correlating them with thermal conductivity. The only property which correlated at all was the ASTM viscosity slope. The thermal conductivity tended to increase with decreasing ASTM viscosity slope.

The best method of correlating the thermal conductivities of the high-molecular-weight compounds is by relating the thermal conductivity to the number of atoms in the longest straight chain. This correlation indicates a trend toward higher thermal conductivity at greater number of atoms in the straight chain. Deviations from this trend show that side chains have a definite effect upon the thermal conductivity. In determining the effects of side chains of different lengths it was found that single carbon atoms attached to the central chain decrease thermal conductivity more than do the presence of two or more atoms in a side chain. In general, it can be said that thermal conductivities of high-molecular-weight liquids increase with increasing chain length and the effect of side chains is to reduce the thermal conductivity.

ACKNOWLEDGMENT

The authors wish to acknowledge the financial support of the study by the U. S. Air Force, Air Research and Development Command, and the University of Michigan Engineering Research Institute. Appreciation is also extended to Prof. A. D. Moore and Prof. M. B. Stout for valuable suggestions.

BIBLIOGRAPHY

1 "The Thermal Conductivity of Liquids Under Pressure," by P. W. Bridgman, Proceedings of the American Academy of Arts and Sciences, vol. 59, 1923, pp. 141–169.

2 "Synthetic Lubricant Fluids From Branched-Chain Diesters," by E. M. Bried, H. F. Kidder, C. M. Murphy, and W. A. Zisman, *Industrial and Engineering Chemistry*, vol. 39, 1947, pp. 484–491.

3 "Thermal Properties of Petroleum Products," by C. S. Cragoe, Bureau of Standards, Miscellaneous Publication No. 97, 1929, 48 pages.

4 "Bestimmung der Wärmeleitfähigkeit des Wassers im Bereich von 0 bis 80°," by M. Jakob, *Annalen der Physik*, vol. 63, 1920, pp. 537–570.

5 "Wärmeabgabe von zylindrischen Flüssigkeitschichten bei natürlicher Konvektion," by H. Kraussold, *Forschung auf dem Gebiete des Ingenieurwesens*, vol. 5, 1934, pp. 186–191.

6 "Thermal Conductivity of Liquids," by M. R. Rao, *Indian Journal of Physics*, vol. 16, 1942, pp. 161–167.

7 "Thermal Conductivity of Liquids," by J. F. D. Smith, *Industrial and Engineering Chemistry*, vol. 22, 1930, pp. 1246–1251.

8 "The Thermal Conductivity of Liquids," by J. F. D. Smith, Trans. ASME, vol. 58, 1936, pp. 719–725.

9 "Untersuchungen über die Wärmeleitung in Flüssigkeiten," by H. F. Weber, Wiedemann's Annalen, *Annalen der Physik und Chemie*, vol. 10, 1880, pp. 103–129.

Discussion

C. F. Bonilla.[5] The data on thermal conductivity of organic liquids in this paper, together with their analysis and the derived method of predicting thermal conductivity, will be helpful to those handling many types of liquids—in particular, the chemical industry. The authors are to be complimented on the care and effort that went into this work.

Fig. 2 of the paper represents an extrapolation to zero thickness, presumably at substantially constant temperature difference, and k is seen to decrease significantly as ΔL approaches zero. Do the authors have any explanation for this effect, in view of the fact that Kraussold's criterion shows that natural convection is negligible at all values of ΔL employed?

It is the writer's theory that extrapolation to $\Delta L = 0$ has two effects: (*a*) Conduction in the fluid sample increases so that any wall-to-wall radiation becomes negligible, and (*b*) radiation within the fluid also becomes negligible. Thus the k extrapolated to $\Delta L = 0$ is the true value of k by molecular conduction alone.

If the values of k were plotted against $(1/\Delta L)$ and extrapolated to $1/\Delta L = 0$ the true value of k by molecular conduction plus internal radiation could be expected, provided the thickness of the sample was not sufficient in any of the tests to cause natural convection.

AUTHORS' CLOSURE

The reason for the decrease in k as ΔL approaches zero, as noted in Fig. 2 by Professor Bonilla, is discussed in the paper under "Proof of the Apparatus."

The apparatus used had a constant heat loss from the test heater for a given temperature difference between the test heater and the lower copper block. This heat loss was by convection and radiation through the annular air space around the test heater to the oil bath below. Calculation of the order of magnitude of these losses shows that they account for the decrease in k shown in Fig. 2.

Thus extrapolation to zero liquid thickness not only eliminates effects of radiation and convection but also causes the effect of the heat loss from the test heater to the oil bath below to become negligible.

[5] Columbia University, New York, N. Y.

Heat Transfer and Fluid Friction During Flow Across Banks of Tubes—V

A Study of a Cylindrical Baffled Exchanger Without Internal Leakage

By O. P. BERGELIN,[1] G. A. BROWN,[2] and A. P. COLBURN[3]

The experimental results of a research program on tubular heat exchangers have been extended from unbaffled rectangular tube banks to a cylindrical baffled exchanger designed so that internal leakage can be eliminated or controlled accurately. The present results represent the first stage, in which internal leakage is essentially absent, and future work will be directed to evaluate the effects of known leakage areas. Pressure drops across a single crossflow section and a single window are measured for viscous and turbulent flow for heating, cooling, and isothermal conditions. The friction results for the crossflow section agree well with previous data on simple crossflow units in the turbulent region, but are somewhat lower in the viscous region.

Nomenclature

The following nomenclature is used in the paper:

A = heat-transfer area based on total outside exposed surface area of tubes, sq ft

A_B = heat-transfer area of tubes in crossflow section, sq ft

A_w = heat-transfer area of tubes in window sections, sq ft

c = heat capacity of oil, Btu/(lb)(deg F)

D_t = outside diameter of tube, ft

D_v = hydraulic diameter of window, ft

f_{Ct} = friction defined by $f_{Ct} = \dfrac{2\Delta p\, g_c \rho}{4G_m^2\, N}\left(\dfrac{\mu}{\mu_s}\right)^{0.14}$, dimensionless

G_m = mass velocity based on S_B, lb/(hr)(sq ft)

G_z = mass velocity based on S_z, lb/(hr)(sq ft)

g_c = conversion factor, 32.2 (mass lb)(ft)/(force lb) (sec)^2, or 4.18×10^8 (mass lb)(ft)/(force lb)(hr)^2

ΔH = loss in head, ft of fluid

h_B = oil-side heat-transfer coefficient in crossflow section, Btu/(hr)(sq ft)(deg F)

h_o = oil-side coefficient of heat transfer based on value of A, Btu/(hr)(sq ft)(deg F)

h_w = oil-side heat transfer coefficient in window section, Btu/(hr)(sq ft)(deg F)

j = heat-transfer factor defined by

$$j = \left(\frac{h_B}{cG_m}\right)\left(\frac{c\mu}{k}\right)^{2/3}\left(\frac{\mu_s}{\mu}\right)^{0.14}, \text{ dimensionless}$$

k = thermal conductivity of oil, Btu/(hr)(ft)(deg F)

L_B = baffle spacing, ft

l = minimum clearance available for flow at restrictions in each row in the crossflow section, in.

l_{avg} = average minimum clearance available for flow at restrictions in all rows in crossflow sections, in.

N = number of major restrictions encountered in crossflow section of bank

N_{Re} = Reynolds number, $\dfrac{D_t G_m}{\mu}$

N_w = estimated average number of restrictions passed in window

n = exponent of velocity as a function of heat-transfer coefficient

Δp = pressure drop across a single crossflow or window section, psf

r = area ratio, A_w/A

S_B = average of minimum cross-sectional areas for rows of tubes in crossflow section, sq ft

S_w = free cross-sectional area in baffle window, sq ft

S_z = geometric mean of S_w and S_B (noting that value of S_B should apply at last row of tubes before baffle lip)

s = minimum clearance between two adjacent tubes, ft

V_m = velocity through S_B, fps

V_w = velocity through S_w, fps

V_z = geometric mean velocity, $V_z = (V_m V_w)^{1/2}$, fps (Note that, strictly, value of V_m to be used in this relation should be based not on average value of V_m but on value for last row of tubes before baffle lip; in present exchanger these values were nearly the same in all cases.)

μ = absolute viscosity at average bulk temperature, lb/(hr)(ft), or lb/(sec)(ft)

μ_s = absolute viscosity at tube surface temperature, lb/(hr)(ft), or lb/(sec)(ft)

ρ = density at average bulk temperature, pcf

Introduction

Previous papers[4,5,6] of this series have dealt with viscous, transitional, and turbulent flow across unbaffled rectangular tube banks with different tube sizes, tube spacings, and tube arrangements. The program is now being extended to include the case of

[1] Professor, Department of Chemical Engineering, University of Delaware, Newark, Del. Mem. ASME.

[2] Research Fellow in Chemical Engineering, University of Delaware. Present address, Merck and Company, Rahway, N. J.

[3] Provost, University of Delaware. Mem. ASME.

Contributed by the Heat Transfer Division and presented at the Annual Meeting, New York, N. Y., November 29–December 4, 1953, of The American Society of Mechanical Engineers.

 Manuscript received at ASME Headquarters, September 3, 1953. Paper No. 53—A-173.

[4] "Heat Transfer and Fluid Friction During Viscous Flow Across Banks of Tubes," by O. P. Bergelin, A. P. Colburn and H. L. Hull, University of Delaware, Engineering Experiment Station, Bulletin No. 2, 1950.

[5] "Heat Transfer and Fluid Friction During Viscous Flow Across Banks of Tubes—III. A Study of Tube Spacing and Tube Size," by O. P. Bergelin, G. A. Brown, H. L. Hull, and F. W. Sullivan, Trans. ASME, vol. 72, 1950, pp. 881–888.

[6] "Heat Transfer and Fluid Friction During Flow Across Banks of Tubes—IV. A Study of the Transition Zone Between Viscous and Turbulent Flow," by O. P. Bergelin, G. A. Brown, and S. C. Doberstein, Trans. ASME, vol. 74, 1952, pp. 953–960.

the cylindrical exchanger containing baffles. The present model is in many ways similar to the conventional shell-and-tube exchanger, but certain modifications have been made to simplify the internal flow pattern. In future work these simplifications will be removed, one by one, until finally the complex conditions of the commercial exchanger will be reached.

In considering the performance of any baffled heat exchanger the leakages known to occur in all exchangers have always been factors of unknown magnitude.[7] The resulting uncertainty has prevented a precise experimental treatment of the effect of baffle spacing and baffle cut-down. Therefore it was felt that the present systematic study of tubular heat exchangers should first consider baffled exchangers without any internal leakage. Later each known type of leakage can be studied and its effect evaluated. The present paper deals with the case of a cylindrical exchanger in which the baffle spacing and cut-down are varied, but in which entrance and exit effects and all internal leakages are eliminated or minimized.

Equipment and Procedure

The over-all experimental apparatus has been described previously[4,6] and so only new features of equipment will be described here. The exchanger, shown partially assembled in Fig. 1, has the dimensions given in Fig. 2 and Table 1A. The unusual features of this exchanger are the gasketed tube sheets, the gasketed baffles, the pressure taps within the tube bundle, and the extra-wide nozzles for the shell-side fluid.

The gasketed tube sheets used in this exchanger are designed[8] so that different baffle arrangements can be made up in the laboratory without cutting out the old tubes and rolling in new ones. In order to be sure that there is no mixing of the oil and water, double tube sheets are used with a vented space between them. The tube sheets are drilled somewhat larger than the tubes and each tube sheet has a sheet of neoprene bonded to one face. Holes somewhat smaller than the tube diameter are cut in the neoprene, and when the tube is pushed through the tube sheet a tight gasket is formed. A sheet of neoprene also is bonded to each baffle and the tube holes drilled out the same way as in the tube sheets. The sheet of neoprene is allowed to extend about $^1/_{32}$ in. beyond the edge of the baffle to form a gasket against the inner wall of the bored shell of the exchanger. In this way two of the major internal leakage paths are closed. The third type of internal leakage, by-passing between the bundle and shell, is not completely eliminated in this exchanger but is minimized. Fig. 2, a cross-section drawing of the exchanger, shows how the tubes are placed as close to the shell as practicable. The narrow side clearance, and the use of spacer bars which also serve as sealing strips, allow little or no leakage past the bundle for the middle half of the exchanger. With small baffle cut-downs the bundle by-passing may be appreciable, but even in the extreme case it is less than in the usual commercial exchanger. A study of by-passing will be made later with an exchanger containing more tubes so that a row of tubes around the periphery may be removed to increase the amount of by-passing.

Entrance and exit effects have been minimized in this exchanger by using large rectangular entrance nozzles as shown in Fig. 1. Moreover, the inner tube sheet is of such thickness that the face of the tube sheet is in line with the edge of the nozzle. In this way the incoming fluid is spread nearly uniformly across the tube bundle and the leaving fluid can escape freely. For narrow baffle spacings a plastic insert is placed in the nozzle and a plastic false

[7] "Shell Side Characteristics of Shell and Tube Heat Exchangers," by Townsend Tinker, General Discussion of Heat Transfer, The Institution of Mechanical Engineers, London, England, 1951.

[8] The original design was developed by J. I. Stevens in 1948, when Stevens was associated with the project as Research Fellow.

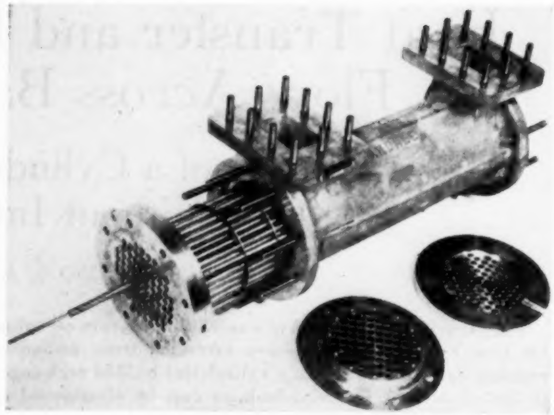

Fig. 1 Partially Assembled Exchanger

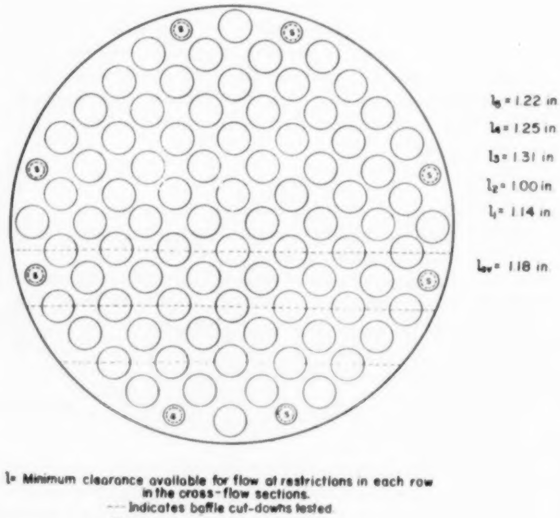

Fig. 2 Diagram of Tube Bundle Showing Cutdowns

tube sheet is used to give the initial and final shell passes the same spacing as the others.

The exchanger, connected for a series of tests, is shown in Fig. 3. The apparatus is insulated by filling the box surrounding the exchanger and headers with vermiculite. Isothermal runs at the operating-temperature level are made to determine the heat loss to the surroundings.

The usual pressure-drop measurements are made at the headers across the whole exchanger. Measurements also are made over a crossflow section and a window section about halfway along the exchanger at the levels of the baffle cutdowns, as shown in Fig. 4. The lines to the manometers are taken off the ends of the dummy tubes and brought out of the water headers through packing glands.

The temperatures of the streams entering and leaving the exchanger are measured with copper-constantan thermocouples located beyond the headers to the exchanger. Temperature differences are measured with multijunction, series-connected, differential thermocouples as described previously.[4]

TABLE 1 DIMENSIONS OF EXCHANGER

A-Basic Dimensions

Inside shell diameter	5.25 in.
Number of tubes	80
Length between tube sheets ..	16-1/8 in.
Baffle thickness	1/8 in. (1/16-in. brass plus 1/16 in. neoprene)
Tube arrangement	Staggered square pattern with 1.25 pitch ratio
Tubes	3/8 in. 18-gage copper tubes cored with 3/16-in. rods

B-Dimensions for Various Baffle Spacings and Cutdowns

Baffle cutdown, % of diameter	18.4 per cent (N = 10)			31.0 per cent (N = 6)			43.7 per cent (N = 2)		
Number of baffles ...	7	13	25	7	13	25	3	7	13
Distance between baffles, in.	1.906	0.976	0.500	1.906	0.976	0.500	3.72	1.906	0.976
Cross-flow area, S_p, sq ft	0.0204	0.0104	0.00535	0.0204	0.0104	0.00535	0.0398	0.0204	0.0104
Window free area, S_w, sq ft	0.0124	0.0124	0.0124	0.0239	0.0239	0.0239	0.0366	0.0366	0.0366
Total heat transfer area, A, sq ft ..	9.90[a]	8.91[a]	8.47	9.85	9.49	8.77	9.59	9.94	9.02
Window heat-transfer area, A_w, sq ft .	1.64	1.61	1.61	4.28	4.40	4.37	5.93	7.21	7.05
Symbol on graphs	○	□	△	●	■	▲	-◇-	-○-	-□-

[a] One dummy tube; in all other cases two dummy tubes were used. Note also that the number of baffles and the plastic false tube sheets affect the heat-transfer area.

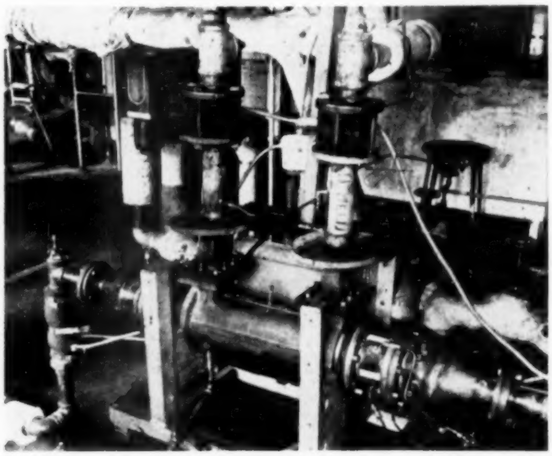

FIG. 3 EXCHANGER CONNECTED FOR TESTS

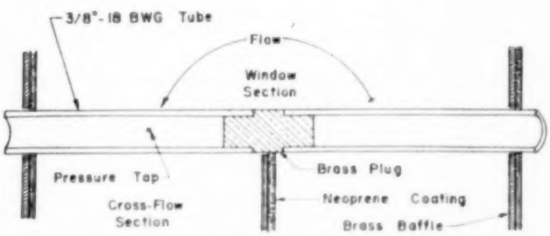

FIG. 4 DETAILS OF INTERNAL PRESSURE TAP

The equipment variables in this set of tests are the spacing and cutdown of the baffles. The range of these variables and the corresponding exchanger constants are given in Table 1B. The fluids used on the shell side of the exchanger are Gulfcrown C oil for low Reynolds numbers and Gulf 896 oil for high Reynolds numbers. The properties of these oils are given in Table 2.

RESULTS OF TESTS

This paper presents the experimental results for oil flowing on the shell side of a baffled cylindrical exchanger without internal leakages. Four baffle spacings and three baffle cutdowns are treated. Heating, cooling, and isothermal runs are reported for the oil at an average bulk temperature of 150 F over a Reynolds number range of 2.5 to 14,000. The average crossflow velocity varies from 0.5 to 10 fps, and the window velocity varies from 0.2 to 10 fps. Water at 125 F is used for cooling and at 175 F for heating.

Average oil film coefficients of heat transfer for the shell side range from 35 to 900 Btu/(sq ft)(hr)(deg F), and the calculated water-film coefficients are 1819 at 125 F and 2365 at 175 F. The oil-film coefficients are calculated by subtracting the resistance of the water film and the metal wall from the over-all coefficients. Heat balances are within ±5 per cent for all but a few runs at very low oil rates. A standard run which was made at the beginning and end of the tests gave identical results and showed that there was no measurable fouling of the heat transfer surfaces during the period of testing.

DISCUSSION OF RESULTS

Pressure Drop

The pressure taps which are located within the tube bundle are at the levels of the edges of successive baffles so that the pressure drop across one crossflow section and across an adjacent window can be measured. The dividing line between these two zones is arbitrarily taken as at the level of the tips of the baffles.

TABLE 2 PHYSICAL PROPERTIES OF TEST OILS

t, deg F	c_p [a], Btu/(lb)(deg F)	k [b], Btu/(hr)(ft)(deg F)	μ [c], lb/(hr)(ft)	$c\mu/k$, None	$(c\mu/k)^{2/3}$, None	ρ, pcf
Gulf Crown "C" Oil						
90	0.476	0.0749	1000	6370	344.0	55.0
110	0.487	0.0744	500	3270	220.0	54.6
130	0.499	0.0739	285	1925	155.0	54.2
150	0.510	0.0734	166	1153	111.9	53.8
170	0.522	0.0729	105	752	82.8	53.4
190	0.533	0.0724	73	538	66.3	53.0
Gulf 896 Oil						
80	0.486	0.0814	10.1	60.4	15.4	50.6
110	0.504	0.0807	6.82	42.5	12.2	49.9
140	0.521	0.0799	4.91	31.9	10.1	49.2
170	0.538	0.0792	3.72	25.3	8.61	48.5
200	0.558	0.0784	2.91	20.6	7.52	47.8

[a] Calculated using equation of Watson and Nelson, *Industrial and Engineering Chemistry*, vol. 25, 1933, p. 880: $c_p = [0.6811 - 0.308s + t(0.000815 + 0.000306s)]\,(0.055K + 0.35)$, where s = specific gravity at 60 F; t = temperature, deg F; K = characterization factor

[b] Calculated using equation of C. S. Cragoe, Bureau of Stds. Misc. Pub. No. 97: $k = 1/12 \dfrac{0.813}{\text{sp gr}} [1 - 0.0003 (t - 32)]$.

[c] Experimentally determined values.

Experiments showed that the pressure drop varies differently with velocity in the two zones and so the discussion of the pressure drop for each zone will be taken up separately. When the pressure drop over the measured zones is multiplied by the number of such zones in the exchanger, with minor corrections for the entrance and exit effects, the results check the measured over-all pressure drop closely, and therefore the measurements are considered representative of all zones in the exchanger.

Crossflow Section. The variation in pressure drop with linear velocity in the crossflow zone is shown in Fig. 5. In this figure the pressure drop is per flow restriction, and the velocity is calculated on the basis of the average of the minimum cross-sectional areas through the restrictions, as shown in Fig. 2.

In order to cover a wide range of Reynolds numbers, two oils of different viscosity are used and these have resulted in one set of data for viscous flow and another for turbulent flow. Heating, cooling, and isothermal runs are all presented, which accounts for the spread of points for any given baffle configuration as would be expected. The line drawn through the turbulent-flow points represents the pressure drop for the previously tested simple crossflow exchanger with the same tube size, arrangement, and spacing. No data are available to provide a similar comparison for the more viscous oil.

In Fig. 6 the same data are shown as the friction factors versus the Reynolds number. Again in the turbulent range there is some spreading as a result of baffle configuration but the line for the simple crossflow unit is fairly representative. In the viscous-flow region the friction factors fall consistently below those for the crossflow exchanger with the difference increasing at the lower flow rates. No explanation has so far been found for this behavior.

Baffle Window. The pressure drop through the baffle window for the lighter oil is shown as a function of the velocity through the window in Fig. 7. The data spread considerably, with those having the highest ratios of crossflow to window velocity being highest. To include this effect, the geometric mean of the crossflow and the window velocities is used as shown in the lower part of Fig. 8. Although the flow conditions in the window are so complicated that probably no simple average velocity is truly representative, the geometric mean velocity does improve the correlation considerably. The viscous-flow data are shown in the upper part of Fig. 8. The geometric mean velocity is found to be more

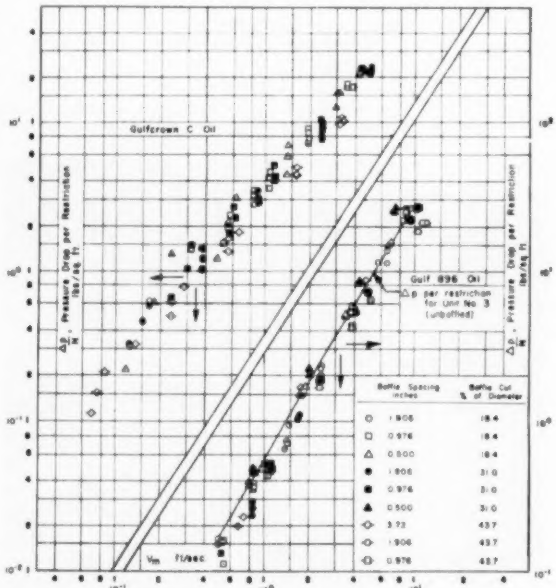

FIG. 5 PRESSURE DROP PER RESTRICTION IN CROSSFLOW AREA

suitable in this case too, but there is still considerable spread for the various baffle configurations. The conditions of flow through a baffle window have not yet been analyzed sufficiently to make a generalized interpretation on the basis of local friction and kinetic losses.

As a preliminary method of attack in a rather simple manner, the following method is suggested for making estimates of pressure drop in the window sections of heat exchangers. For turbulent flow through the crossflow section, Fig. 5 shows an intercept at V_m = 1 fps of from 0.403 to 0.576, with the best line passing through about 0.446; thus

$$\frac{\Delta p}{N} = 0.446\, V_m^{2} \qquad [1]$$

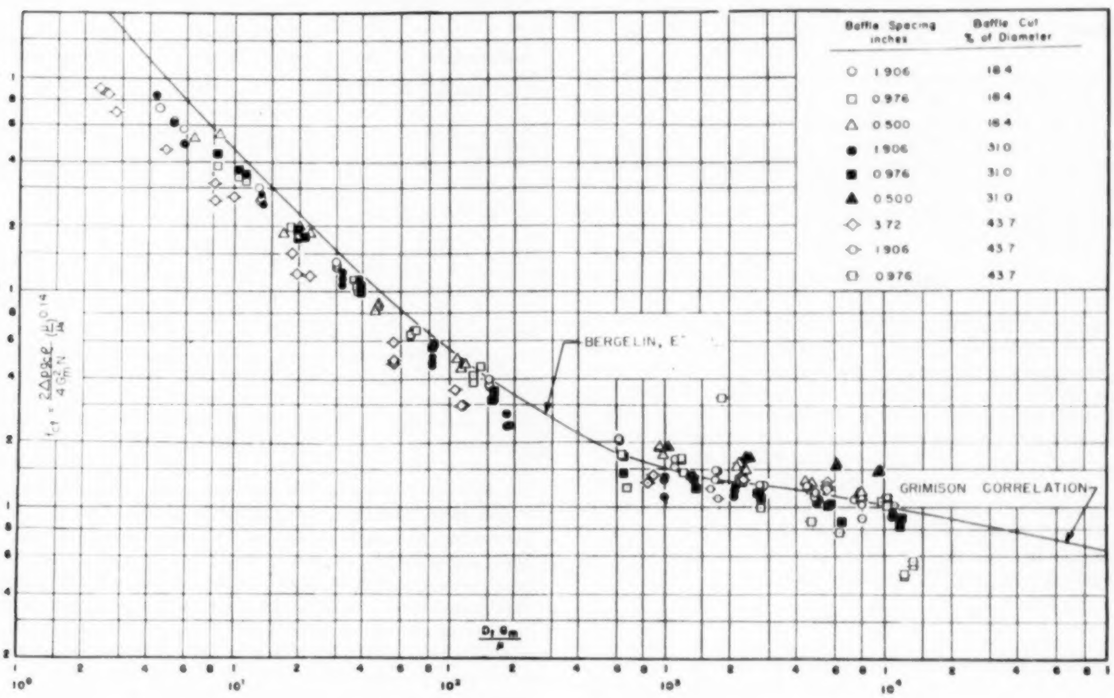

Fig. 6 Friction Factor f_{ct} for Crossflow Section

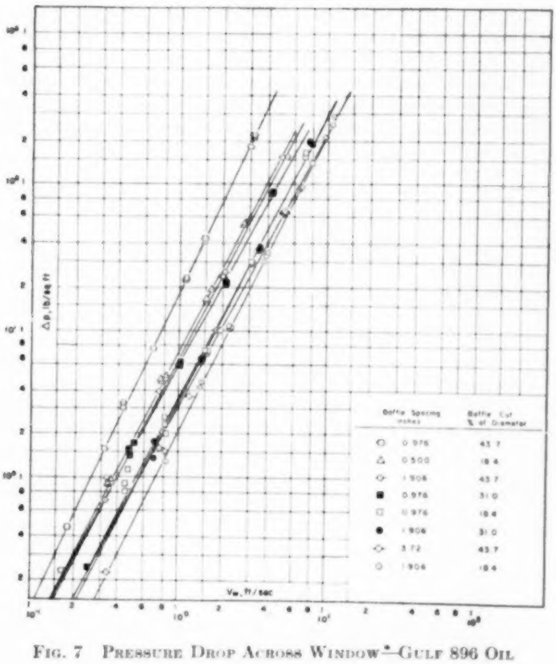

Fig. 7 Pressure Drop Across Window—Gulf 896 Oil

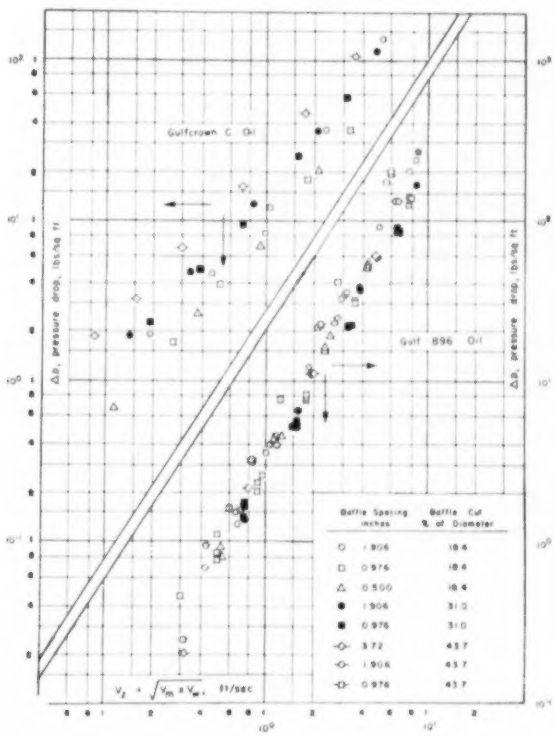

Fig. 8 Pressure Drop Across Window as a Function of V_z

whence
$$\frac{\Delta H}{N} = \frac{\Delta p}{N\rho} = \frac{(0.446)(64.4)}{49}\,\frac{V_m^2}{2g_c} = 0.6\,\frac{V_m^2}{2g_c} \ldots [2]$$

That is, the loss in head per row of tubes can be estimated as about 0.6 of a velocity head.

In the baffle window there is, in this exchanger, flow across tubes plus a complete reversal of direction, and also flow along the tubes. If, for turbulent flow, the friction for the flow along the tubes is neglected and the loss owing to reversal of direction is estimated as 2 velocity heads, the total window pressure drop can be estimated as

$$\Delta p_w = (2 + 0.6N_w)\,\frac{\rho V_z^2}{2g_c} \ldots\ldots\ldots\ldots [3]$$

where the velocity head $\rho V_z^2/2g_c$ is determined from the geometric mean velocity V_z, and N_w is an estimated number of restrictions passed in the window. On the basis of the present data, $^1/_2$ of the number of restrictions above the baffle is suggested, although in the present case, as Fig. 2 shows, there is so little free space above the final restriction that this restriction is neglected, giving N_w equal to 1, 3, and 5 for the three baffle-cuts shown.

For viscous flow a similar procedure is used but instead of the velocity head a viscosity-velocity unit, defined as $V\mu/s$ and using lb-ft-sec dimensions, is used. For the crossflow section, from Fig. 5, the best line for the isothermal data passes through a value of 3.25 psf at $V_m = 1$ fps. Thus

$$\frac{\Delta p}{N} = 3.25V_m \ldots\ldots\ldots\ldots [4]$$

Since the viscosity at 150 F is, from Table 2, equal to 166 lb/(hr)(ft) or to 0.046 lb/(sec)(ft), and the minimum clearance tube-to-tube is 3/32 in. or 0.0078 ft

$$\frac{\Delta p}{N} = \frac{(3.25)(0.0078)}{(0.046)}\,\frac{V_m\mu}{s} = 0.55\,\frac{V_m\mu}{s} \ldots\ldots [5][3]$$

That is, the pressure loss in pounds per square foot can be estimated as 0.55 velocity-viscosity unit per row of tubes or per restriction.

In the baffle window the friction across and along the tubes for viscous flow may be much more important than the kinetic-energy loss in reversal of direction of flow so the latter can be neglected except at velocities above 1 fps. Allowing 0.8 unit loss for friction during longitudinal flow for each ratio of L_B to D_v and 0.55 per row for friction across tubes, the expression for pressure drop in the window can be written as

$$\Delta p_w = \frac{0.55\,N_w V_z \mu}{s} + \frac{0.8\,V_z\mu}{D_v}\left(\frac{L_B}{D_v}\right) + \frac{2\rho V_z^2}{2g_c} \ldots\ldots [6]$$

where N_w is estimated as before, and Δp_w = pressure loss in psf for one window.

When this method of estimating pressure drop is applied to the three window sections covered by the present experiments, the results given in Table 3 are obtained at a value of V_z of 1 fps.

The agreement between calculated and experimental results is fairly good considering the complicated conditions in the baffle window and, until more thorough methods are developed, this procedure may prove useful for estimates.

Heat Transfer

The values of heat-transfer coefficients are first plotted versus the linear velocity through the average of the minimum cross-sectional areas of the restrictions within the baffled section as shown in Fig. 9. A comparison of these results with those of the simple crossflow unit is shown by the line representing such data. For turbulent flow the results fall into three groups with the higher values occurring with the smaller values of baffle cutdown. It is apparent that the tubes in the window area for the larger windows do not transfer heat as rapidly as those in the baffled section. Within each configuration there is a slight variation between the heating and cooling runs, as would be expected.

It is rather surprising to note that for the smallest window the rate of heat transfer is higher than for the similar simple crossflow unit represented by the dotted line. One possible explanation is that, in the crossflow exchanger where the fluid entered in smooth flow, the first rows of tubes may have had low heat-transfer rates because of the entrance effect, and thus lowered the average for the ten rows. In the baffled exchanger, on the other hand, each window turnaround may have caused enough turbulence to maintain a high rate of heat transfer throughout the exchanger. For the two larger baffle windows, the effects of the low window velocity and the short crossflow section combine to give a lower rate of heat transfer.

For heat transfer it was not considered feasible to make temperature measurements within the bundle in order to separate the window from the crossflow zone, as was done in measuring pressure drops. However, the evident effect of baffle configuration in Fig. 9 indicates that the rate of heat transfer in the window differs from that in the crossflow zone, and that the effect is undoubtedly some function of the baffle dimensions. For the whole exchanger, the total heat transfer can be considered as the sum of that in the baffled section and in the window area. For the case of a relatively large number of baffles the mean temperature difference can be considered the same in each area. Then

$$h_o A = h_B A_B + h_w A_w \ldots\ldots\ldots\ldots [7]$$

or

$$h_B = h_o / \left[1 - r + r\left(\frac{h_w}{h_B}\right)\right] \ldots\ldots\ldots\ldots [8]$$

where $r = A_w/A$.

The crossflow experiments can be represented by

$$h_B = bV_m^n \ldots\ldots\ldots\ldots [9]$$

As a first approximation it will be assumed that the same relationship holds in the baffle window when the geometric mean velocity is used, or

$$h_w = bV_z^n = bV_m^{n/2}V_w^{n/2} \ldots\ldots\ldots\ldots [10]$$

Dividing Equation [10] by Equation [9]

$$\frac{h_w}{h_B} = \left(\frac{V_w}{V_m}\right)^{n/2} = \left(\frac{S_B}{S_w}\right)^{n/2} \ldots\ldots\ldots\ldots [11]$$

Substituting for the ratio of h_w/h_B in Equation [8]

[3] This is a dimensional equation; to express it as dimensionless it can be written

$$\frac{\Delta p}{N} = \frac{(0.55)\,(32.2)}{g_c}\,\frac{V_m\mu}{s} \ldots\ldots\ldots\ldots [5a]$$

TABLE 3 PRESSURE LOSS IN WINDOW AREA, PSF, AT V_z = 1 FPS

Turbulent Flow						
Baffle cutdown	18.4 per cent			31 per cent		43.7 per cent
Calc'd,[a] Eq. [3]	2.0			2.9		3.8
Exp'l, Fig. 8	2.6			2.6		4.3
Viscous Flow						
Baffle cutdown	18.4 per cent			31 per cent		43.7 per cent
Baffle spacing, in.	1.91	0.98	0.50	1.91	0.98	3.72
Calc'd,[b] Eq. [6]	11.1	8.2	6.6	18.0	14.8	29.8
Exp'l, Fig. 8	12.0	8.5	7.8	16.0	14.0	25.0

[a] $\Delta p = (2 + 0.6N_w)\,\frac{49}{64.3} = 0.76\,(2 + 0.6N_w)$

[b] $\Delta p = \frac{(0.55)\,(0.046)N_w}{0.00782} + \frac{(0.8)\,(0.046)}{(0.031)}\,\frac{L_B}{D_v} + \frac{2(57)}{64.3} = 3.25N_w + 1.18L_B/D_v + 1.77$

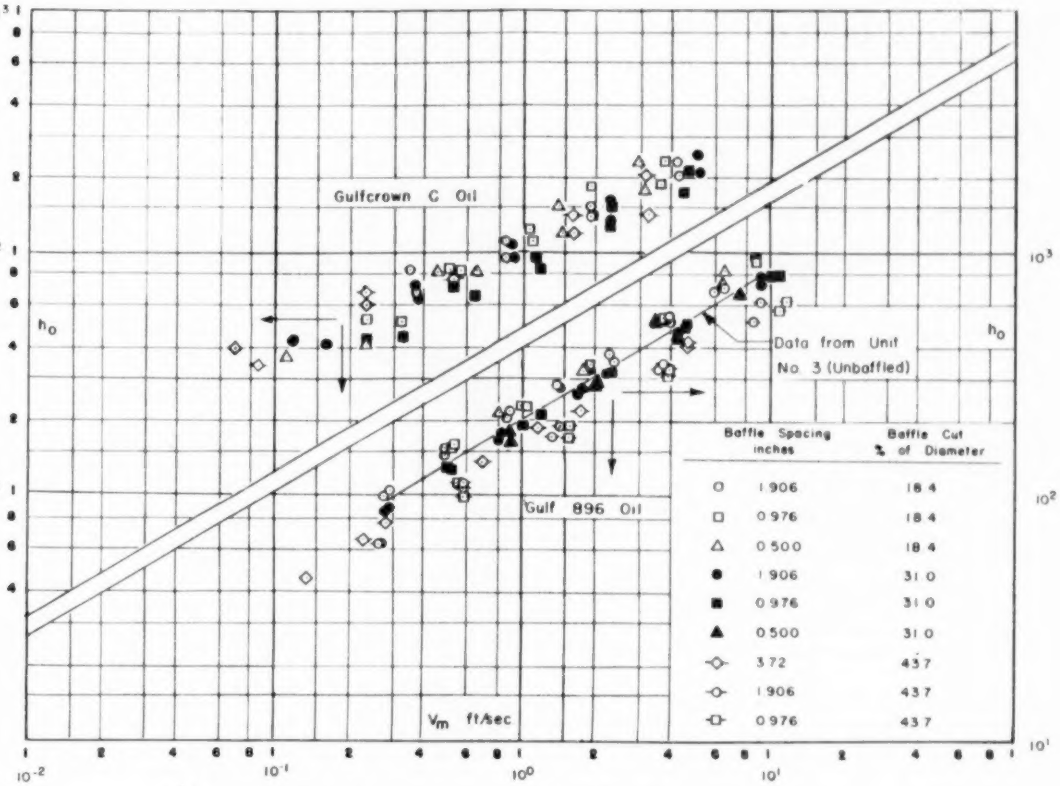

Fig. 9 Oil-Film Coefficient of Heat Transfer—Heating and Cooling

$$h_B = h_o / \left[1 - r + r\left(\frac{S_B}{S_w}\right)^{n/2}\right] \qquad [12]$$

From Fig. 9, the values for n are found to be 0.6 for turbulent flow and 0.48 for viscous flow. When the observed heat-transfer coefficients for the whole exchanger are corrected in this manner to give values of h_B, Fig. 10 shows that the spread of the data is much less and, for turbulent flow, the agreement with the simple crossflow exchanger is greatly improved.

The corrected heat-transfer coefficients are plotted as j-factors in Fig. 11, with the line representing the case of the simple crossflow exchanger. In the turbulent range the agreement is fairly good but the data for the large cutdown are still low, indicating that the value of b in Equation [10] is probably lower than in Equation [9], especially for large cutdowns. It is hoped that additional studies in these laboratories will permit experimental determination of heat transfer in the window area separately from the baffle section to resolve this problem.

In the viscous region, the data are consistent among themselves but fall below the line for simple crossflow units, similar to the friction data in Fig. 6. So far no satisfactory explanation has been found for this behavior, and further study of this region of flow is under way.

To use the heat-transfer results in design, it is suggested for the present that the heat-transfer coefficients in the baffle section and in the window be predicted separately and then combined using Equation [7]. For the baffled section, Fig. 11 would be used in the usual manner. For the window area, Fig. 11 also would be used, except the value used for velocity would be G_e not G_m.

Conclusions

1 For turbulent flow the pressure drop per restriction in the crossflow section of a cylindrical heat exchanger having no internal leakage is practically the same as the pressure drop in a simple crossflow exchanger of similar tube arrangement. For viscous flow the pressure drop is somewhat less than for the simple crossflow exchanger.

2 The pressure drop through a baffle window, where the window contains tubes, is a function of both the velocity through the window and the velocity across the tubes in the window. The geometric mean of the window velocity and the crossflow velocity is more suitable for correlation but is not wholly satisfactory.

3 For turbulent flow the loss in head in flowing through a baffle window can be estimated as the sum of the frictional resistance of the tubes plus two velocity heads for the change in flow direction, all based on the geometric mean velocity. For viscous flow the loss in head owing to change in direction is negligible below a velocity of 1 fps; the frictional resistance for flow across and along the tubes in the window area is estimated utilizing a newly defined velocity-viscosity unit, also based on the geometric mean velocity.

4 For turbulent flow, fair agreement of the heat-transfer data for the whole exchanger with data from the simple crossflow exchanger of similar tube arrangement is obtained if correction is made for a different velocity in the window area. For viscous flow the correction helped agreement among the data for various cutdowns but, as with the friction results, the data in general fell somewhat lower than results in the simple crossflow exchanger.

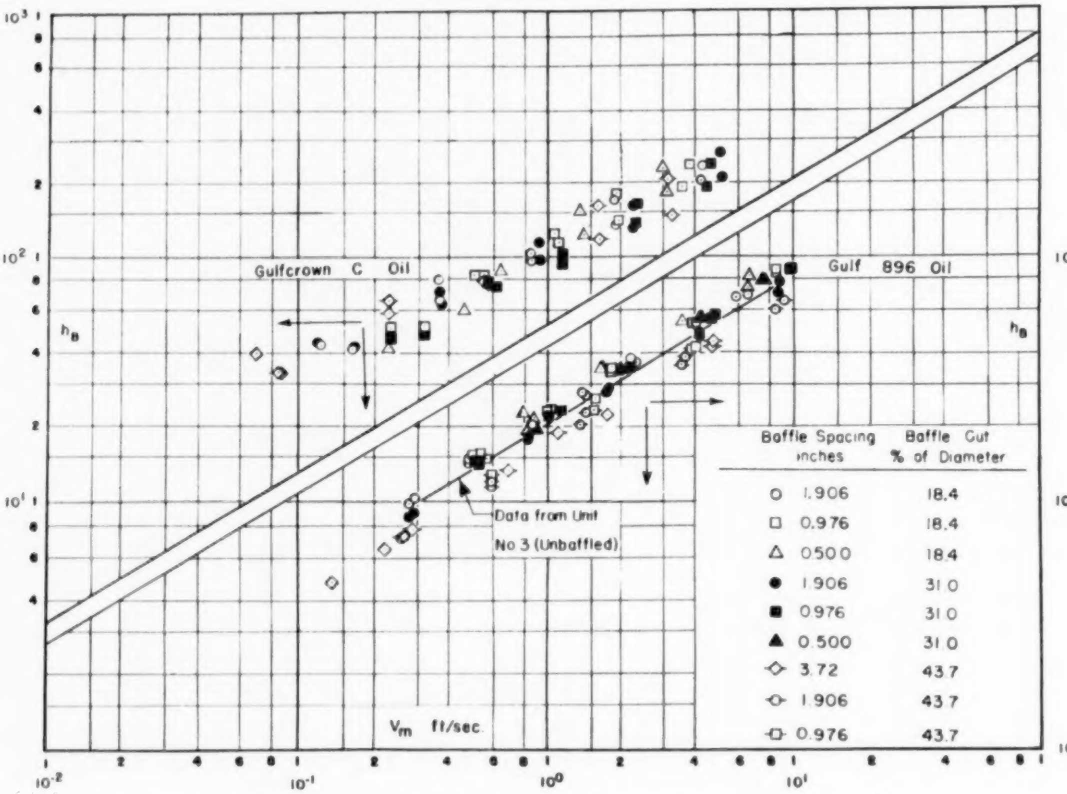

Fig. 10 Oil-Film Coefficient of Heat Transfer in Crossflow Section—Heating and Cooling

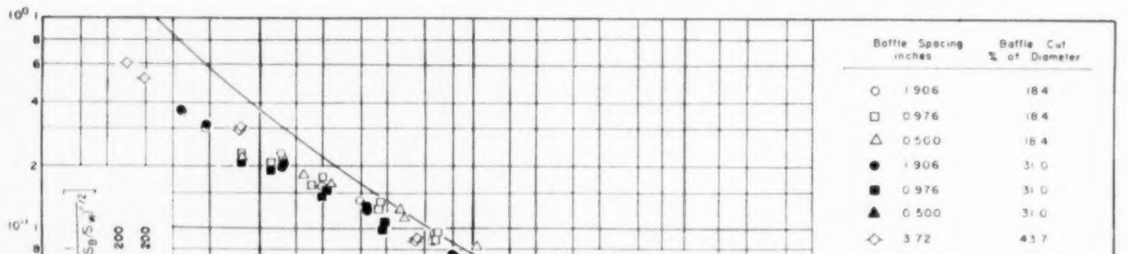

Fig. 11 Corrected Heat Transfer Factor j for Entire Exchanger

It should be pointed out that the foregoing conclusions are based upon experiments in which internal leakages were believed to be negligible. For commercial exchangers allowances must be made for the important effects of such leakages.

ACKNOWLEDGMENT

The authors acknowledge the many valuable suggestions by the ASME Special Advisory Committee of the Heat Transfer Division, which is sponsoring this co-operative research project. The committee at the time of the work was composed of W. H. McAdams, Chairman, C. H. Brooks, A. P. Colburn, S. Kopp, A. C. Mueller, B. E. Short, W. H. Thompson, T. Tinker, and P. R. Trumpler. The help of A. Wurster in the design and construction of the test unit was invaluable. Assistance in the experimental work was given by Research Fellows K. J. Bell, J. J. Fusco, and J. F. Tompkins. Funds and equipment were kindly furnished by the American Petroleum Institute, the Tubular Exchanger Manufacturers' Association, Andale Company, and the E. I. du Pont de Nemours and Co. The oil was provided by the Gulf Oil Corp.

Discussion

D. A. Donohue.[10] These remarks are prefaced by an expression of admiration for the excellent research program being conducted at the University of Delaware under the guidance of the authors.

In a paper[11] by the writer some years ago, it was shown that in all heat exchangers for which experimental data had been published, only part of the total flow penetrated the tube bundle while most of the remainder by-passed to flow through the annulus between the tube bundle and its enclosing shell. The fraction of flow penetrating the tube bundle varied in the different units tested but for the case of 50 per cent penetration in turbulent flow the pressure drop would be 25 per cent and the heat-transfer coefficient 67 per cent of that obtainable with 100 per cent penetration. As a consequence the heat exchanger would have to be 50 per cent larger than if full flow penetration had occurred.

Since that time two papers have been published on attempts made to force all of the fluid to flow into the tube bundle. In the first of these Williams and Katz[12] employed a tube layout in which an outer row of tubes was moved into the annulus and a space left between this outer tube circle and the tube bundle. Much greater, if not complete, flow penetration resulted.

In the other paper, which is the present publication, the shell has been completely filled with tubes and open areas filled in with dummy tubes to choke off by-passing. It appears from Figs. 6 and 11 of this paper that complete or very nearly complete flow penetration has been achieved. Having indicated the extent to which flow may by-pass the tube bundle, it is advisable in this connection to recall the floating-head, removable-tube-bundle-type heat exchanger.[11] Its inherent construction is such that a sizable open annulus exists between the tube bundle and shell through which considerable by-passing occurs. Therefore the results of the present paper and of Williams and Katz[12] are not directly applicable to the floating-head, removable-tube-bundle-type heat exchanger which is perhaps the most commonly used construction for industrial heat exchangers. The University of Delaware study plans to remove peripheral tubes from the tube bundle in order to observe the effects.

[10] Chemical Construction Corporation, New York, N. Y.

[11] "Heat Transfer and Pressure Drop in Heat Exchangers," by D. A. Donohue, *Industrial and Engineering Chemistry*, vol. 41, 1949, pp. 2499–2511.

[12] "Performance of Finned Tubes in Shell-and-Tube Heat Exchangers," by R. B. Williams and D. L. Katz, Trans. ASME, vol. 74, 1952, pp. 1307–1320.

TABLE 4 CONSTRICTIONS IN CROSSFLOW PATHS

Size baffle cutout, per cent of diam	No. of constrictions between baffle edges	No. of constrictions between centers of cutout
18.4	10	11
31	6	9
43.7	2	7

The idealized average path of a fluid flowing through a segmentally baffled shell was described some 19 years ago by Perrone[13] as consisting of two components: One in crossflow normal to the tubes extending from the center of gravity of one baffle cutout to the center of gravity of the next successive baffle cutout, the other parallel to the tubes having a length equal to the baffle spacing. This concept has been accepted generally as a rational method of analysis.

In this paper the authors have not separated the pressure drop into exactly these same components but instead have divided it into a crossflow component extending from the straight edge of one baffle to the straight edge of the next successive baffle, and into another component which includes both the orifice effect of flow through the baffle cutout plus the crossflow distance from the center of gravity of the opening to the straight edge of the baffle. For comparison the number of constrictions in each of the two different crossflow paths for each of the three different-size baffle cutouts tested are given in Table 4 of this discussion.

It may be noted that for the 43.7 per cent cutout the crossflow component included with the orifice effect is 2.5 times that between baffle edges. It would seem that a method of correlation which lumps the crossflow effect with the orifice effect necessarily will be complex and empirical because it includes the effect of the size of cutout on the crossflow component and the effect of tube layout on crossflow penetration.

The authors located pressure taps at each side of one baffle edge and at the edge of the next baffle. These readings give their two pressure-drop components, namely, crossflow from the edge of one baffle to the edge of the next, and through the baffle cutout involving both parallel and crossflow. The pressure loss observed in this single baffled compartment multiplied by the number of compartments in the exchanger was checked against the measured over-all pressure drop. Unfortunately, in many cases the over-all value differed from the sum of the components by 10 to 30 per cent. If one component were assumed to be correct then the other could be off by as much as twice these amounts. Possible reasons for this variation may be that the pressure drop is not uniform through each compartment, or that kinetic energy is dissipated in eddy motion at dead spots.

In any event it appears that measurements are needed at more locations in order to account for the spread between component and over-all pressure-drop values. In addition, it is suggested that pressure taps be installed at the center of the cutout and that the distance between these taps be varied in an attempt to isolate the orifice-discharge component of pressure drop.

Regarding the experimental technique used to evaluate the coefficient of heat transfer, it is found that when the quantity of oil is small the heat balance of the oil and water streams diverges greatly in some cases and confirmation of the Btu/hr of heat transferred as calculated from the oil quantity and temperatures is lacking. This could be overcome by reducing the quantity of water circulated. Since in these tests h deviates from a straight-line relation with Reynolds number at low values of Reynolds number it would be desirable to have a check on h by means of a close heat balance between the two fluids.

A. F. Fritzsche.[14] This fifth report on the results of the re-

[13] "Pressure Drop and Heat Transfer in Exchangers," by S. A. Perrone, *Oil and Gas Journal*, vol. 33, March 28, 1935, pp. 71–72, 75–76.

[14] Winterthur-Seen, Switzerland

search program on tubular heat exchangers conducted at the University of Delaware shows that the experimental work has been carried out with the usual care and attention to detail for which the leaders of the project have once more earned our acknowledgments and thanks. The tests have been performed on a cylindrical exchanger in which the leakage areas between tubes and baffles and between baffles and shell have been eliminated in a most ingenious manner. The authors also assume that the third and most serious type of internal leakage, that between the tube bundle and the shell, has been almost completely eliminated in the design of the exchanger. The deviation of the experimental results from those previously measured in the corresponding simple crossflow exchanger model for which the authors can offer no explanation, demonstrates, however, that the by-passing of the tube bundle is still appreciable in the low Reynolds number range.

It is clear that such a partial by-passing would tend to give values of the friction and heat-transfer factors which are too low when correlated in the manner used by the authors in their Figs. 6 and 11. Because of the leakage around the bundle the actual or effective flow velocity between the tubes is smaller than the mean or apparent flow velocity based on the total free cross-sectional area, and therefore both the pressure drop and heat-transfer coefficient will actually be lower than the values to be expected at the mean velocity.

Tests conducted by the writer some years ago,[15] which were also described in a communication discussing the papers presented by T. Tinker to the General Discussion on Heat Transfer in London, September, 1951,[16] not only confirm this explanation in a qualitative way, but afford an approximate check on the amount of deviation which is to be expected as a result of the by-pass areas obtaining in the exchanger used here.

These tests were performed on a rectangular tube bundle similar to those used in the previous experiments at the University of Delaware, the side walls of which could be assembled at different distances from the outermost row of tubes. With this apparatus it was thus possible to determine the connection between the actual flow velocity through the tube bundle and the size of the by-pass areas, and the results of the tests were plotted nondimensionally, showing the ratio of effective to apparent flow velocities as a function of the ratio of effective to ideal flow areas (the ideal flow area corresponding to a tube bundle without any leakage flow).

According to these results an increase in the by-pass area reduces the flow velocity through the tube bundle more strongly in a bundle of small tube pitch than in one with widely spaced tubes and this reduction increases appreciably with decreasing Reynolds number. This is fully in accordance with the results under discussion, which check well with the earlier correlations (within the spread resulting from secondary influences) in the turbulent region but which deviate increasingly at the lower Reynolds numbers.

The ratio of the effective to the ideal flow areas is somewhat difficult to determine in the staggered square arrangement of tubes used here. It is, however, to be expected that the value of 1.15 determined as the mean value for the tube rows concerned from the dimensions given in Table 1 is fairly representative. The tests just described indicate a decrease of the actual flow velocity between the tubes as against the apparent velocity based on the mean area by a factor of about 0.9 at $N_{Re} = 10^4$ and a factor of about 0.8 at $N_{Re} = 100$, increasing still further for smaller Reynolds numbers to a factor of perhaps 0.7 at $N_{Re} = 5$ (extrapolated!). From these figures it can be seen that even a small by-pass area influences the flow in a baffled heat exchanger to a high degree in the range of viscous flow. If the curves representing the earlier correlations obtained on simple crossflow exchangers in Figs. 6 and 11 are now transposed toward lower Reynolds numbers in accordance with the factors previously indicated, the correlation with the test results on the baffled heat exchanger becomes almost as good in the laminar region as it is in the turbulent régime.

The tests performed by the writer covered but two tube pitches and only Reynolds numbers between about 200 and 5000, and are to be considered as being more of a preliminary nature. The unbaffled rectangular exchangers used in the earlier parts of the University of Delaware research program seem to be ideally suited to conduct the necessary confirmation tests and to extend the study to tube bundles with a wider range of tube pitches, tube layouts, and particularly to the region of laminar flow, and to nonisothermal conditions. It is believed that the study of the by-pass flow which is envisaged with a baffled exchanger containing a large number of tubes, some of which can be removed to increase the leakage flow, will not provide the same amount of detailed information as the tests on the unbaffled exchangers proposed in the foregoing.

[15] "Gestaltung und Berechnung von Oelkühlern" (Design and Calculation of Oil Coolers), by A. F. Fritzsche, 1953, Verlag Leemann, Zürich, Switzerland.

[16] Proceedings of the General Discussion on Heat Transfer, London, England, The Institution of Mechanical Engineers, September, 1951, p. 217.

Authors' Closure

The authors appreciate the comments of Mr. Donohue who previously has contributed to the empirical correlation of heat-exchanger data. With regard to his comments, the authors realize the importance of the bundle by-pass stream, as pointed out in the Fritzsche discussion, but purposely attempted to minimize the size of this stream in the present study. On the method of handling crossflow and window pressure drop, the method of Perrone served its purpose when no information was available on conditions within the bundle, but the authors believe that their own method is to be preferred now that data on component effects are available. The average deviation of the over-all pressure drop from the sum of the components is far less than the extreme figures mentioned in the discussion. However, additional pressure taps are being placed in the new model tube bundle in order to assist in investigating local pressure-drop effects more fully. The proposal to reduce the water rate at low oil rates, in order to obtain better heat balances, is a good suggestion and will be considered in future experimental work.

The by-pass area discussed by Dr. Fritzsche, undoubtedly does have an effect upon the pressure drop and rate of heat transfer, especially at low Reynolds numbers. The correction factors, suggested by Dr. Fritzsche on the basis of his experiments, tend to explain the deviations at low Reynolds numbers shown in Figs. 6 and 11 of the paper. Until better information is available, the authors recommend the use of the correction curves presented by Dr. Fritzsche in the references cited in his discussion, although his data are all in the turbulent or near-turbulent region and this bundle by-pass effect is, no doubt, much greater in magnitude at very low Reynolds numbers. It is the hope of the authors that information on the bundle by-pass-leakage stream, especially at low Reynolds numbers, can be obtained during the course of the present investigation.

In closing, the authors wish to call attention again to the monograph written by Dr. Fritzsche and cited in his discussion. This 100-page monograph contains much information on the design of heat exchangers in addition to the material on the by-pass stream, and should be known to all working in this field.

AN ASME PAPER

Its Preparation, Submission and Publication, and Presentation

To a large degree the papers prepared and presented under the ASME sponsorship are evidence by which its professional standing and leadership are judged. It follows, therefore, that to qualify for ASME sponsorship, a paper must not only present suitable subject matter, but it must be well written and conform to recognized standards of good English and literary style.

The pamphlet on "AN ASME PAPER" is designed to aid authors in meeting these requirements and to acquaint them with rules of the Society relating to the preparation and submission of manuscripts and accompanying illustrations. It also includes suggestions for the presentation of papers before Society meetings.

CONTENTS

Price 40¢. No discount allowed. *A remittance must accompany all orders for $5.00 or less. U. S. Postage Stamps are acceptable.*

THE AMERICAN SOCIETY OF MECHANICAL ENGINEERS

29 West 39th Street, New York 18, N. Y.